Neurovascular Coupling in the Visual Cortex

By:

Katie Boyd

A thesis submitted in partial fulfilment of the requirements for the degree of Doctor of Philosophy

University of Sussex

Submission Date: September 2019

Statement

I hereby declare that this thesis has not been and will not be, submitted in whole or in part to another University for the award of any other degree.

Signature:

Acknowledgements

Thank you so much to Catherine for your unending support and enthusiasm for my work. You really helped me to see the big picture and get excited again when I felt lost in all the hours of ImageJ. I've learned so much from you, and through what was a bit of a wobbly time for me, I'm not sure any other supervisor could have got me through this process with the same level of compassion and understanding.

To my 5D15 people, I'm going to miss all of you so very much. You are the most lovely, supportive bunch I could have asked for. Please still invite me to stuff. Orla, you are a Kween, you are so supportive and give wonderful advice. Your poetry has brought me to tears, and I will so miss your wee googly eyes and voice like a toddler. Good things really do come in the very smallest of packages. Laura, you are an immuno master, and we went through the incredible struggle of the viral injection together- I am beyond grateful for all your help (and chit-chat!), your passion for cats is infectious, and I will treasure my dinosaur mug for many years to come. Devin, as terrible as we are to one another, we are unfortunately undeniably besties. We have shared a pain like no other in birthing these theses (Thesises? Thesis'?) together, and I want to thank you dearly for letting me freak out and vent at you via text when I needed someone who understood the thesis panic (not that you had much choice in the matter). Kira you are the greatest pal and the undisputed goddess of MATLAB: I'm certain I couldn't have done my PhD without you, and you have been a saint for the amount of help and sage counsel you've given me (and for all the times you've let me sleep on your sofa!). I for sure owe you an extremely classy and overpriced bottle of alcohol, and can't wait to hear you blasting some Alanis Morisette on Karaoke now this is all over! Dori you are my codespiration! I really don't think I'd have my new job without your encouragement on my coding journey, not to mention all the cute dogs you've sent me that get me through the day- I'm so glad I've brought you around to the pure, unadulterated joy of puppies; and I don't know what I would done without having you to share some extremely niche Belinda in-jokes with. You are all wonderful, and I feel so lucky to have had you all around me during this time.

Many thanks to all the support staff that helped keep my animals happy and healthy, and to Rozan, Tristan, and Chrysia of Lagnado lab for being really helpful and training me when I was trying my hand at something new.

Finally, thank you to my family for all their support throughout my eight years(!) at Sussex; for putting a roof over my head whenever I have needed it, and firmly believing I'm the cleverest person no matter the evidence to the contrary. Kermit, you may not have been the most helpful, but I wouldn't have it any other way. Tom, you've supported me when I've been at my lowest ebb, reassured me, and most importantly, bought me many bottles of wine. Thank you for being so understanding when I've had to work long into the evenings, making me stop when I needed to, and being there beside me throughout.

Acronyms

AA	Arachidonic Acid
αSMA	alpha smooth muscle actin
AMPAR	α-amino-3-hydroxy-5-methyl-4-isoxazolepropionic acid receptor
ATP	Adenosine Triphosphate
BBB	Blood Brain Barrier
BO	Branch Order
BOLD	Blood Oxygen Level Dependent
$CaCl_2$	Calcium Chloride
Ca^{2+}	Calcium
CBF	Cerebral Blood Flow
cGMP	Cyclic Guanosine Monophosphate
CO_2	Carbon Dioxide
COX	Cyclooxygenase
cpd	Cycles per degree
DAG	Diacylglycerol
dH_2O	Distilled Water
EET	Epoxyeicosatrienoic Acids
fMRI	Functional Magnetic Resonance Imaging
FWHM	Full Width Half maximum
GABA	Gamma-Aminobutyric Acid
GCamP	Genetically Encoded Calcium Indicator
GLUT-1	Glucose Transporter 1
IS	Intersoma
K^+	Potassium
KCl	Potassium Chloride
$MgCl_2$	Magnesium Chloride
mGLUR	Metabotropic Glutamate Receptor
MLC	Myosin Light Chain
NaCl	Sodium Chloride
$NaHCO_3$	Sodium Bicarbonate
NaH_2PO_4	Monosodium Phosphate
NMDAR	N-methyl-D-aspartate receptor
nNOS	Neuronal Nitric Oxide Synthase
NO	Nitric Oxide
NOS	Nitric Oxide Synthase

NVC	Neurovascular Coupling
PBS	Phosphate Buffered Saline
PDGFRβ	Platelet-derives Growth Factor Receptor Beta
PET	Positron Emisson Tomography
PFA	Paraformaldehyde
PG	Prostaglandin
PGE_2	Prostaglandin E2
PLA2	Phospholipase A2
PLD	Phospholipase D
Pop	Population
PV	Parvalbumin
Pyr	Pyramidal
SGC	Soluble Guanylyl Cyclase
SMC	Smooth muscle cell
SST	Somatostatin
VIP	Vasoactive Intestinal Peptide
2P	Two Photon
20-HETE	20-Hydroxyeicosatetraenoic acid

Table of Contents

University of Sussex
Katie Boyd
Psychology Ph.D
Neurovascular Coupling in the Visual Cortex

Abstract

This research aimed to improve understanding of neurovascular coupling, focussing on the V1 area of the visual cortex. Neurovascular coupling is the process by which the energetic requirements of the brain are met by increases in local blood flow to areas of neuronal activity. The precise mechanisms underlying this are yet to be fully elucidated, however, it is likely to involve multiple cell types (including vascular mural cells, interneurons and astrocytes) through multiple possible pathways. Increasing our understanding of this process is of great importance: functional magnetic resonance imaging (fMRI) is a widely used technique that measures local changes in blood flow in order to extrapolate findings to neuronal activity. However, little is known about the relationship between increases in blood flow and the activity of specific neuronal subtypes underlying it. This therefore limits the conclusions that can be drawn and the level of detail in which it can be understood. Furthermore, a more nuanced understanding of the characteristics of the vasculature and how this relates to its functionality is required in order to deepen understanding of the role different vessel types and their accompanying vascular mural cells might play in neurovascular coupling, and more specifically how neuronal activity might differentially affect various parts of the vasculature with differing properties.

Neurovascular coupling was probed using an *in vivo* mouse model with a chronic awake head-fixed preparation, which allowed sporadic bouts of volitional locomotion. Through this method we were able to observe varying changes in vascular diameter and neuronal intracellular calcium with manipulation of a visual stimulus and varying patterns of locomotion. The function of the vasculature was also characterised in terms of vessel branching order, diameter and inter-soma distance of vascular mural cells; and using *ex vivo* immunolabellling, markers of vascular function were also characterised in relation to these characteristics.

Chapter 1

Introduction

1.1 Neurovascular Coupling

1.1.1 Theory and History of Neurovascular Coupling

Brain tissue requires a constant supply of oxygen and glucose to maintain normal function (Bicher, Reneau, Bruley, & Knisely, 1973), the disruption of which leads to pathophysiological consequences that form the basis of many brain disorders (Mergenthaler, Lindauer, Dienel, & Meisel, 2013). The brain has a particularly high energy requirement compared to other tissues, comprising 2% of overall bodyweight, but demanding 20% of the body's energy at rest (Sokoloff, 1960). This energy is primarily required to restore ion gradients after action and synaptic potentials (Attwell & Laughlin, 2001). The dependence on a constant supply of energy necessitates specialised regulation of the brain's blood supply: local increases in neuronal activity are spatially and temporally coupled to vascular dilation, and hence increases in the regional blood supply, a phenomenon known as neurovascular coupling (NVC). This increase in blood flow in response to neuronal activity underlies the blood-oxygen dependent (BOLD) signal used in functional magnetic resonance imaging as a surrogate measure of neuronal activity in human imaging studies (see Hall, Howarth, Kurth-Nelson, & Mishra, 2016).

It was initially thought that the brain did not play a role in the regulation of its own blood flow (Friedland & Iadecola, 1991; Iadecola, 2017). However this started to change in the late 1800s, first in human studies using participants with skull abnormalities, finding that varying types of stimulus, ranging from physical to emotional, led to changes in brain volume; a relationship thought to be mediated by haemodynamic influence (Mosso, 1880). Further research using various animals but predominantly dogs, look at changes in brain volume to a plethora of stimuli, such as stimulation of sensory nerves, muscular movements, and a variety of drugs, and found that the simulated brain metabolic activity increased brain volume (Roy & Sherrington, 1890). Further work was not carried out until the 1930s, when it was shown that light stimulation increased the temperature of the visual cat cortex (Schmidt & Hendrix, 1938), and later, methods to quantitively measure cerebral blood flow (CBF) using a nitrous oxide tracer were developed to look at net CBF over the entirety of the brain (Kety, 1950). Changes in regional blood flow were first studied in the 1970s using radioactive tracers (Lassen, Ingvar, &

Skinhøj, 1978), which paved the way for future positron emission tomography (PET) and fMRI studies used to measure regional CBF changes. The first MRI study to look at local changes in blood flow in humans was carried out in 1992 (Kwong et al., 1992), and since then, the use of fMRI to understand brain activity has become widespread, and with it, research to further understand the NVC that underlies the BOLD signal garnered through fMRI on a cellular level has increased, with citations of the neurovascular unit increasing from less than 200 in 2001, to over 6500 in 2016 (Iadecola, 2017). With this increased interest, much has been learned about the neurovascular unit. Initially, it was thought that local blood flow is controlled by a negative feedback system, wherein reduced oxygen or glucose, or increased CO_2 in response to neuronal activity acted as a metabolic signal to increase blood flow (Tian et al., 1995). However it was found that oxygen and glucose did not affect blood flow (Lindauer et al., 2010; Mintun et al., 2001; Powers, Hirsch, & Cryer, 1996). Furthermore, the extracellular pH is not congruent with what might be expected if there were a build-up of CO_2 (Astrup et al., 2008). While there are some feedback mechanisms that contribute in fairly minor ways to neurovascular coupling (such as via adenosine, produced during hydrolysis of ATP) (Attwell et al., 2010); the major mechanisms of functional hyperaemia are feedfoward, whereby neurons signal directly to blood vessels, or via astrocytes (Attwell et al., 2010). There are multiple potential pathways through which this can occur, detailed in the following section.

1.2 Pathways involved in NVC

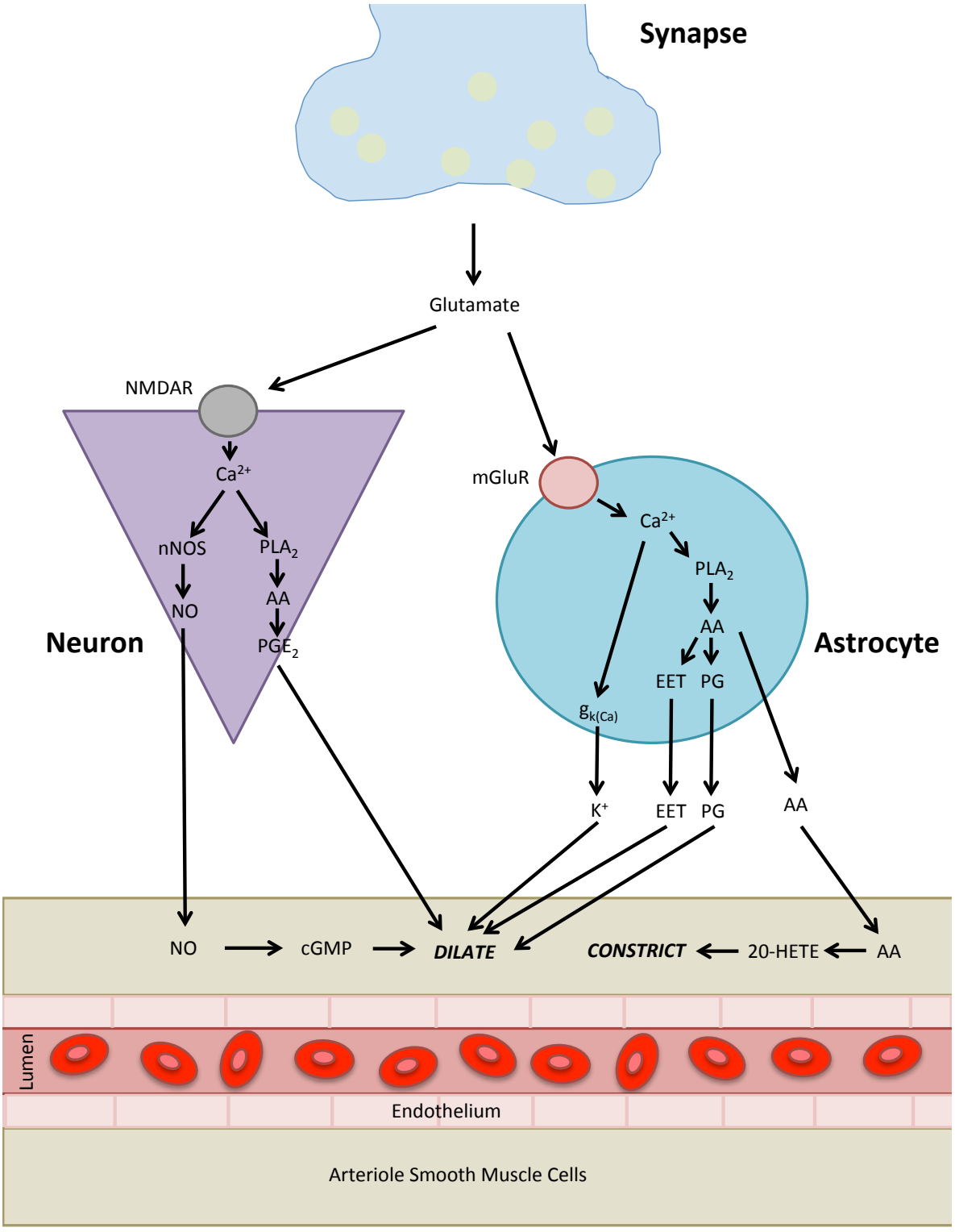

Figure 1.1. Major pathways mediating blood vessel response to glutamate (adapted from Attwell (2010)). *Schematic describing molecular pathways implicated in dilation or constriction of the vessel in response to glutamate release, both neuronally and through astrocytes.*

The canonical view of the pathways involved in NVC is outlined in Figure 1.1, and was suggested based on multiple studies from various different laboratories. The pathways shown here describe glutamate release acting on NMDAR receptors on neurons to increase Ca^{2+}, leading to nNOS-mediated release of NO, activating smooth muscle guanylate cyclase, and leading to cGMP levels that dilate the vessel. In addition to this, arachidonic acid (AA) can be generated from the increased Ca^{2+}, leading to prostaglandin (PG) generation through COX2. Alternatively, via astrocytes, it is suggested that metabotropic glutamate receptor (mGluR) activation by glutamate leads to increased Ca^{2+}, and therefore increased AA. It is postulated that this leads to expression of EETs and prostaglandins, both of which are vasodilators, as well as 20-HETE, which constricts (see Attwell (2010) for a review of these pathways).

However, there is a large degree of controversy regarding specifically these astrocytic pathways. There is controversy concerning the plausibility of astrocyte Ca^{2+} increases potential to contribute significantly to NVC, due to the small size and slow speed of these Ca^{2+} events (Nizar et al., 2013); but other studies have indicated that the degree of Ca^{2+} increase is actually integral in determining whether dilation or constriction occurs in the vessel (Girouard et al., 2010). This has led to further research that delves further into the context of these differing pathways and their potential relationships with differing vessel types.

1.2.1 NVC Pathways for Differing Vessel Types

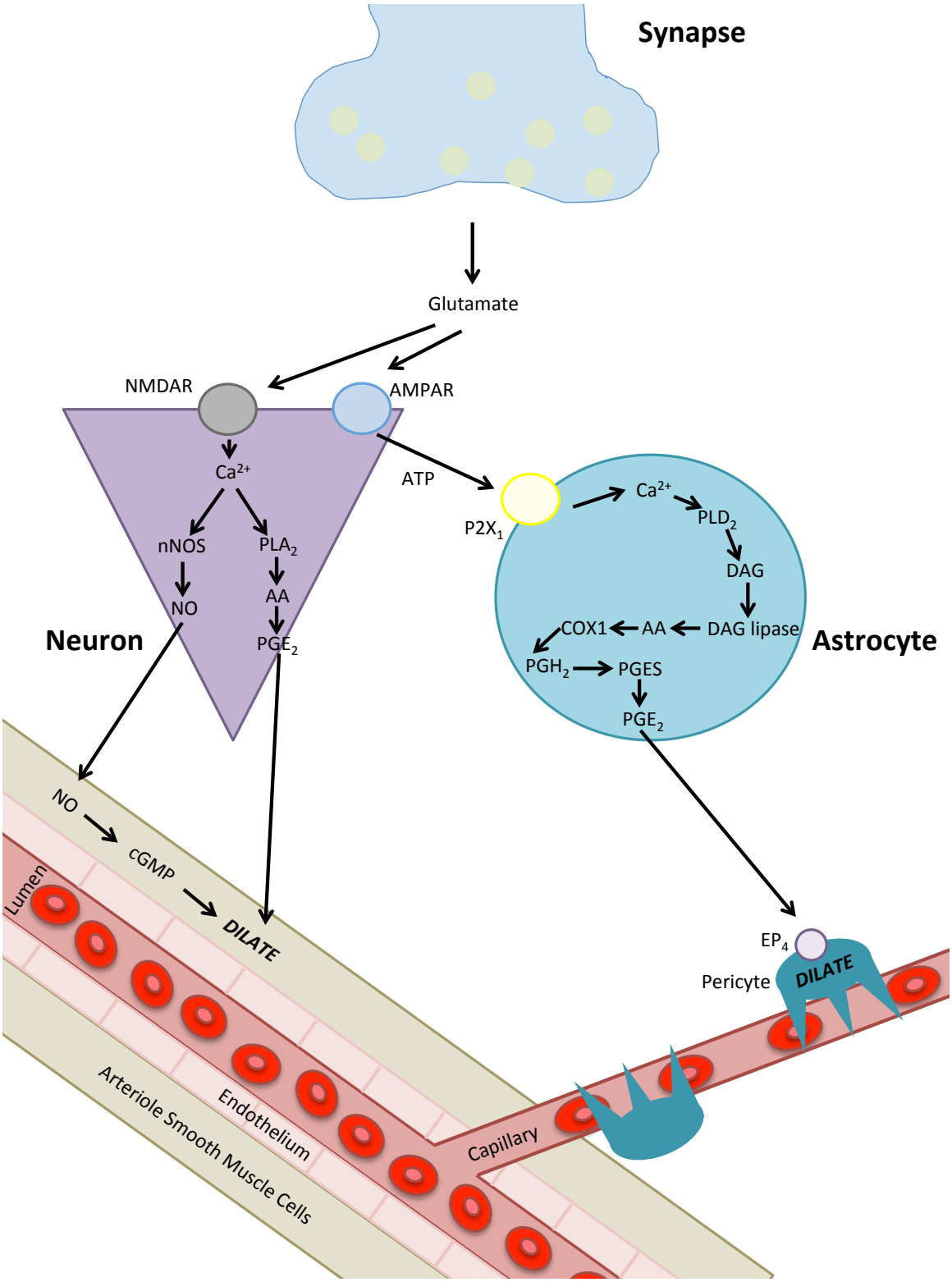

Figure 1.2. Major pathways mediating blood vessel response to glutamate response (adapted and updated from Attwell (2010) and Mishra et al. (2016)).
Schematic describing molecular pathways implicated in dilation or constriction of arterioles and capillaries in response to glutamate release, both neuronally and through astrocytes.

There may be many contextual factors that might affect the pathways implicated in NVC, such as region and oxygen level (Attwell et al., 2010). One such factor is the vessel type to which neuronal activity is coupled. Although both capillary-associated pericytes and arteriole-associated smooth muscle cells (SMCs) have their vasoactivity regulated by actomyosin (Mishra et al., 2016), regulation of muscle contraction could occur via different mechanisms. Indeed, it was shown that differing signalling cascades modulate blood flow changes at the levels of the capillary and arteriole (Mishra et al., 2016), which has allowed development of the previous canonical theory of NVC pathways (see Figure 1.2).

Rather than through a mGluR5 (the existence of which in the mature brain is debated (Sun et al., 2013)); the postsynaptic neuron is implicated in astrocytic control of NVC. The ATP release from post-synaptic neurons activates $P2X_1$ ATP receptors on astrocytes, leading to increased Ca^{2+} in the astrocyte, activating PLD_2 (and not PLA_2 as previously thought). This leads to DAG production, which is converted to AA, which is metabolised to PGE_2. This acts on EP_4 receptors on pericytes, to selectively constrict capillaries (Mishra et al., 2016).

NVC properties can be influenced by the signals coming from neurons (possibly via astrocytes) and the responses of the vasculature to these signals. In my PhD research I investigated the factors shaping NVC at both these levels, studying how different neuronal populations' activity is reflected in vascular response, and how NVC properties vary across the vascular bed.

1.2.2 Neuronal Subpopulations and NVC

As pyramidal cells have the potential to dilate various forms of blood vessel through different pathways, it appears likely that excitatory activity is well coupled with cerebral blood flow. Some researchers also consider pyramidal cells to be important in synthesis of PgE_2, and also identified this as the primary prostaglandin in mediation of vessel dilation (Lacroix et al., 2015), further supporting that close coupling is likely between pyramidal cell activity and vessel dilation. It has also been suggested that the translation of this excitatory

signal to blood vessel dilation also relies upon the post-synaptic neuron, both for direct signalling to arterioles, as well as in order to mediate between glutamate release from the pre synaptic neuron and activation of vaso-regulatory astrocytes (Mishra et al., 2016). The post-synaptic neuron is very likely an interneuron. Interneurons are capable of extensive innervation of local blood vessels (Perrenoud, Rossier, et al., 2012), and nNOS is largely expressed in GABAergic interneurons, with these nNOS-expressing GABAergic neurons constituting approximately 20% of interneurons in the cortex (Tricoire & Vitalis, 2012). In addition to this, activating certain subtypes of interneuron has been shown to dilate blood vessels, for example, serotonin-expressing interneurons (Perrenoud, Rossier, et al., 2012), as well as NOS and vasoactive intestinal peptide (VIP) –expressing interneurons (Cauli et al., 2004) have all been shown to dilate local blood vessels; while parvalbumin (PV) (Urban, Rancillac, Martinez, & Rossier, 2012), somatostatin (SST) and Neuropeptide Y - expressing interneurons have been shown to constrict vessels (Cauli et al., 2004).

However, there has also been some seemingly conflicting work within certain interneuron subtypes: while stimulating an individual SST-expressing interneuron (therefore identifying causality) was shown to elicit vascular constriction (Cauli et al., 2004); correlationally SST interneurons demonstrated increased activity with basolocortical pathway stimulation, which also elicited increased CBF (Kocharyan, Fernandes, Tong, Vaucher, & Hamel, 2008). Further research has found that a subset of nNOS-expressing interneurons are also SST-expressing (Perrenoud, Geoffroy, et al., 2012), indicating potential ability to dilate vessels. Importantly, increasing diversity is being revealed within SST interneurons in terms of their morphology and function, as well as variations in expression of other neuropeptides such as Neuropeptide Y (which was also found to constrict vessels on a cell to vessel basis (Cauli et al., 2004), but correlate positively in terms of activity with CBF (Kocharyan et al., 2008)), which has already led to subgroups of SST interneuron to be theorised (Riedemann, Straub, & Sutor, 2018)). It is therefore plausible that diversity might be found in SST interneuron function in regards to vascular constriction and dilation, and indeed within other subtypes of interneuron. It should also be noted that these subtypes can and

likely do overlap, except between SST, VIP and PV, which have been shown to be distinct and to not co-express (Xu, Roby, & Callaway, 2010).

It is therefore of interest in the current work to measure the response from both pyramidal cells that might dilate vessels directly through PgE_2 (Lacroix et al., 2015), as well as via interneurons and astrocytes (Mishra et al., 2016); and also to study these interneurons themselves, which dilate arterioles through NO release, and demonstrate synaptic activation that generates astrocyte-mediated capillary dilations (Mishra et al., 2016). Co-expression with nNOS (Perrenoud, Geoffroy, et al., 2012) and the fact that SST activity has been shown to both increase and decrease haemodynamic response depending on the duration of activation (Lee et al., 2019) makes this an interesting interneuron subtype to probe. By studying how pyramidal cell and SST interneuron activity changes concurrently with vessel dilation, we might potentially identify which neuronal subtypes drive NVC, and gain more information on the subtype activation that co-occurs with the BOLD response.

1.3 What is an Arteriole?

NVC properties change across the vascular bed (e.g. Mishra et al. (2016), Hill et al. (2015)) so the first focus of my research was to investigate where in the vascular network transitions between different functions occurred and how these mapped onto previous descriptions of vessel types.

Classically, smooth muscle cells (SMCs) were thought to be responsible for brain blood flow regulation, dilating and constricting arteries and arterioles in response to signals generated by neuronal activity. SMCs consist of bands of muscle with contractile ability that act to regulate blood flow. Constriction occurs when myosin light chain (MLC) is phosphorylated, allowing cross-bridge cycling with smooth muscle actin. MLC phosphorylation is promoted by increased intracellular calcium and activation of MLC kinase, or decreased activation of MLC phosphatase, for example by activation of Rho kinase (Webb, 2003). Conversely, dilation occurs when the intracellular calcium

concentration is reduced, and/or the activity of MLC phosphatase is promoted. Second messenger molecules generally regulate smooth muscle cell tone by either altering the intracellular calcium concentration, often by altering the membrane potential and therefore regulating calcium entry through voltage-gated channels, or by activation of receptors that lead to alterations in the cyclic nucleotides that regulate MLC phosphatase (see Hamilton, Attwell, & Hall (2010)). Potassium channels on SMCs are a major target of neurovascular coupling signals, their activation resulting in hyperpolarisation, thus promoting dilation (Longden, Hill-Eubanks, & Nelson, 2015).

In addition to SMCs on arterioles, capillary pericytes have more recently been shown to also regulate cerebral blood flow (Peppiatt, Howarth, Mobbs, & Attwell, 2006, Hall et al., 2014). Pericytes are located on capillaries and classically possess a different morphology from SMCs: while SMCs appear as rings wrapping around the vessel, pericytes are spatially isolated and possess a 'bump on a log' morphology, with processes that emanate from these 'bumps' (Hamilton et al., 2010). However, there has been controversy in the field as to whether pericytes can be considered contractile or not (Attwell, Mishra, Hall, O'Farrell, & Dalkara, 2016). While Hall et al. (2014) found that sensory stimulation induced dilation of pericyte-covered capillaries before arterioles, and predicted that up to 84% of blood flow increase was produced by this capillary dilation, Hill et al. (2015) argued that capillary pericytes lack the smooth muscle actin required for this cell type to be contractile, and that, unlike SMCs, pericytes lacking smooth muscle actin were not contractile. However, this apparent discrepancy in findings appears to be due to differences in how pericytes and SMCs are defined (Attwell et al., 2016). Zimmerman's beautiful drawings in the 1920s (Zimmermann, 1923) first illustrated the lack of an abrupt change between SMCs and pericytes, instead showing a gradual transition in cellular morphology between rings of smooth muscle, pericytes with circumferential and longitudinal processes, and mid-capillary pericytes with only longitudinal processes. Importantly, however, Zimmerman classed all cells with processes, as opposed to classic rings of smooth muscle, as pericytes (Zimmermann, 1923, Krueger & Bechmann, 2010). Hartmann et al. (2015) used transgenic

mice to visualise individual pericytes and attempted a more specific classification of pericyte subtypes, describing smooth muscle-pericyte hybrids, mesh pericytes, and thin strand pericytes, each possessing differing levels of smooth muscle actin and morphologies (e.g. with circumferential and/or longitudinal processes) and therefore differing capacities for contractility, all of which points towards a gradual transitioning between SMCs and pericytes. Conversely, Hill et al. (2015) used a much more limited definition of pericytes, classifying those cells with only longitudinal processes as pericytes and any cell with circumferential processes as an SMC (including those with the classic pericyte bump on a log morphology). These cells with circumferential processes (which would usually be termed pericytes) were found to express smooth muscle actin and to be contractile. In short, the data agrees that vascular mural cells on vessels of small calibre, commonly termed pericytes, are contractile up to approximately 4 branches from diving arterioles, while the evidence is less clear for a contractile role for mid-capillary pericytes.

This debate over the very definition of a pericyte, and their functional properties, indicates how much more research is required in order to understand the role of these cells within the cerebrovascular system more fully, how their function changes across the vascular tree, and whether indeed the rigid classification of arteriole and capillary; and SMC and pericyte is a reflection of the reality of the changing functionality across the vascular tree.

Confusion regarding how to define different points of the vasculature has led to apparent disagreements in the literature. It is therefore of great importance to characterise the function of differing vessel types. This can be achieved both through investigating where functional markers for various more arteriole- or capillary-like functions start and terminate, as well as through in vivo imaging in order to probe the contractile ability of various points of the vasculature, which can also be characterised in terms of the vascular mural cells present, as well as resting diameter and branch order. This might aid in not only to improving understanding of the functionality of arterioles and capillaries, but also in determining the meaningfulness and utility of classification of these vessels in this

discontinuous manner at all.

1.3.1 Markers for Vascular Function

There are many possible markers of vasculature function, some of which are more closely associated with what might classically be considered arteriole-like function, and others that are more closely associated with traditionally capillary-like functionality. Some markers are described below.

Elastin

To maintain blood flow to the brain at a constant level despite being pumped by the heart in a discontinuous manner, a large degree of vascular resistance is required. This is provided mainly by the basal tone of penetrating and parenchymal arterioles (Cipolla, 2009). Elastin fibres are found in cerebral arteries and arterioles and provide the vessel with the compliance required to smooth out the blood flow and allow more uniform flow in capillaries (Vrselja, Brkic, Mrdenovic, Radic, & Curic, 2014). Studying the point at which elastin expression in the vasculature terminates provides one indication of a switch in functionality between arteriole- and capillary-like vessels.

Alpha smooth muscle actin

Alpha smooth muscle actin (αSMA) is a contractile protein, and like elastin, is also classically associated with arteriole rather than capillary function. Due to its contractile role in vascular mural cells, knowing the point at which alpha smooth muscle actin terminates should allow the locale of the switch in function between contractile and non-contractile vessels. This is especially interesting given that although alpha smooth muscle actin is widely accepted to be present in vascular smooth muscle cells, their presence in (and therefore the contractile ability of) pericytes is more controversial (Attwell et al., 2016). Hill et al. (2015) found that smooth muscle cells expressed αSMA and were contractile, while pericytes that did not express αSMA were not contractile. Nehls & Drenckhahn (1991) however showed αSMA expression on some pericytes, but not at the mid-capillary; while

other studies have indicated that αSMA is sometimes expressed at the mid-capillary (Bandopadhyay et al., 2001). It has also been shown that mid-capillary pericytes can respond to neuronal activity, which might lead to relaxation of the capillary wall and an increase in CBF (Rungta, Chaigneau, Osmanski, & Charpak, 2018). It is therefore important to elucidate the termination point of alpha smooth muscle actin to understand how this relates to the vessel dilation that occurs across the vascular network, as well as to understand the morphological properties of the cells and vessels where this functional transition occurs. Comparing this to the termination points of elastin will also shed light on whether an abrupt switch between arteriole and capillary function exists, as both markers are classically associated with arterioles.

Glucose transporter 1

Glucose is an essential metabolic substrate, and the disproportionate energetic needs of the brain (Sokoloff, 1960) mean that it is reliant upon constant availability of glucose. In order for cells to take up glucose, transporters allowing it to move from the blood, down its concentration gradient and into the cell are necessary. Of the two primary glucose transporters in the brain (glucose transporters one and three), glucose transporter one is the most prominent and is typically expressed in capillary endothelial cells of the blood brain barrier. The capillary bed is the site where most nutrient transport occurs (Cervós-Navarro, Kannuki, & Nakagawa, 1988), and evidence indicates that structural deviations in the capillary bed lead to changes in nutrient transport across the blood brain barrier, potentially causing functional neuronal changes associated with diseases such as Alzheimer's (Jong, Vos, Steur, & Luiten, 1997). As this function is integral for maintaining healthy neuronal function, it is important to know at which point in the vascular tree nutrient transport begins and ends and whether this is a function dominated by the capillary bed as is widely believed.

Platelet-derived growth factor receptor beta (PDGFRβ)

PDGFRβ is a classic pericyte marker (Hutter-Schmid & Humpel, 2016). Pericytes are important in the form and function of the blood brain barrier (BBB) (Armulik et al., 2010): a barrier of tightly packed endothelial cells at the interface between the blood and central nervous system (Hawkins & Davis, 2005), allowing the bathing microenvironment of the central nervous system to be controlled and allow optimal functioning. In embryonic mice that lack PDGFRβ, there are no pericytes in the central nervous system and a leaky BBB is evident, indicating an important role for pericytes in the structure of the BBB (Daneman, Zhou, Kebede, & Barres, 2010). In the adult brain, hypomorphic PDGFRβ alleles also lead to BBB breakdown, demonstrating that this is not exclusive to embryos. Blood brain barrier maintenance is therefore traditionally considered a capillary function due to the presence of pericytes on these vessels. Staining for PDGFRβ in the cortex may therefore allow the location in the vascular tree of blood brain barrier maintenance to be determined.

Nestin

Angiogenesis, the process whereby new blood vessels are formed from pre-existing vessels, is an important process in allowing flexibility of the central nervous system: if a brain region is hypo-perfused, it allows new vessels to be formed so that its metabolic demands can be met.

Nestin is an intermediate filament protein that can be used as a marker for angiogenesis, as it is found in proliferating but not mature endothelial cells (Suzuki, Namiki, Shibata, Mastuzaki, & Okano, 2010). Previous research has also located its expression in some capillary pericytes (Birbrair et al., 2015). Therefore, looking at the transition points of nestin staining will provide further evidence of the beginning and end points of this typically capillary-associated function.

1.4 Manipulating Neuronal Activity in V1

The V1 area of the mouse visual cortex demonstrates expression of excitatory pyramidal cells, as well as VIP, SST and PV interneurons (Pakan et al., 2016). One way to gain

understanding of the roles of various subpopulations of neuron in NVC therefore might be to look in the visual cortex at the response from the vasculature as the balance of activity between these subpopulations changes during stimulus change. In order to do this, it is necessary to understand how to stimulate different patterns of activity in these different populations using different stimuli.

Previous work has stimulated these excitatory and inhibitory cells through use of a black and white drifting grating, and importantly, shown that it is possible to manipulate the balance of activity between them through subtle and easy to implement alterations to the drifting grating (Adesnik, 2017). This work by Adesnik used whole cell recordings in layer 2/3 of V1 and showed that by increasing the size or the contrast of the drifting grating, the ratio of excitatory to inhibitory activity shifted towards inhibition, showing for the first time that this excitation/inhibition ratio is not fixed, and indicating potential importance for the ratio of activity of these cell types in processing visual stimuli. Furthermore, although both excitatory and inhibitory activity increase with contrast, they decrease with stimulus size, a phenomenon termed ‘surround suppression’, indicating that the general level of activity is also important in processing these changes. Suppressing SST interneurons specifically enhanced both the excitatory and inhibitory activity garnered in response to increasing stimulus size, thus implicating this interneuron subtype in modulating the general levels of activity in response to changing stimulus size.

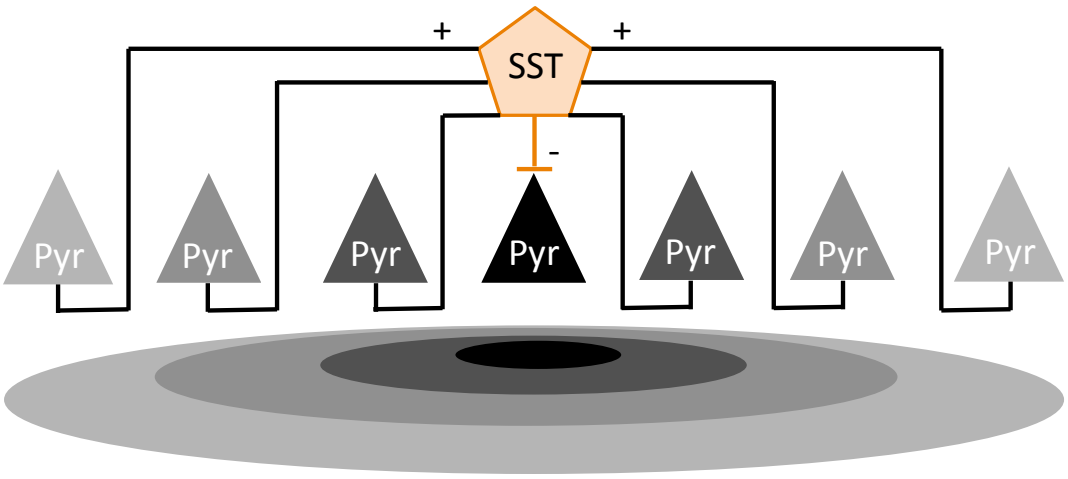

Figure 1.3. Schematic demonstrating circuitry thought to contribute to surround suppression in layer 2/3, adapted from Adesnik, Bruns, Taniguchi, Huang, & Scanziani (2012).
Size of visual stimulus is indicated by grey circles, with lighter grey circles to indicate increasing stimulus size. As stimulus size increases, adjacent pyramidal cells (shown in a colour corresponding to the stimulus that activated them) are recruited to increase SST (orange) excitation through horizontal axons (black lines).

This was consistent with previous work that explored the role of SST in surround suppression in more detail, and provided an explanation for how SST activity could increase as net activity decreased within a region with increased stimulus size (Adesnik et al., 2012). In cortical layer 2/3 of V1, as the visual stimulus size increases, a wider spread of pyramidal neurons are recruited, even though net pyramidal cell activity decreases overall. In this way, there can be a decrease in firing at the centre of the stimulus, as additional pyramidal cells are recruited at the edge of the stimulus in order to adequately excite SST through horizontal axons (Figure 1.3).

These findings on surround suppression were supported and extended using optogenetics to activate both the SST and PV interneuron subtypes. This work also implicated SST in surround suppression but added further depth to our understanding of the interaction between neuronal subtypes as stimuli are manipulated in different ways. It was found that as in primate studies, in rodents there is weaker surround suppression to changing stimulus size when the stimulus is low contrast compared to when it is higher contrast, and that the stimulus size that elicits the largest net neuronal activity also increased under these circumstances. It was also found that this effect was modulated by PV interneuron

activation (Nienborg et al., 2013). It therefore appears that depending on the stimulus, complex interactions between neuronal subtypes can occur in order to drive processing of these stimulus changes.

Luminance of a visual stimulus can also play a role in neuronal activation in V1. In macaque, luminance preferences for specific cells were found (Peng & Van Essen, 2005), however, it appears that response to luminance might overlap a great deal with neuronal response to detection of other features, and therefore the context in which the luminance change occurs is likely important in its processing. In cat V1, while cells with selective activity for changes in luminance were found, there was also a great deal of overlap with cells that were responsive to changes in contrast (Dai & Wang, 2012). This study found three subpopulations of neurons that responded to different stimulus changes: a small subpopulation responded solely to luminance changes, a larger subpopulation responded to contrast changes of the stimulus, and many cells responded to both changes in contrast and luminance. This means that in the context of contrast change, concurrent change in luminance might recruit a small subset of additional cells, but mostly the cells that respond to luminance also respond to contrast. These more diverse cells were also less selective with their orientation tuning and receptive field, thus demonstrating the possible diversity in function of individual cells in encoding certain features. However, research focussing on specific roles of excitatory and inhibitory cells, and the roles of individual subtypes appears to be lacking.

All of these methods of manipulation present an opportunity not just to understand neuronal activity per se in terms of visual processing, but to also look at the relationship of various neuronal subtypes with the vasculature in order to understand which patterns of neuronal activity underpin dilations of blood vessels, and therefore the BOLD signal acquired through fMRI. A stimulus might therefore be changed in contrast and size in order to change the general levels of activity in V1, and to change the balance between excitatory and inhibitory activity in order to look at their relative contributions to NVC.

1.4.1 Locomotion

In addition to features of the visual stimulus driving differential activation of neuronal populations in V1, behavioural state can also dramatically modulate firing patterns. For example, it appears that locomotion and visual stimulus can interact in complex and diverse ways. Vision is of great import during locomotion on account of spatial navigation, leading to interesting relationships between changing visual stimulus and running behaviour that are extremely dependent on context. Looking at LFP has shown a doubling of the visually evoked firing rate as an animal transitions from stillness to running (Niell & Stryker, 2010); and further research has delved into specific neuronal subtypes in order to better understand the circuitry underlying visual processing during locomotion, both with and without a visual stimulus.

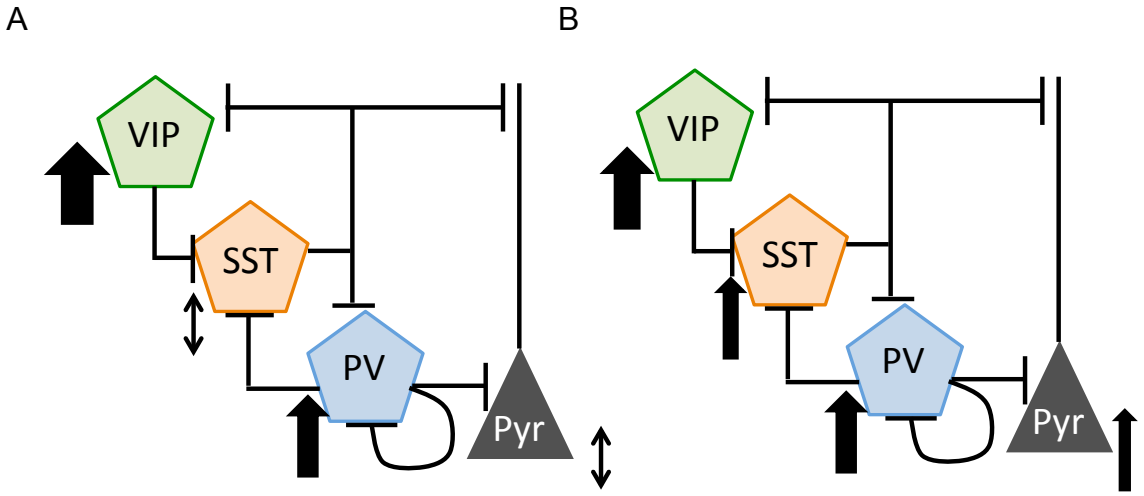

Figure 1.4. Schematic indicating connectivity and activity of different neuronal subtypes in darkness (A) and with a visual stimulus (B) during locomotion. Arrow weight indicates the size of response and up and down arrows indicate the small, variable responses found in these cell types. Adapted from Pakan et al. (2016).

Pakan et al. (2016) sought to probe the validity of the disinhibition theory: that during locomotion response gain of pyramidal cells is caused by disinhibition, mediated by interneurons; and to understand variability in previous studies that probed the activity of specific neuronal subtypes during locomotion. They looked in layers 2/3 and 4 of mouse V1, and found that locomotion during stimulus presentation increased the activity of all subtypes tested: VIP, SST, PV and pyramidal cells (Figure 1.4 B). As the disinhibition

theory, supported by previous research, relied upon inhibition of SST, this finding was inconsistent with this theory. However, in darkness, while VIP and PV interneurons still showed increased response to locomotion, both SST interneurons and excitatory pyramidal cells showed inconsistent activity and were mostly non-responsive during locomotion (Figure 1.4 A), thus explaining how inconsistent findings regarding SST activation might have been yielded if there was variability in the presence of visual stimulus. It was posited that locomotion-triggered neuromodulatory inputs (for example, cholinergic and noradrenergic) could activate all of the neuronal subtypes studied here, but might remain subthreshold in their modulation of SST in darkness, where VIP and PV neurons become activated by locomotion and inhibit SST interneurons and pyramidal cells. However, visual input might allow adequate excitatory and SST activation to overcome VIP and PV inhibition and respond to modulatory inputs. This indicates that the visual context is extremely important when studying locomotion, and can produce variable results depending on the stimulus presentation; and points towards diversity in cell response depending on these factors.

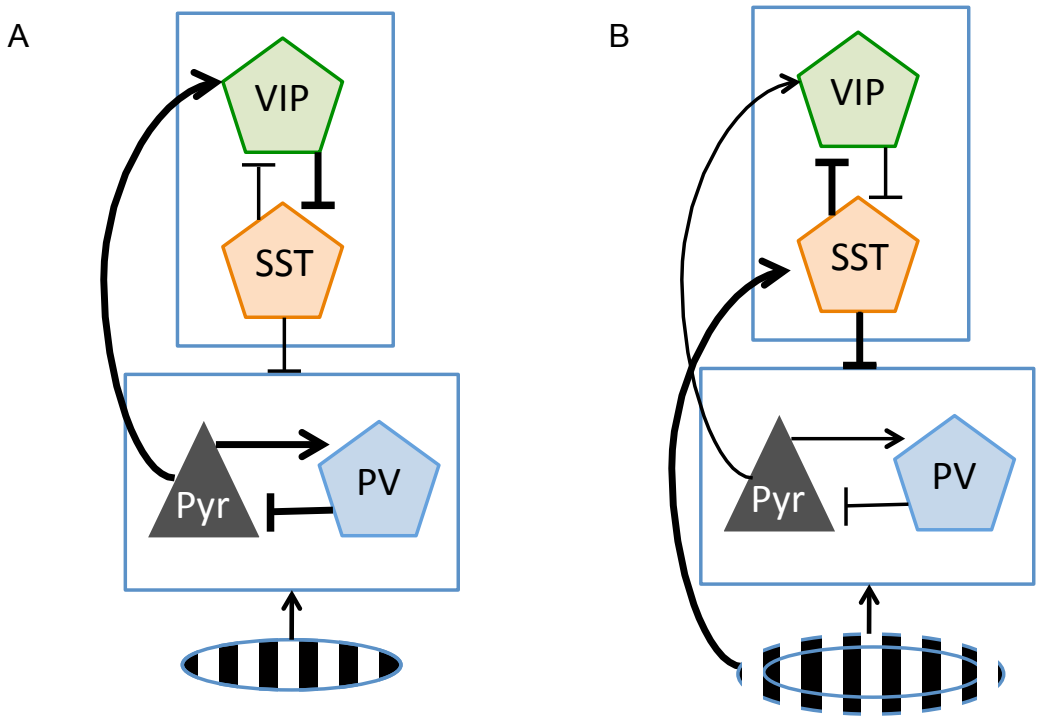

Figure 1.5. Schematic indicating connectivity and activity of different neuronal subtypes to small stimulus (A) and large stimulus (B). Arrow weight indicates the size of response. Adapted from Dipoppa et al. (2016).

Further to this, visual context and its relationship with locomotion has been further studied in the context of more subtle changes. Dipoppa et al. (2016) studied stimulus size in conjunction with locomotion, and found further evidence to contradict the simpler disinhibition model in layer 2/3 of rodent V1. SST activation was increased in response to locomotion when a large stimulus or a full field grey screen was presented, with little effect on VIP activation. To the small stimulus, locomotion increased VIP interneuron response, with little effect on SST interneurons. Both VIP and SST appear to therefore be activated by running, which they theorised put them in 'competition', with variations in visual input more strongly activating one over the other. Response to a small stimulus reflects the disinhibition theory: VIP interneurons are more strongly activated, and this suppresses the SST interneurons, which prevents them from inhibiting pyramidal cells and PV interneurons (Figure 1.5 A). A larger stimulus however more strongly stimulates SST, which suppresses VIP cells and thus more strongly inhibits pyramidal cells and PV interneurons (Figure 1.5 B). PV activity in this case was regardless of stimulus, tightly related to excitatory cell

activity. The pattern of SST activation here indicates that Adesnik's (2012) findings hold during locomotion as well as in the absence of running.

What we might therefore expect based on the literature, is for running during a stimulus presentation to increase SST, VIP, PV and pyramidal cell activity, but for only VIP and PV activity to increase during running without visual stimulus. If a visual stimulus is smaller during locomotion, there is likely to be greater VIP activation as well as pyramidal cell and PV activity compared to when the stimulus is larger, when SST is stimulated and inhibits these other neuronal subtypes.

Locomotion therefore presents another method with which to manipulate activity of various neuronal subpopulations in order not just to understand V1 circuitry, but how these energy requirements are met across different behavioural contexts, and how the activity of specific subtypes relates to response from the vasculature across different brain states.

1.5 Aims and Hypotheses

The current body of work aimed to contribute towards elucidating the mechanisms of NVC in the V1 region of the mouse visual cortex. There were two broad aims within this:

1. To understand how vessel function changes throughout the vascular tree and what features of the vasculature predict these functional changes.
2. To understand which type of neurons drive neurovascular coupling in the visual cortex, and thus whether vascular dilation better reflects excitatory or SST inhibitory interneuron activity.

Aim 1 was investigated through use of functional vascular markers in order to investigate whether there is meaningful separation between arteriole and capillaries using various different methods of identifying the vasculature (branch order, diameter, and distance between vascular mural cells, termed inter soma distance). Additionally, in vivo imaging of different points of the vascular tree was carried out to characterise contractile ability based on the available aforementioned characteristics of the vessel. Based on the difficulty in the field in identifying specific vessel types and their corresponding vascular mural cells, as well as findings of continuous change in the morphology of vascular mural cells, the current work hypothesises that there will not be a single transitional point between arteriole and capillary functions, but that different markers classically associated with arteriole-like function will terminate at different points in the vascular network, while markers classically associated with capillary-like function will start at different points. Regarding the in vivo experiments, it is hypothesised that αSMA expression should align with the contractile ability of the vessel: i.e. vessels that have diameters, branch orders, and IS distances that indicate they should express αSMA will possess more contractile ability than those that should not express αSMA.

Aim 2 was probed through concurrently recording vascular diameter changes and activity of differing neuronal subtypes in order to understand the neuronal activity that is underpinning the BOLD signal acquired through fMRI. Specifically, it was aimed to study

the activity of pyramidal cells, and SST interneurons. SST interneurons were prioritised above other interneuron subtypes due to controversy regarding their role in NVC, as well as divergence between SST interneurons and excitatory activity during surround suppression (Adesnik, 2017), potentially providing an interesting opportunity to separate out the relative functions of these neuronal subtypes in NVC. We then also aimed to look at PV and VIP interneurons to elucidate their relationship with vessel dilation, but were unable to get expression from these. It is hypothesised that there should be a high degree of correspondence between excitatory cells and vessel diameter due to previous findings that pyramidal cell activity directly influences vessel dilation (Lacroix et al., 2015), and its role in dilating vessels through interneurons and astrocytes (Mishra et al., 2016). Thus both pyramidal cell activity and blood vessel diameter is expected to increase with increasing stimulus contrast or decreasing stimulus size. The relationship between SST interneurons and vessel dilation is less clear based on previous literature, but it appears that generally, there is a positive relationship between SST activity and blood vessel dilation. It is therefore hypothesised that increased SST activity will generally co-occur with increased blood vessel dilation, but that this might be less consistent than within pyramidal cells, due to findings that SST interneurons can also constrict blood vessels (Cauli et al., 2004), and it is therefore possible that different experimental procedures (i.e. different stimulus manipulations or levels of locomotion) might reveal differing degrees of correspondence between SST and vessel dilation.

Chapter 2

Materials and Methods

2.1 Animal Preparation

The following methods were carried out in line with the Animals (Scientific Procedures) Act 1986, under approval of the UK Home Office.

2.1.1 Animals

Male and female mice of a C57BL/6J background were used, bred in house (founder mice were generous gifts from David Attwell, UCL (NG2-DsRed mice) or Leon Lagnado (GCaMP6f mice)) and weighing between 18 and 35g. Mice were transgenic, either being NG2-DsRed (in order to visualise vascular mural cells (results from these mice are shown in chapter 3)) (n = 4), Thy1-GCaMP6f (in order to visualise excitatory pyramidal cells (results from these mice are shown in chapters 3 to 6)) (n = 3), or heterozygous SST cre GCaMP6f crossed (in order to visualise SST-expressing inhibitory interneurons (results from these mice are shown in chapters 3 to 6)) (n = 5). At the time of surgery, mice were aged between 8 to 16 weeks, and were imaged between the ages of 12 weeks and 7 months.

2.1.2 Surgery

This procedure describes an open skull window, and largely follows the protocol described by (Goldey et al., 2014), but we made some adaptations. One of the most crucial changes is splitting the surgery into two parts: the *preparation*, which includes preparing and sterilising the surgical site, and the *surgery*, from which point onwards everything used is sterile to maintain asepsis. This adaptation ensures that the surgical procedure is in line with the guidelines of the Laboratory Animal Science Association (LASA) as described in their report “Guiding Principles for Preparing for and Undertaking Aseptic Surgery” (Jennings & Berdoy, 2010).

2.1.2.1 Materials

1. Microdrill Burrs ϕ07 and ϕ14 (Interfocus Ltd., UK)
2. Coverslips 5mm and 3mm diameter, thickness #1 (Biochrom Ltd. UK)
3. Spear Sponges surgical (Fine Science Tools, UK)

4. Norland Optical glue 1oz. NOA 61 (Edmund Optics Ltd., UK)
5. Dexadresson 50ml (dexamethasone) (Cliffe Veterinary group, UK)
6. Buprecare (buprenoriphine) (Cliffe Veterinary group, UK)
7. Isoflurane (Cliffe Veterinary group, UK)
8. Long autoclavable swabs (VWR, UK)
9. Vetbond (St Paul, US)
10. Eye Ointment VitA-POS (Scope Ophthalmics, UK)
11. Unifast Trad Self Cure Liquid (Kent Express, UK)
12. Unifast Trad Powder Pink (Kent Express, UK)
13. Vanna Spring Scissors (Fine Science Tools, UK)
14. Bonn Microprobe (Fine Science Tools, UK)
15. Watchmakers Forceps
16. Scalpel No. 3 for blade No. 10A or No. 15
17. Surgical Scissors
18. Dumont #55 Forceps Inox (Fine Science Tools, UK)
19. Dumont #5SF Forceps Inox Super Fine Tip (Fine Science Tools, UK)
20. Surgical Calipers Stainless Steel 0.5mm increments (Fine Science Tools, UK)
21. Stereotax (Stoelting, US)
22. Head Mount (Kopf Instruments, Inc, CA)
23. Heating plate with temperature controller (World Precision Instruments, US)
24. Betadine (Purdue Products, USA)
25. Hair removal cream (Veet, Reckitt Benckiser, UK)
26. 70% Ethanol
27. Hibiscrub (Centaur Services, UK)
28. Sterile drapes, gown and gloves
29. Black tempera powder (Reeves, UK)
30. Head Post (made in-house)
31. Microdrill (Saeshin Precision Ind. Co., Korea)
32. Compressed air duster

33. Gelfoam (Avitene Ultrafoam, Bard Davol Inc., US)
34. Sterile Saline (Eyewash)
35. Rubber rings

2.1.2.2 Surgical Preparation

Prior to surgery, animals were housed in a 12-hour light/dark cycle, at an average temperature of 22°C. Food and water was freely available.

Animals were first anaesthetised with 4% isoflurance in pure oxygen until the frequency of breathing reduced to ~1.5 Hz, and then maintained at between 0.5%-2% isoflurane, with percent isolfurane being reduced in response to slow or irregular breathing, and gasping. Body temperature was maintained at 37 degrees Celsius through use of a heated mat connected to a temperature controller (World Precision Instruments, US). Mice were secured on a stereotaxic frame (Stoelting, US) with a head mount (Kopf Instruments, Inc, CA) to ensure stability. Just before surgery, animals were given 120 µg subcutaneous (SC) dexamethasone to prevent inflammation of the brain and neural oedema, 1.2 µg SC of the analgesic buprenorphine, and 525µL of SC saline in order to prevent dehydration, and 6.25 µg of SC metacam (meloxicam; non-steroidal anti-inflammatory/analgesic). Eyes were kept moist with opthalamic ointment (e.g. VitA-POS, Scope Ophthalmics, UK).

Hair was trimmed from the site of surgery and removed with hair removal cream (Veet, Reckitt Benckiser, UK). Then the area was washed with saline, then sterilised with 70% ethanol and antiseptic (betadine, Purdue Products, USA) using a cotton-tipped applicator (e.g. VWR, UK).

2.1.2.3 Surgery

Aseptic technique was used throughout the surgery. Hands were washed with 4% chlorhexidine gluconate (e.g. Hibiscrub, Centaur Services, UK) prior to putting on a sterile gown and sterile gloves. Sterilisation of the required equipment was achieved by autoclaving.

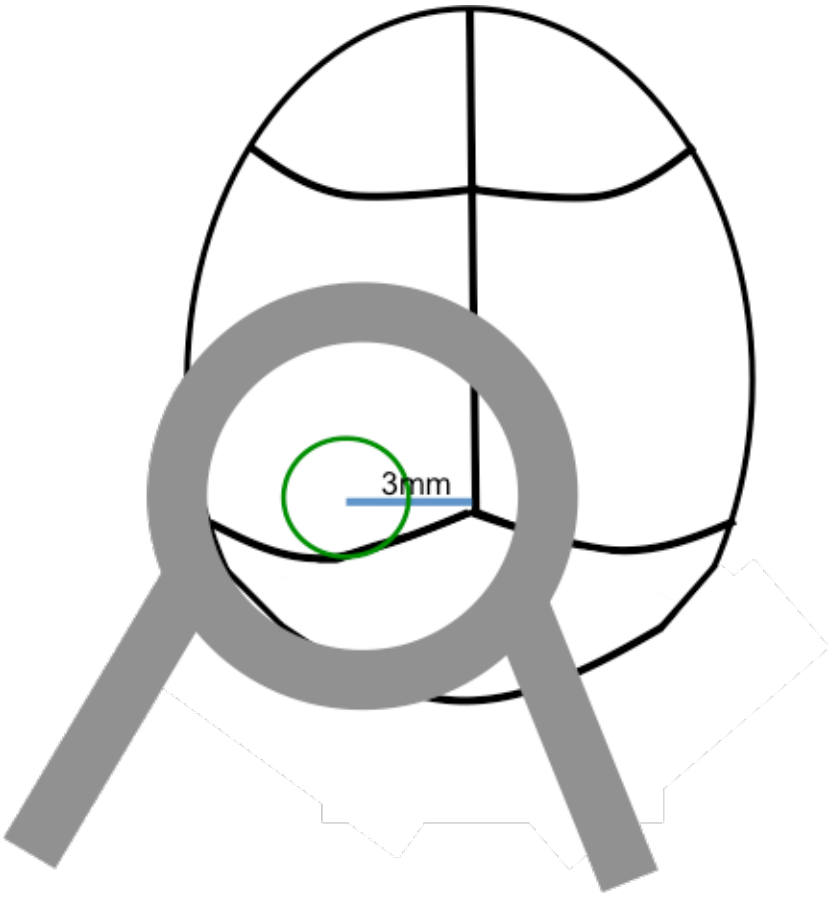

Figure 2.1. Schematic of drilled area/window placement (green), with distance from lambda shown (blue). Headplate placement is shown in grey.

The skin, membrane and some neck muscle were cut away with small spring scissors to expose an adequate area of skull around V1 (3mm to the left of the lambda) (see Figure 2.1). The muscle and skin was sealed with the cyanoacrylate tissue adhesive Vetbond (3M, St Paul, US).

To increase adhesion of the cement, the skull was roughened with blunt forceps and scored with a surgical scalpel blade. Dental cement (Unifast Trad Self Cure Liquid and powder, Kent Express Limited, UK) mixed with light-shielding black tempera powder (Reeves, UK) was then applied to the skull, avoiding the area of interest, and the head plate was applied (approximate placement shown in Figure 2.1). A microdrill (Saeshin Precision Ind. Co., Korea) was used to remove any excess cement and drill around the area of the skull to remove it (shown in Figure 2.1), stopping intermittently to apply saline and cool the area. When the skull was removed, bleeding was controlled with gelfoam

(Avitene Ultrafoam, Bard Davol Inc., US). The dura was then removed with super fine forceps (Dumont #5SF Forceps, Fine Science Tools) to allow optical access to deeper cortical layers.

The glass window (consisting of three circular coverslips: one 5 mm coverslip with two 3 mm coverslips, to create a plug effect glued together using UV-curing optical cohesive) was then placed over the visual cortex and secured with Vetbond and dental cement. Finally, two rubber rings were glued to the head plate and secured with dental cement to create an imaging well as described by (Goldey et al., 2014).

Mice were then allowed to wake by gradually lowering the percentage of isoflurane to 0%, and maintained body temperature using a recovery heat chamber set at 38^{o}C. Mice were closely monitored until they were observed to be active and grooming.

Mice were administered wet food mash with 10 µg metacam mixed through for three days after surgery and monitored daily. Mice were allowed a minimum of 1 week to recover prior to carrying out any further experimental procedures.

2.1.3 Habituation

During habituation, mice were handled daily, and were head fixed for short periods of time on a cylindrical treadmill where they would later be imaged. These periods of head fixing were gradually increased over the period of ~1-2 weeks until mice appeared comfortable on the wheel for over an hour. At which point, imaging could be carried out. This allowed mice at least 3 weeks, but usually >4 weeks to recover prior to any imaging, by which point, Microglial and astrocyte inflammation has been shown to have subsided (Holtmaat et al., 2009). Although some imaging was carried out between 3-4 weeks post-surgery, the majority of imaging started after a month, and so this should have allowed adequate time for recovery (Holtmaat et al., 2009). A horizontal treadmill (Flying saucer, Small n Furry)

was also provided during this period and throughout imaging to increase the likelihood of locomotion behaviour.

2.2 Visual Stimulation

Visual gratings were used to stimulate V1 (PsychoPy). Grating stimuli were displayed for five seconds with a twenty-second inter-stimulus interval. The five seconds prior to stimulus onset was used as a baseline. Screens were placed 17 cm from the mouse. The luminance of the grating has a sinusoidal distribution (sine-wave gratings) for all variations on the grating stimulus. The phase of the grating was 0.033 of a phase per frame, shown at 60 frames per second.

The grating alternated between two spatial frequencies for all stimulus types: 0.04 and 0.2 cycles per degree. In some experiments, the grating stimulus was also varied by contrast (5%, 25%, 63% and 100%) (Figure 2.2), whereby 100% is the maximum contrast allowed by the Psychopy software, and 0% is a uniform, grey screen with no contrast. The contrast value in Psychopy is multiplied by the colour value in order to vary its intensity. Where the stimulus was varied by contrast, it was shown as a full screen stimulus (220 degrees). In some experiments, the stimulus was varied by size, whereby either a full screen (220 degree) or smaller, circular (20 degree) stimulus was shown (Figure 2.3). Where the stimulus was manipulated by size, the contrast was shown at 100%. The stimulus conditions (the differing contrasts or stimulus sizes) were randomised in the order they were shown. Only contrast or size was manipulated in a given experiment, however, the same mice did experience these different stimulus manipulations across different experimental days. It was not possible to achieve equiluminescence between stimulus types, despite calibrating the gamma curve. It is therefore possible that any modulation by contrast or stimulus size could in part be due to changes in luminescence.

In chapter 3, only the highest contrast, largest stimulus was used in order to look specifically at responses from differing parts of the vasculature to the stimulus that elicited the strongest, most robust response. However, both 0.2 and 0.04 cpd spatial frequencies were shown.

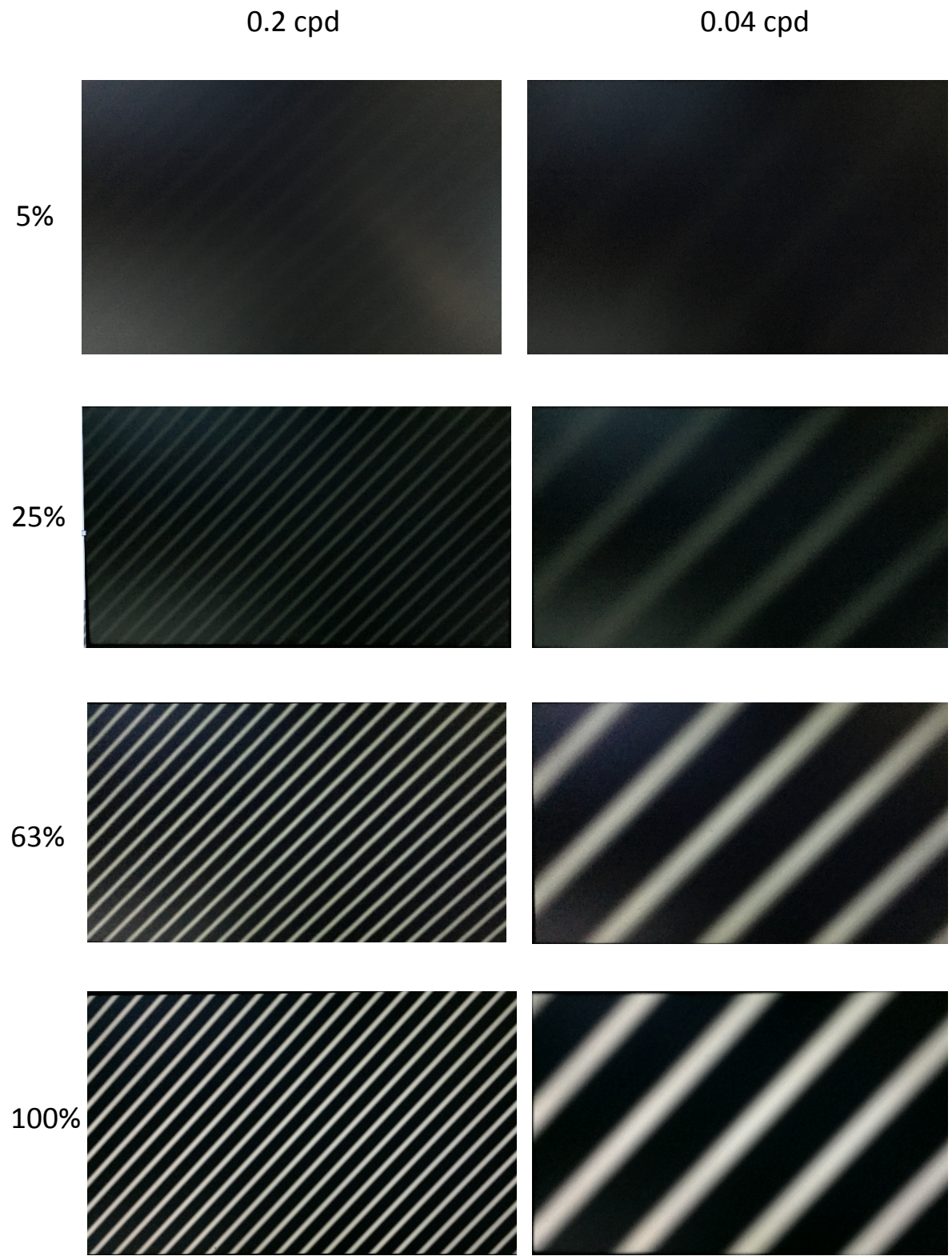

Figure 2.2. Visual stimuli shown, varied by contrast and spatial frequency.
A drifting grating was shown either at 0.2 cycles per degree (left) or 0.04 cycles per degree (right). And was also varied by contrast, shown at 5%, 25%, 63% or 100% contrast.

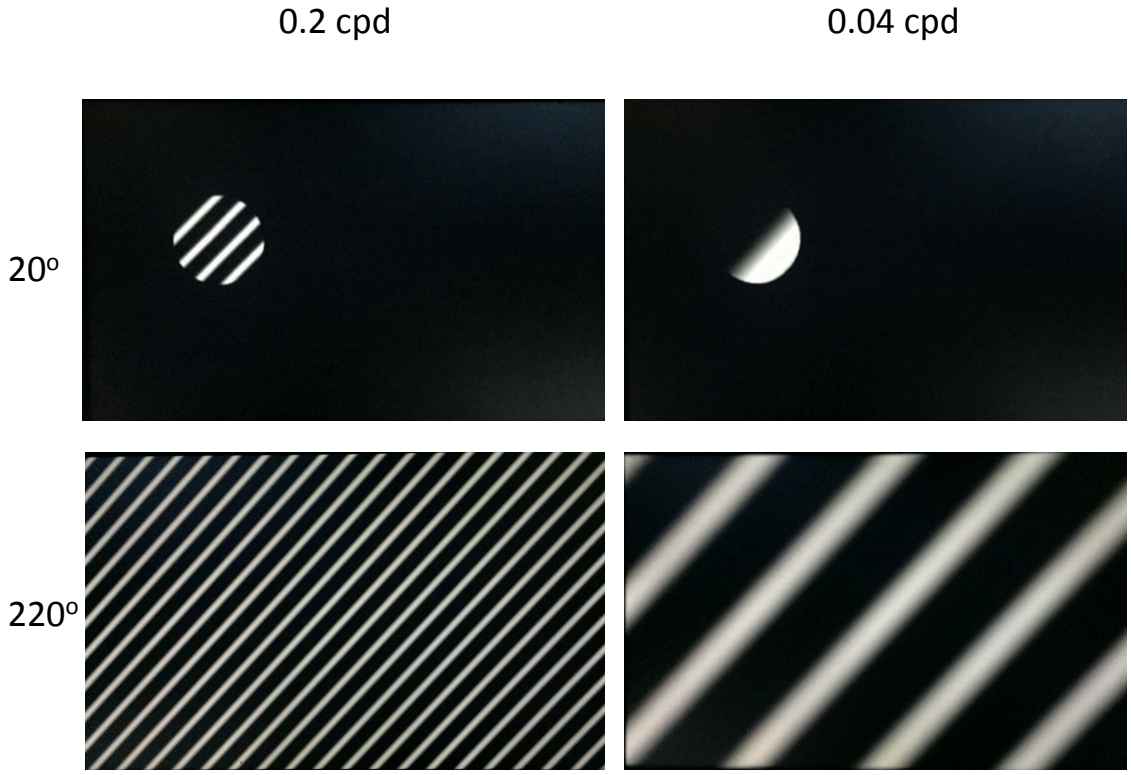

Figure 2.3. Visual stimuli shown, varied by size and spatial frequency.
A drifting grating was shown either at 0.2 cycles per degree (left) or 0.04 cycles per degree (right). And was also varied by size, either to 20 or 220 degrees.

2.3 Experimental Imaging Procedure

In order to visualise changes in vascular diameter, the blood serum was labelled using dyes with a dextran moiety to prevent them from crossing the blood brain barrier and leaking from the vessels. The dye used was dependent upon the experiments: where there was a green calcium indicator in the GCaMP6 mice, a red dye colour was necessary (Texas Red Dextran, Sigma-Aldrich). Where DsRed-labelled pericytes were imaged, which were red, a green dye colour was necessary (FITC Dextran, Sigma Aldrich).

Approximately 20 minutes before imaging, mice were injected using a 29 gauge needle with 2.5% (w/v) Texas Red Dextran or FITC dextran dissolved in saline (70 kDa intravenously via tail vein, Sigma-Aldrich). In some experiments in which Texas Red Dextran was used, a 3 kDA version was injected subcutaneously to achieve the same result. This allowed contrast between the vessel and the surrounding tissue, which was maintained throughout the 1-3 hour imaging sessions.

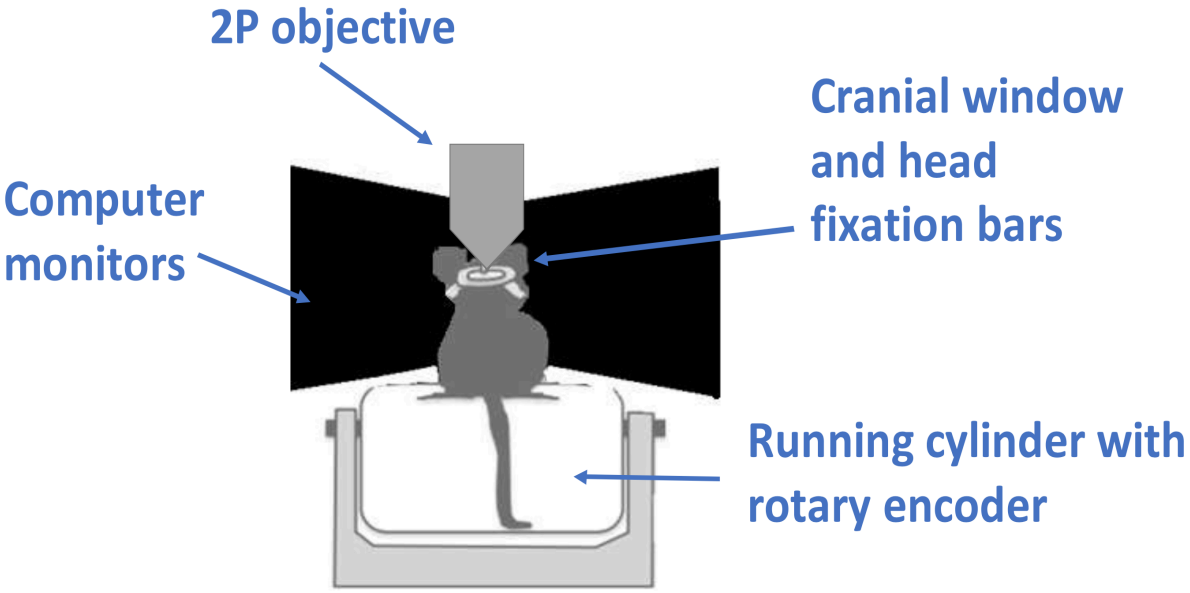

Figure 2.4. Experimental setup for imaging. Mice were head fixed atop a cylindrical treadmill fitted with a rotary encoder, with the 2P objective placed above the window to the visual cortex. Two computer monitors were placed in front of the mouse showing the stimuli shown in figures 2.2 and 2.3.

Mice were then head fixed using both of the protruding connection sites of the titanium head plate (see (Goldey et al., 2014)) on a polystyrene cylindrical treadmill, allowing volitional locomotion at any time. This was fitted to a rotary encoder to allow locomotion to be measured (Figure 2.4). The microscope and treadmill setup were positioned upon a damping optical table (SmartTable, Newport, UK). Above the head fixed mouse was a two-photon microscope (Scientifica, UK), and mice had in front of them (at a 17cm distance) two computer screens (Asus), which displayed the visual gratings (from Psychopy), or were left dark to allow locomotion to be measured in isolation. Individual mice were imaged on multiple different days and experienced all possible visual stimulus conditions (across both the contrast and size manipulation).

Mice were imaged with a two-photon microscope (SP5, Leica), a high numerical aperture water-dripping objective (Olympus, 20x aperture), and a Titanium Sapphire laser (Chameleon, Coherent, US). For each animal, different regions of the cranial window were measured from in different sessions. Experiments were recorded using SciScan software (Scientifica, UK). Laser power used varied between 200 μW and 5 mW, generally increasing with the depth of tissue imaged. Pixel dwell time was 4 μS (in order to balance between signal to noise and speed of acquisition). Pulse frequency was 2 Hz with a pulse duration of 2 ms every 2 frames. Image acquisition was carried out at 7 frames per second. Pixel size differed depending on the zoom used: when imaging locally to a vessel, the pixel size was approximately 0.148 μm, while when the population calcium activity was imaged (with a wide field view), the pixel size was 1.980 μm. The zoom had to be varied between vessels when imaging locally due to differences in vessel diameter, so there was a small degree of variability in pixel size here. As the zoom was consistent across wide field population imaging, the pixel size was always consistent.

When visual stimulation was used, the space between the head post imaging well and the objective was light-sealed using low light transmission masking tape (e.g. T743-2.0 high-performance black masking tape, Thorlabs Ltd, UK). Tissue was excited at 940 nm

wavelength in order to visualise the calcium and Texas Red Dextran simultaneously, and 980 nm in order to visualise NG2 DsRed-labelled pericytes and FITC Dextran simultaneously.

In order to ensure that the area of imaging chosen was responsive to visual stimuli, initially an area for imaging was identified by showing a high contrast grating stimulus and looking for visible changes in vascular diameter at the pia and/or changes in calcium activity (depending on its availability). In experiments in which the grating stimulus size was manipulated, this was also carried out with the small (20 degree) stimulus, which was moved around the screen until the location that elicited the greatest response from the calcium and/or vasculature was found. It was also necessary to identify that the vessel of interest was on the arterial rather than the venous side of the vascular tree, due to the role of arterioles and capillaries in cerebral blood flow regulation. Where NG2-DsRed signal was available, this was used as a method by which to identify that the chosen vessel was on the arterial side of the vascular tree. Where this signal was not available (in Thy1-GCaMP6f or SST cre GCaMP mice), the direction of blood flow from a capillary (in which red blood cells are visible) was used to help verify that the vessel from which it branched was an arteriole.

High magnification movies of individual vessels and their surrounding pyramidal cell or SST interneuron activity were taken, as well as low magnification wide field movies of cell activity as a population (although this wide field view was unable to garner adequate resolution to look at changes in vascular diameter). During high magnification imaging of the vasculature, motion artefacts that might give the appearance of vasculature diameter change were avoided by: ensuring that imaging began at the midline of the vessel and maintaining the focal plane at this point throughout imaging to avoid artefactual dilations; looking for changes in the surroundings of the vessel (e.g. appearance or disappearance of excitatory cells, SST-interneurons, or vascular mural cells) that might indicate a change in Z position; and by also imaging cross sections of vessels, in which changes in Z position will affect the apparent diameter less, assuming a constant diameter along its length.

The depth of imaging was conducted from just below the pia (from the 0^{th} order diving arteriole), down to approximately 700 μm below the surface of the brain. However it was usually not possible to achieve optical access this deeply, and so imaging usually stopped at approximately 200 μm below the surface of the brain. The order in which sections of the vasculatures of varying depths within the tissue were recorded was varied in order to avoid any potential systematic effects, for example, animal fatigue or prolonged heating of the sample (Picot et al., 2018).

2.4 Background to Two-Photon

Due to the light scattering properties of most biological tissues, high resolution in deep tissue has only become possible with the use of two-photon excited fluorescence microscopy, used in the current experiment. The premise for two-photon microscopy is that absorption of two photons simultaneously (within ~ 10xe(-18) seconds) by a fluorophore results in excitation, which leads to emission of a fluorescence photon. The necessity of two lower energy photons rather than one higher-energy photon for excitation renders excitation of a fluorophore more unlikely. As deeper in the tissue, light scattering becomes increasingly prominent and problematic for high-resolution imaging; the requirement of the more unlikely scenario of two photon absorption allows adequate resolution to be maintained hundreds of micrometres into the tissue (Ricard et al., 2009). However, high laser power is required to increase the likelihood of two-photon absorption and gain adequate fluorescence, which can cause tissue damage. To ameliorate this, the laser is pulsed in order to allow high laser power while avoiding burning the tissue. This was very relevant to the current study, as the high laser power could lead to bursting of blood vessels, or more subtly, might affect contractile ability of the vessel through swelling and/or unseen damage to the vessel or its vascular mural cells.

The fluorescence produced by two-photon absorption is then collected by the PMT (photomultiplier tube). This works to translate photon absorption into the emission of an

electron, and increasing the electrons that are generated through electrodes, with all the electrons eventually being captured with a collection electrode. The light intensity is then represented as a pixel eventually in the image.

2.5 Analysis of Two-Photon Data

Data analysis was performed using ImageJ (NIH, Bethesday, MD, USA) and MATLAB (Mathworks Inc, USA).

2.5.1 Vascular Analysis

Vessel diameter movies were first preprocessed in ImageJ to remove motion artefacts. This was achieved through the ImageJ plugin 'Template matching' (Tseng et al., 2011) (see Figure 2.5 B1, B2). The processed movie was then loaded into MATLAB and a script was run to extract the diameter of the vessel across the length of the vessel and across time. This involved skeletonizing the vessel so that a line equidistant between the two vessel edges was drawn (see Figure 2.5 B3, where the skeleton is visible). The diameter was then calculated along each pixel of the skeleton by way of a plot of the light intensity perpendicular to the skeleton (Figure 2.5 B3). The full width half maximum (FWHM) of the yielded intensity curves was used to calculate diameter. The vessel diameter was averaged along the vessel, across multiple skeletal points to allow smoothing over time and space (Figure 2.5 B3). This was achieved with a sliding time window across 5 pixels of the skeleton. The window then moves back 2 pixels to measure another 5 pixels and averages the FWHM for these (this process is demonstrated in Figure 2.5 B3, wherein the overlap of sections that were averaged on the pixels of the skeleton is shown). Measuring from these overlapping sections allows spatial smoothing. This is repeated for every frame of the vessel over time.

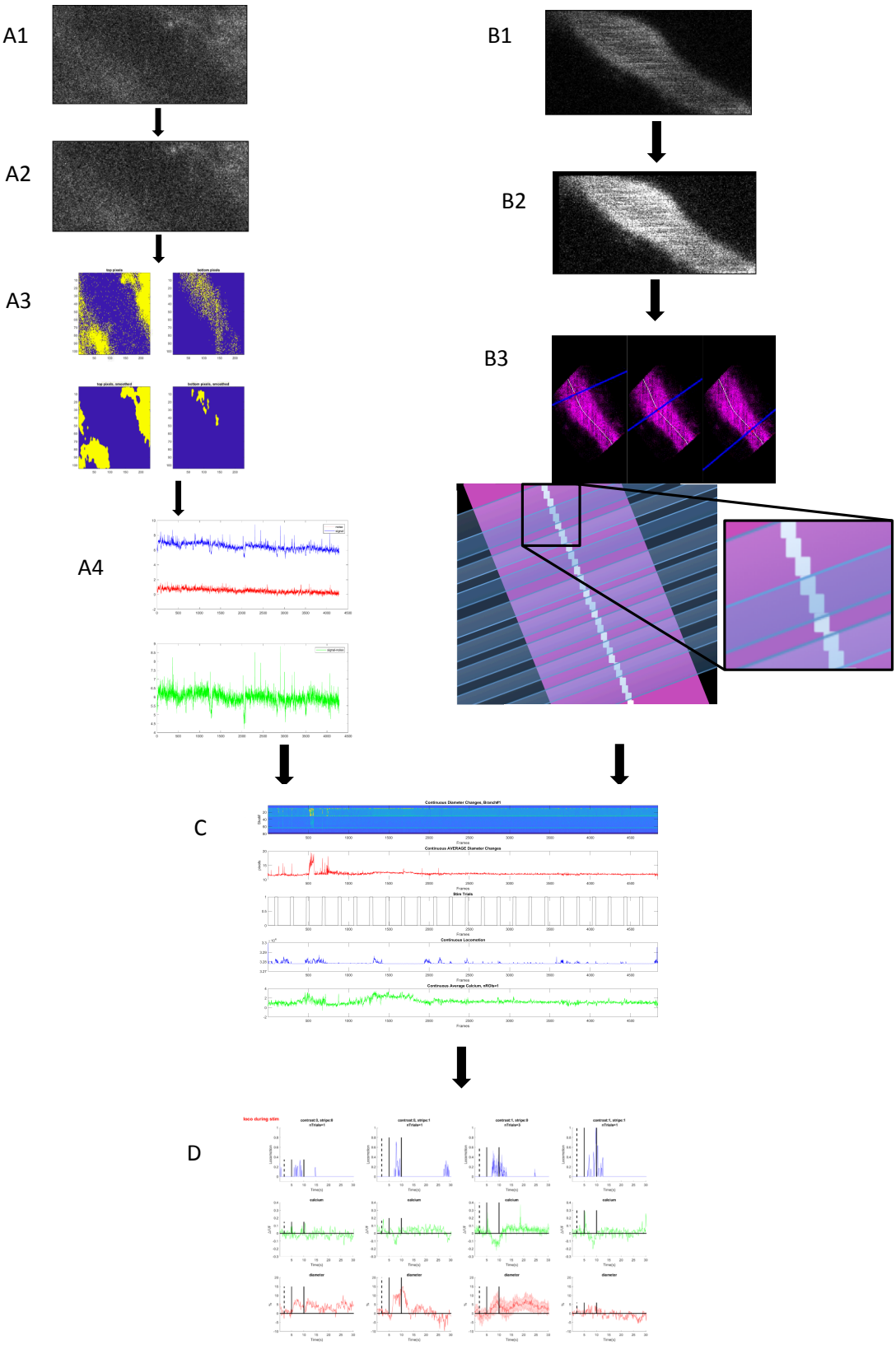

Figure 2.5. Steps of analysis of neuronal activity and vascular diameter change.
A1, A2, B1, B2 *show the registration of the images (note the change in dimension of the image in* ***A2*** *and the black edge in* ***B2*** *due to image stabilisation).* ***A3*** *shows the top and bottom pixels that were selected and smoothed.* ***A4*** *shows the traces from the top (blue) and bottom (red) pixels selected, the red trace is taken away from the blue trace, leaving the trace shown in green, which is used for further analysis.* ***B2*** *shows the brightening of the vessel to improve edge detection.* ***B3*** *shows the acquisition of the full width half maximum, which is taken over overlapping sections of the vessel.* ***C*** *shows the vessel response, visual stimulus onset and offset, running speed, and neuronal activity over the duration of the imaging of one vessel.* ***D*** *shows this data cut around the stimulus and split into groups based on the type of stimulus shown (i.e. Level of contrast and spatial frequency) and pattern of locomotion (in this example, loco during stim is shown).*

2.5.2 Calcium Activity Analysis

The registration coordinates from the vessel were used to register the calcium to stabilise the calcium image, removing motion artefacts and to ensure that the same area of tissue was being sampled for the vessel and neuronal calcium (Figure 2.5 A1, A2). This image was then loaded into MATLAB where the top 20% highest intensity pixels (measured as the maximum value across all experimental trials) were selected (Figure 2.5 A3). The 1-5% of pixels with the lowest maximum value were then selected, and this signal was subtracted from the signal measured from the top 20% (Figure 2.5 A4). The threshold for these low intensity pixels was selected case by case in order to select an adequately small selection of pixels that would not capture any neuronal activity, while ensuring that a large enough sample of pixels was taken so as to ensure this selection was representative of the background activity, and avoid adding noise to the final signal after the subtraction. Any bleed through from the vessel channel was identified and removed so as not to be mistaken for neuronal activity (this was rarely necessary). This method was chosen in order to allow insight into the net activity, while preventing artefacts due to increases in signal from the background (i.e. non-neuronal activity) that might be caused by factors such as any light that might leak through the light-sealing tape (although this was tested and found to be extremely minimal) or general changes in fluorescence in the tissue that might be caused by factors such as changing levels of nicotinamide adenine dinucleotide (NADH) (Ince, Coremans, & Bruining, 1992).

2.5.3 Analysis of Visual Stimulation and Locomotion

A continuous trace of all trials for the resultant calcium change and vascular diameter change was then plotted for each vessel, alongside the concurrent running speed and onset and offset point of stimulus presentations (Figure 2.5 C).

In experiments in which there was a stimulus presented, the stimulus presentations were cut around in order to garner a pre-stimulus, stimulus and post-stimulus period. The

stimulus period was 5 seconds long, and the baseline was cut 5 seconds before this, giving a 5-second pre-stimulus period. The post-stimulus period was cut 20 seconds after the offset of the stimulus presentation (see Figure 2.5 D for an example trace). These were then sorted based on the type of stimulus shown, i.e. the level of contrast shown, or the size of the stimulus shown (Figure 2.5 D).

The stimulus dataset was also sorted based on the temporal pattern of locomotion in relation to the stimulus presentation, i.e. when locomotion occurred in relation to the stimulus presentation. In all locomotion groups, the post-stimulus locomotion was ignored, as it should not have bearing on the response to the stimulus. Therefore all groups may contain some locomotion during the post-stimulus period. The ‘No Loco’ group contained no bouts of locomotion during the stimulus and pre-stimulus period. The ‘Loco during stim’ group contained bouts of locomotion during the stimulus presentation, but not during the pre-stimulus period. The ‘Loco before & during stim’ group contained locomotion bouts during both the pre-stimulus and stimulus period. It should be noted that trials in which there was only locomotion during the pre-stimulus period were measured and sorted, however this pattern of locomotion was very rare and the N was not adequate to look at this data subset individually.

Where there was no stimulus presentation, and spontaneous bouts of locomotion in the absence of visual stimulus were looked at, calcium and vessel responses were instead cut around the onset of the locomotion. The pre-locomotion baseline was the 4-second period prior to locomotion (however it is of note that there is a slight increase in running speed visible prior to the sudden increase in running speed that occurs at the 4-second time point, although traces did not show any obvious response to this). Response to this locomotion onset from 4 seconds onwards was then used as the ‘locomotion onset’ period and measured over a further 4.3 seconds (see Figure 3.4 D for an example trace of the locomotion).

After acquiring and sorting all of the trials, it was then necessary to exclude noisy trials that showed erratic activity. These might have occurred due to warping of the image of the vessel, or any other issues that might have affected the edge detection abilities of the code during vessel analysis, or excessive movement that might have meant a small area remained in the frame after registration (which might also affect the neuronal channel). This was achieved by calculating the standard deviation over the baseline period. This was averaged for each locomotion group, due to the added variability that might be possible if there were locomotion bouts during the pre-stimulus period. Where spontaneous locomotion was studied, the baseline period prior to locomotion onset was used, and averaged over all trials. The cut-off point for exclusion from the dataset was if the standard deviation of a trial was 1.5x greater than the mean. This threshold sufficed to remove noisy trials, but was not too stringent so as to remove low levels of diameter change. The included trials were then averaged for each vessel, and these data were used to produce traces and peak values to stimulus. The peak values to stimulus specifically were obtained by calculating the maximum value during the stimulus period (where there was a stimulus) or locomotion onset period (where spontaneous locomotion was studied) for each vessel.

2.6 Functional Markers Associated with Vascular Function

Immunohistochemistry was employed in chapter 3 in order to characterise different points of the vasculature in terms of functional markers. Details of this are provided in chapter 3, but briefly, immunohistochemistry and some analysis had already been carried out by another research student in order to identify the start and termination points of functional markers. These included αSMA, elastin, PDGFRβ, GLUT-1 and nestin, each of which is associated with more arteriole- or capillary-like function. These start and termination points were identified in terms of vascular mural cell inter soma distance (the distance between soma of vascular mural cells), vascular diameter, or vessel branch order; however an alternative method of branch order was originally employed that added a branch order to the penetrating arteriole with ever branch away from it. This differs from the widely used classical method, which assumes homogenous functionality across the length of the

penetrating arteriole, and therefore classifies its entire length as branch order 0, regardless of any branches away from it.

The purpose of the current research was therefore to go through all of the images used and reclassify the branch orders using the classical method for comparison, as well as to complete analysis of IS distance and diameter

2.7 Statistical Analysis

Statistical tests are applied throughout experimental chapters (3 – 6). These were predominantly independent measures (due to the severe loss of N that would have occurred had repeated measures tests been carried out) two-tailed two-way and one-way ANOVAs (chapters 3 – 5) and correlations (chapters 3 and 6). Where appropriate, Bonferroni post-hoc tests were completed to test multiple comparisons.

Chapter 3

Characterising the Vasculature

3.1 Introduction

Vessels that supply energy to the brain can be categorised into arteries, arterioles and capillaries, while venules and veins remove waste products. Here, we aim to investigate the morphology and function of the vessels on the arterial side of the vascular tree, as it is here that vessels have contractile ability and are therefore able to dynamically regulate blood supply (Hall et al., 2014).

Arterioles are covered in bands of vascular smooth muscle cells that are classically considered to be contractile (Hill et al., 2015), while capillaries exhibit more spatially isolated pericytes with a “bump-on-a-log” morphology that are classically considered to support vessel function through nutrient transportation, blood brain barrier maintenance and angiogenesis (Cervós-Navarro et al., 1988; Nakagawa et al., 2009; Ozerdem & Stallcup, 2003). However, recent research has controversially indicated that many of these pericytes are also contractile and regulate neurovascular coupling (Attwell, Mishra, Hall, Farrell, & Dalkara, 2015; Hall et al., 2014). This has led to disagreements in the literature as to the respective roles of pericytes and smooth muscle cells (Hall et al., 2014; Hill et al., 2015), and confusion regarding the nomenclature that should therefore be used in reference to varying types of vessel (arteriole or capillary) and their respective vascular mural cells (smooth muscle cells and capillaries) (Attwell et al., 2016; Damisah, Hill, Tong, Murray, & Grutzendler, 2017; Hill et al., 2015).

It is suggested that the cause of this issue is a lack of clear morphological and functional difference between arterioles and capillaries. The current research therefore aims to investigate whether there is a clear transition point between vascular smooth muscle cells and pericytes and arterioles and capillaries by determining how the function and morphology of the vessels and their vascular mural cells transitions between classic arterioles and capillaries.

One important aspect of this controversy is regarding where vessels do and do not dilate. While it is agreed upon that arterioles and first order branches dilate (Hall et al., 2014; Rungta et al., 2018); there is controversy closer to the mid-capillary, where there is disagreement over whether the smaller dilations observed here are active or passive (i.e. that the diameter might be increasing with increased blood flow to the region, but that this is being controlled elsewhere in the vascular tree) (detailed in Attwell et al. (2015)). It has been argued that these vessels closer to the mid-capillary are unable to control blood flow due to less consistent (but still present in some cells) αSMA (integral in contractile ability of vascular mural cells) expression (Bandopadhyay et al., 2001) and due to processes that do not encircle the vessel; however even these pericytes lacking circumferential processes might be able to control diameter change by relaxing and decreasing the stiffness of the vessel wall (Rungta et al., 2018), and thus increases in vessel diameter actively induced by vascular mural cells might occur even in the mid-capillary. It is therefore of great interest to characterise the degree of dilation that occurs across the vascular tree, which here was carried out both to a visual stimulus and to spontaneous locomotion (which has been shown to increase CBF response in the somatosensory cortex (Huo, Smith, & Drew, 2014)).

After establishing which vessels dilate, it is of interest to know how this aligns with functional markers, especially the aforementioned αSMA, which is important in determining ability to dilate (Brozovich et al., 2016). Its presence in capillary pericytes has been controversial, for example, Nehls & Drenckhahn (1991) found that some pericytes expressed αSMA, but not mid-capillary pericytes; while Bandopadhyay et al. (2001) found that some mid-capillary pericytes do in fact express αSMA; and recent research has revealed that αSMA might not have been previously detected in mid-capillary due to its instability in PFA (Alarcon-Martinez et al., 2018). There is therefore a large degree of uncertainty and controversy around this marker, where it is expressed, and how exactly that relates to vascular function. Therefore, characterising dilation and aligning this to this functional marker is of great use in improving understanding of the nature of αSMA

expression throughout the vascular tree, and how this impacts the degree of dilation where it is and is not present.

The vasculature can be characterised more than just in terms of contractile ability. See chapter 1 for details of the functional markers, but briefly, aside from αSMA, the markers that were studied included what is classically considered another arteriole marker: elastin (pulsatile flow); and classical capillary markers: PDGFRβ (blood brain barrier regulation), nestin (proliferative capacity), and GLUT-1 (nutrient transport). We aimed to characterise the start and termination points of these in order to improve understanding of how different functions in addition to contractility begin and end across the vascular tree. This was completed with a view to characterising the transition from arteriole-like functions (contractility and pulsatile flow) to capillary function (such as blood brain barrier regulation and nutrient transport). It was aimed to learn whether this change occurs in an abrupt manner that signals a clear transitional point between what could be considered an arteriole and what could be considered a capillary, or whether this occurs in a more gradual manner, with less consistent stop and start points between differing markers that correspond with the same vessel type (e.g. an arteriole).

Another area of controversy is how to define different zones of the vasculature. One extremely common and easy-to-implement method is branch order. This is easy to use in vivo and also doesn't require visualisation of vascular mural cells. Usually, vessels are categorised according to their branch order away from the penetrating arteriole using 0 or 1 to classify the entire length of the penetrating arteriole (for example, Alarcon-Martinez et al., (2018) and Hill et al. (2015)). However, the morphology of mural cells also changes down the penetrating arteriole (Grant et al., 2019; Hartmann et al., 2015), which suggests that vascular function changes too. Therefore an alternative method of defining branch order that might account for this change over the penetrating arteriole was investigated. Here, each branch away or down from the penetrating arteriole resulted in an increment of 1 branch order.

Vessels also vary in their vascular diameter: arterioles have a greater diameter than capillaries and vessels, from as large as ~70 μm in arterioles (Harper, Bohlen, & Rubin, 1984) down to ~5 μm in capillaries. As vessels decrease in their diameter, the functional properties of mural cells is likely to change, as they transition from smooth muscle cells (on vessels > 10 μm in diameter), to circumferential 'mesh' pericytes (on vessels of 6 – 10 μm in diameter), to thin strand pericytes (on vessels of 4 – 6 μm in diameter) (Hartmann et al., 2015). However, it is not clear, based on diameter, where the boundary between an arteriole and capillary should be drawn, being anywhere from 5 -10 μm (Attwell et al., 2016). This further supports the notion that the nomenclature has become confused. It would be useful to know at what diameter of vessel any meaningful functional transitions occur, to better define categories of vessel (such as capillary or arteriole).

A third way of identifying the vasculature is through the distance between the soma of the vascular mural cells, termed inter soma (IS) distance. Because pericyte cell length increases along the vascular tree, while contractility may decrease (Grant et al., 2019), IS distance may serve as a useful indicator of mural cell morphology, and may be a useful indicator of vascular function. IS distance of pericytes found upstream of the αSMA termination point is also smaller than that of vascular mural cells downstream of the αSMA termination point (Grant et al., 2019). Looking at the vascular mural cells themselves might therefore provide a useful way of defining the vasculature.

Aims and Justifications for Current Study

The current study aimed to characterise the degree of dilation throughout the vascular tree, using various methods of identifying a given point of the vasculature. Within this, it was aimed to determine which method of determining branch order best reflects dilation of different branches, and along the length of the penetrating arteriole. We also aimed to look at how functional markers correspond with the dilation observed at different points. Using branch order, IS distance and diameter, we looked to characterise the start and termination

points of different vascular functional markers to: 1. Understand the transition of function between arterioles and capillaries, and 2. To elucidate which method of characterising the vascular tree is most consistent in identifying these start and stop points of functional marker expression.

As the IS distance is a reflection of changing vascular mural cell morphology (as the longitudinal processes and increased soma length towards the capillary end of the vasculature contribute towards greater IS distance), it is hypothesised that this method might best reflect the changing vascular function, especially in relation to contractile ability. It was also hypothesised that the different functional markers corresponding to arteriole- vs. capillary-like function would not transition at one distinct point, but at variable different points, thus indicating that the functionality between arterioles and capillaries transitions in a gradual, continuous manner. Additionally, it was hypothesised that the predicted termination point of αSMA (based on immunohistochemistry findings) would correspond with a decrease in contractile ability of vessels in vivo.

3.2 Methods and Materials

3.2.1 Ex Vivo

3.2.1.1 Experimental Solutions

Standard aCSF: for use during slicing

In dH2O mix 124 mM NaCl; 26 mM $NaHCO_3$; 2.5 mM KCl; 1 mM NaH_2PO_4; and 1 mM Kynurenic acid. This can be stored at 4^{o}C for 1-2 weeks. On the day of slicing, add 1 mM $MgCl_2$; 2 mM $CaCl_2$, and 10 mM Glucose.

3.2.1.2 Animals

Animal procedures were carried out in accordance with UK Animals (Scientific Procedures) Act 1986, with the approval of the local ethics committee. Male and female mice aged between 6 – 20 weeks and expressing the fluorescent DsRed protein under the control of the NG2 promoter were used. A minimum of 3 animals were used in each condition and on at least 3 different experimental days.

3.2.1.3 Immunohistochemistry

Primary antibody	Supplier	Dilution (in BPS)	Secondary antibody	Supplier	Dilution (in PBS)
Rabbit anti alpha smooth muscle actin	Abcam	1:200	AF 647 goat anti-rabbit IgG Or AF 488 donkey anti-rabbit IgG	Life technologies	1:500
Rabbit anti GLUT-1	Abcam	1:200	AF 647 goat anti-rabbit IgG	Life technologies	1:500
Chicken anti GFAP	Abcam	1:200	Goat anti-chicken IgY CF488	Sigma	1:500
Rabbit anti PDGFRβ	Santa Cruz Biotechnology	1:200	AF 647 goat anti-rabbit IgG Or AF 488 donkey anti-rabbit IgG	Life technologies	1:500
Chicken anti Nestin	Abcam	1:200	Anti-chicken IgY CF488	Sigma	1:500

Fluorescent dye	Supplier	Dilution (in oxygenated slicing solution)
AF 633 hydrazide (elastin dye)	Life technologies	1:1,000

Table 3.1. Antibodies, dyes and dilutions used

All animals were culled using methods approved by Schedule 1 of the Animals (Scientific Procedures) Act 1986. NG2 DsRed mice were culled by cervical dislocation followed by decapitation. The brain was dissected and anterior and posterior coronal sections were removed with a razor blade. The brain was mounted against a block of agarose using cyanoacrylate glue and submerged in ice cold slicing solution bubbled with 95% oxygen, 5% CO_2 in the vibratome. 200 μm slices of cortex were taken and kept in room temperature slicing solution for 30 minutes, before being fixed in 4% PFA for 30 minutes. After thorough washing in 0.1M PBS, immunohistochemistry was conducted using primary antibodies for markers of classically arteriole-like (α-smooth muscle actin and elastin) or capillary-like functions (PDGFRβ, nestin, and GLUT-1). Slices were washed in 0.1M PBS before being labelled with a 6-hour incubation of secondary antibody. Slices were then mounted onto microscope slides (Vectashield Hard Set mounting medium, Vector Laboratories USA), sealed with nail varnish, and stored shielded from light sources at 4^{o}C.

Slices were imaged using sequential scans for each wavelength on a Leica SP8 confocal laser-scanning microscope. Wide field z-stacks were taken of penetrating arterioles and the downstream capillary bed using the 20x air objective, then projected as maximum intensity projections and merged together (to show the entire length of vessel imaged) using the MosaicJ plugin from ImageJ software (NIH, Bethesda, MD, USA). Specific regions of interest, including transition points of markers, were acquired with a 63x oil immersion objective.

Immunohistochemistry and imaging were completed by research students (Matthew Hammond-Hayley, Davina Amin). For elastin, α-smooth muscle actin (αSMA), PDGFRβ, and nestin; the diameters, inter soma distances and branch orders of the vessels at which

these markers began and ended had been calculated, however branch order calculation was completed assuming differences in function along the length of the penetrating arteriole. This meant that at a branch point on the penetrating arteriole, the branch order was considered to increase by one both for the capillary and the penetrating arteriole itself (see Figure 3.1 for an example image, and Figure 3.7 for a more detailed schematic). However, the classical method of determining branch order assumes that the penetrating arteriole retains the same function throughout its length regardless of any branches away from it, and is classified as branch order zero throughout. The current research therefore recalculates branch order using the classical method, and compares these two possible methods of determining branch order, as well as inter soma distance and vascular diameter.

3.2.2 In Vivo

3.2.2.1 Animal Subjects

Adult male and female C57BL mice aged between 3 – 8 months were used in these experiments. Mice expressed a genetically coded calcium indicator to allow for concurrent measurement of intracellular calcium release from specific subpopulations (see chapter 5), these were Thy1-GCaMP6f and heterozygous SST cre GCaMP6f crossed mice (described further in main methods). Where IS distance was measured, NG2-DsRed mice were instead used in order to visualise the vascular mural cells. Animals were housed in a 12-hour reverse light/dark cycle to encourage locomotion during imaging.

3.2.2.2 Animal Surgery

Animal procedures were performed in accordance with the Animals (Scientific Procedures) Act 1986. Surgical procedures are detailed in the main methods section (chapter 2). A craniotomy was carried out over V1 on the left hemisphere and a glass window was fitted. A stainless steel head plate was fixed to the skull to stabilise the head of the mouse during imaging.

3.2.2.3 Experimental Procedure

Mice were allowed to recover and were then habituated to the experimental setup (see chapter 2).

Approximately twenty minutes prior to an experiment, mice were injected with 2.5% (w/v) Texas Red Dextran (70kDa) into the tail vein. In some experiments, 2% (w/v) Texas Red Dextran (3kDa) was injected subcutaneously to achieve the same result. Where NG2-DsRed mice were used, FITC-Dextran was injected into the tail vein instead. This labelled the blood serum and allowed contrast between the vessel and the surrounding tissue. The dextran moiety of the dye prevents this dye from crossing the blood brain barrier and leaking. This remained detectable in the vasculature for 3-4 hours.

The two-photon microscope was then used to measure changes in diameter (Figure 3.1), while the GCaMP6f genetically encoded calcium indicator allowed concurrent imaging of activity of neuronal subpopulations. Pixel size varied somewhat with the field of view, but the vast majority of vessel imaging used a pixel size of 0.148 µm, which appeared small enough to detect dilation in small capillary vessels (Figure 3.3).

A test stimulus (the grating stimulus) was first presented to test for visible neuronal activity and/or vascular dilation at the pia to ensure that the brain region to be imaged was responsive to visual stimulus. Pial dilation and wide field neuronal activity were clearly visible to the eye, and so this was sufficient to ensure that the correct location was imaged, as evidence by the high vessel response rate during experimentation (Figure 3.4). It was also necessary to determine whether a vessel was on the arterial or venous side of the vascular tree, as only arterioles and their surrounding cells were to be imaged. To achieve this, within the predetermined region, a vessel would be chosen and the first capillary branch (in which there were visible red blood cells) was imaged using a line scan to determine the flow direction. Where NG2-DsRed mice were imaged, the morphology of the

vascular mural cells was used to ensure that the arterial side of the vascular tree was measured from.

Where GCaMP6f mice were used, mice were presented with a visual stimulus, comprised of a drifting grating presented at either 0.2 or 0.04 cycles per degree spatial frequencies. While the drifting grating was also varied by size (a 20 degrees circular stimulus, or 220 degrees (full screen) stimulus, both presented at 100% contrast) or by contrast (5%, 25%, 63% or 100%, all presented as a full screen stimulus) for other experimental purposes, here the data reflects trials from the greatest contrast (100%) and the largest stimulus size (full screen). GCaMP6f mice were used in this chapter to determine response frequencies and compare methods of determining branch order in vivo.

Where NG2-DsRed mice were used, mice were presented only with a full screen stimulus at 100% contrast, also varied by spatial frequency between 0.2 and 0.04 cycles per degree. NG2-DsRed mice were used in this chapter for any ex vivo work and to compare IS distance against other methods of determining location within the vascular network in vivo. Other than this, the mice used in vivo were Thy1 GCaMP6f and SST cre x GCaMP6f mice.

Mice were also able to run at will on a cylindrical treadmill. The results in the following section omit any trials in which locomotion occurred during the stimulus or pre-stimulus period (5 seconds prior to stimulus onset). Spontaneous locomotion trials are also shown.

3.2.2.4 Vessel Processing

Details of the analysis of the vessels are detailed in chapter 2. Briefly, ImageJ registered vessel images, removing movement artefacts. The diameter of the vessel was measured along its length, and across time to determine the diameter changes of the vessel. Where cross sections were imaged, these were either processed in the same manner, or where this was not possible, (when the code was unable to form a skeleton, usually on account of

size and/or shape of the cross section), the area of the vessel was measured over time, and the diameter was extracted from this.

This was then cut into trials around the stimulus presentations, and split into groups based on which size/contrast was shown, which spatial frequency was shown, and the level of locomotion. For the purpose of the current experiment, only trials in which no locomotion occurred 5 seconds before or during stimulus presentation were included. The maximum value from within the stimulus presentation period was then calculated and used as the measure of peak response in all further analysis.

Where spontaneous locomotion was the variable of interest, vessel response was cut around locomotion onset. No stimulus presentation occurred during this behaviour, but screens were switched on, providing a small amount of light.

Trials were then discounted if the standard deviation across the pre-stimulus or pre-locomotion (when studying spontaneous locomotion) baseline was greater than 1.5x the average standard deviation over the baseline period in order to prevent bias in the results from noise and only capture genuine vessel responses. The peak response was then taken by calculating the maximum percent diameter change during stimulus presentation (or locomotion onset where spontaneous locomotion is studied). All of the remaining vessels were used in the dataset, but responding vessels were isolated to compare their response (see figure 3.4). Responding vessels were defined as vessels for which the peak value during stimulus or locomotion was equal to or more than 2 times greater than the standard deviation over the baseline period of that vessel. This threshold was chosen out of several tested as it appeared to best discriminate between vessels that showed no response and vessels and did respond, without categorising small diameter changes as a non-response (evidence by the traces in figure 3.4) This ensured that the response to the stimulus/locomotion was greater than the noise occurring during the baseline period.

In order to measure inter soma distance in vivo, ImageJ was used to draw a line between the centre of each cell and measure the length. It was necessary to z-project the stack to a certain extent to gain required resolution to visualise vascular mural cells. To minimise the error incurred by not accounting for this difference in depth, it was ensured that soma were relatively close together in the Z-stack (within < 20 frames, imaging at ~10 frames per plane, with Z-spacing set to 1 μm) in order to be counted. This may have added 1-2 μm of error, but likely no more than the error involved in hand measuring the IS distance inherently (as a pericyte soma is approximately 10 μm in length (Figure 3.12) and measuring by eye, one is unlikely to measure from the exact centre of the soma each time).

3.2.2.5 Data Analysis

All data analysis was performed using MATLAB (Mathworks) and SPSS.

3.3 Results

3.3.1 Does Branch Order Reflect Function in vivo?

Branch order is a widely used method of defining different zones of the vascular tree. Traditionally this is carried out by classifying the penetrating arteriole as branch order 0, and every branch from the penetrating arteriole as branch order 1. From branch order 1 onwards, the branch order increments with every new branch (termed the 'classical' method in the current work, see Figure 3.2 A for a schematic of this branch order classification system). The current research was carried out in order to assess the validity of this method of determining branch order, and to establish whether a more accurate reflection of vascular function might be to increment the branch order of the penetrating arteriole with every branch down it (i.e. not treating it as one homogenous unit, but as a vessel that changes in function with every branch from it, similarly to its branches). This method also leads to the reclassification of the branches from the penetrating arteriole depending on how many penetrating arteriole branches have occurred between that branch and the pia (this is termed the 'alternative' method, see Figure 3.2 B for a schematic of this branch order classification system). This was also completed in order to understand whether this widely used method of vessel identification is a meaningful way in which to characterise the vasculature at all.

In order to assess the function of different zones of the vessel, first it was established that we could visualise vessel dilations across different diameters (in order to ensure that dilations from high branch order capillaries could be captured); and as vessels had to be analysed in different ways depending on their orientation in the tissue (i.e. some were viewed longitudinally, and some as a cross section), whether this affected results. Branches were then classified using both the classical and alternative method, the degree of their dilation was measured, and the dilations observed across branches using both methods of classification were assessed.

3.3.1.1 Vessel Diameter Change: Checking dilations

In order to look at how vessel diameter changes to stimulus presentation, it was first necessary to check our experimental setup and analysis. In GCaMP6f mice, vessels were imaged both with a longitudinal and cross sectional view (Figure 3.1), both through necessity to image the diving penetrating arteriole, and to allow a check that dilations seen in the longitudinal vessels weren't caused by a change in the focal plane. Dilations to the stimulus were seen both with a longitudinal view and a cross sectional view of the vessel (Figure 3.2, see Figure 3.1 for an example image), and there wasn't a significant difference between responses of vessels depending on how they were imaged (Figure 3.2). It was also shown that the resolution used allowed dilations to be captured in capillaries (Figure 3.3).

It was also decided to include the entire dataset of vessels in our analyses, without discriminating based on responsiveness in order to capture the full spectrum of behaviour from the vasculature. However, we first checked whether results might be drastically different if only responsive vessels (those for which the maximum value during stimulus or locomotion was two times greater than the standard deviation of the baseline period) were used in the analysis. Figure 3.4 shows very similar responses from vessels whether or not non-responsive vessels were included within the dataset.

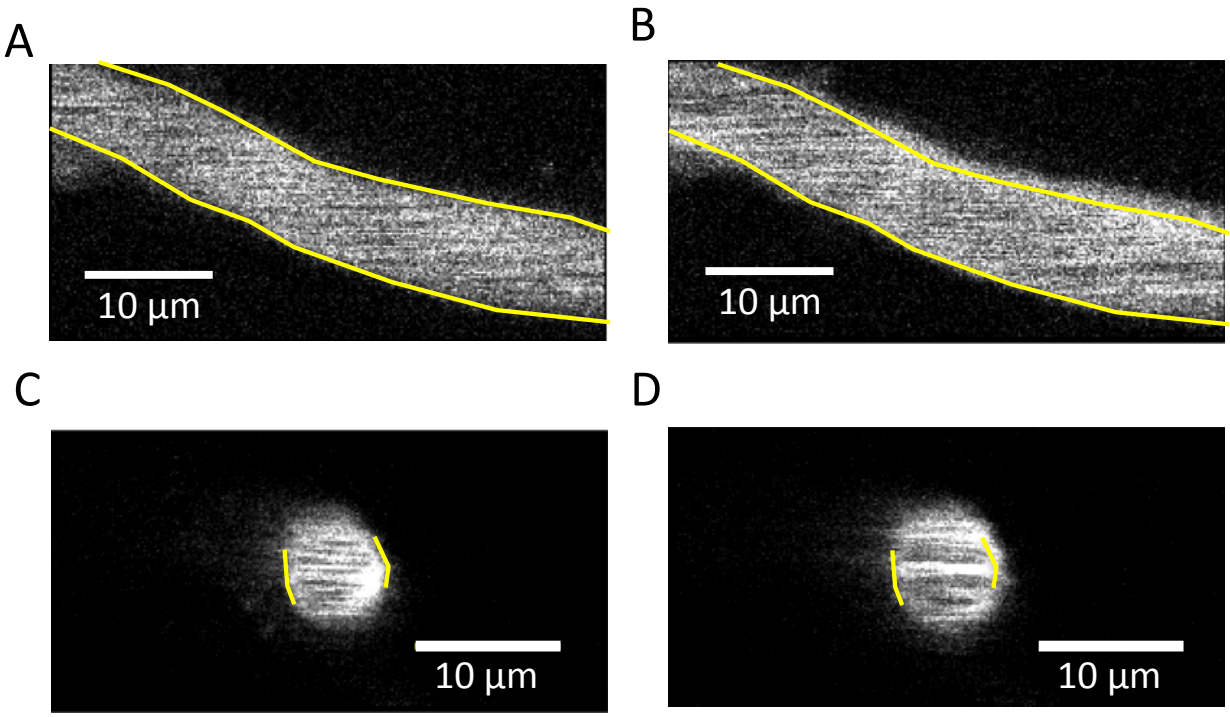

Figure 3.1. Example vascular responses to visual stimulation within longitudinal and cross sectional views of the vasculature.
Baseline diameters are indicated in red. ***A.*** *A longitudinal vessel before stimulus, then* ***B.*** *during stimulus indicates an increase in diameter with the stimulus presentation.* ***C.*** *A pre-stimulus diving vessel imaged with a cross sectional view can also be seen to dilate to the stimulus in* ***D.***

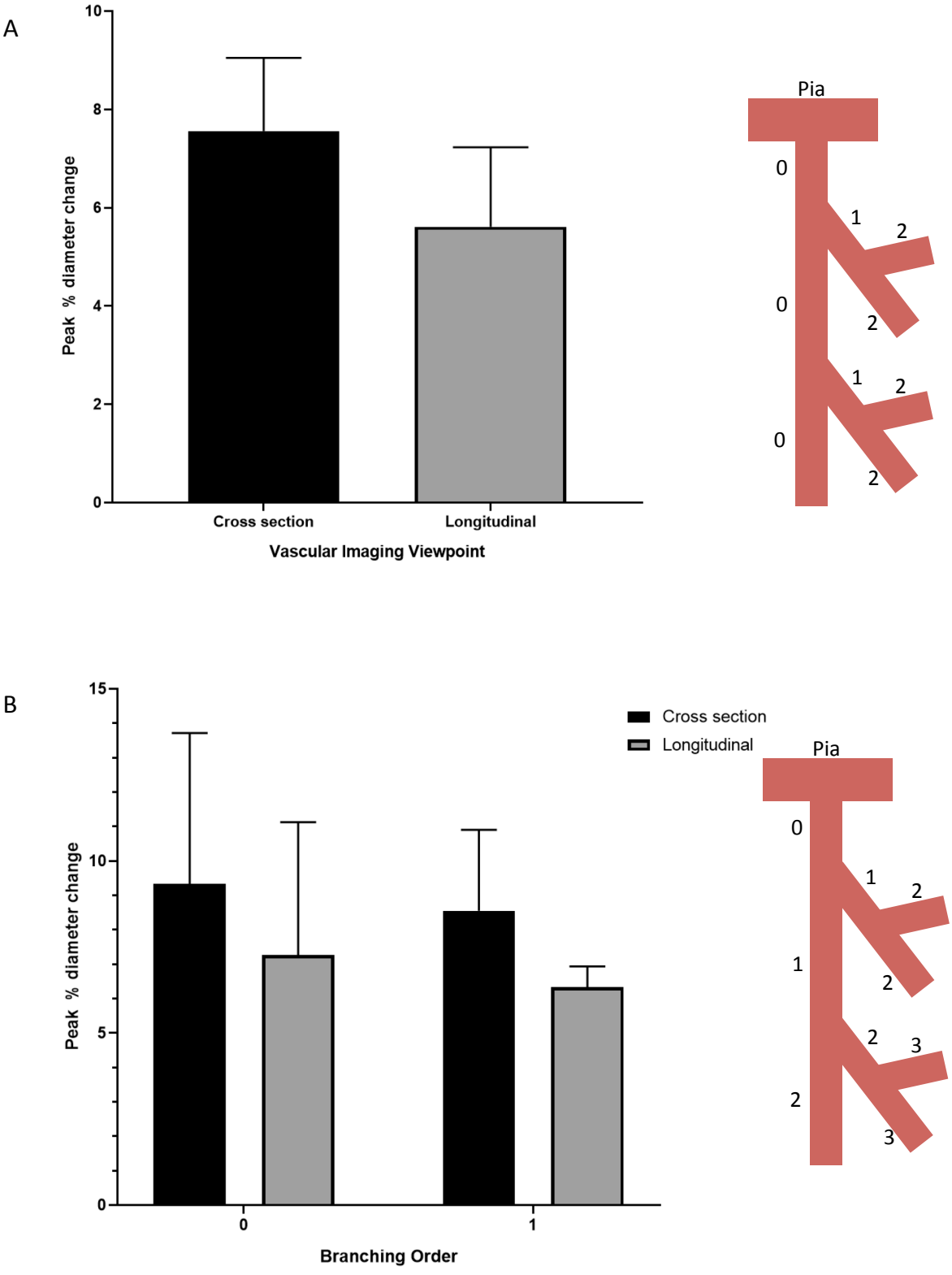

Figure 3.2. Comparison of peak diameter changes yielded from the same branching order using the two different methods of branch order determination and splitting by whether the vessels were imaged and analysed as cross sections or longitudinally.
A *uses the method of branch order determination in which the entirety of the penetrating arteriole is classified as branching order 0 (right) and looks only at vessels that were classified as branch order 0 using this method. The cross sectional view is compared against the longitudinal view of the vessels imaged to ascertain whether differences in peak diameter change were seen between these two views of the vessel. Cross section: N = 21, longitudinal: N = 17.* ***B*** *uses the alternative method of branch order determination (in which 1 branch order is added to the penetrating arteriole with every branch away from it (right)). Here, peak diameter changes of cross sectional and longitudinal views of the vessel were compared across both branch orders 0 (Cross section: N = 4, longitudinal: N = 7) and 1 (Cross section: N = 11, longitudinal: N = 26)(right).*

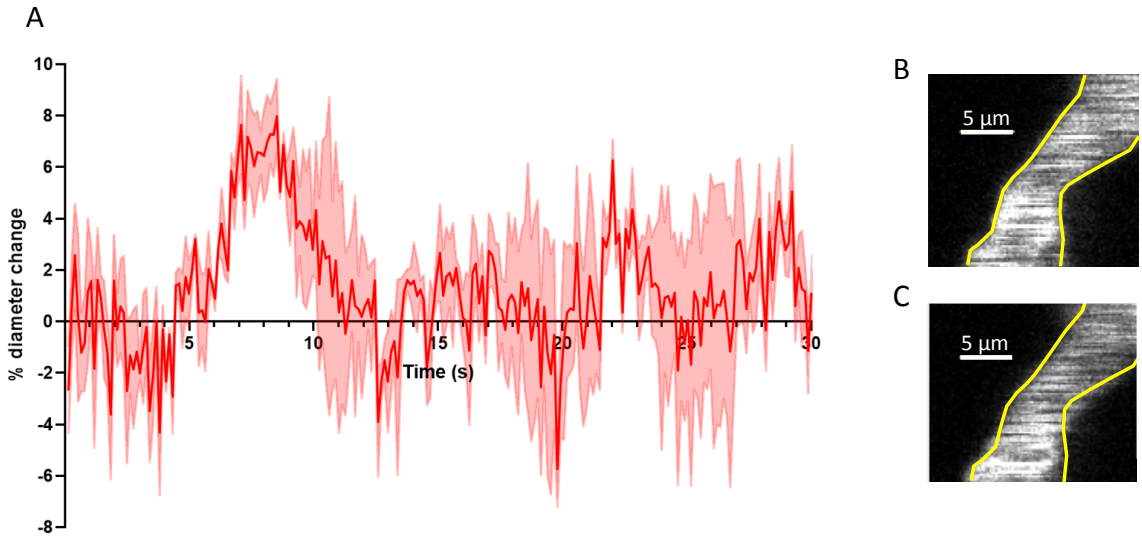

Figure 3.3. Trace to 100% contrast 0.2 cpd from a 5 µm diameter capillary (+/- 1 SEM)
A *Averaged trace across trials for a 5 µm vessel shown in* ***B****. Stimulus presentation of 100% contrast and a 0.2 cycle per degree spatial frequency occurred between the 5 and 10 seconds time points.* ***B*** *Vessel from which the diameter changes were extracted, before stimulus presentation. Yellow lines indicate vessel diameter along the length of the vessel during this baseline period****. C*** *Vessel shown in* ***B*** *during a stimulus presentation, with the same yellow lines to demonstrate diameter change. N = 1 vessel.*

3.3.1.1.1 Comparing the cross sectional and longitudinal views

The two methods used to measure vascular diameter were: a longitudinal view (along the length of the vessel: Figure 3.1 (A, B)) or a cross sectional view (through the width of the vessel: Figure 3.1 (C, D)). Concerns had previously been raised to our lab that false dilations might be acquired simply from changes in the focal plane of the longitudinal viewpoint. We therefore measured the peak vascular diameter change to stimulus from either cross sectional or longitudinal views. In these measurements, vessels were classified using both classifications of branching order. First, the classical method of branch order determination was used, in which the entirety of the penetrating arteriole is classified as branching order 0 (Figure 3.2 A). Using this method, cross sections and longitudinal vessels that were classed as branching order 0 were compared for the degree of peak dilation they exhibited. Using an independent samples t-test, here was no difference between whether vessels were imaged and analysed as longitudinal or cross sectional vessels ($t(36) = .886$, $p = .381$). The alternative method of branching order determination (shown in figure 3.2 B) was also implemented to test the difference between cross sections and longitudinal vessels, in case any bias is implemented by using either method of branch order classification. Using this method, both branching orders 0 and 1 could be analysed due to the larger N of branch order 1 cross sections yielded when branch order is incremented along the penetrating arteriole. A two-way ANOVA was conducted with branch order and vessel viewpoint (whether the vessel was imaged and analysed as a cross section or a longitudinal vessel) as factors. For both of these branch orders, again there was no significant difference in peak dilation depending on whether the vessel was viewed as a cross section or longitudinal vessel ($F(1, 44) = .909$, $p = .346$). It therefore isn't the case that greater dilations are observed using the longitudinal view, as has previously been speculated.

It was established that dilations could be captured across the spectrum of vessels, importantly including capillaries in which the small resting diameter renders any changes in diameter more difficult to capture due to the resolution required. The trace in figure 3.3 A

demonstrates that diameter changes were possible to detect in a 5 μm capillary (Figure 3.3 (B, C)).

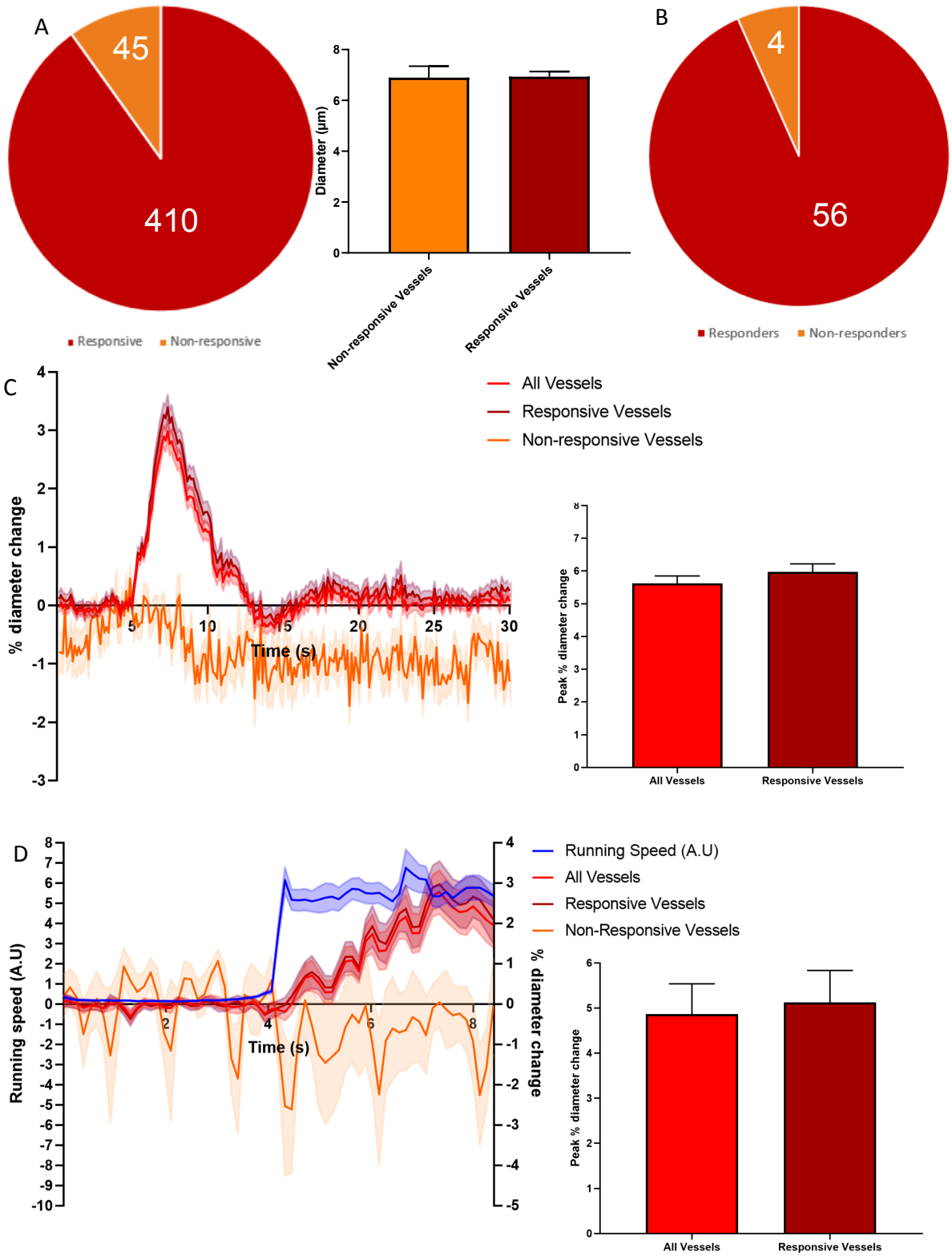

Figure 3.4 Response frequencies, traces, and max responses to 100% contrast, full screen stimulus, collapsing across spatial frequency, split up by whether vessels were responsive to the stimulus; and response frequencies, traces, and max responses to spontaneous locomotion (no stimulus presentation), split up by whether vessels were responsive to locomotion onset (+/- 1SEM).
*N for stimulus data = 455, N for spontaneous locomotion data = 60. Vessels were defined as responsive if the maximum value during the stimulus/locomotion onset was twice as large as the standard deviation across the baseline. The number of responders and non-responder are shown in **A** to the 100%, full screen stimulus (both 0.2 and 0.04 cpd spatial frequencies are included), along with comparison of the mean resting diameters of vessels that did and did not respond; and **B** to spontaneous locomotion onset. In **C**, responses are shown both as a trace (left) and the peak response from all vessels is compared against responsive vessels (right). In **D**, responses are shown to the onset of spontaneous locomotion, comparing vessel responsiveness in the same manner as **C**, but also showing locomotion in blue.*

3.3.1.1.2 Vessel Response Frequency

All vessels were included in the analysis regardless of response level, including non-responders. This served to allow the full spectrum of response to the visual stimulus or spontaneous locomotion to be looked at (throughout the following chapters). However, it is therefore beneficial to ascertain the proportion of vessels that responded and whether the results are changed at all by omitting non-responsive vessels. Vessels were classified as responsive in terms of how great the peak response to stimulus or locomotion was in comparison to the noise in the baseline: the maximum value of diameter change during stimulus presentation or locomotion had to be two times greater than the standard deviation of the baseline (pre-stim/pre-locomotion) period.

In terms of the response frequency, looking at the stimulus dataset, of a possible 455 vessels measured form, 410 were responsive, demonstrating a 90.1% response rate (Figure 3.4 A). As contractile ability of small capillaries is disputed (Hill et al., 2015), and because it is more difficult to capture the small dilations that might occur in these vessels, it would seem more likely that smaller diameter vessels would be (or at least appear) non-responsive. However, in an independent samples t-test there was no difference between responsive and non-responsive vessels in their resting diameter ($t(436) = 0.07189$, $p = .9429$) (Figure 3.4 A), indicating that small vessel dilations occurred to the same extent as larger vessel dilations. Within the spontaneous locomotion dataset, 56 vessels of a possible 60 were responsive, demonstrating a 93.3% response rate (Figure 3.4 B). This demonstrates that the majority of vessels were responsive, and indicates that the proportion of non-responsive vessels might not be large enough to bear a great influence on the results.

Traces of the responses from vessels that were responsive or non-responsive as well as the entire dataset of vessels were also plotted in order to gain more information about the difference between these three groups (Figure 3.4 C). The traces indicate that non-responsive vessels were captured through the method that was employed to distinguish by

vessel responsiveness, as these vessels were not shown to dilate, and indicate that there is very little difference between the responses of all the vessels compared to the responsive vessels alone. The peak responses to the stimulus (a 100% contrast, full screen drifting grating, presented at both a 0.2 and 0.04 cycles per degree spatial frequency) was slightly greater from responsive vessels, but did not differ significantly between the vessels as a whole, and the responsive vessels alone ($t(859) = -.826$, $p = .409$) (Figure 3.4 C).

Similarly, during spontaneous locomotion, non-responsive vessels were successfully differentiated, and traces from all vessels and just responsive vessels appear similar in that the error overlaps to a very large degree. A comparison of the peak vascular diameter change to locomotion onset shows very similarly to the stimulus data, that there is a slightly greater maximum response from responsive vessels, but that there is no statistically significant difference between all vessels and just the responsive vessels ($t(114) = -.271$, $p = .787$) (Figure 3.4 D).

3.3.1.2 Examining different branch order classification systems

The two methods of branch order classification (classifying the entirety of the penetrating arteriole as branch order 0, or not (see figure 3.2)) were next assessed in GCaMP6f mice. Both methods of classification demonstrate the greatest degree of dilation within lower order vessels (closer to the pia or penetrating arteriole depending on the method used), before plateauing. These plateaus begin at similar points within the two methods, and also showed that using the alternative method; branch order 0 demonstrates greater dilations than most of the other branch orders (Figure 3.5). The penetrating arteriole does not show the same degree of dilation throughout its length regardless of branches, and so categorising its entirety as branch order 0 is unlikely to be a meaningful way of categorising this vessel (Figure 3.6). This taken with comparisons between different sections of the vessel that might be classified as the same branch order using the two different methods,

leads us to believe that while the first two sections of the penetrating arteriole (before and directly after the first branch away from it) dilate to similar degrees; after the second branch, the penetrating arteriole dilates to a lesser degree and behaves more akin to the branches away from the penetrating arteriole (Figure 3.7).

Based on this, the alternative method of determining branch order was selected to be used for all further work where appropriate, due to the variation in capacity to dilate across the length of the penetrating arteriole (Figure 3.6), and the otherwise similar profiles of dilation across different branch orders (Figure 3.5).

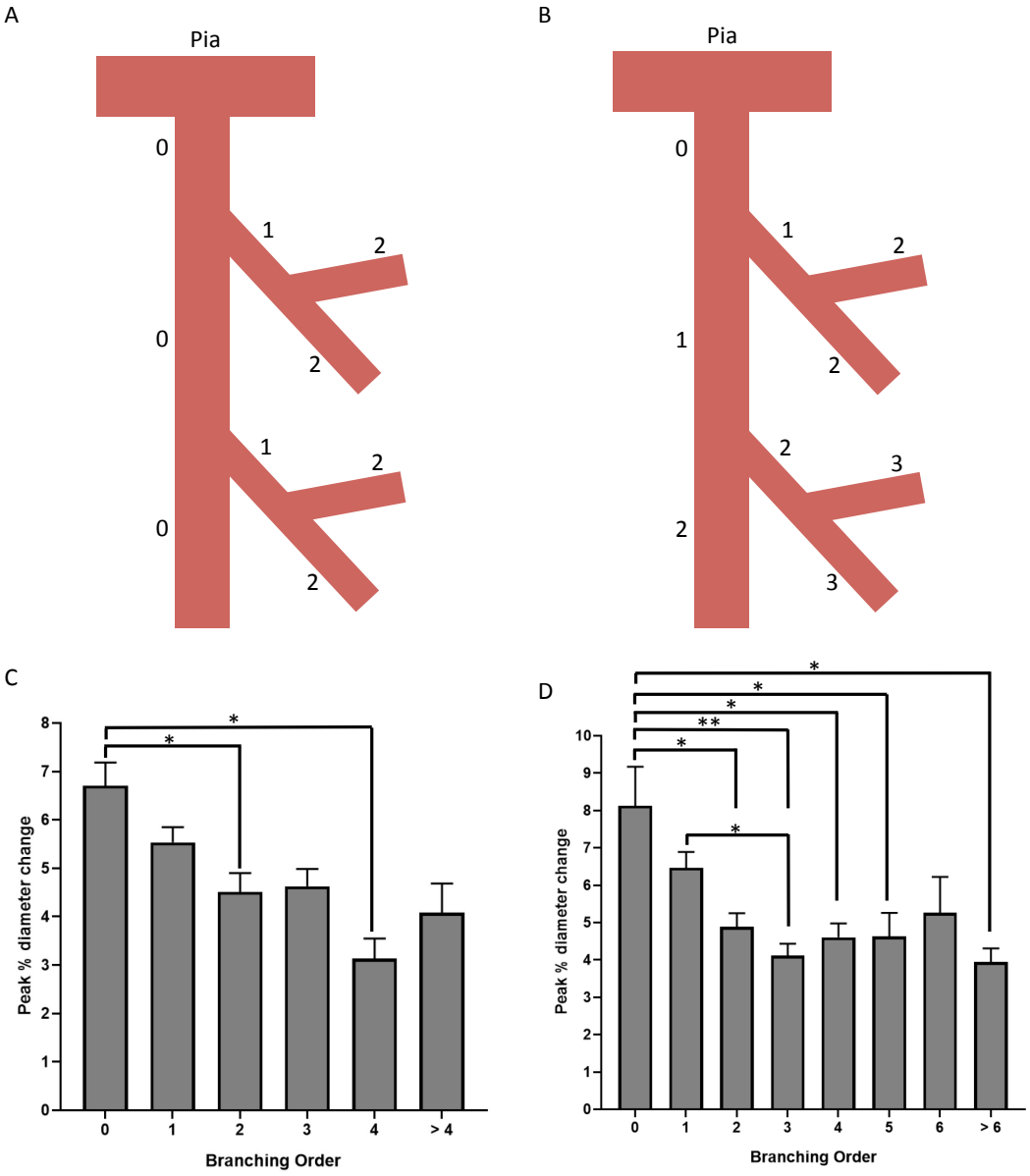

Figure 3.5. Schematics of alternative methods of classifying branching order, and diameter changes to the 100% contrast, full screen stimulus from different branching orders of the vasculature, split up by branching order using the different methods of classification (+/-1SEM).
The two spatial frequencies are collapsed. All data were taken from the 'No Locomotion' group. Two methods of determining branching order were used: ***A*** *The entirety of the penetrating arteriole is classified as branching order 0, each branch from the penetrating arteriole is considered branching order 1, and onwards from branching order 1, each branch adds 1 to the branching order,* ***B*** *Sections of the penetrating arteriole are reclassified with every branch that occurs, adding 1 with every branch (i.e. Classification occurs in the same way as described from branching order 1 onwards in* ***A****, but this is also applied to the penetrating arteriole). The classification of each branch from the penetrating arteriole therefore depends on the presence of branches further towards the pia.* ***C*** *average maximum diameter change for each branching order using the method shown in* ***A,*** *BO (branch order) 0 N = 156, BO 1 N = 129, BO 2 N = 73, BO 3 N = 45, BO 4 N = 22, BO > 4 N = 16;* ***D*** *shows the same data shown in* ***C,*** *but uses the classification system show in* ***B****, BO 0 N = 55, BO 1 N = 117, BO 2 N = 85, BO 3 N = 68, BO 4 N = 54, BO 5 N = 28, BO 6 N =17, BO > 6 N = 18.*
** p < .05*
*** p < .001*

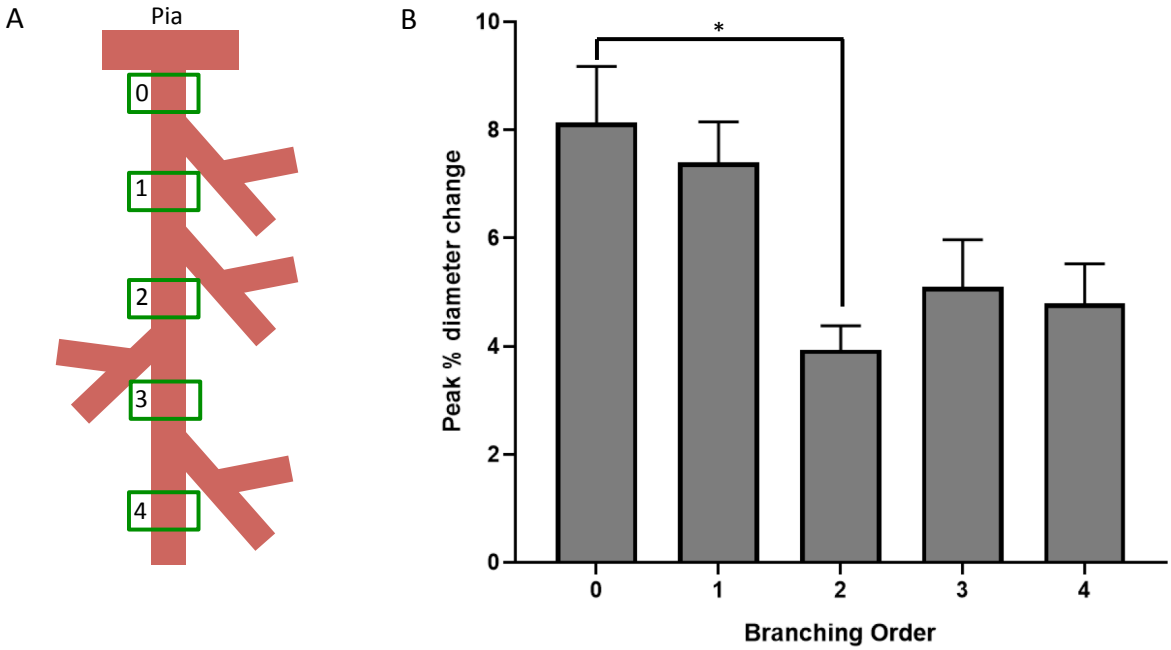

Figure 3.6. Schematic of areas of the penetrating arteriole measured from, and the peak diameter changes to the 100% contrast, full screen stimulus yielded from these areas (+/-1SEM).
*Diameter change responses to the 100% contrast presented over the full screen, collapsing over the two spatial frequencies. All data were taken from the 'No Locomotion' group. Regions of the penetrating arteriole measured from are shown in the schematic **A**. Mean responses from each of these regions are shown in **B**. BO 0 N = 55, BO 1 N = 54, BO 2 N = 25, BO 3 N = 5, BO 4 = 11.*
** p < .05*
*** p < .001*

3.3.1.2.1 Comparing classification methods across the vasculature

A one-way ANOVA was conducted to look at the effect of branching order on the degree of peak diameter change that occurred within vessels when the entirety of the penetrating arteriole was classified as branching order 0 (i.e. using the classical method). A Bonferroni post-hoc test determined between which branching orders there were differences.

There was a significant main effect of branching order ($F(5,435) = 5.073$, $p < .001$), whereby degree of dilation generally decreased as branching order increased (Figure 3.5 C). Specifically, differences were significant between branching orders 0 and 2 ($p = .007$), and 0 and 4 ($p = .006$), with no further significant differences between the branching orders.

A one-way ANOVA was then conducted to look at the same dataset, but with the branching orders reclassified so that different sections of the penetrating arteriole were allocated different branching orders using the alternative method described in Figure 3.5 B.

As with the prior method of classification, there was a significant main effect of branching order ($F(7, 433) = 5.820$, $p < .001$). A Bonferroni test revealed significant difference between branching orders 0 and 2 ($p = .001$); 0 and 3 ($p < .001$); 0 and 4 ($p = .001$); 0 and 5 ($p = .018$); 0 and >6 ($p = .011$); and 1 and 3 ($p = .011$). The significant differences between branches (here, but also using the classical method) indicates that we can yield a significant degree of separation in functionality between branches, suggesting that there is utility in using branch order. Separating out the penetrating arteriole based on its branches appears to differentiate branch order 0 from other vessels in the vasculature, suggesting that including all the responses throughout the penetrating arteriole might be diluting this response (Figure 3.5 D).

A repeated measures t test directly comparing the degree of dilation from branch order 0 using the classical vs. the alternative method was conducted to assess the impact of labelling the entirety of the penetrating arteriole as branch order 0, compared to the section

closest towards the pia, before the first branch. This difference was close to but not significant ($t(263)= 1.811$, $p = .0713$), however the trend towards greater dilation at branch order 0 using the alternative method of determining branch order, and the increased differentiation this produced from other branches (Figure 3.5 D) still warranted further research characterising different sections of the penetrating arteriole in order to understand whether its capacity for dilation changes along its length. Aside from this, there appears to be a relatively high degree of consistency between the methods of branch order classification in terms of the pattern of dilation that occurs across branch orders, and neither method appears to consistently increase the variability that occurs within a branch order.

3.3.1.2.2 Comparing different sections of the penetrating arteriole

The differences between different branching orders of the penetrating arteriole (using the alternative method, (shown in Figure 3.5 B)) was then examined in order to test the validity of classification of the entirety of the penetrating arteriole as branching order 0.

A one-way ANOVA showed that on the penetrating arteriole alone, there was a significant main effect of branching order on the magnitude of peak diameter change ($F(4,145) = 2.727$, $p = .032$). A Bonferroni test showed that the only significant difference occurred specifically between branching orders 0 and 2 ($p = .038$) (Figure 3.6), but this does suggest some degree of changing function along the length of the penetrating arteriole. Additionally, the decrease in peak dilation that occurs as branch order increases, until branch 2 at which point there is a plateau, is consistent with the previous findings that included all branches (using both the classical and alternative methods of branch order) (shown in Figure 3.5). This might suggest that changes in function occur along the length of the penetrating arteriole as it branches in a similar manner to branches away from the penetrating arteriole, and that it might therefore make sense to classify penetrating arteriole branches in the

same manner as horizontal ‘capillary’ branches (i.e. the alternative method better reflects vascular function).

3.3.1.2.3 Comparing sections of the penetrating arteriole against equivalent capillary branching orders

In order to further probe the two different methods of determining branching order, different sections of the vasculature that could be classified as branching order 1 (Figure 3.7 A) were compared in terms of the peak dilation elicited by the stimulus (Figure 3.7 B). This was then also carried out for branching order 2 (Figure 3.7 C, D). Both branching orders 1 and 2 were tested, as although the difference in dilatory capacity between these branches within the penetrating arteriole were not significantly different (Figure 3.6 B); the peak diameter change does appear to plateau at branching order 2 and above, regardless of the method used to determine branch order (Figures 3.5 and 3.6).

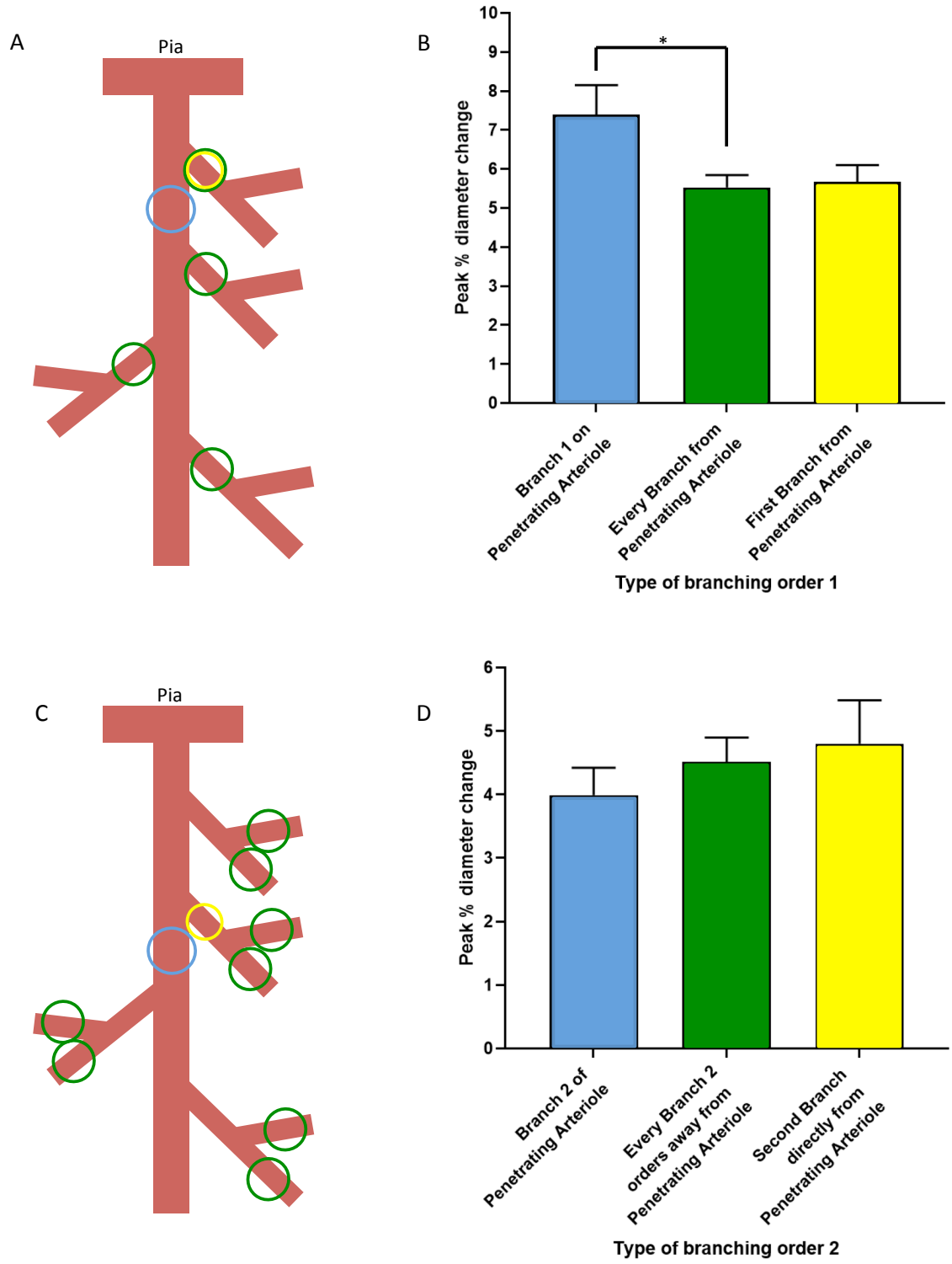

Figure 3.7. Schematic of branches of the vasculature measured from, and a comparison of the corresponding peak diameter changes to the 100% contrast, full screen stimulus yielded from these areas (+/-1SEM).

*Diameter change responses to the 100% contrast presented over the full screen, collapsing over the two spatial frequencies. All data were taken from the 'No Locomotion' group. Regions of the penetrating arteriole measured from are shown in the schematics **A** and **C**. **A** shows different branches that might be considered 'Branching order 1' using two possible methods of determining branching order (described in Figure 4.5). These branches include what could be considered branching order 1 on the penetrating arteriole itself (after the first branch away) (blue) (N = 54); the very first branch away from the penetrating arteriole (yellow) (N = 63); and every branch branching directly from the penetrating arteriole (green) (N = 129) **B** shows the peak diameter changes that occurred within these branches, **C** shows the different branches that might be considered 'Branching order 2', including branching order 2 on the penetrating arteriole itself (after 2 branches away from the penetrating arteriole further towards the pia) (blue) (N = 26); the second branch from the pia that branches directly from the penetrating arteriole (yellow) (N = 34); and all branches that branch directly from the green labelled branches in **A** (green) (N = 73).* $p < .05$, ** $p < .001$.*

A one-way ANOVA compared three types of first order vessel: 1. Branching order 1 on the penetrating arteriole itself, garnered using the alternative method (Figure 3.7 A (blue)). 2. The first branch from the penetrating arteriole, closest towards the pia, classified as branching order 1 by both of the methods described (Figure 3.7 A (yellow)); and 3. Every branch directly from the penetrating arteriole (classified as such using the classical method (Figure 3.7 A (green)).

There was a significantly different degree of dilation to visual stimulation depending on which type of branching order 1 the vessel was ($F(2, 243) = 4.291$, $p = .015$). A Bonferroni test revealed the only clearly significant difference was between Branching order 1 on the penetrating arteriole itself (1), and every branch directly from the penetrating arteriole (3) ($p = .015$). The difference between branching order 1 on the penetrating arteriole (1) and the first branch from the penetrating arteriole (2), while non-significant, was close to significance ($p = .065$) (Figure 3.7 B). This suggests some difference in function between this specific point on the penetrating arteriole, and the branches that could be labelled as the same branch point using the alternative method of branch order determination.

Branching order 2 was then tested similarly with a one-way ANOVA, which compared: 1. Branching order 2 on the penetrating arteriole itself, garnered using the alternative method (Figure 3.7 C (blue)); 2. The second branch that occurs directly from the penetrating arteriole, classified as branching order 2 by the alternative method (Figure 3.7 C (yellow)); 3. Every branch off branches classified as branching order 1 using the classical method (Figure 3.7 C (green)). There was no significant effect of which type of branching order 2 the vessel was ($F(2, 130) = 0.445$, $p = .642$) (Figure 3.7 D), suggesting similarity in degree of response between all three ‘types’ of branch order 2.

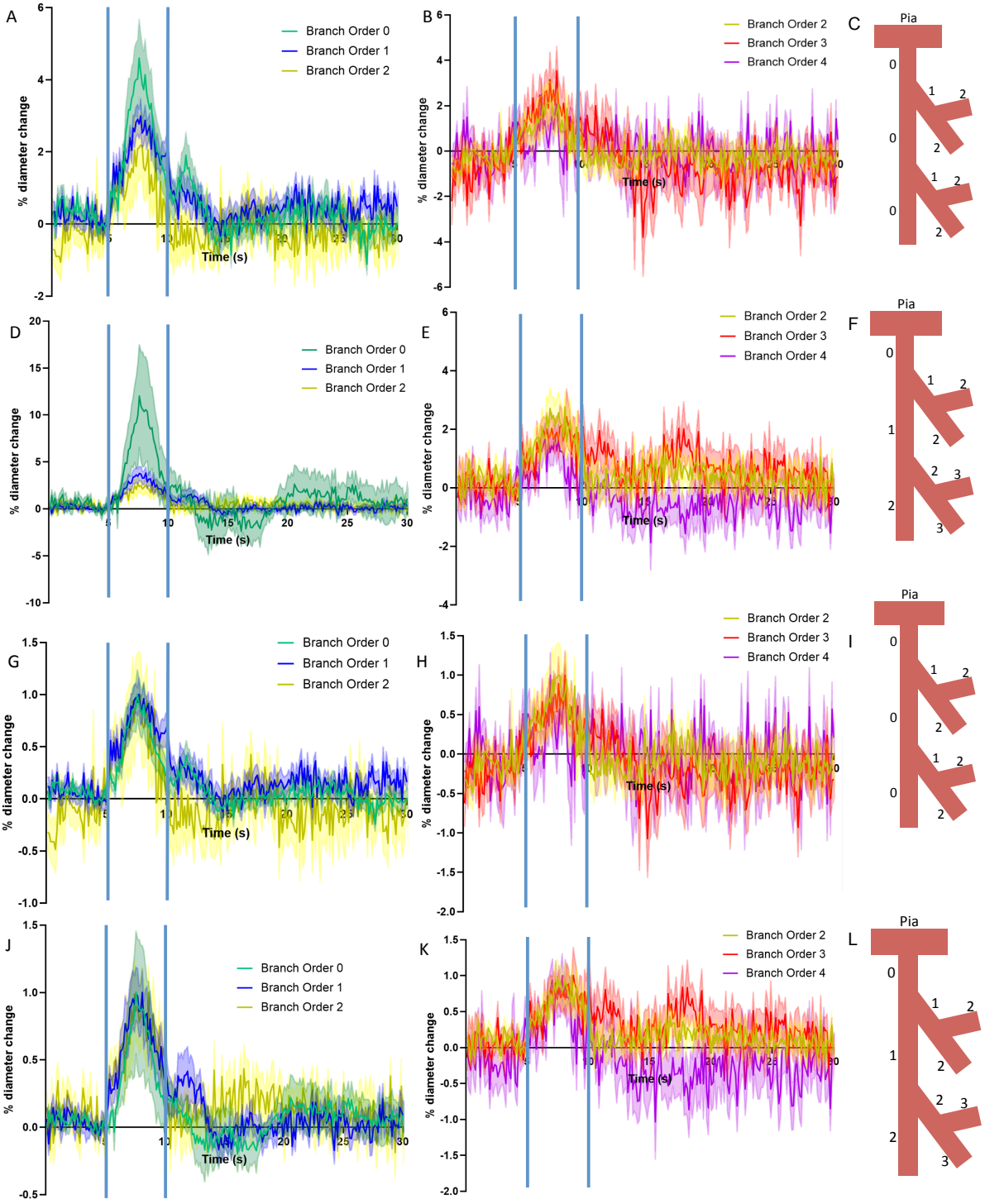

Figure 3.8. Traces of vessel responses to 100% contrast and 0.2 cpd spatial frequency split by branch order (+/-1SEM).

*Stimulus occurs between the 5 and 10-second time points (shown with blue lines). In **A** branch order is determined using the method shown in the schematic in **C** (the classical method, in which the entirety of the penetrating arteriole is classified at branch order 0). **A** shows dilation traces to the 100% contrast with a spatial frequency of 0.2 within branching orders 0, 1 and 2 (BO 0 N = 36, B1 N = 40, B2 N = 14), while **B** shows branching orders 2, 3, and 4 (B3 N = 10, B4 N = 7). In **D** branch order is determined using the method shown in the schematic in **F** (the alternative method where each branch adds 1 to the branch order classification of the penetrating arteriole). **D** shows the responses to the same stimulus within branches 0 (N = 5), 1 (N = 36) and 2 (N = 15), while **E** shows response within branches 2, 3 (N = 12), and 4 (N = 18). **G** shows the results in **A** normalised to the maximum response during the stimulus presentation in order to show the time course more clearly. **H** shows the results in **B** but also normalised to the maximum response. **I** shows the method of branching order determination used in **G** and **H**. **J** shows the max-normalised data from **D**, **K** shows the max-normalised data from **E**. **L** shows the method of branch order determination used in **J** and **K**.*

3.3.1.2.4 Time courses of different branch orders

The time courses were also compared using the traces in order to get an overview of how each vessel branching order responds temporally to the stimulus presentation. The original traces in which the peak is normalised to the baseline vessel diameter indicate no difference between branch orders 0 to 4, regardless of the method of branching order determination used (Figure 3.8 A-F). These traces were then each normalised to the maximum percent change in dilation during the stimulus period, to better allow comparison of the time courses (Figure 3.8 (G-L). There still weren't any clear differences in the onset time of diameter change, and using both methods of branching order classification, there is a large degree of overlap between the standard errors of each branching order. This suggests that neither branch order determination method is more meaningful over the other in terms of characterising the time course of dilation over the vascular tree.

3.3.1.2.5 Spontaneous Locomotion

Diameter responses to spontaneous locomotion were then looked at. 'Spontaneous locomotion' in the current experiment refers to locomotion that did not occur during stimulus trials (i.e. was not triggered by visual stimuli), but occurred only in the presence of a low level of ambient light (which might increase levels of activity from certain neuronal subtypes compared to complete darkness (Pakan et al., 2016), potentially impacting the degree of vessel dilation compared to spontaneous locomotion in complete darkness). We tested both how vessels responded to spontaneous locomotion as a whole, and also within specific branch orders.

It was found that there were clear increases in diameter during locomotion onset, and that these increases in diameter to locomotion occurred at least from branch order 0 to 2 tested here (Figure 3.9). Different branch orders tested responded similarly in terms of their peak response (Figure 3.10).

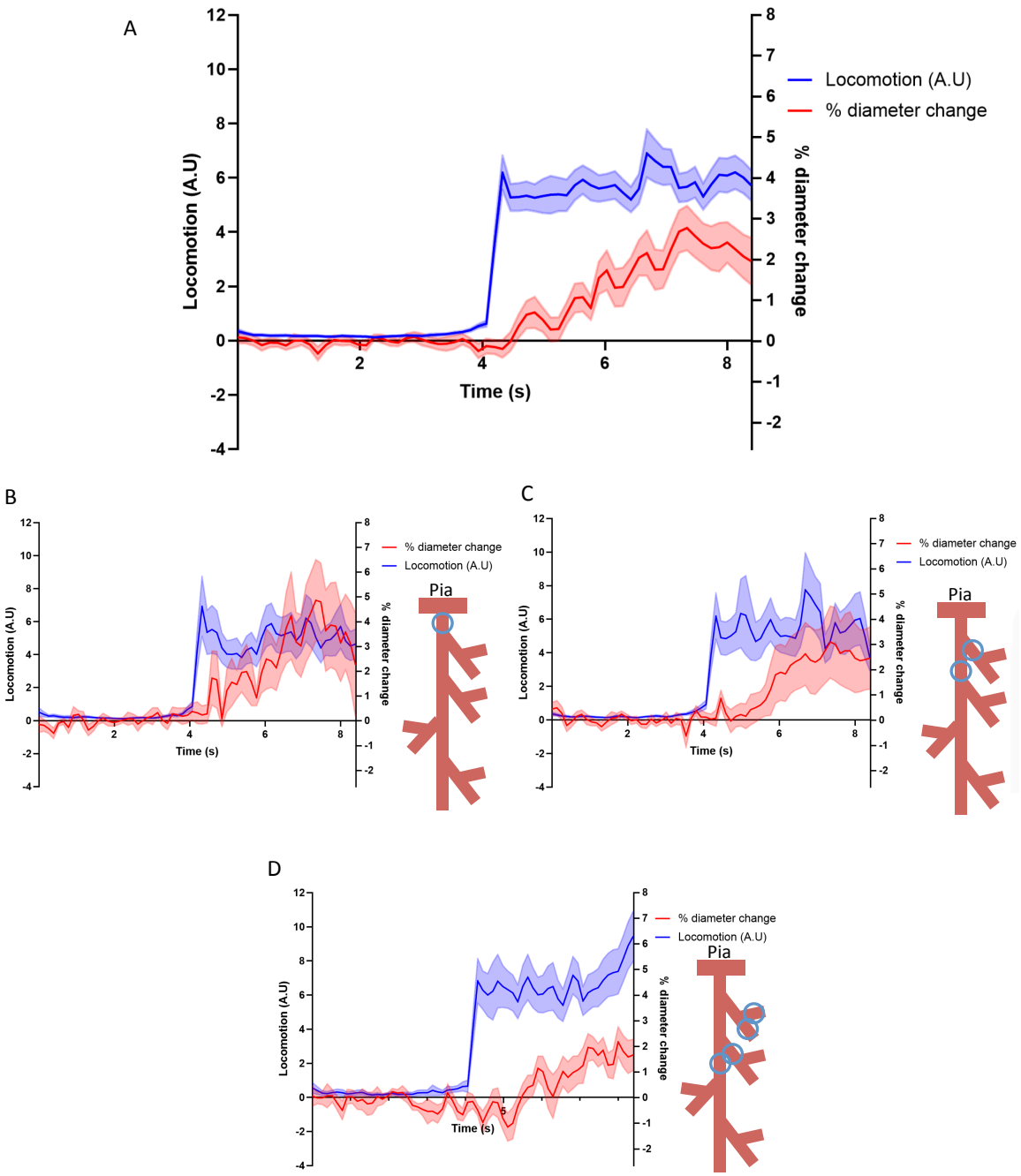

Figure 3.9. Averaged vascular diameter change (red), and spontaneous locomotion traces (blue) (arbitrary units) over the entirety of the vasculature and divided by branching order (+/- 1SEM). *Locomotion level is shown in blue, vascular diameter change is shown in red. Spontaneous locomotion onset is shown in varying branching orders using the 'alternative' method of determining branch order.* ***A*** *shows the response from all the vasculature in the dataset (N = 60);* ***B*** *shows the response of branch order 0 (N = 13).* ***C*** *shows the response from branch order 1 (N = 16); and* ***D*** *shows the response from branch order 2 (N = 13).*

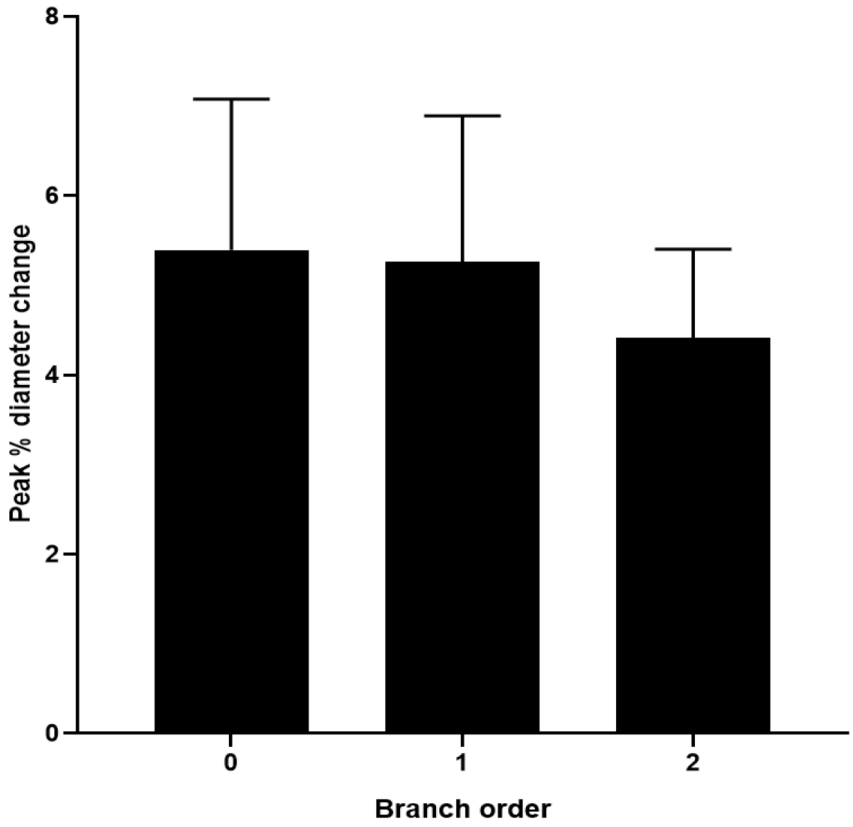

Figure 3.10. Peak vascular diameter during spontaneous locomotion onset split by branch order (+/- 1SEM).
BO 0 N = 13, BO 1 N = 16, BO 2 N = 13.

Figure 3.9 shows clear increases in vessel diameter to the onset of spontaneous locomotion. Increased vessel diameter was observed within branching orders 0, 1 and 2 (schematics indicate which branch orders within the vascular tree fall within the branch order tested). A one-way ANOVA revealed that peak dilations to locomotion onset did not differ significantly between branch orders ($F(2, 36) = .1232$, $p = .4273$), suggesting that the vessels tested between branch orders 0 and 2 dilated to similar extents to spontaneous locomotion (Figure 3.10), however the lower N available within spontaneous locomotion data compared to the stimulus dataset makes it unclear whether or not this is a deviation at all from the pattern of dilation between branch orders within the stimulus dataset. There is a reduction at branch order 2, which is consistent with that dataset, but as the difference is not significant, it is not possible to conclude whether or not these results are consistent with those found within dilation to a visual stimulus.

3.3.2 Do Other Methods of Classifying the Vasculature Reflect Function?

Having established that branch order can be used to distinguish dilatory capacity between zones of the vascular tree, it is of interest to probe other methods that might also be used to identify a given point of the vasculature, in order to assess the validity of these methods. One of these is the resting diameter of the vessel, and the other is the distance between the soma of vascular mural cells (pericytes or smooth muscle cells), termed inter soma (IS) distance. Using DsRed mice, these two methods were each applied to characterise a given point of the vasculature, in order to see how diameter and IS distance related to the degree of dilation from a vessel. It was found that neither IS distance nor diameter correlated significantly with peak diameter change, although both did trend ($p = .1033$, and $p = 0663$ respectively), suggesting that while there is some degree of variation in the degree of vascular reactivity depending on vessel diameter and IS distance, it cannot be concluded that certain vessels are contractile and others are not purely based on either of these characteristics, and it appears that the majority of dilations fell below 5% throughout the vascular network (Figure 3.11).

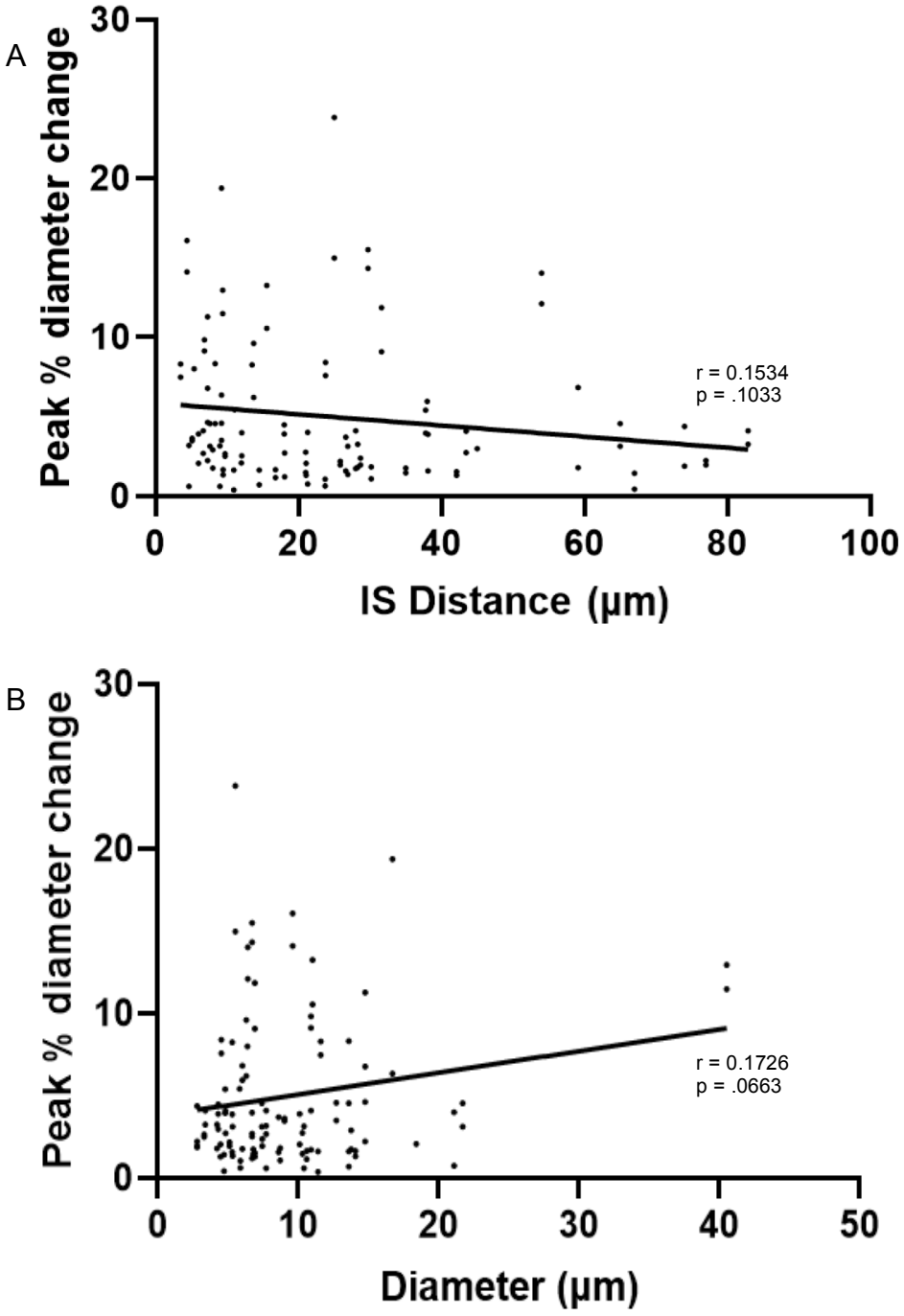

Figure 3.11. Correlation between peak diameter change and differing methods of defining the vasculature.
A *Correlation between the maximum diameter yielded to a stimulus presentation and inter soma distance;* ***B*** *Correlation between the maximum diameter yielded to a stimulus presentation and vascular resting diameter. N = 116.*

Comparing diameter change with IS distance, while there was a trend towards a negative correlation, this was not significant ($F(1,112) = 2.698$, $p = .103$). It is clear that there is a large degree of variation away from the linear regression line ($R^2 = 0.024$), demonstrating the large variety of dilations that occur throughout the vasculature at various IS distances. The Pearsons r of 0.1534 suggests that the correlation is weak (Figure 3.11 A), and so IS distance cannot be used reliably to inform what dilation to expect.

Resting diameter trended towards a positive correlation with peak diameter change, however, this was only nearing significance ($F(1,112) = 3.440$, $p = .066$). And, again there was a very large degree of variation away from the linear regression line ($R^2 = 0.030$), suggesting that resting diameter also doesn't explain a lot of the variation in the data. The Pearsons r of 0.1726 suggests that like IS distance, the correlation between diameter and vascular dilation is weak (Figure 3.11 B), and overall it seems that branch order is a better method to inform the degree of dilation that might be expected from a given point in the vascular network.

3.3.2 How do Methods of Classifying the Vasculature Correspond to Functional Markers?

Having shown that in vivo, degree of dilation decreases from branch order 0 until it plateaus at branch order 2; it is of interest to see how this aligns with vascular functional markers. In particular, αSMA is used as a marker of the contractile ability of vascular mural cells and so intuitively it might be the case that αSMA starts at branch order 0, and termination occurs at branch order 2. However, we also garner smaller dilations in higher order vessels up to branch order 6 (and perhaps beyond) of ~5% (see figure 3.5), so it might be the case that these smaller dilations also correspond with αSMA expression. Using immunohistochemistry to measure the termination point therefore provides the opportunity to reveal what degree of in vivo dilation might be αSMA-mediated.

Additionally we can employ different methods of characterising a given point in the vasculature (i.e. the termination point can be identified in terms of branch order, but also diameter and IS distance). The way in which branch order and IS distance were determined is shown in figure 3.12. By identifying the termination points using these different methods, we can also determine whether branch order is a meaningful method to use when characterising vascular markers (as it appeared to be when looking at dilation), or if a different method of identifying the zones of the vascular tree is more consistent in identifying functional marker placement.

Other functional markers might also be interesting that, like αSMA, are also classically synonymous with either arteriole or capillary function. These were also studied in order to characterise the transition from arteriole to capillary, and the manner in which this happens. If arteriole and capillary markers are spatially distinct and transition at a consistent point (using any of the methods of determining a given point of the vasculature employed), then this this would support the notion that these vessel types and their vascular mural cells should be treated in a discontinuous, categorical manner. However, if there is a large degree of variability in the start and termination points, and if the arteriole and capillary markers overlap, then this might indicate that there isn't a meaningful point where we can switch between the label of 'arteriole' and 'capillary' or 'smooth muscle cell' and 'perictye'. In order to investigate this transition in function, start and termination points of another arteriole-associated functional marker were tested (in addition to αSMA) (Elastin: involved in pulsatile flow (see chapter 1 for more information)); as well as typically capillary-associated markers (Nestin: involved in angiogenesis; GLUT-1: glucose transporter; and PDGFRβ: blood brain barrier maintenance).

It was found that some classical capillary-associated markers were expressed throughout the vasculature. PDGFRβ and GLUT1 were both expected to be found only among capillaries: that is high branch order, high IS distance, low diameter vessels. However, both were actually expressed among all branch orders, diameters and IS distances of the vessel

(Figure 3.15 and 3.16). Elastin and αSMA did both label arterioles (labelling can be seen in Figure 3.13), but did not terminate at the same points when measured using diameter, branch order or inter soma distance (Figure 3.17). The start point of capillary-associated nestin labelling (can be seen in figure 3.14) overlapped with αSMA but not elastin. This overlap occurred over all methods of identifying points of the vasculature, but did vary, with significant overlap between αSMA termination and nestin onset occurring only when vessels were identified by branch order and IS distance, but not diameter. There were differences in the patterns of expression depending on the way in which the vasculature was classified; e.g. αSMA termination was most specifically pinpointed using diameter (Figure 3.17 C), while respective onset and termination of nestin and elastin was most specifically identified using IS distance (Figure 3.17 B). This suggests that care should be taken in choosing a method of characterising the vasculature, and casts doubt on the validity of separating out the vasculature and its vascular mural cells into the discontinuous categories arteriole and capillary, and smooth muscle cells and pericytes.

The termination point of αSMA did not align with the dilatory capacity of the different branch orders of the vessel. Dilation switched from being larger (~6-7%) at branch order 1 to plateauing at ~5% for all further branch orders, while αSMA terminated at branch order 5 (in the middle between the plateau in dilation that occurs between branch orders 2 and >6). This indicates that branch order might not be a very meaningful method of determining functional marker location. Specifically for αSMA, it appears that diameter is the most reliable and consistent method of characterising the vasculature for the purpose of predicting where it might terminate, as αSMA terminates in a relatively small range between 6 and 7 μm (Figure 3.17 C); though this termination point still does not appear to reliably predict dilation based on dilations that were previously measured across vessels of different diameters (Figure 3.11 B).

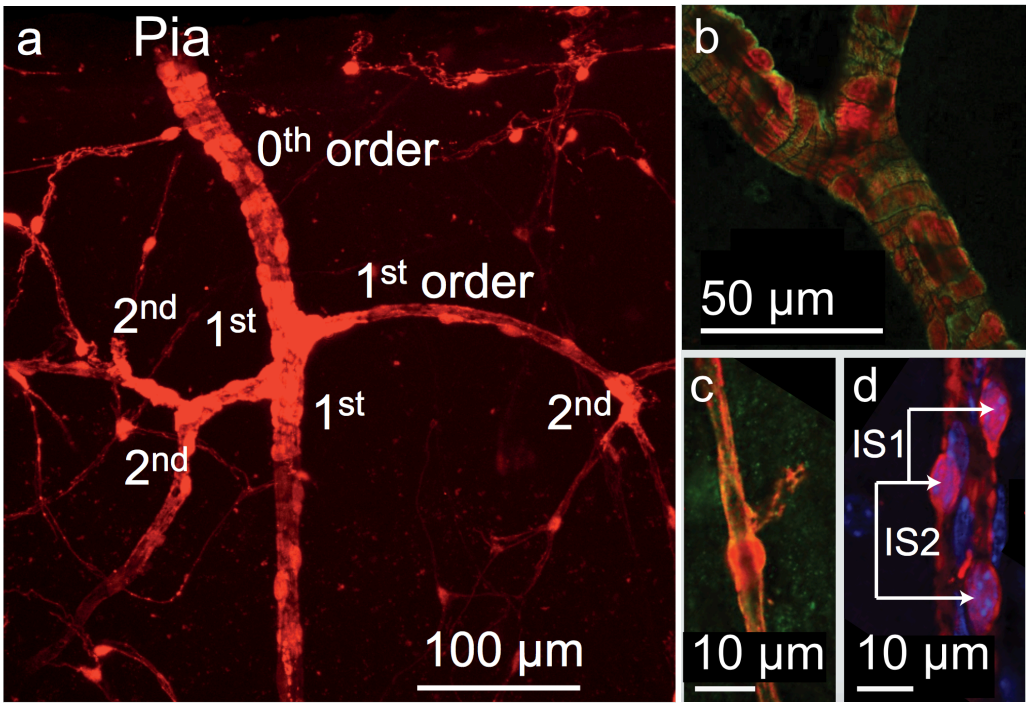

Figure 3.12. Method of determining branch order and inter soma distance.
A *NG2/DsRed-labelled vascular mural cells (red), classified by branch order. NG2/DsRed was co-labelled with functional markers such as αSMA (**B, C**: green) or the nuclear label DAPI (**D**: blue). The method used to determine inter soma distance is shown in **D**: the distance between each vascular mural cell was measured.*

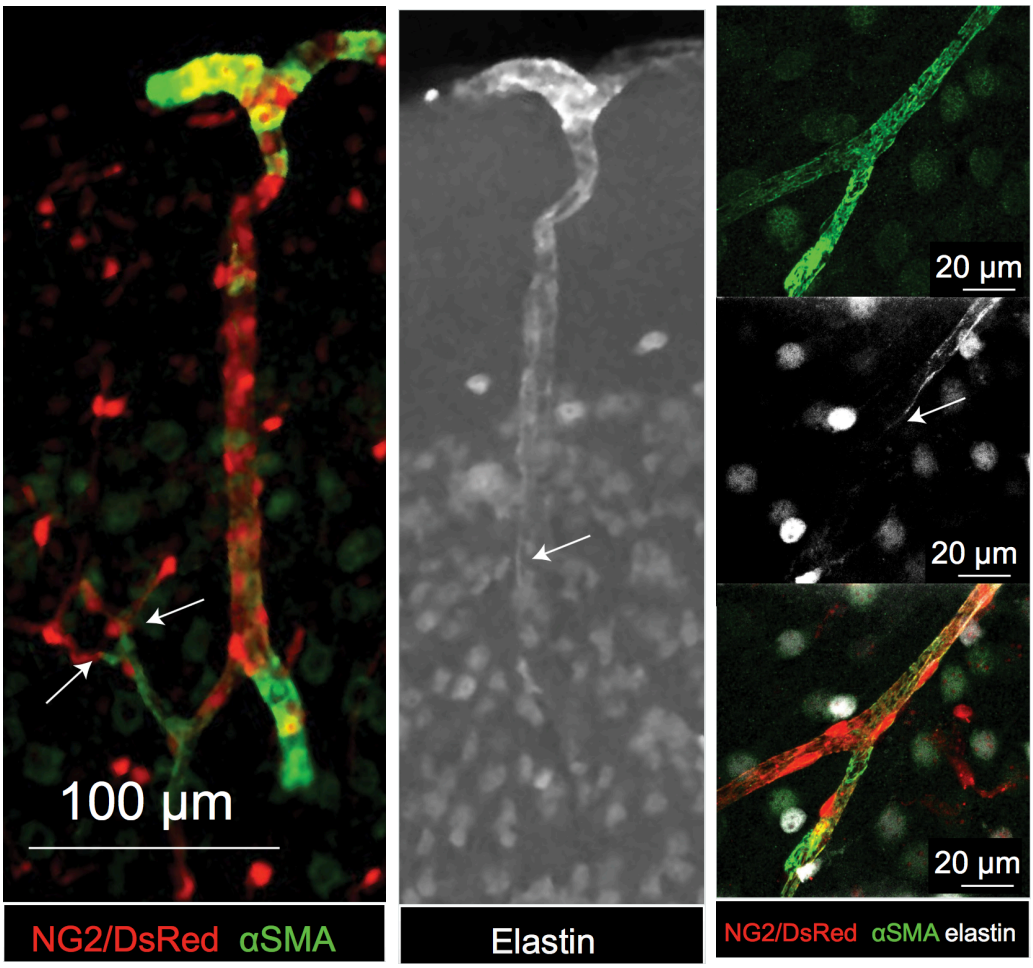

Figure 3.13. Cortical forebrain slices labelled for classical arteriole vascular markers.
NG2 DsRed (red) positive vascular mural cells co-labelled for αSMA (green) and elastin (white).

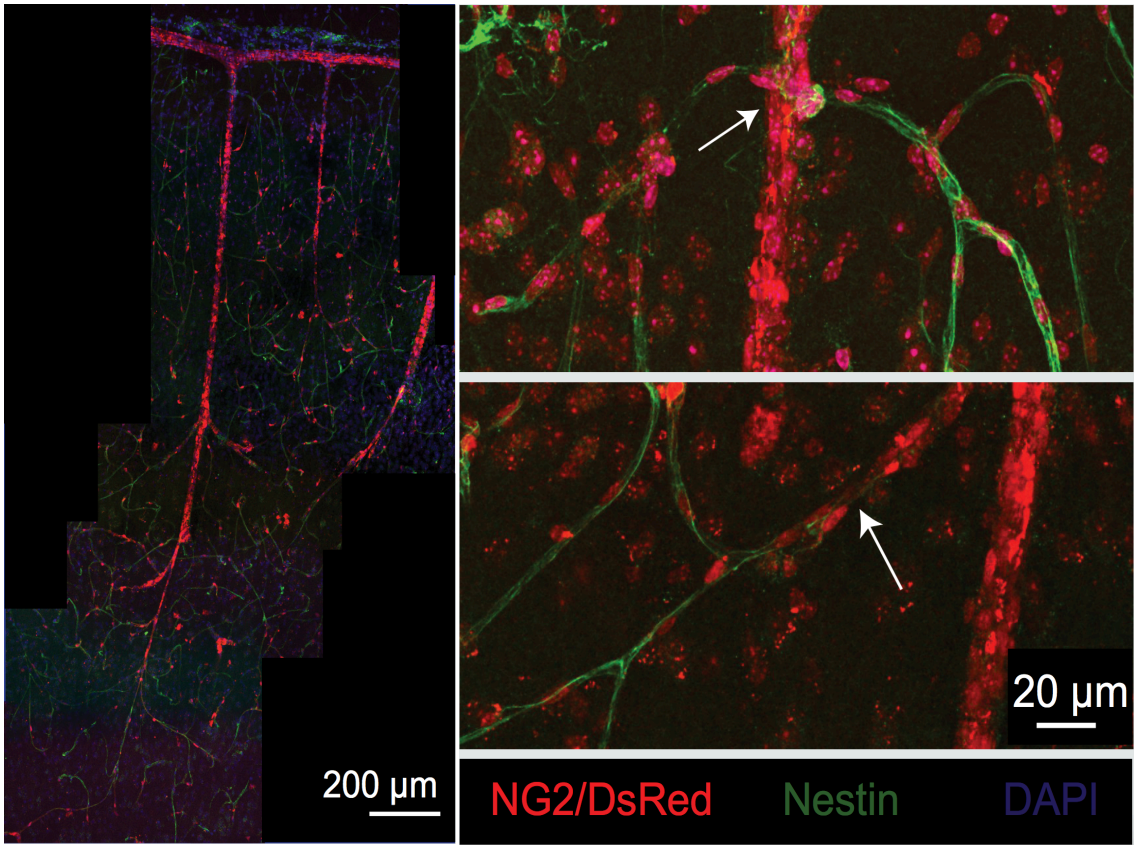

Figure 3.14 Cortical forebrain slices labelled for the capillary vascular marker Nestin (green).
Nestin (green) labelling of endothelial cells, with NG2/DsRed (red). Arrows illustrate point of expression onset.

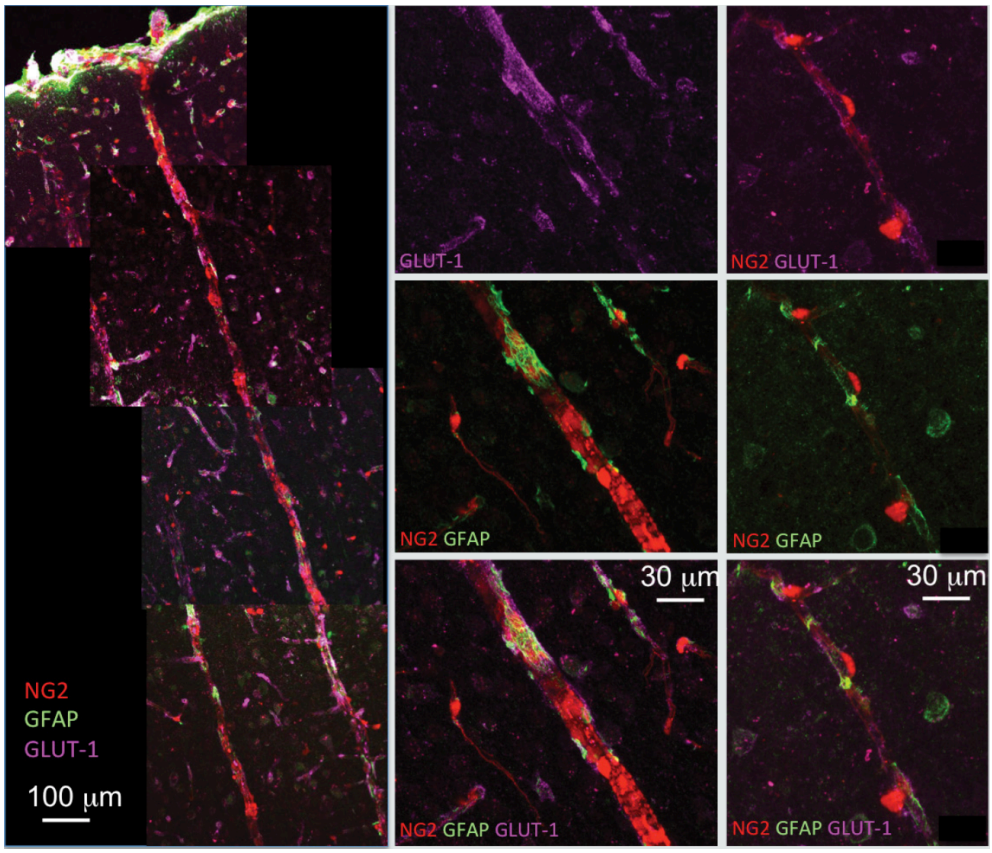

Figure 3.15 Cortical forebrain slices labelled for the capillary vascular marker GLUT 1 (purple).
GLUT 1 labelling co-labelled with NG2 (red) and GFAP (green), GLUT 1 expression was expressed throughout the vasculature on larger or smaller vessels.

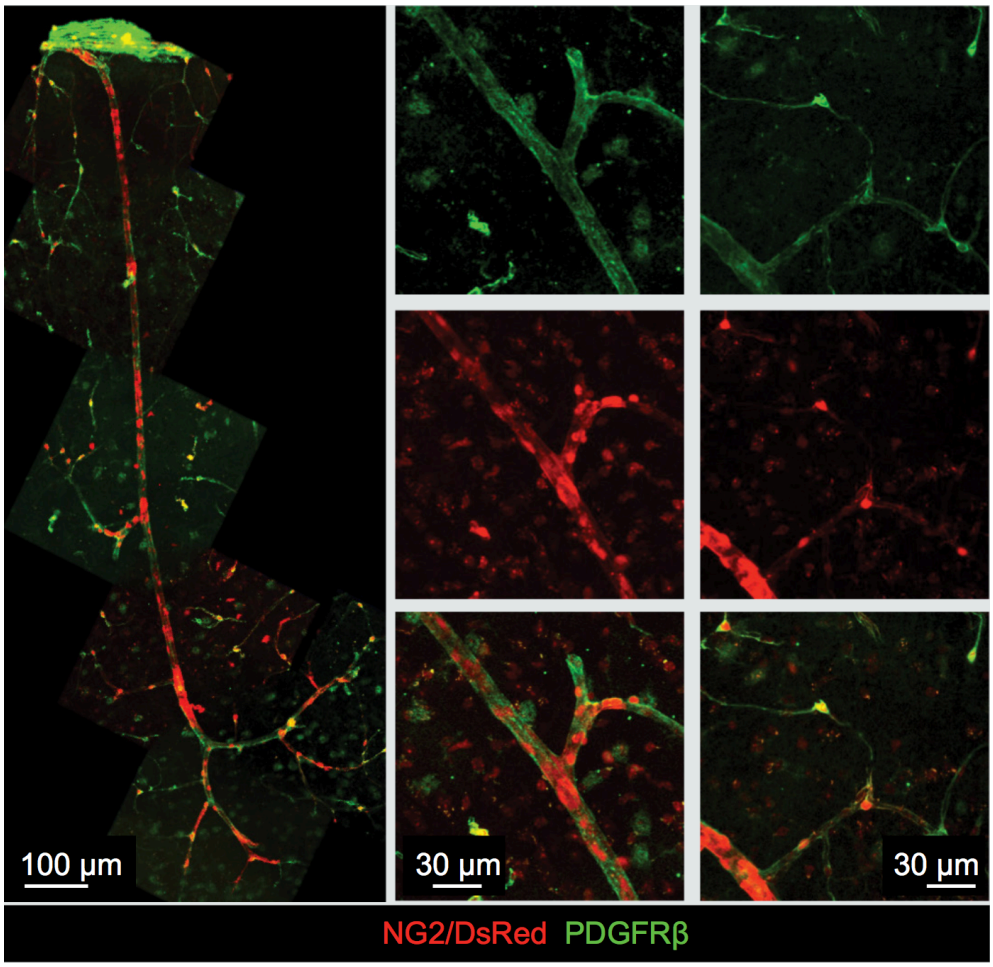

Figure 3.16. Cortical forebrain slices labelled for capillary vascular marker PDGFRβ (green). *PDGFRβ co-labelled with NG2-DsRed (red) expressed throughout the vasculature.*

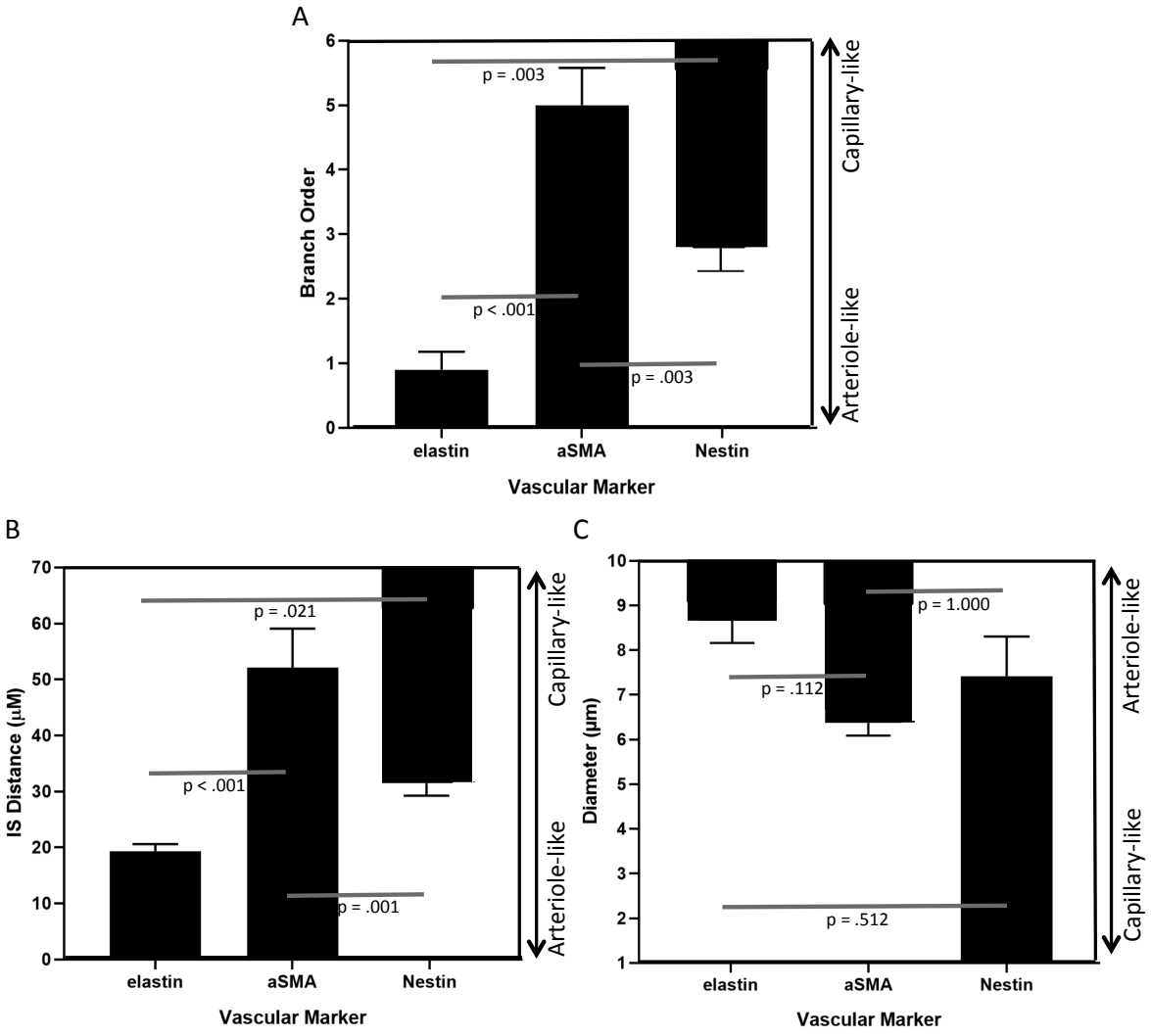

Figure 3.17. Branching order, inter soma distance of vascular mural cells and vascular diameter as methods to determine vascular marker start (nestin) and endpoints (αSMA and elastin) (+/-1SEM)
*Bars indicate in which direction expression continues, e.g. in **A,** αSMA expression occurs from branch order 0 up to ~5, while nestin expression starts from branch 3 and continues throughout the farther branches of the vasculature. **A** shows the termination points of elastin (N = 10) and αSMA (N = 6) and the start point of nestin (N = 10) by branching order. **B** shows the same start and termination points of the previous vascular markers, using IS distance as a measure. **C** shows the nestin termination and αSMA and elastin start points by diameter: as vessel diameter is approximately inversely related to inter soma distance of the vascular mural cells and branch order the direction of the onset and termination of these markers is reversed.*

3.3.2.1 How Do Classically Arteriole- and Capillary- associated Markers Transition Across the Vascular Tree?

A one-way ANOVA with a Bonferroni post hoc test was carried out on the data shown in figure 3.17 for each method of categorising the vasculature. Using branch order, there was an overall significant difference between marker the start and termination points of the markers based on which marker type was looked at ($F(2, 23) = 25.762$, $p < .001$), which might indicate that there is not one specific point of functional transition. Specifically, there was a difference between elastin offset and nestin onset, which is significant, and αSMA and nestin significantly overlap (Figure 3.17 A). Using inter soma distance, likewise, there is an overall difference based on marker on the start and termination points ($F(2, 23) = 25.393$, $p < .001$) there is a significant difference between the offset of elastin and the onset of nestin (Figure 3.17 B). Both branch order and IS distance therefore strongly support a functional change in the vasculature both at the transition between elastin and no elastin, and then, further down the vascular tree, a change from non-nestin to nestin expression; i.e. a heterogenous change from arteriole-like to capillary-like function rather than a binary change. Using diameter as a measure of morphology, the overall difference between markers in their transition points was non-significant ($F(2, 24) = 2.628$, $p = .093$); there were no significant differences between the transition points of the functional markers measured. While there is an overlap between αSMA and nestin, this was non-significant (figure 3.17 C). It is therefore ambiguous as to whether using diameter, there is any overlap between arteriole-like markers and nestin, as there is no clear division between them, and while αSMA and nestin appear to overlap, this does not occur to a significant degree, indicating that it isn't consistent. However, this does suggest that there is at least sometimes overlap between αSMA and nestin, but that it doesn't occur in as consistent a manner using diameter as a characteristic of the vessel as when using branch order or IS distance; but this still indicates a lack of a clear consistent transition point and doesn't support discontinuous categorisation of the vessel.

It appears that IS distance is the most consistent method of defining the elastin termination and nestin onset, as it shows the smallest degree of error of any of the methods employed (Figure 3.17 B); while αSMA appears to be most consistently predicted by vessel diameter (Figure 3.17 C), again due to the very small degree of error here. This tentatively suggests that perhaps different functional markers might vary in which methods of characterising the vasculature best predict their placement.

3.3.3 Are Diameter and Inter Soma Distance Related in vivo?

As both IS distance and diameter predicted the placement of different functional markers, but generally, IS distance appeared to be the most consistent predictor, these two methods of characterising the vasculature were directly correlated in order to understand how they relate to one another. This is also useful to be aware of due to the fact that in order to measure IS distance, it is necessary to use NG2 DsRed mice, which is unlikely to be possible in all experimental paradigms. It is therefore useful to know to what extent diameter can be used as an approximation of this. It has already been established that branch order is a useful way to specifically predict dilation, but that this does not align with expression of the functional markers. Therefore establishing an easily implemented method of characterising the vasculature other than branch order that might better reflect what is being expressed across the vasculature is of great utility.

Diameter and IS distance appear to reflect one another relatively well (Figure 3.18), and diameter is likely a useful measure to predict expression of functional markers where IS distance is unavailable (Figure 3.18).

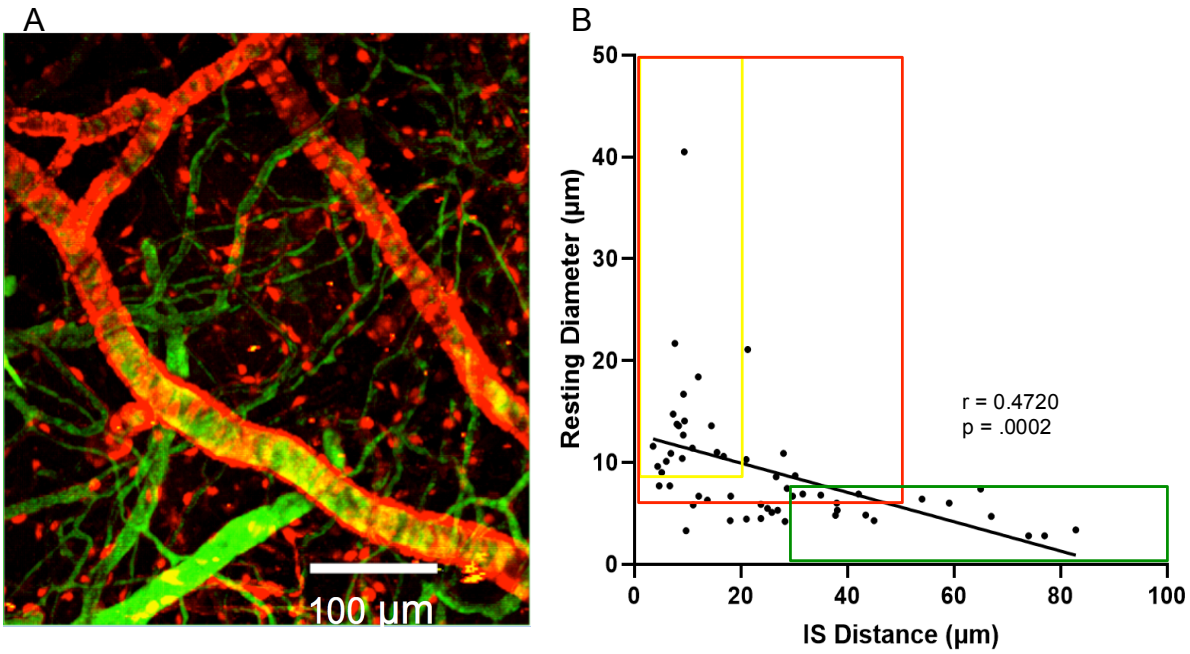

Figure 3.18 In vivo correlation between Inter Soma Distance and Vascular Diameter.
A *In vivo z-stack of V1 vasculature showing vascular lumen (green) and NG2-DsRed (red).* ***B*** *Correlation between Inter soma distance and vascular diameter overlaid with the expected corresponding vascular markers Elastin (yellow), αSMA (red) and nestin (green) that might be predicted based on immunohistochemistry findings. N = 57.*

The relationship between IS distance and diameter showed a medium correlation (r =0.4720 , $F(1, 112) = 15.77$, $p < .0002$), whereby for a given diameter decrease, IS distance increases to a greater extent. Specifically, a 5 µm decrease in vessel diameter predicts a 25 µm increase in IS distance. This helps explain why the overlap between αSMA and nestin was not significant using diameter to characterise vessels (Figure 3.17, predicted placement of functional markers can be seen in figure 3.18); as the variability in start and termination markers was general slightly greater (except for αSMA) than when using IS distance; but the relatively small changes in vessel diameter compared to IS distance render the overlaps that do occur non-significant. This relationship between IS distance and diameter demonstrates some variability ($R^2 = 0.2228$), which appears most prominent at lower IS distance vessels (Figure 3.18).

3.4 Discussion

The vasculature was probed in vivo in order to understand what methods could be used to predict dilation; most importantly whether the extensively used method of branch order could predict dilation, but also IS distance and diameter. It was then checked whether the degree of dilation corresponded with functional markers, and the transition between functional markers was more generally characterised in order to understand the transition of arteriole to capillary function.

3.4.1 Results Summary and Interpretation

It was confirmed that in vivo dilations could be captured even in smaller vessels, and the sensitivity of our experimental setup and analysis was supported by the relatively high response rate from vessels. Whether vessels were imaged as cross sections or longitudinally didn't affect the degree of diameter change captured to a significant degree, confirming that dilations seen longitudinally are unlikely to be the result of a change in focal plane, as has been suggested to us informally. All of the vessels compared here were taken from the penetrating arteriole through necessity (as this vessel typically dives vertically into the tissue, requiring it to be imaged cross sectionally), and therefore any slight difference between cross sections and longitudinal vessels could be due to the longitudinal data here being taken from a slightly different conformation of penetrating arteriole that did not dive as is typical (i.e. it would not have been diving completely vertically into the cortex as would be the norm, but might extend more in the x-y direction as it dives, such that it would be imaged as a longitudinal vessel). It is possible that these penetrating arterioles with a more atypical conformation might functionally vary compared to the majority of typical penetrating arterioles imaged here.

Looking at branch order, regardless as to whether the penetrating arteriole was classified as branch order zero across its length (classical method), or reclassified with each branch (alternative method), the degree of dilation appears to plateau at branch order 2. There

also doesn't appear to be a great deal more variability in the degree of dilation for each branch in all further branches. This suggests that dividing the penetrating arteriole by branch order does not have a large effect of the results, and also suggests that sections of the penetrating arteriole dilate comparably to the corresponding branches. There is also a clear greater degree of dilation within branch order 0 using the alternative method compared to the classical method, indicating that this top part of the penetrating arteriole, closest to the pia, possesses the greatest dilatory capacity. For this reason, the penetrating arteriole itself was investigated in order to directly assess the validity of classifying the entirety of the penetrating arteriole as branch order zero. This demonstrated that there are differences in the degree of dilation along the length of the penetrating arteriole. Again this reduces and plateaus at branching order two, suggesting that the responses from the branch orders within the penetrating arteriole using the alternative method reflects that of the responses from the branches away from the penetrating arteriole. This was somewhat confirmed by direct comparisons between equivalent branch orders on the penetrating arteriole and away from the penetrating arteriole. It appears that while within branch order one, the penetrating arteriole dilates to a greater extent than the equivalent branches; within branch order two, there are no differences between the penetrating arteriole and the equivalent horizontal branches. Altogether, it therefore appears that on the penetrating arteriole, branch orders zero and one behave equivalently to one another, and all the sections of the penetrating arteriole beyond this, as well as all of the branches measured away from the penetrating arteriole also dilate to a similar extent. Purely in terms of contractile ability, it therefore seems like the vasculature might be categorisable into these two discrete groups. This might also be reflected in responses to spontaneous locomotion, whereby dilation also decreased at branch order 2, although this difference was not significant, likely due to the lower N within the spontaneous locomotion data. This all suggests that branch order is a useful was to define zones of the vasculature in order to predict vessel dilation, as it was able to separate out two discrete sections with different degrees of dilation. The alternative method of determining branch order reflects this pattern

of dilation across the vascular tree better than the classical method, and was therefore employed in all further use of branch order.

The time course for dilations appeared to reveal no difference between branch orders, although higher branch orders did show some noise, rendering the profile of the dilation less clear. Previous research in anaesthetised animals has found branch order one to peak more quickly than the penetrating arteriole or higher order branches (Rungta et al., 2018). However, this was not replicated here, perhaps due to our use of awake animals. Previous work has shown that the time course of haemodynamic response is delayed through use of anaesthesia (Pisauro, Dhruv, Carandini, & Benucci, 2013), and so the time courses for dilation are likely to have been affected by this. Additionally, Rungta et al. (2008) measured from olfactory bulb, which has different vascular architectures, and different neural-vascular anatomies (Tiret, Chaigneau, Lecoq, & Charpak, 2009).

Having established the dilation that occurs at different branch orders, we next looked at whether this aligns with where we might expect functional markers to terminate. αSMA is known for its importance in contractile ability of vascular mural cells (Brozovich et al., 2016), and so we might expect this to align with any decrease in peak dilation (which occurred at branch order 2), or potentially, as there was no branch order tested where no dilation was observed, for αSMA expression to continue up to and beyond branch 6 (if this dilation of higher order branches were to be αSMA-mediated). However neither of these outcomes was the case, and αSMA expression actually terminated at branch order 5. Branch order might not therefore be the most informative way in which to characterise the vasculature for the purpose of understanding expression of αSMA. While both IS distance and resting diameter showed a trend to correlate with peak diameter change, neither correlation was significant, and there was a great deal of variation around the linear regression line. This demonstrates a lot of variability in function away from what might be expected based on the characteristics of the vasculature, and casts some doubt on our ability to decipher the functionality of a given vessel based on physical characteristics such

as IS distance or diameter. This might be caused by the similar responses observed in swathes of the vascular bed (I.e. using branch order, we showed that similar responses occurred throughout most of the vasculature). We know that the cell morphology changes throughout this large zone in which similar dilation occurred, as differences in vessel diameter and IS distance have been reported (Grant et al., 2019), and so it seems that this might explain the large degree of variability in the correlation between IS distance/diameter and degree of dilation. Indeed figure 3.11 demonstrates that a large proportion of dilations are <5% in magnitude, and that dilations of this magnitude do occur across a wide variety of IS distances and diameters. However, at certain IS distances and diamaters, we see a very large degree of variability in the magnitude of dilation that occurs (figure 3.11), which might suggest that this isn't the only factor involved in the weak correlations. This might be due to the changes in dilation along the penetrating arteriole: the sudden change in dilatory capacity after the second branch away from the penetrating arteriole might mean that sections of the vessel with similar diameters and IS distances demonstrate very different dilatory capacities.

The start and termination points of other functional markers were also studied in addition to αSMA in order to characterise the transition between arteriole (using classically arteriole-associated markers) and capillary (using classically capillary markers). All of these markers had their start and termination points on the vascular tree characterised in terms of branch order, IS distance, and diameter in order to examine which were the most reliable anatomical markers of vascular function. While PDGFRβ is considered the classical pericyte marker (for example, (Miners, Schulz, & Love, 2017)), here it was actually found throughout the vasculature, including in SMCs (a finding that has been replicated elsewhere (Bernier et al., 2018)). This indicates that even though this marker is widely used to look at pericytes, it does not serve to distinguish pericytes from smooth muscle cells. Furthermore, GLUT-1 is implicated in nutrient transport, a function associated with capillary function. However this was also expressed throughout the vasculature, suggesting this

function that is classically capillary-associated might occur within any vessel, including those carrying out more classically arteriole-like functions as well.

Elastin expression was limited to low branch order, high diameter, small IS distance vessels (mostly limited to the penetrating arteriole), but expression of αSMA was much more widespread. It is interesting that these two arteriole-associated markers showed different termination points, as this suggests variety in function within αSMA-expressing vessels, and therefore a lack of homogenous function within ‘arterioles’. This arteriole-associated marker spread from branch zero to five, and furthermore, expression continued to diameters of ~6 μm, which is well within the diameter at which vessels are classically classified at capillaries (Attwell et al., 2016). This in itself suggests that a broad range of vessels are likely to possess αSMA–mediate contractile ability, including those classically identified as capillaries. The overlap found between nestin and αSMA suggests that some contractile vessels also retain proliferative capacity (in addition to blood brain barrier function and nutrient transport due to the ubiquitously expressed PDGFRβ and GLUT-1). This supports the idea that there are vessels with overlapping functionality between what is classically considered arteriole-like and capillary-like, supporting the idea that categorical distinction between arterioles and capillaries is not especially meaningful, and is likely to lead to conflicting results when the line of demarcation is left to individual interpretation. Furthermore, it appeared that the method that is most consistent in identifying the onset or termination for a given marker might vary depending on the marker, although overall, IS distance most consistently reported the start and termination points of the markers as it displayed the least variability. αSMA termination was quite specifically predicted by diameter, which might suggest that if available, using both of these measures might be of value in specifying the locations of different functional markers, as the most specific method might vary. However the lack of any differences within diameter between the markers suggests that the degree of variability was quite high for the other markers (relative to the smaller scale of diameter compared to IS distance). However, as it is often difficult to ensure that the vascular mural cells can be visualised in order to use IS distance,

the relationship between IS distance and diameter was measured in order to test the utility of using diameter instead. Given what was found to be a relatively close correlation between these two methods of characterising vessels, it seems that they are related, and that there is some validity in using diameter where IS distance is not available to identify the placement of vessel functional marker expression. Interestingly, more of the variability in this correlation seems to come from lower IS distance vessels. This could potentially be due to a more consistent IS distance between the bands of smooth muscle cells that might occur over a range of larger diameter vessels. Although mural cell morphology does change along the length of the penetrating arteriole, based on images from Grant et al. (2019) it appears that there is some variability in diameter within areas showing low IS distance bands of smooth muscle cells on this vessel, and so this might especially be the case on the penetrating arteriole. This suggests that diameter of high IS distance vessels might be more accurately predicted than low IS distance vessels, which one should be aware of if trying to use diameter as a proxy measure. Work in further chapters does not have NG2-DsRed signal available in order to visualise vascular mural cells, and so a mixture of the available methods (diameter, which predicts αSMA termination relatively well; and branch order, which predicts dilation) were implemented in order to understand any differences across the vasculature.

3.4.2 Limitations of the Current Study

The current study characterised the vasoreactivity of specific vessels, the reduction in which should (but didn't using branch order) correspond with αSMA expression, allowing the behaviour of the vessel corresponding to that marker to be understood. The activity corresponding to other markers could however not be measured (such as smoothing pulsatile flow, or nutrient transport). Contractile function was therefore the only function characterised in the current study, but it would also be very informative to gain evidence of other classically arteriole- or capillary-like functions in order to better understand how these other functions transition across the vasculature, and if indeed functions such as blood-

brain barrier regulation and nutrient transport are as ubiquitous as the markers for these suggest.

Within the NG2-DsRed mice, dilations were variable, leading us to believe that even the more arteriole-like vessels vary a great deal in the extent to which they dilate. However, within these transgenic mice, the underlying neuronal activity is unknown and the context for any dilation or lack thereof is therefore also unknown. It is possible that this variability is not a factor of the maximum dilatory capacity of the vessel, but the activity occurring in the region varying for an unknown reason (for example, inattention, arousal, sleep; or just variations in the choice of region within the cortex (although this was avoided through a test stimulus)). Crossing NG2-DsRed mice with mice with a calcium indicator in order to also attain both vascular mural cell and neuronal information would help to get a fuller picture of what is underlying the vessel response.

Lastly, during immunohistochemistry, slices were fixed in PFA, which since completing this research, has been shown to affect the stability αSMA expression in the mid-capillary. This might have affected the extent of our αSMA staining in this region, and it's possible that it may have in reality continued further than we were able to record here.

3.4.3 Future Directions

There are other markers that might be of interest in characterising not just the degree of dilation, but the mechanisms by which dilation occurs throughout the vasculature. One of these is nNOS, which catalyses the production of NO, which has been shown to mediate dilation of arterioles but not capillaries (Mishra et al., 2016). It would therefore be interesting to characterise the expression of nNOS throughout the vasculature in order to further characterise where exactly this cut-off point (if there is a consistent one) might lie. Further to this, it would be informative to look at soluble guanylate cyclase (SGC): the only known receptor for nitric oxide. Although it is expected that nNOS and SGC are likely to co-localise, it will be of interest to study whether this is indeed the case, as for example, the

presence of SCG further from the pia than nNOS would indicate the ability of smaller vessels to dilate to nitric oxide.

It would also be interesting to be able to draw direct links between functional marker labelling and the function itself. For example, to thoroughly characterise the contractile response to stimulus of a given set of vessels in vivo, and then to relocate these vessels for immunolablling in order to see what markers, such as αSMA, nNOS or SGC might be expressed and underlying the responses observed.

3.4.4 Conclusions

The penetrating arteriole changes in contractile ability as it branches, and functionality becomes more akin to the branches (i.e. it becomes more 'capillary'-like as it branches). The 'alternative' method of determining branch order appeared to capture this most accurately over the traditional method, because the penetrating arteriole responses changed dramatically down its length at it branched. However, this change in function did not align with αSMA expression, suggesting that αSMA expression was not the only factor determining the degree of dilation in SMCs and pericytes.

In fact, there doesn't appear to be a sudden switch between arteriole-like to capillary-like function in terms of markers. Inter soma distance and diameter don't appear to strongly predict function in terms on contractile ability due to a large degree of variability, but do somewhat predict functional marker expression (although even within IS distance, the more reliable predictor overall, there was still variability).

Having established that there is heterogeneity of the vasculature to dilate, but that dilation is relatively consistent across the capillary bed, in chapter 6, we investigated neurovascular coupling properties of capillaries and arterioles in visual cortex.

Chapter 4

Vascular Responses to Stimulus Change in V1 of the Visual Cortex

4.1 Introduction

The BOLD signal is a measure of the ratio of oxy- to deoxyhaemoglobin in the blood obtained through fMRI (Le Bihan, 1996), and allows regions of the brain in which there is an increase in oxygenated blood to be identified. This method is widely used to infer increased neuronal activity in regions of increased cerebral blood flow (Logothetis, Pauls, Augath, Trinath, & Oeltermann, 2001), due to the mostly linear relationship between these variables, termed neurovascular coupling (although this may only be true within the cortex (Devonshire et al., 2012)). In spite of this indirect measurement of neuronal activity, fMRI is widely used both in research and diagnostics (Devonshire et al., 2012; Iadecola, 2017). It is therefore vital to optimise our understanding of the underlying neuronal activity that occurs when we obtain the BOLD response.

In order to better understand the relationship between neuronal activity and the BOLD signal, it is necessary to measure changes in blood flow in order to correlate the degree of cerebral blood flow change with activity of neurons. Changes in blood vessel diameter reflect the increase in oxygenated blood seen in the BOLD signal (Tian et al., 2010), and therefore measuring individual blood vessel diameter changes in conjunction with changes in surrounding neuronal activity allows the neuronal activity underlying BOLD to be probed.

V1 is a prime target in which to look at this relationship, on account of the wealth of previous research that has demonstrated manipulation of neuronal activity through changes in visual stimulus (see chapters 1 and 5 for further details). Previous research has made extensive use of the drifting grating to manipulate neuronal activity in V1, and has found that changes in the contrast or size of a drifting grating alters the balance of excitatory and inhibitory neuronal activity (Adesnik, 2017) (see chapter 5 for further details). If the balance of activity between different neuronal subtypes can be shifted, this presents the opportunity to probe how the vasculature behaves in response, and therefore clarify how the activity of certain neuronal subtypes is related to and drives changes in vascular diameter.

It is known that blood flow increases to the presentation of a grating stimulus. In humans, fMRI has been used to probe sensitivity to different contrasts of a radial grating in V1, and found increasing MR signal with increasing contrast (Tootell et al., 1998), showing that increases in cerebral blood flow are sensitive to somewhat subtle changes in context such as contrast. This is interesting considering the oxygenated blood provided that 'overshoots' the requirements of the region (Devor et al., 2011), which might lead one to consider cerebral blood flow response as somewhat less precise to the needs of the region than it appears to be in reality.

There is a dearth of research looking at blood vessel response and stimulus size, but it has been found that LFP increases with the presentation of a smaller stimulus, while gamma power increases with a larger stimulus (Berens, Logothetis, & Tolias, 2010; Gieselmann & Thiele, 2008). Variance in BOLD is best explained by LFP in the range of 20-60 Hz (Goense & Logothetis, 2008) and the gamma band has been characterised as laying at approximately 40Hz (Gold, 1999), but ranging between 25-100 Hz (Hughes, 2008). Either the local LFP or more specifically the gamma band therefore could reflect variance in BOLD, and should become more active to different sized stimuli, and it is therefore somewhat ambiguous what might occur with cerebral blood flow in response to stimulus size change. Elucidating this could therefore be extremely informative in understanding what pattern of neuronal activity co-occurs with the blood vessel response, especially as responses from specific neuronal subpopulations clearly diverge during stimulus size change (see chapter 5 for further discussion).

Aside from size and contrast, another variable regarding the drifting grating that can be altered is spatial frequency, the number of bars per degree of visual angle. This is a less well-researched area, especially within rodents. In the cat cortex, BOLD signal differentiated between spatial frequencies that varied between 0.8 and 0.04 cycles per degree, and it was found that these changes in BOLD correlated with changes in spiking

(specific neuronal subtypes were not identified) (Kim et al., 2004). However, another study looking at spatial frequency differentiation in humans found that the BOLD response did not separate spatial frequencies of 0.5 and 3 cycles per degree out, but using MEG (a measure of magnetic field generated by neuronal activity) did (Muthukumaraswamy & Singh, 2008). The research here is therefore somewhat sparse and mixed, but it appears that it is possible to differentiate spatial frequencies based on cerebral blood flow response, although this might vary depending on the experimental parameters employed.

Mice were also able to run freely on a cylindrical treadmill during the presentation of these changing stimuli, leading to another possible modulating factor in the form of locomotion. While locomotion is more difficult to look at in the context of an fMRI study, there has been previous research looking at the neuronal response to the interaction between a grating stimulus presentation and locomotion. This has shown that locomotion causes a strengthening in the neuronal activity, allowing neurons to encode more information about visual stimuli during locomotion to improve stimulus discriminability. This occurs through increased firing rate in the upper layers, and through decreasing noise correlations in layer 5 (Dadarlat, Michael, & Stryker, 2017). It might therefore be expected that this increased firing rate might be accompanied by an increase in local blood flow to meet its energetic requirements, with perhaps a decrease in CBF in the lower layers where there is a decrease in synchronised activity.

Aims and Justifications for Current Study

The current research aimed to use two-photon imaging of awake mice in order to investigate changes in vascular diameter, a direct correlate of BOLD signal (Tian et al., 2010). Vessels across the arteriole side of the vasculature were measured from, on account of their active role in blood flow regulation (Hall et al., 2014). A drifting grating stimulus was varied either by contrast and spatial frequency, or by stimulus size and spatial frequency in order to probe how vessels respond to subtle changes in a stimulus, and furthermore to elicit differential activation of excitatory and inhibitory neuronal

subpopulations (see chapter 5). As there is evidence of changes in BOLD in response to alterations in grating contrast, it is expected that there should be changes in vascular diameter as contrast is manipulated. There is less previous research looking into stimulus size, but based on evidence of change in LFP, it would be expected that vascular diameter might also be affected by this variable. Likewise regarding spatial frequency, given some contrary evidence across species of BOLD response to changing spatial frequency, this intimates that any change elicited might be relatively subtle and require a high level of resolution to detect diameter changes, and are likely to be dependent on the spatial frequencies selected for testing. Here, looking at stimulus contrast and size in interaction with spatial frequency, as well as in the presence or absence of locomotion allowed extensive manipulation of the vasculature and neuronal activity to maximise any potential differences.

It was hypothesised based on increased overall neuronal activity with increasing contrast (Adesnik, 2017) as well as the increased MR that has been shown with increasing contrast (Tootell et al., 1998), that blood vessel dilation would increase with increasing contrast to supply the energetic demands of neuronal activity. As overall neuronal activity decreases with increased stimulus size, but SST activity increases (Adesnik, 2017), there is greater uncertainty in how blood vessel diameter might change with stimulus size, but as all other neuronal activity in Adesnik's (2017) study decreased, it is hypothesised that blood vessel dilation is likely to correspond with this and also decrease in dilation, as this would best reflect the overall activity of the region. As locomotion increases neuronal activity in V1 (Niell & Stryker, 2010), it was also hypothesised that locomotion would lead to increased vessel dilation.

As activity from specific neuronal subtypes was measured concurrently locally to the vasculature (chapter 5), through these manipulations, it was then possible to determine the relationship between vessels of different branching orders and diameter, and neuronal activity (see chapter 6).

4.2 Methods and Materials

Details of the methods used in this chapter can be found in the main methods section (chapter 2).

4.2.1 Animal Subjects

Adult male and female C57BL mice aged between 3 – 8 months were used in these experiments. GCaMP6f mice that expressed a genetically coded calcium indicator to allow for concurrent measurement of intracellular calcium release from specific subpopulations (see chapter 5) were used. These included Thy1 GCaMP6f and SST Cre GCaMP6f crossed mice (further detailed in the main methods). Animals were housed in a 12-hour reverse light/dark cycle to encourage locomotion during imaging.

4.2.2 Animal Surgery

Animal procedures were performed in accordance with the Animals (Scientific Procedures) Act 1986. Surgical procedures are detailed in the main methods section (chapter 2). To summarise, a craniotomy was carried out over the V1 area of the visual cortex on the left hemisphere and a glass window was fitted over the area. A stainless steel head plate was fixed to the skull to stabilise the mouse during imaging.

4.2.3 Experimental Procedure

Mice were allowed to recover and were then habituated to the experimental setup (see chapter 2).

Approximately twenty minutes prior to an experiment, mice were injected with 2.5% (w/v) Texas Red Dextran (70kDa) into the tail vein. In some experiments, 2% (w/v) Texas Red Dextran (3kDa) was injected subcutaneously, both of which allowed visualisation of the vascular lumen.

The two-photon microscope was then used to measure changes in diameter (Figure 3.1), while the GCaMP6f genetically encoded calcium indicator allowed concurrent imaging of activity of neuronal subpopulations. Changes in vascular diameter were detectable even in small capillary vessels (Figure 3.3).

It was ensured the region was stimulated by a test stimulus, and that the vessel was on the arterial side of the vascular tree as previously described. Mice were then presented with a visual stimulus, comprised of a drifting grating that was varied either by size (a 20 degrees circular stimulus, or 220 degrees (full screen) stimulus, both presented at 100% contrast) or by contrast (5%, 25%, 63% or 100%, all presented as a full screen stimulus), with both stimuli being varied by spatial frequency (0.04 or 0.2 cycles per degree).

4.2.4 Vessel Processing

Details of the analysis of the vessels are detailed in section 2. In summary, ImageJ was used to remove movement artefacts. The diameter across the length the vessel was determined, and this was measured across time to determine the diameter changes of the vessel. Where cross sections were imaged, these were either processed in the same manner, or where this was not possible, the area of the vessel was measured over time, and the diameter was extracted from this.

This was then cut into trials around the stimulus presentations, and split into groups based on which size/contrast was shown, which spatial frequency was shown, and whether there was 1. No locomotion before or during the stimulus (No loco); 2. Locomotion only during the stimulus (Loco during stim); or 3. Locomotion in the pre-stimulus and stimulus period (Loco before & during stim). The maximum value from within the stimulus presentation period was then calculated and used as the measure of peak response in all farther analysis.

4.2.5 Data Analysis

All data analysis was performed using MATLAB (Mathworks) and SPSS.

4.3 Results

Here the vascular responses to changes in stimulus presentation and locomotion events are reported. The aim was to generate a range of different sized vascular responses by presenting stimuli of varying contrast (5%, 25%, 63%, 100%) or size (20 degrees, or 220 degrees (full screen)). Both stimulus types were also varied by spatial frequency (0.2 or 0.04 cycles per degree). Throughout this section, where there is a stimulus presentation, the maximum response during the stimulus period is reported from vessels as a % change, with the first 5 seconds before stimulus taken as the pre-stimulus baseline period. Where spontaneous locomotion is presented, the maximum percent value during the locomotion onset period is reported. Vessels were imaged both longitudinally and in cross section (see Figure 3.1 A and B) and cross sectional view (Figure 3.1 C and D) to allow data to be collected from a variety of vessels throughout the vascular tree and to ensure that vascular diameter changes were observed within each of these perspectives (see chapter 3 for a comparison of the dilation elicited from these different viewpoints of the vessel).

It can be observed that the vessels imaged generally responded to the drifting grating stimulus as a full screen, 100% contrast, with a slight increase in diameter visible at the offset of the stimulus, before dipping below, and then returning to baseline (Figure 4.1 (1)). This response to stimulus onset appears increased in the presence of locomotion only during the stimulus (Figure 4.1 (2)).

4.3.1 Examining Responses to Varying Contrast and Spatial Frequency

The diameter change response traces of vessels throughout the vasculature to the highest contrast (Figure 4.1) show that there was vascular response to the high-contrast grating stimulus. The peak diameter responses are plotted for each contrast and spatial frequency, showing the maximum diameter changes averaged over all vessels to each contrast (Figure 4.3). This is broken down further by the pattern of locomotion that occurred before and during the stimulus presentation, with no locomotion pre- or during the stimulus (No

loco), no locomotion in the 5-second pre-stimulus period, but locomotion during the stimulus (Loco during stim), and locomotion both within the pre-stimulus and the stimulus period (Loco before & during stim) (locomotion traces of the locomotion-positive groups are shown in figure 4.2). The vessels sampled from were sensitive to contrast, spatial frequency, and to the level of locomotion (Figure 4.3).

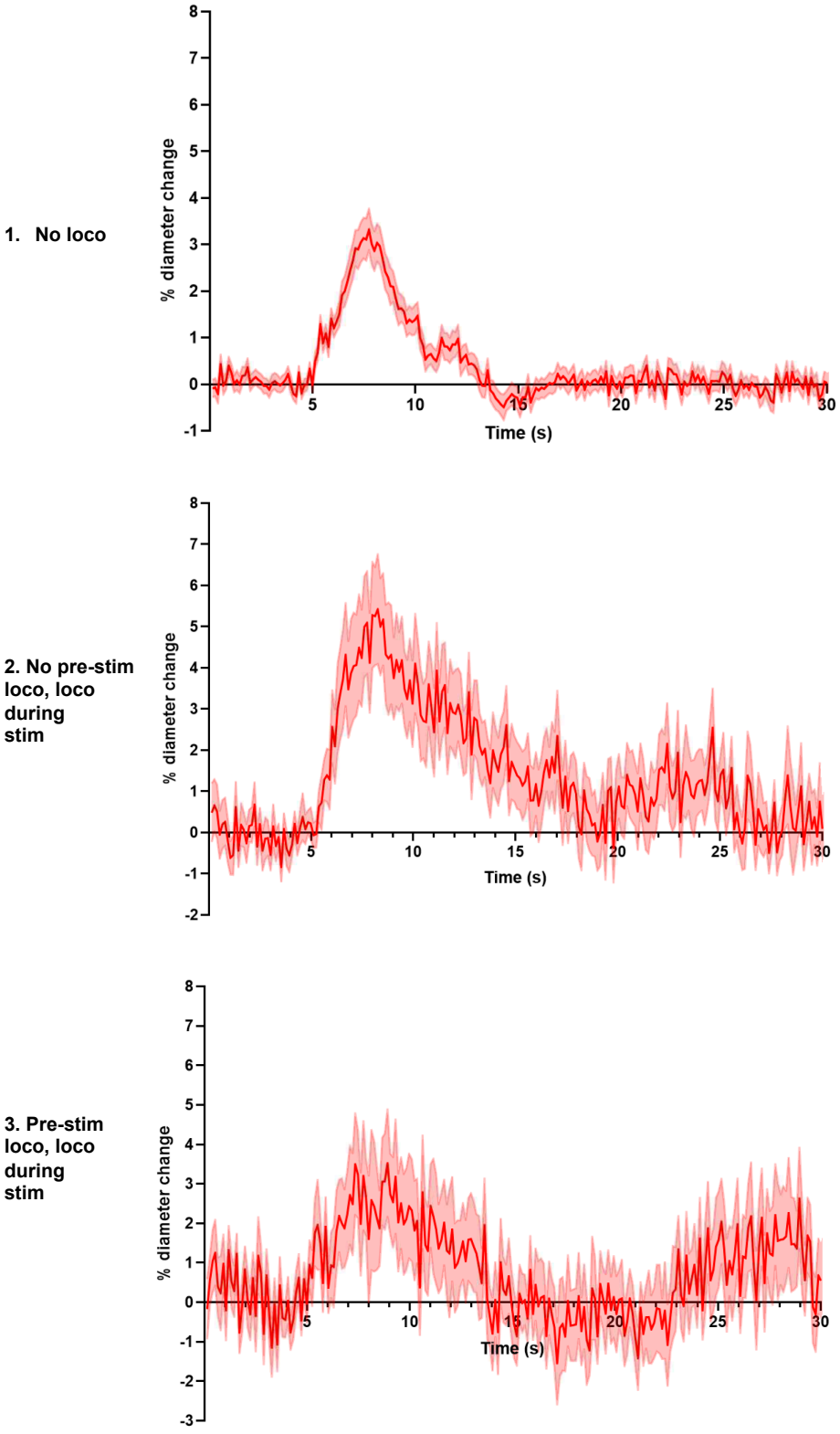

Figure 4.1. Averaged diameter change traces within varying patterns of locomotion (+/-1SEM). *All data used here were taken from the 100% contrast with a spatial frequency of 0.2 cycles per degree. The stimulus onset is at 5 seconds, and stimulus offset is at 10 seconds. During the pre- and post-stimulus period, a plain grey screen was displayed. Mice were able to freely run at will, and so data are split up into* ***1.*** *No locomotion during the pre-stimulus or stimulus period (N = 116),* ***2.*** *No locomotion in the pre-stimulus period, but locomotion during the stimulus period (N = 37), and* ***3.*** *Locomotion during the pre-stimulus and stimulus period (N = 21).*

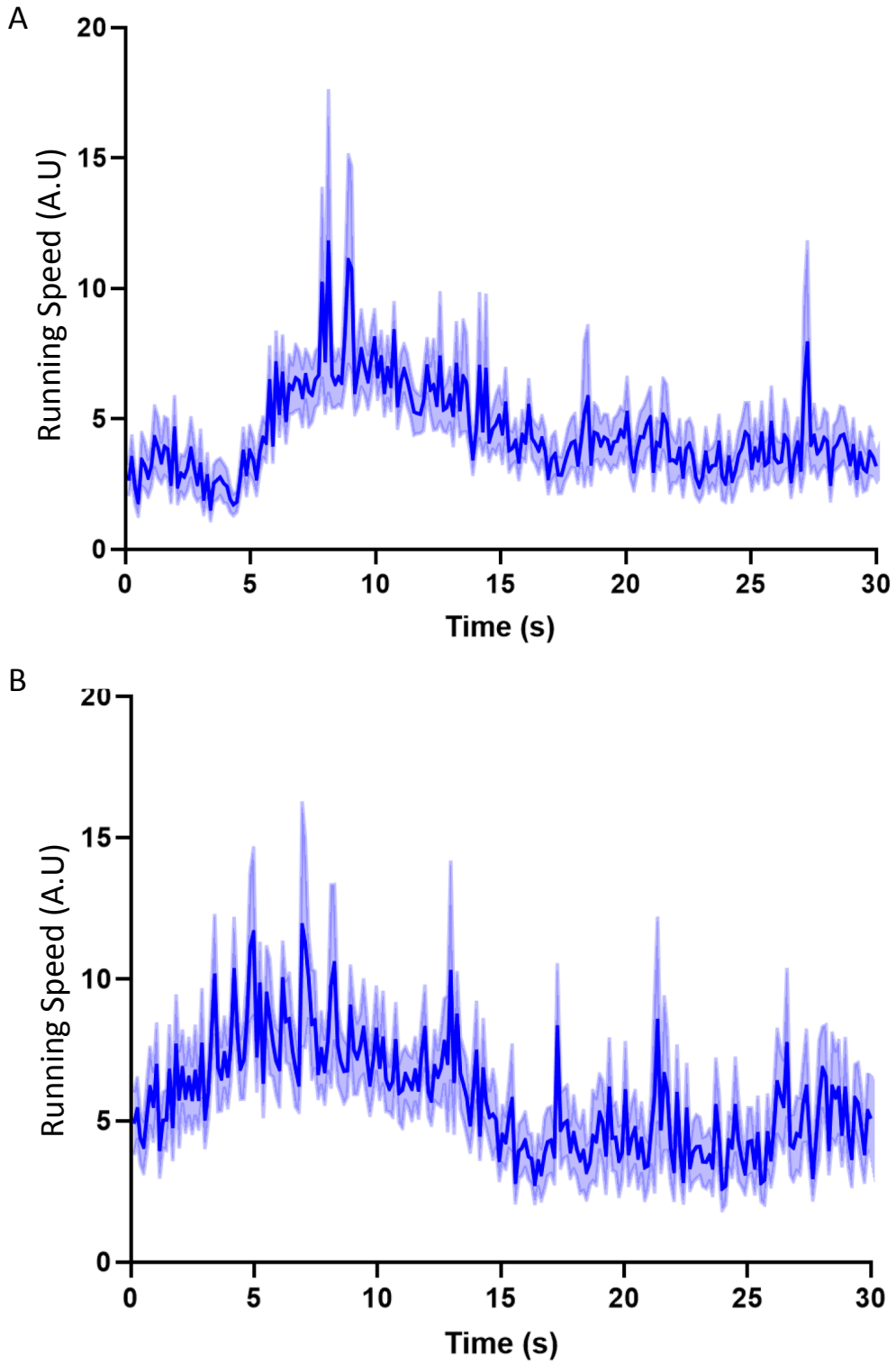

Figure 4.2. Averaged locomotion traces throughout contrast stimulus trials (arbitrary units) (+/- 1SEM). *All data used here were taken from the 100% contrast with a spatial frequency of 0.2 cycles per degree. The stimulus onset is at 5 seconds, and stimulus offset is at 10 seconds. During the pre- and post-stimulus period, a plain grey screen was displayed.* ***A*** *shows the locomotion that occurred when there was no pre-stimulus locomotion, but there was locomotion during the stimulus (N = 37).* ***B*** *shows the locomotion that occurred when there was both pre-stimulus locomotion, and locomotion during the stimulus presentation (N = 21).*

1. No loco

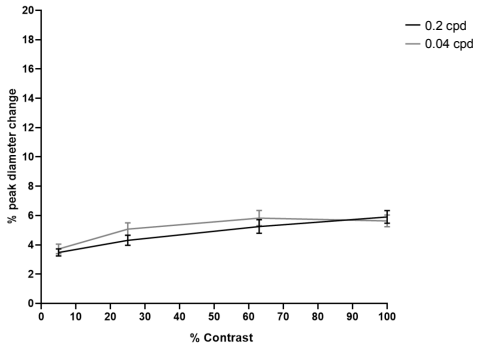

2. No pre-stim loco, loco during stim

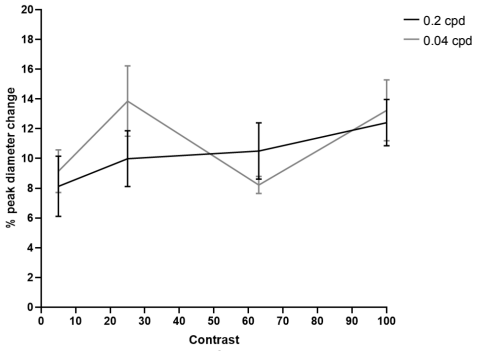

3. Pre-stim loco, loco during stim

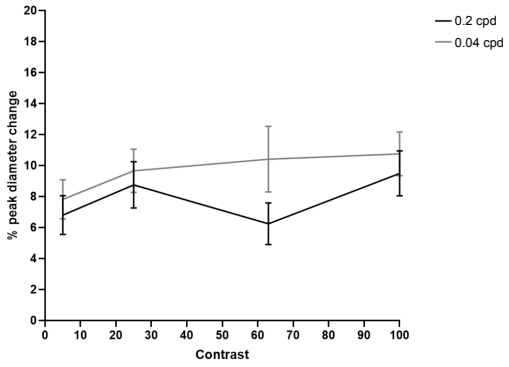

4. No loco vs. loco comparison

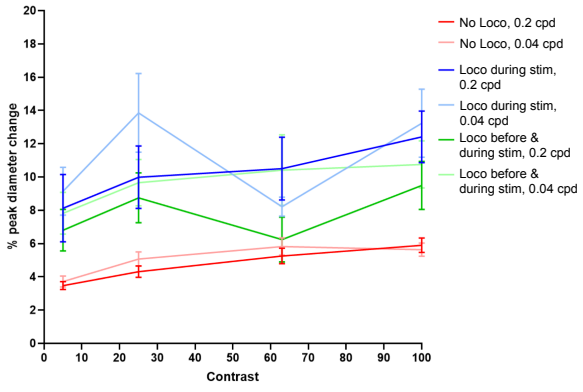

Figure 4.3. Peak blood vessel diameter change in response to varying stimulus contrast and locomotion (+/-1SEM).
*Averaged maximum blood vessel changes (%) during presentation of a drifting grating that was shown at 4 different contrasts and 2 different spatial frequencies from the entire dataset (all measured branching orders, diameters and responsiveness levels); divided into trials in which there was no locomotion in the pre-stimulus or stimulus period (**1**) (5% Contrast, 0.2 cpd N = 100; 0.04 cpd N = 96; 25% Contrast, 0.2 cpd N = 110, 0.04 cpd = 110; 63% Contrast 0.2 cpd N = 99; 0.04 cpd = 99; 100% Contrast 0.2 cpd N = 112; 0.04 cpd N = 109), trials in which there was no locomotion in the pre-stimulus period, but locomotion in the stimulus period (**2**) (5% Contrast, 0.2 cpd N = 13; 0.04 cpd N = 19; 25% Contrast, 0.2 cpd N = 23, 0.04 cpd = 19; 63% Contrast 0.2 cpd N = 26; 0.04 cpd = 25; 100% Contrast 0.2 cpd N = 37; 0.04 cpd N = 32), and trials in which there was locomotion both in the pre-stimulus and stimulus period (**3**) (5% Contrast, 0.2 cpd N = 17; 0.04 cpd N = 16; 25% Contrast, 0.2 cpd N = 19, 0.04 cpd = 15; 63% Contrast 0.2 cpd N = 9; 0.04 cpd = 19; 100% Contrast 0.2 cpd N = 19; 0.04 cpd N = 24). All locomotion groups are compared in **4**.*

4.3.1.1 Interaction between Contrast, Spatial Frequency, and Locomotion

The degree of diameter change increased significantly with increasing contrast ($F(3, 1143) = 9.08$, $p < .001$). A Bonferroni test revealed these differences to be significant specifically between 5% and 25% ($p = .007$), 5% and 60% ($p < .001$), 5% and 100% ($p < .001$), 25% and 100% ($p = .002$), and 60% and 100% ($p = .045$). It therefore appears that the vasculature is capable of differential responses to varying contrasts, and is quite sensitive to changes in contrast. There was also a significant main effect of spatial frequency ($F(1,1143) = 5.171$, $p = .023$), whereby 0.04 cycles per degree elicited a greater vascular diameter increase than 0.2), so vessels also appear to discriminate changes in the spatial frequency of the grating. There was a significant main effect of locomotion group ($F(2, 1143) = 96.175$, $p < .001$), whereby 'Loco during stim' was significantly greater than 'Loco before and during stim' ($p = .004$) and greater than 'No loco' ($p < .001$). 'Loco before and during stim' was also significantly greater than 'No Loco' ($p < .001$), so the vessels tested here showed increased diameter during locomotion, and had adequate sensitivity to distinguish between the 2 groups that were locomotion-positive, but over different periods (Figure 4.3 (4)).

4.3.2 Examining Responses to Varying Stimulus Size and Spatial Frequency

As with contrast, the stimulus size data shows the peak values to the stimuli presented, which were varied by stimulus size, spatial frequency, and the three aforementioned patterns of locomotion. Figure 4.4 demonstrates that blood vessels responded both to the stimulus size and spatial frequency of the stimuli, as well as to the level of locomotion that occurred.

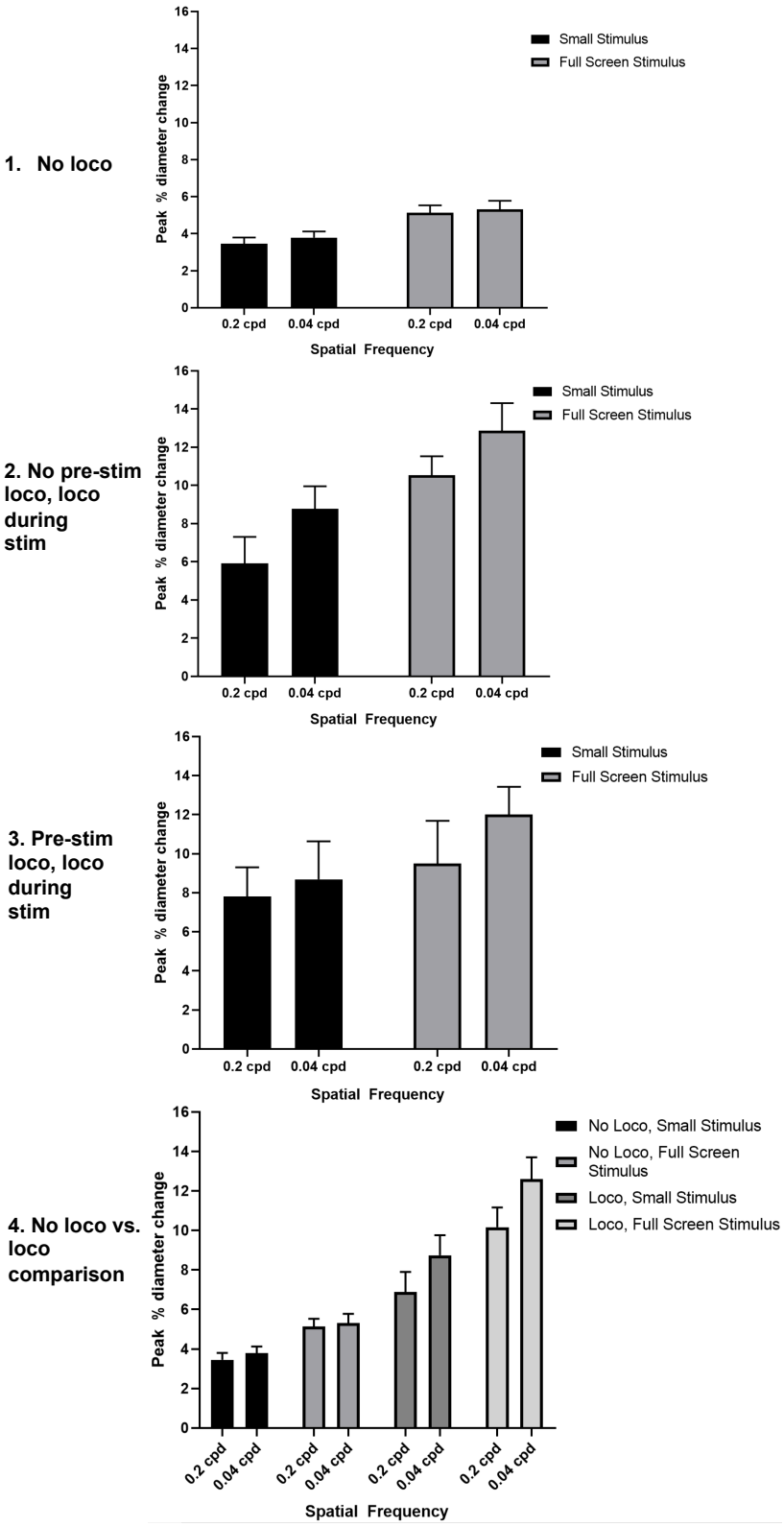

Figure 4.4 Peak blood vessel diameter change in response to varying stimulus size and locomotion (+/- 1SEM).

*Averaged maximum blood vessel changes (%) during presentation of a drifting grating that was shown at 2 different stimulus sizes and 2 different spatial frequencies from the entire dataset (all measured branching orders, diameters and responsiveness levels); divided into trials in which there was no locomotion in the pre-stimulus or stimulus period (**1**) (Small stim 0.2 cpd N = 113, 0.04 cpd N = 113; Full stim 0.2 cpd N = 113, 0.04 cpd N = 109), trials in which there was no locomotion in the pre-stimulus period, but locomotion in the stimulus period (**2**) (Small stim 0.2 cpd N = 23, 0.04 cpd N = 36; Full stim 0.2 cpd N = 39, 0.04 cpd N = 47), and trials in which there was locomotion both in the pre-stimulus and stimulus period (**3**) (Small stim 0.2 cpd N = 24, 0.04 cpd N = 19; Full stim 0.2 cpd N = 22, 0.04 cpd N = 20). Locomotion-positive groups were collapsed across in **4** due to lack of significant difference (Locomotion positive: Small stim 0.2 cpd N = 47, 0.04 cpd N = 55; Full stim 0.2 cpd N = 61, 0.04 cpd N = 67)).*

4.3.2.1 Effect of Stimulus Size, Spatial Frequency and Locomotion on Vascular Diameter

Stimulus size was then investigated as an alternative method of stimulus manipulation. A two-way ANOVA revealed a significant main effect of stimulus size ($F(1, 666) = 25.447$, $p < .001$), whereby surprisingly, the larger, full screen stimulus elicited a greater vascular diameter increase than the smaller (20 degree) stimulus (Figure 4.4 (1, 2, 3, 4)). There was also a significant main effect of spatial frequency ($F(1, 666) = 7.334$, $p = .007$), in which 0.04 cpd elicited a greater response that 0.2 cpd. This difference between spatial frequencies appears much more prominent in the presence of locomotion, but the interaction is non-significant (Figure 4.4 (1, 2, 3, 4)). This was investigated further in figure 4.5. There was also a significant main effect of locomotion group ($F(2, 666) = 58.319$, $p < .001$), in which 'Loco during stim' was significantly greater than 'No loco' ($p < .001$); and 'Loco before and during stim' was also greater than 'No loco' ($p < .001$); but unlike within the contrast data, there was no significant difference between the two groups in which locomotion occurred at some point during the stimulus or pre-stimulus period ($p = 1.000$), for this reason these two locomotion-positive groups are collapsed across to compare the effect of the presence against absence of locomotion in figure 4.4 (4).

There was also a significant interaction between stimulus size and locomotion group ($F(2, 666) = 3.023$, $p = .049$), as the magnitude of the discrepancy in diameter change between the stimulus sizes appears to be heightened during locomotion compared to no locomotion.

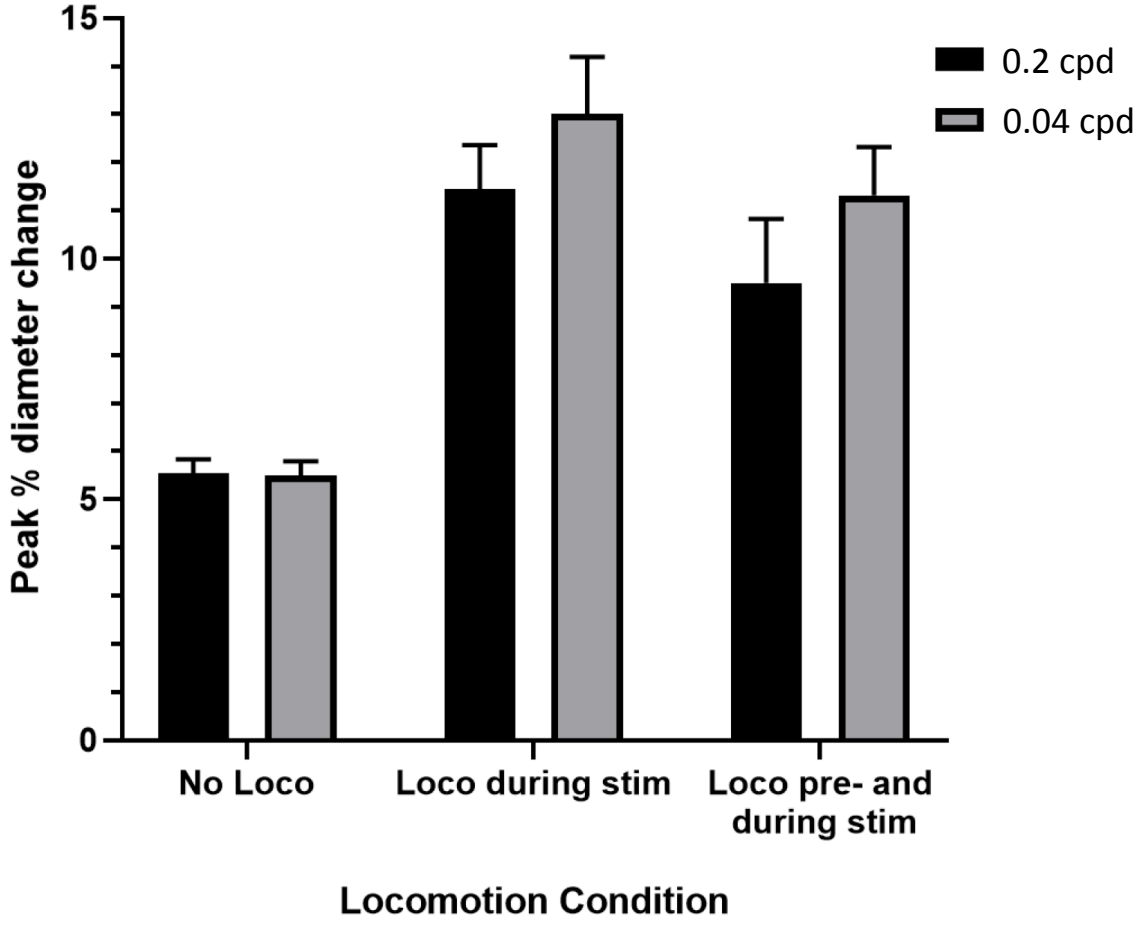

Figure 4.5. Mean peak responses to 100% contrast, comparing spatial frequency across locomotion conditions (+/- 1SEM).

Mean maximum responses to the 100% contrast shown over a full screen, collapsing over the surrounding stimuli (i.e. If the stimulus was shown in the context of different contrast stimuli or different size stimuli). Here, this dataset is split up by spatial frequency (0.04 or 0.2 cycles per degree) and locomotion group (No locomotion, locomotion only during the stimulus, or locomotion during the pre-stimulus and stimulus period). No loco, 0.2 cpd N = 224, 0.04 cpd N = 217; Loco during stim 0.2 cpd N = 76, 0.04 cpd N = 79; Loco pre & during stim 0.2 cpd N = 76; 0.04 cpd N = 79).

4.3.3 Locomotion and Spatial Frequency

Due to what appears to be a non-significant interaction between locomotion and spatial frequency in figure 4.5, the 100% contrast, full screen stimulus was taken from both the dataset in which contrast was manipulated, and the dataset in which stimulus size was manipulated (as the full screen stimulus shown where size was manipulated was the same as the 100% contrast stimulus shown where contrast was manipulated) and collapsed across to allow an increase in N to probe a potential interaction between the locomotion group and the spatial frequency of the grating. The locomotion-positive groups elicited significantly greater peak diameter change than the no locomotion group ($F(2, 675) = 73.637$, $p < .001$), with no significant difference between the locomotion-positive groups themselves ($p = .106$). There was greater peak dilation elicited from a spatial frequency of 0.2 cycles per; however this was non-significant ($F(1, 675) = 3.399$, $p = .066$). However even with the increased N of the combined datasets, there was not a significant interaction between locomotion and spatial frequency ($F(2, 675) = 1.413$, $p = .244$), indicating that locomotion does not consistently elicit different responses to differing spatial frequencies consistently.

4.4 Discussion

Two-photon imaging was employed to probe how the V1 vasculature responds to changes in a visual stimulus and locomotion.

4.4.1 Results Summary and Interpretation

4.4.1.1 Responses to Contrast Changes

Vessels increased their diameter significantly with increasing contrast, and it should therefore be expected that at least some of the neuronal subtypes implicated in NVC also show a pattern of increasing activity with increasing contrast. Thus our chosen stimulus set is appropriate to investigate NVC between different neuronal populations and individual vessels in visual cortex. These results successfully replicate findings from fMRI studies of increasing BOLD response in V1 in response to increasing contrast, but on the level of individual vessels within a rodent model and are congruent with previous neuronal studies that show increasing neuronal activity with increasing contrast (Adesnik, 2017), demonstrating the expected NVC response.

This dataset also showed that the vasculature was sensitive to which spatial frequency was shown, however a lack of interaction with contrast suggests that the vessels respond to these two features independently. This is interesting due to the somewhat mixed results within the few studies that have looked at blood flow changes in response to changes in spatial frequency. The BOLD signal of cats was able to differentiate gratings with spatial frequencies of 0.8 and 0.04 cycles per degree (Kim et al., 2004); while BOLD signal in humans was unable to differentiate between 0.5 and 3 cycles per degree (Muthukumaraswamy & Singh, 2008). The differentiation here therefore could be due to the somewhat similar spatial frequencies used by Kim et al. (2004); however, as neuronal activity was able to differentiate the spatial frequencies used by Muthukumarawamy & Singh (2008) where BOLD could not, this suggests that sensitivity of the experimental paradigm is important, and so it could be that using individual blood vessels with the pixel resolution employed, we are able to differentiate these subtle differences.

The vasculature within the dataset also differentiated between the three different patterns of locomotion. Both of the groups in which locomotion occurred during the stimulus presentation showed significantly greater dilations to the stimulus than did the group in which no locomotion occurred. There was also greater dilation where locomotion only occurred during the stimulus presentation, compared to when it occurred before and during the stimulus. As all of the trials were normalised to the pre-stimulus baseline period, if the diameter is increased during this baseline period to locomotion, then this will lessen the degree of normalised dilation (compared to if there was no dilation during the pre-stimulus period). It can therefore be concluded both that locomotion during the stimulus increases the degree of blood vessel dilation (in accordance with the increased neuronal activity that might be expected (Dadarlat et al., 2017)), and that locomotion before the stimulus increases blood vessel dilation during this period adequately to differentiate the stimulus peak from the other locomotion group.

4.4.1.2 Responses to Stimulus Size Changes

There was significantly greater dilation to the full screen stimulus size compared to the smaller stimulus. As gamma band activity increases with a larger stimulus, this suggests that this activity might be reflected in the blood vessel response (Berens et al., 2010; Gieselmann & Thiele, 2008). However, there was difficulty placing the small stimulus, which might have led to the receptive field of the cells tested not being stimulated, perhaps causing an unexpected pattern of neuronal activity and therefore blood vessel response between the smaller and larger stimuli. This is examined further in section 5, in which activity of neuronal subtypes is measured to the different sized stimuli; however based on the current finding, it would be expected that neuronal subtypes involved in NVC would increase their activity with increasing stimulus size.

Similarly to the contrast data, the 0.04 cycles per degree spatial frequency elicited greater blood vessel dilation than did 0.2 cycles per degree. The lack of interaction with stimulus

size suggests that again, this difference is independent from other contextual factors of the stimulus shown. Furthermore, there was also greater dilation in response to the presence of locomotion during stimulus presentation than when there was no locomotion, although here, the two locomotion-positive groups were not differentiated by the blood vessels. Therefore within this dataset, any pre-stimulus increase in diameter caused by locomotion was not large or consistent enough to differentiate the normalised peak to stimulus from the condition in which there was no pre-stimulus locomotion. Potentially within the stimulus size dataset, there was too much variability to pick apart this effect. In the vast majority of trials, mice exhibited no locomotion in the pre-stimulus and/or stimulus period, which reduces the power we have when looking at effects of locomotion. There was however an interaction between locomotion and stimulus size, so that there was a greater discrepancy between the degrees of dilation between stimulus sizes in the presence of locomotion. Locomotion is known to increase selectivity for certain features within cells (Dadarlat et al., 2017), so it seems likely here that this interaction is caused by an increase in selectivity for the larger stimulus size when there is locomotion, and furthermore that the underlying neuronal activity of some populations is increasing discrimination between the different stimuli.

4.4.1.3 Locomotion and Spatial Frequency

There was a non-significant trend for different degrees of discrimination between spatial frequencies depending on whether the mouse was running during the stimulus or not. Therefore the data from 100% contrast and the full screen size stimulus (which are the same stimulus) were collapsed across. This was completed in order to increase the sample size and therefore establish whether there might be a meaningful interaction whereby during locomotion, the vasculature differentiates to a greater extent between the different spatial frequencies. However, this interaction was non-significant. Although it is conceivable that spatial frequency is another feature that cells might become more selective for with locomotion, this was not supported by the current data.

4.4.2 Limitations of the Current Study

In the current study, locomotion was investigated in terms of the pattern in which it occurred in regards to the stimulus. While this is very valuable in terms of understanding what happens when locomotion occurs at certain time points in relation to the stimulus, there is more complexity to be explored in addition to this. Our current method of locomotion categorisation does not account for locomotion speed, and differences that might occur in response to running, that might vary from walking or even 'flickering' behaviour (in which the mouse moves for short periods, but the movement does not develop into a walk or a run).

It would also be of benefit to have been able to acquire more trials in which locomotion occurred. There was some difficulty in eliciting volitional locomotion, despite provisions of a wheel in the home cage and a reverse light/dark cycle to encourage locomotion during the experimental period. Locomotion was volitional and not trained; however, mice chose not to run for the majority of trials, which led to a lower N within the locomotion data, and therefore an increase in variability of these data.

As previously discussed (see chapters 2 and 3), there is also the issue that vessel diameter could potentially appear changed due to changes in the plane of focus on a longitudinally imaged vessel, especially during locomotion. However, this issue has been avoided through the use of cross sectional images in the dataset, which respond comparably to longitudinal vessels (and trended towards responding to a greater extent that longitudinal vessels, supporting a lack of artefactual dilations of longitudinal vessels). In addition if this were playing a role in the diameter changes, then there is no reason this would yield consistent dilations (especially as it was ensured all imaging began with the focal point on the widest point of the vessel), and would if anything, add noise to the dilations that were yielded to locomotion here.

It appears that there is a good degree of sensitivity to changes in vascular diameter within small vessels (Figure 3.3), but it might be useful to use linescans in order to measure

diameter for comparison (in order to see if it's possible any smaller dilations might not be visualised), as well as to garner more information on changes in speed of blood flow, which would help to provide further information about changes in cerebral blood flow in response to the stimuli.

4.4.3 Future Directions

The next logical step is to examine neuronal activity of various subtypes and look at the degree of NVC that occurs. This is examined in chapters 5 and 6.

Further to this, as spatial frequency is a less studied manipulation of the drifting grating, it might be interesting to probe this further, to look into a greater range of spatial frequencies, find the optimal spatial frequency to maximally dilate vessels, and look at whether this corresponds with the optimal spatial frequencies that have been found to stimulate neuronal activity in V1 maximally. Furthermore it could be seen if this aligns with specific neuronal subtypes better than others. This could prove especially interesting, due to findings of sensitivity to spatial frequency within the vasculature that are not replicated in chapter 5 when focussing on neuronal activity.

It also might be interesting to probe further into which types of stimulus variation interact with locomotion, due to some variations in stimulus interacting (stimulus size), while others did not (spatial frequency and contrast). It is interesting that stimulus size was discriminated between more in the presence of locomotion, while other features were not. This size difference is a particularly obvious manipulation compared to contrast and spatial frequency, and one could speculate that this is implicated in the significant interaction here. Further research that might focus solely on locomotion and its interaction with varying stimulus manipulations might therefore be valuable in order to understand the characteristics of features that are more heavily discriminated.

Future research could also look at the specifics of locomotion and how they affect the vasculature. For example, it is possible that locomotion induced by the stimulus (i.e. that in the 'Loco during stim' group) was motivated by a greater level of arousal, and so it would be interesting to attempt to disentangle the effects of arousal and locomotion itself (discussed further in chapter 5). It might also be interesting to look at how walking and running behaviour might vary in their effects on processing, as different levels of arousal are likely to underlie these different behaviours, and intuitively the motor feedback itself should be different for these different behaviours.

4.4.4 Conclusions

Vascular diameters were successfully manipulated in such a way that varied as the stimulus and state of the animal were changed. Differing diameter changes were elicited by alterations in stimulus contrast, size and spatial frequency, as well as in the presence and absence of locomotion. The corresponding activity of various neuronal subtypes that were measured for their intracellular calcium change concurrently will next be examined. Changes in vascular diameter will then be examined in direct comparison with neuronal activity in order to draw conclusions about neurovascular coupling.

Chapter 5

Pyramidal Cell and Somatostatin Interneuron activity in V1 of the Visual Cortex

5.1 Introduction

One area of knowledge that requires improvement in order to better understand the BOLD signal is which specific neuronal subpopulations become active concurrently with the BOLD response. Relatively little is known about the activity of various neuronal subpopulations that underlies and correlates with increased blood flow under various different conditions, and it is therefore necessary to further our knowledge regarding the patterns of activity that occur under various different circumstances. The V1 area of the visual cortex is a prime target for this: there exists already research probing the circuitry under certain conditions, thus allowing an improved understanding of any findings; as well as established methods by which to study the area, allowing us to use different stimuli to subtly manipulate the activation of neuronal subpopulations in V1.

5.1.1 Excitatory and Inhibitory activity to Drifting Grating in V1

Drifting gratings are an established method of stimulating the primary visual cortex (Cossell et al., 2015). Previous research by Adesnik (2017) showed that altering the contrast or size of a drifting grating impacts the ratio of excitatory and inhibitory activity in Layer II/III of V1. Intracellular whole cell recordings from awake mice indicated that as contrast increased (with grating size remaining stable), both excitatory and inhibitory activity increased; however excitatory activity increased more at lower levels of contrast than did inhibitory cells. As the contrast increased, the ratio of excitatory to inhibitory activity tilted towards inhibition. When response to stimulus size was measured, it was found that the ratio of excitatory to inhibitory activity also tilted towards inhibition as stimulus size was increased. In addition, the overall magnitude of both excitatory and inhibitory response declined as stimulus size increased due to surround suppression. Somatostatin expressing interneurons played a key role in this surround suppression, changing the overall magnitude of response but not shifting the excitatory-inhibitory activity ratio, and so can also show a separate pattern of activity from overall interneuron activity from other subtypes in this context. Indeed, previous research has also shown that as the size of a

stimulus increases further beyond the receptive field of a neuron, pyramidal cell activity decreases, but SST expressing interneuron activity increases. Furthermore, the perturbation of SST activity weakens the surround suppression of pyramidal neurons (Adesnik et al., 2012). New unpublished research from the same lab indicates that there is also contrast dependent surround suppression, whereby as contrast increases, SST increases its size tuning gain (Johnson, Geng, Hoffman, Adesnik, & Wessel, 2018).

Regarding spatial frequency, early research in cat V1 found that cells with a small receptive field were very specifically sensitive within various different spatial frequency ranges (varying between 0.2 and 2 cycles per degree), with each being sensitive within a narrow range. Cells with a larger receptive field also had broader response range to varying spatial frequency, with peak frequencies between 0.25 and 0.7 cycles per degree (Maffei & Fiorentini, 1973). However, specific neuronal subtypes were not identified in this work. More recent work in anaesthetised mice has compared parvalbumin (PV) expressing interneurons against a generic population of neurons, and found no difference in preferred spatial frequency, which was ~0.03 cycles per degree (Runyan et al., 2010). This suggests that a range of neuronal subtypes are likely to show a preference for approximately this spatial frequency. This is supported by further research in which a check for optimal spatial frequency was carried out, which found that for excitatory cells, a spatial frequency of 0.035 cycles per degree gave an optimal response (Okun et al., 2015). However, a range of spatial frequencies are often used within visual processing research without explicit testing or justification.

5.1.2 Effect of Locomotion on V1

Locomotion also has an effect on visual processing, which can be separated out into an effect of changing arousal levels, and motor feedback (Vinck, Batista-Brito, Knoblich, & Cardin, 2015). Using pupillometry, the effects of these on local field potentials (the summed synaptic amplitude) have been somewhat disentangled: while arousal suppresses

spontaneous firing, it increases signal-to-noise ratio during the presentation of a drifting grating, seeming to increase the extent to which the brain is driven by these external inputs. Locomotion itself was responsible for increased anticipatory firing to movement and during movement. Locomotion speed and arousal (measured through pupil diameter) were found to be closely correlated as mice transition to a higher-arousal state, just preceding or during locomotion (Vinck et al., 2015), and it is therefore important to be aware of these co-occurring states that enact somewhat different effect on LFP during locomotion.

On the level of the V1 circuitry, using two-photon imaging of awake mice, Pakan et al. (2016) found that in V1, pyramidal cell activity increases during locomotion, possibly due to disinhibition mediated by inhibitory interneurons. However this was not the case in the absence of a visual stimulus (in absolute darkness), an effect that based on Vinck et al.'s previous finding, could be arousal-driven. Locomotion also increased pyramidal cell activity, SST, vasoactive intestinal peptide (VIP), and PV expressing interneuron activity in the presence of some form of visual stimulation. SST interneurons and pyramidal cells were the only subtypes for which increases to locomotion did not persist in darkness. Furthermore, the size of a visual stimulus affects the activity of different neuronal subtypes, with SST activity increasing with size, but VIP, and PV interneurons, as well as pyramidal cells decreasing their activity (Dipoppa et al., 2016), which appears consistent with the changes in activity that occur to this stimulus change in the absence of locomotion (Adesnik, 2017).

This research highlights the importance of context when considering the effects of locomotion on neuronal subtypes, and the complex interactions that take place between locomotion, arousal, and the visual environment.

Aims and Justifications for Current Study

The current research aimed to use two-photon imaging of awake mice to probe the activity of different neuronal subpopulations both locally to the vasculature and at a population

level. Specifically, excitatory activity and SST-expressing interneuron activity were measured in response to a drifting grating that was varied either by contrast and spatial frequency, or by stimulus size and spatial frequency. SST was prioritised as the interneuron subtype of interest due to its role in surround suppression as stimulus size increases (Adesnik et al., 2012). Some SST-expressing interneurons have been found to co-localise with nitric oxide synthase, suggesting some may dilate vessels (Perrenoud, Geoffroy, et al., 2012). However, general activity (and therefore cerebral blood flow) should decrease in a region as stimulus size increases, while SST activity should increase to facilitate this (Adesnik et al., 2012). This creates a situation in which as general activity decreases, activity of what might be a vasodilatory subtype (SST) could be increasing. For this reason, it is of great interest to examine excitatory activity and SST-expressing interneuron activity locally to the vessel and as a broader population to understand the pattern of activity that occurs during surround suppression and how this relates to the response of the blood vessel. Furthermore, as new research indicates a role for SST in surround suppression in the context of contrast change (Johnson et al., 2018), this neuronal interaction might also be of interest in the context of contrast. Co-occurring vascular diameter changes should illuminate how this changing pattern of activity impacts cerebral blood flow (see chapter 4 and chapter 6).

Regarding spatial frequency, previous research has not very thoroughly probed spatial frequency and its effect on specific subpopulations, especially not in collaboration with changing contrast or stimulus size, or with locomotion. This was therefore added as another variable to the drifting grating stimulus in the present research in order to allow more extensive manipulation of the levels of different neuronal subpopulation activity for the purpose of later correlation with the corresponding vascular response, as well as to garner information about the roles of excitatory and SST interneuron activity in processing of differing spatial frequencies. Previous research has also confirmed that mice have adequate visual acuity for the spatial frequencies selected (Teichert, Lehmann, & Bolz, 2018).

As mice were awake and head fixed upon a cylindrical treadmill, locomotion data were also garnered at various time points during the stimulus presentation. This is further reason excitatory cells and SST-expressing interneurons were of particular interest: findings that these subpopulations increase their activity to locomotion only during the presentation of a visual stimulus, and are very context-dependent in their activity (Pakan et al., 2016) renders them interesting targets to investigate how their activity level might change with changing size or contrast of a visual stimulus during bouts of locomotion, which has not yet been studied as far as the author is aware. This will also be interesting in the context of later comparisons against the vasculature, to investigate the extent to which changes in vascular diameter might reflect these highly context-dependent changes in neural activity (see chapter 6).

Based on the previous results gleaned by Adesnik (2017), it was hypothesised that both excitatory and SST activity would increased with increasing stimulus contrast, and that with increasing stimulus size, excitatory activity would decrease, while SST activity would increase. As previous research has found that increases in pyramidal cell and SST activity only occur to locomotion in the presence of a visual stimulus, it was predicted that activity of both of these subpopulations would increase to locomotion in the presence of a visual stimulus, but not without a stimulus. However, as in the absence of stimulus, there was some ambient light from the screens, there is some uncertainty as to whether this extremely low level of visual stimulus would be adequate to elicit increased neuronal activity to spontaneous locomotion.

5.2 Methods and Materials

Details of the methods used in this chapter can be found in the main methods section (chapter 2).

5.2.1 Animal Subjects

Adult male and female C57BL mice aged between 3 – 8 months were used in these experiments. Transgenic mice were used (Thy1 GCaMP (n = 3) and heterozygous SST cre GCaMP crossed (n = 5)), in fluorescent signal was elicited by increased intracellular calcium to allow the measurement of changes in neuronal activity in either excitatory pyramidal cells, or SST interneurons. Animals were housed in a 12-hour reverse light/dark cycle to encourage locomotion during imaging.

5.2.2 Animal Surgery

Animal procedures were performed in accordance with the Animals (Scientific Procedures) Act 1986. Surgical procedures are detailed in main methods section (chapter 2). To summarise, a craniotomy was carried out over the V1 area of the visual cortex on the left hemisphere and a glass window was fitted over the area. A stainless steel head plate was fixed to the skull to stabilise the mouse during imaging.

5.2.3 Experimental Procedures

After recovery, habituation of the mice was carried out detailed in main methods (chapter 2).

Mice were injected with a fluorescent dye (see chapter 4) to allow imaging of the vascular lumen.

The two-photon microscope was then used to concurrently measure intracellular calcium release and corresponding vessel diameter both locally to the vessel (see Figure 5.1 A, B) and at a population level (only available for the trials in which contrast was varied) (see Figure 5.1 C, D).

It was determined that the region was responsive to the stimulus either through vasodilation at the pia or neuronal activity. It was also ensured that the vessel to be imaged was on the arterial side of the vascular tree by determining the direction of blood flow from a capillary.

Mice were then presented with a visual stimulus, comprised of a drifting grating that was varied either by size (a 20 degrees circular stimulus, or 220 degrees (full screen) stimulus, both presented at 100% contrast) or by contrast (5%, 25%, 63% or 100%, all presented as a full screen stimulus), with both stimuli being varied by spatial frequency (0.04 or 0.2 cycles per degree). In order to test response to spontaneous locomotion, no stimulus was presented, but the screens were left on (meaning there was a low level of ambient light). Screens were positioned at a 17cm distance from the mouse. Locomotion by the mouse was also recorded from a rotary encoder.

5.2.4 Cell Processing

Details of calcium analysis are detailed in chapter 2. In summary, images were processed in ImageJ to remove movement artefacts. In MATLAB (Mathworks), the 20% highest intensity pixels were selected and the 1-5% lowest intensity pixels were subtracted from this in order to avoid artefacts from background, non-cellular signal (this bottom signal was varied in order to ensure that cell activity was not included, but that the selection wasn't so small as to add noise to the remaining data. The threshold for this varied image by image).

Cell responses were then cut around the stimulus period, allowing a 5-second pre-stimulus and a 25-second post-stimulus period, with 5 seconds of stimulus. The traces were then normalised to the pre-stimulus period, calculated as Δf/f. A subset of the trials were eliminated based on pre-stimulus noise. The maximum value averaged across trails was then calculated for each vessel and used as the peak value to stimulus presentation for that vessel.

Within spontaneous locomotion, similarly trials were cut around locomotion onset, to give a 4-second baseline period and a 4.3-second locomotion onset period. As with stimulus trials, traces were normalised to the pre-stimulus period. And the peak value was calculated in the same manner, but calculating the maximum from the entirety of the locomotion onset period (4.3 seconds).

5.2.5 Data Analysis

All data analysis was performed using MATLAB (MathWorks) and SPSS.

5.3 Results

The following chapter reports neuronal responses from pyramidal neurons and SST expressing interneurons in response to variations in a drifting grating by 4 contrasts (5%, 25%, 63%, 100%) or by 2 sizes (20 degrees, or 220 degrees (full screen)). Both stimulus types were also varied by spatial frequency (0.04 or 0.2 cycles per degree). Throughout this section, where there is a stimulus presentation, the maximum response during the stimulus period is reported from calcium as a Δf/f value, with the first 5 seconds before stimulus taken as the pre-stimulus baseline period. Where spontaneous locomotion is presented, the maximum Δf/f value during the locomotion onset period is reported.

5.3.1 Examining Responses to Varying Contrast and Spatial Frequency Locally to the Vasculature

The maximum responses of pyramidal cells and SST interneurons during stimulus presentation to varying contrast and spatial frequencies of drifting grating, averaged over all vessels, are shown in Figure 5.2. This is broken down further by the pattern of locomotion that occurred before and during the stimulus presentation, with no locomotion pre- or during the stimulus (No loco), no locomotion in the 5-second pre-stimulus period, but locomotion during the stimulus (Loco during stim), and locomotion both within the pre-stimulus and the stimulus period (Loco before & during stim). Both pyramidal activity and SST interneuron activity show increases in activity with increasing contrast, and in interaction with locomotion, differentiated clearly between excitatory and SST activity. Both subtypes increase with locomotion, but while the differential response to varying contrast is retained in the presence of locomotion in SST interneurons, pyramidal cells failed to discriminate different contrasts during locomotion of the mouse (Figure 5.2).

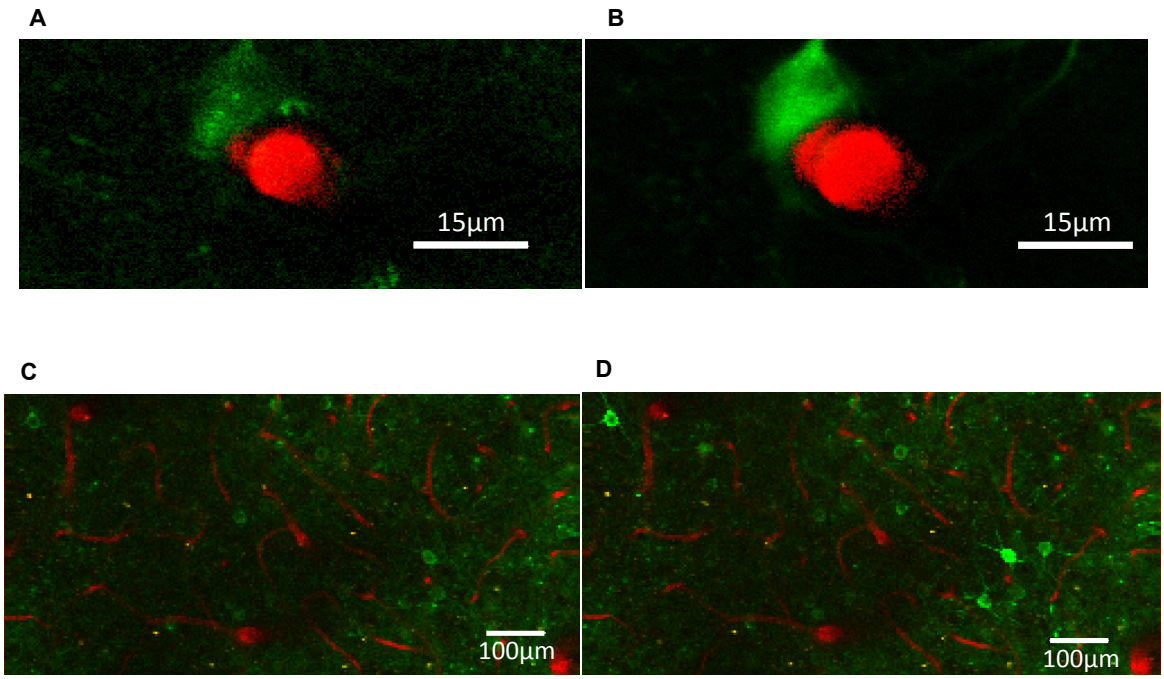

Figure 5.1. Example excitatory activity from pyramidal neurons before and during visual stimulation. ***A.*** *Pyramidal cell presented a blank grey screen (green) and its local vessel (viewed as a cross section) (red),* ***B.*** *Pyramidal cell stimulated by a drifting grating presentation and changing intensity.* ***C.*** *Population view of excitatory activity during blank grey screen presentation.* ***D.*** *Population activity changing intensity with stimulus presentation.*

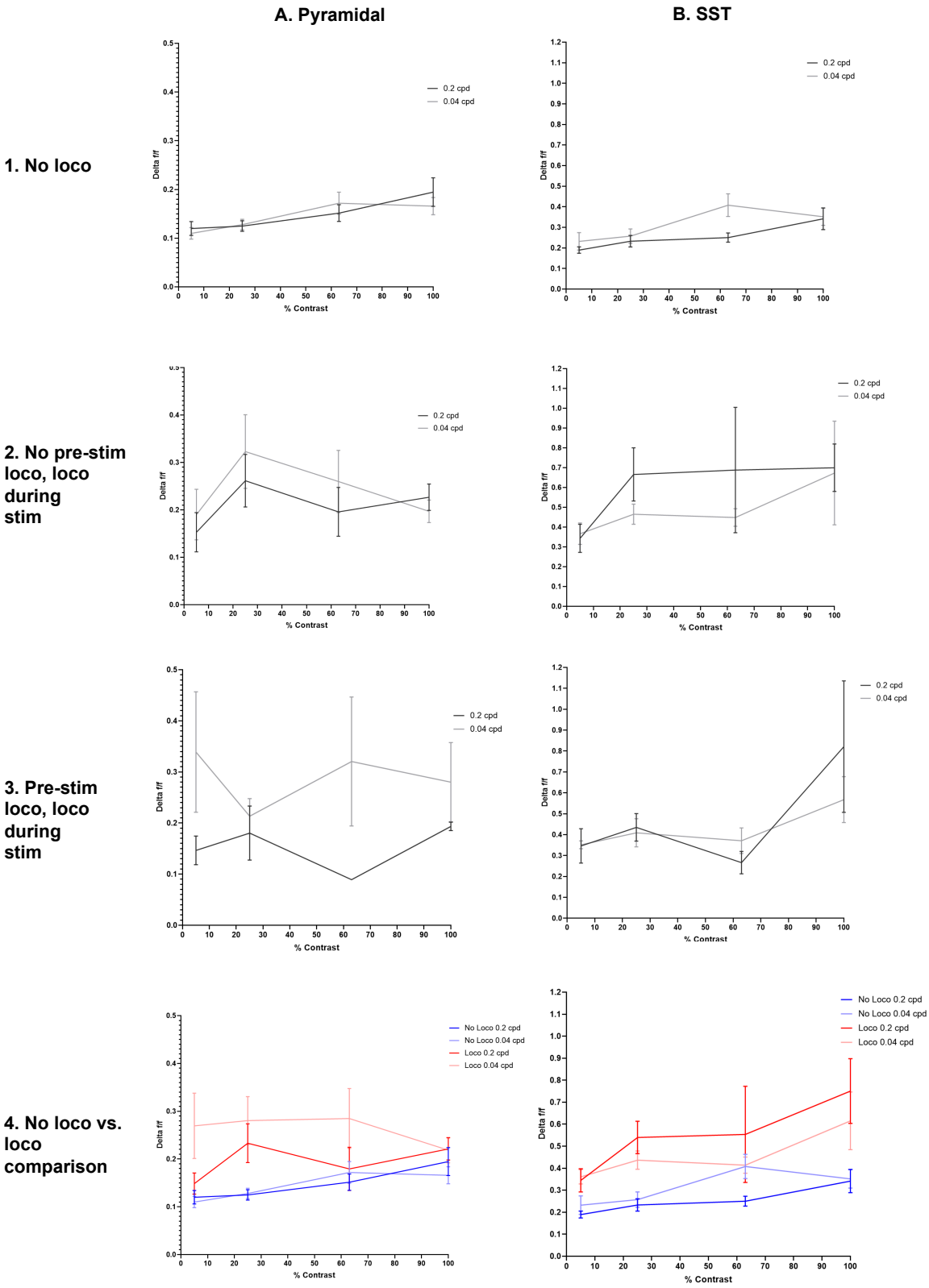

Figure 5.2. Excitatory and SST-expressing interneuron activity in response to varying stimulus contrast locally to the vasculature (+/- 1SEM). *Average maximum calcium responses (Delta f/f) during presentation of a drifting grating that was shown at 4 different contrasts and 2 different spatial frequencies measuring from* ***A.*** *pyramidal cells showing excitatory activity and* ***B.*** *SST-expressing interneurons. Mice were able to freely run at will, and so data are split up farther into* ***1.*** *No locomotion during the pre-stimulus or stimulus period (Pyramidal: N = 49-52; SST: N = 47-60);* ***2.*** *No locomotion in the pre-stimulus period, but locomotion during the stimulus period (Pyramidal: N = 4-17; SST: N = 8-22), and* ***3.*** *Locomotion during the pre-stimulus and stimulus period (Pyramidal: N = 2-8; SST: N = 7-16). Due to no significant difference between the two groups in which any locomotion occurred, this was collapsed across in* ***4.*** *for a direct comparison of no locomotion vs. locomotion during the stimulus (Pyramidal N = 12-23; SST: N = 16-38).*

5.3.2 Effect of Contrast, Spatial Frequency and Locomotion on Local Excitatory and SST-Interneuron Activity

A two-way ANOVA revealed a main effect of neuronal subtype, whereby SST activity was greater that excitatory activity to the stimuli ($F(1, 1297) = 53.958$, $p < .001$). There was also a main effect of contrast ($F(3, 1297) = 4.229$, $p = .006$); and contrast had a significant interaction with neuronal subtype ($F(3, 1297) = 2.873$, $p = .035$), suggesting the different neuronal subtypes are differentially modulated by the changing contrast. There was also a main effect of locomotion ($F(2, 1297) = 10.026$, $p < .001$), which did not interact with any other variables. A Bonferroni test revealed a significant difference between 'No loco' and 'Loco during stim' ($p < .001$); and 'No loco' and 'Loco before & during stim'. However, there was no difference between the two conditions in which locomotion occurred ($p = 1.000$), which is interesting considering the results in chapter 4 in which the vessels did differentiate between these locomotion groups. These two locomotion groups are therefore collapsed across in figure 5.2 (4, A; 4,B). There was no significant effect of spatial frequency ($F(1, 1297) = .003$, $p = .958$), nor any significant interactions with any other variables, suggesting that this did not have an effect on response from either of the neuronal subtypes.

Due to the neuronal subtype by contrast interaction; a two-way ANOVA was conducted on the individual neuronal subtype datasets. Interestingly, within excitatory activity it was found that there was no significant effect of contrast, however contrast did interact with locomotion and was very close to significance ($F(6, 521) = 2.081$, $p = .054$). Figure 5.2 (A, 1-4) suggests while there is an effect of contrast when there is no locomotion, when there is locomotion, this effect is attenuated. However, within SST interneuron activity, it was found that there was a significant main effect of contrast ($F(3, 598) = 7.428$, $p < .001$), with increasing activity as contrast increased (Figure 5.2 (1, B)). A Bonferroni test showed that within contrast, significant differences occurred specifically between 5% and 100% ($p < .001$), and 25% and 100% ($p = .002$). There was also a significant effect of locomotion ($F(2, 598) = 17.181$, $p < .001$), which unlike the excitatory activity, did not interact with contrast.

This suggests that excitatory and SST interneuron activity can be differentiated on the basis of contrast, and especially well in interaction with locomotion.

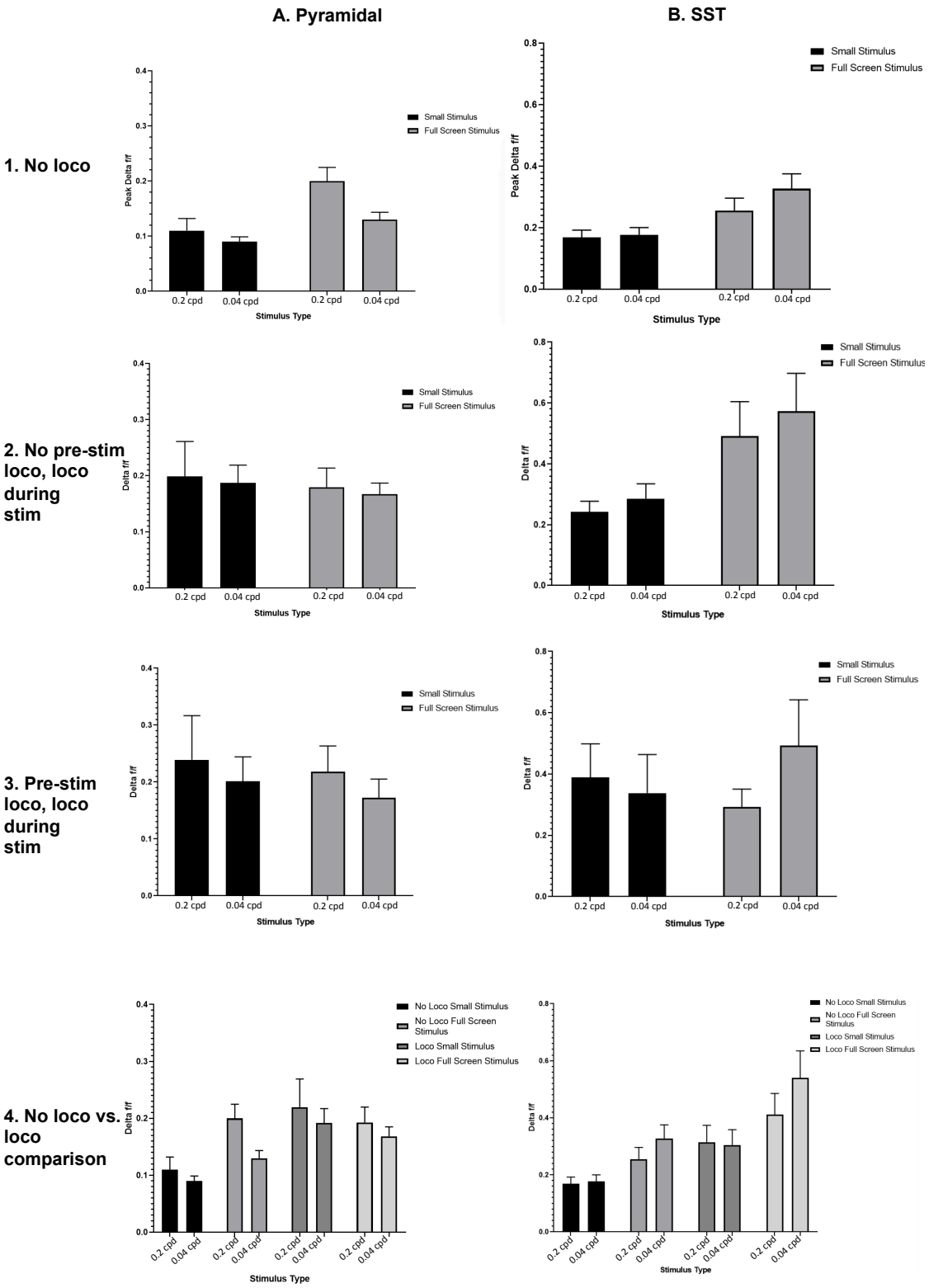

Figure 5.3. Excitatory and SST-expressing interneuron activity in response to varying stimulus size locally to the vasculature (+/- 1SEM). *Average maximum calcium responses (Delta f/f) during presentation of a drifting grating that was shown at 2 different sizes and 2 different spatial frequencies measuring from* ***A.*** *pyramidal cells showing excitatory activity and* ***B.*** *SST-expressing interneurons. Mice were able to freely run at will, and so data are split up farther into* ***1.*** *No locomotion during the pre-stimulus or stimulus period (Pyramidal N = 70-76; SST N = 37-39),* ***2.*** *No locomotion in the pre-stimulus period, but locomotion during the stimulus period (Pyramidal N = 14-31; SST N = 9-16), and* ***3.*** *Locomotion during the pre-stimulus and stimulus period (Pyramidal N = 9-15; SST N = 10-13). Due to no significant difference between the two groups in which any locomotion occurred, this was collapsed across in* ***4.*** *for a direct comparison of no locomotion vs. locomotion during the stimulus (Locomotion: Pyramidal N = 29-41; SST = 18-27).*

5.3.3 Effect of Stimulus Size and Spatial Frequency and Locomotion on Local Excitatory and SST-Interneuron Activity

Looking at both excitatory activity and SST interneuron activity, there was significantly more SST activity than excitatory activity ($F(1, 652) = 57.907$, $p < .001$); and incongruent with the literature, the full screen stimulus elicited significantly more activity than the small (20 degree) stimulus ($F(1, 652) = 8.020$, $p < .005$). Similarly to the prior findings with the contrast stimuli, there was also a significant interaction between neuronal subtype and stimulus size ($F(1, 652) = 12.542$, $p < .001$), suggesting that these subtypes are differentially modulated by the different sized stimuli. There was also a significant main effect of locomotion group ($F(2, 652) = 16.014$, $p < .001$), which was only significant between 'No loco' and 'Loco during stim' ($p < .001$); and 'No loco' and 'Loco before & during stim' ($p < .001$). There was no difference between the two conditions in which locomotion occurred ($p = 1.000$). Again, due to a significant result when comparing these locomotion groups within the vasculature in chapter 4, it is interesting that this difference is not significant in either of the neuronal subtypes tested here. There was a significant interaction between neuronal subtype and locomotion group ($F(2, 652) = 2.341$, $p = .010$), suggesting that the neuronal subtypes responded differently to differing patterns of locomotion. There was also a significant interaction between stimulus size, neuronal subtype and locomotion group ($F(2, 652) = 3.555$, $p = .029$), and based on figure 5.3, it appears this might be based on an attenuated response to stimulus size within excitatory activity in response to locomotion, where this is not the case with SST interneurons. There was no significant main effect of spatial frequency ($F(1, 652) = 0.896$, $p = .344$), and this variable did not have any significant interactions, suggesting that also in the context of stimulus size, spatial frequency does not have an effect either. Due to the neuronal subtype interactions found here, further two-way ANOVAs were conducted on the individual neuronal subtypes.

Stimulus size ($F(1, 425) = .075$, $p = .785$) had no effect on excitatory activity. There was a significant main effect of locomotion, whereby locomotion with stimulus presentation

elicited more activity than stimulus presentation alone (Figure 5.3 (4, A)). However, as previously, a Bonferroni test revealed that this difference was only significant between ‘No loco’ and ‘Loco during stim’ ($p < .001$); and ‘No loco’ and ‘Loco before & during stim’ ($p < .001$). There was no significant difference between the two groups in which locomotion occurred ($p = .575$). These locomotion groups were therefore collapsed across in figure 5.3 (4, A). Similarly to the contrast stimuli, there was an interaction between stimulus size and locomotion that was close to significance ($F(2, 425) = 2.927$, $p = .055$), further supporting the idea that locomotion masks the effect of the stimulus on the excitatory activity (Figure 5.3 (2, A; 3, A)).

Within the SST interneurons, there was a significant main effect of stimulus size ($F(1, 229) = 9.998$, $p = .002$), whereby there was increased activity in response to the larger, full screen stimulus, compared to the smaller (20 degree) stimulus (Figure 3 (1, B; 2, B; 4, B)). There was a main effect of locomotion ($F(2, 229) = 8.674$, $p < .001$) whereby locomotion with stimulus presentation elicited more activity than stimulus presentation alone (Figure 5.3 (4, B)). A Bonferroni test revealed that this difference was only significant between ‘No loco’ and ‘Loco during stim’ ($p < .001$); and ‘No loco’ and ‘Loco before & during stim’ ($p = .009$). There was no significant difference between the two groups in which locomotion occurred ($p = .1000$). These locomotion groups were therefore collapsed across in Figure 5.3 (4, B).

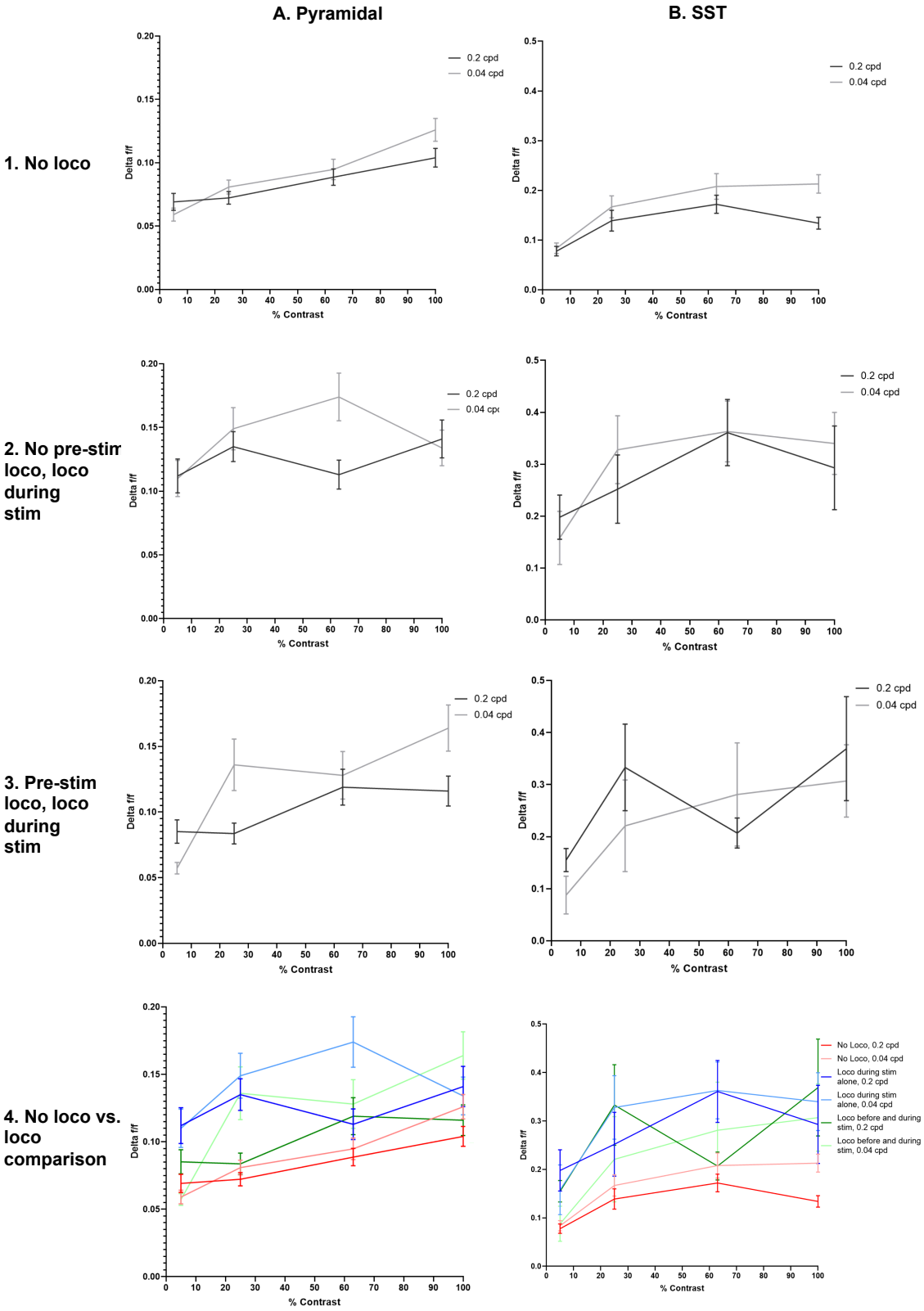

Figure 5.4. Excitatory and SST-expressing interneuron activity in response to varying stimulus contrast as a population (+/- 1SEM). *Average maximum calcium responses (Delta f/f) during presentation of a drifting grating that was shown at 4 different contrasts and 2 different spatial frequencies measuring from* ***A.*** *pyramidal cells showing excitatory activity and* ***B.*** *SST-expressing interneurons. Mice were able to freely run at will, and so data are split up farther into* ***1.*** *No locomotion during the pre-stimulus or stimulus period (Pyramidal N = 46-55; SST N = 48-63),* ***2.*** *No locomotion in the pre-stimulus period, but locomotion during the stimulus period (Pyramidal N = 11-22; SST N = 8-20), and* ***3.*** *Locomotion during the pre-stimulus and stimulus period (Pyramidal N = 8-17; SST N = 9-18). The three locomotion groups are shown together in* ***4.*** *for direct comparison.*

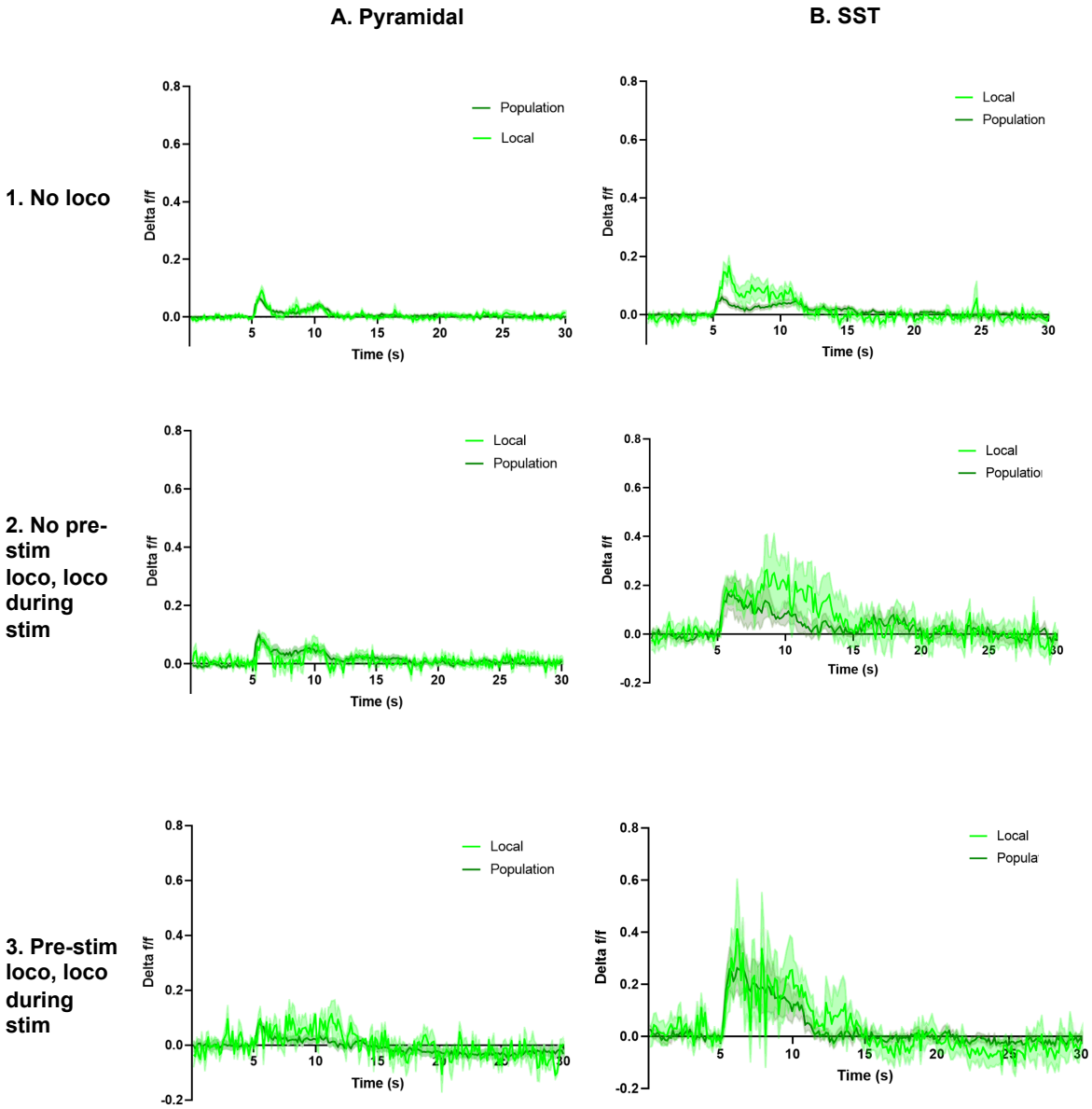

Figure 5.5. Averaged excitatory and SST-expressing interneuron activity (Delta f/f) traces comparing local activity (light green) and population activity (dark green) (+/- 1SEM).
*All data used here were taken from the 100% contrast with a spatial frequency of 0.2 cycles per degree. The stimulus onset is at 5 seconds, and stimulus offset is at 10 seconds. During the pre- and post-stimulus period, a plain grey screen was displayed. Pyramidal cells (excitatory activity) is shown in column **A**; SST-expressing interneuron activity is shown in column **B.** Mice were able to freely run at will, and so data are split up farther into **1.** No locomotion during the pre-stimulus or stimulus period (Pyramidal: Local N = 49-52, Pop N = 46-55; SST: Local N = 47-60, Pop N = 48-63), **2.** No locomotion in the pre-stimulus period, but locomotion during the stimulus period (Pyramidal: Local N = 4-17, Pop N = 11-22; SST: Local N = 8-22, Pop N = 8-20), and **3.** Locomotion during the pre-stimulus and stimulus period (Pyramidal: Local N = 2-8, Pop N = 8-17; SST: Local N = 7-18, Pop N = 9-18).*

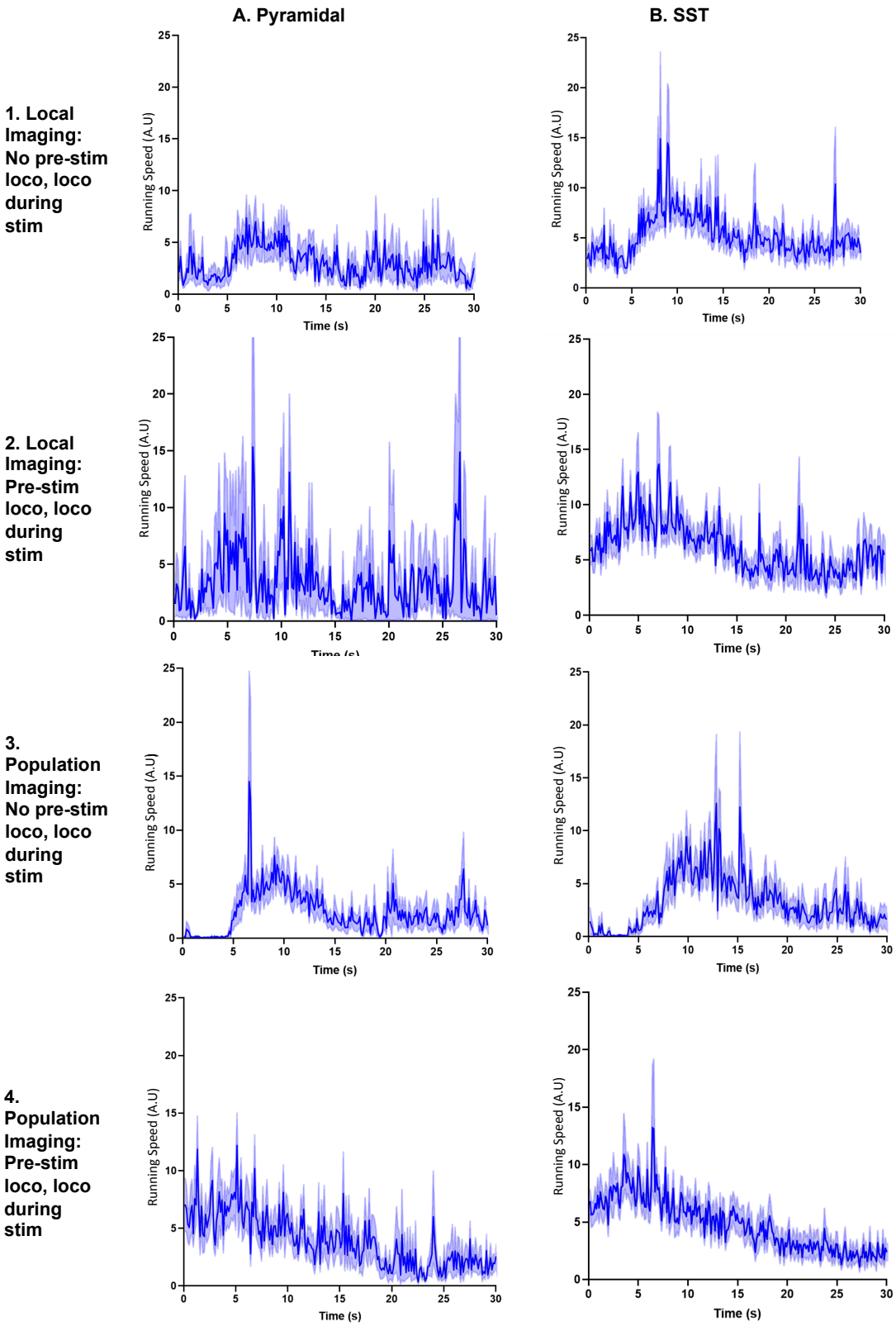

Figure 5.6. Averaged locomotion traces throughout contrast stimulus trials (arbitrary units) (+/- 1SEM). *All data used here were taken from the 100% contrast with a spatial frequency of 0.4 cycles per degree. The stimulus onset is at 5 seconds, and stimulus offset is at 10 seconds. During the pre- and post-stimulus period, a plain grey screen was displayed. Locomotion traces within excitatory activity are shown in column **A**, and within SST interneuron activity is shown in column **B**. Locomotion data is further divided by whether it was recorded during local (rows **1** and **2)** or population imaging (rows **3** and **4**). Data in which locomotion occurred during the stimulus but not in the pre-stimulus period is shown in rows **1** and **3**, and data in which locomotion occurred during the pre-stimulus and stimulus period are shown in rows **2** and **4**. (N is the same as that shown for calcium in Figure 5.5).*

5.3.4 Examining Responses to Varying Contrast, Spatial Frequency and Locomotion as a Population

In addition to measuring neuronal activity locally to the vasculature (Figure 5.1 (A and B)), within the changing stimulus contrast experiments, each imaging session of a vessel was repeated with a wide field view (Figure 5.1 (C and D)). This was carried out to allow insight as to the activity of each neuronal subtype as a population, in addition to the small groups of cells local to the vasculature; thus showing whether calcium responses local to vessels are reflected in the cells as a population. Overall the patterns of activity between local and population activity were somewhat similar, especially within SST interneurons, in which for both data with and without locomotion, similar effects of contrast and locomotion were evident (see figures 5.2 and 5.4), suggesting a degree of consistency between local and population activity. However, here there was some response to variation in spatial frequency that was not evident within the local cells. Within the excitatory activity, similar patterns of activity were observable, however, there were some differences, predominantly an apparently reduced masking of the effect of contrast in the locomotion trials (Figure 5.4 (4, A)) (although it appears this is still somewhat present (see Figure 5.4 (2, A)). The cells viewed as a population were also able to differentiate spatial frequencies, where this was not the case within the local neuronal activity (Figure 5.4).

5.3.5 Effect of Contrast, Spatial Frequency and Locomotion on Population Excitatory and SST-Interneuron Activity

The traces of the pyramidal cell and SST interneuron activity to the highest contrast stimulus, a 0.2 cycle per degree spatial frequency, and no locomotion show that both local and population calcium peak to the onset of the stimulus, and then drop back down to baseline after the stimulus offset (Figure 5.5 (1, A; 1, B)). It is evident from the traces that locomotion-positive data are somewhat more variable than the data without locomotion. However, there are still clear increases in both local and population calcium from pyramidal cells and SST interneurons to the highest contrast stimulus (Figure 5.5 (2, A; 2, B; 3, A; 3, B)). The corresponding locomotion traces for the same subset of the data are shown in

Figure 5.6 for both the excitatory (Figure 5.6 A) and SST (Figure 5.6 B) interneuron activity both within local (Figure 5.6 (1 and 2)) and population (Figure 5.6 (3 and 4)) activity. This shows locomotion occurring within the expected time frames, however, the locomotion traces within the pre-stimulus period of the 'No pre-stim loco, loco during stim' group (i.e. Where there should be no locomotion) do appear somewhat less variable during the pre-stimulus period during population imaging.

A two way ANOVA was conducted on the population activity, which found a significant main effect of neuronal subtype ($F(1,1260) = 147.244$, $p < .001$). SST interneuron activity was greater than excitatory activity; this is consistent with the local activity and suggests that there is greater overall SST activity than excitatory in V1 in response to the stimuli. Importantly, unlike the local activity, there was a significant effect of spatial frequency whereby 0.04 cycles per degree was greater than 0.2 cycles per degree. There was also a significant main effect of contrast ($F(3, 1260) = 19.803$, $p < .001$), which interacted with neuronal subtype ($F(3, 1260) = 5.810$, $p = .001$), indicating that consistently with the local neuronal activity, as a population, the different neuronal subtypes respond somewhat differently to the stimulus. Neuronal subtype did not demonstrate a significant interaction with spatial frequency ($F(1, 1260) = 0.211$, $p = .646$), indicating that as a population, the subtypes do not respond differently to spatial frequency. There was a main effect of locomotion ($F(2, 1260) = 44.091$, $p < .001$), which showed a significant interaction with neuronal subtype ($F(2, 1260) = 12.05$, $p < .001$), indicating that the neuronal subtypes respond to locomotion, but that this might occur somewhat differently to one another. To probe these neuronal subtype interactions, the neuronal subtypes were individually tested with a two-way ANOVA.

Looking just at the pattern of excitatory activity alone, it is not entirely aligned with that of local activity (see figure 5.2 and figure 5.4), as there is a significant main effect of contrast within the population calcium (Figure 5.4 (2, A; 3, A)) ($F(3, 625) = 16.612$, $p < .001$). A Bonferroni test revealed these differences to be significant between 5% and 25% ($p =$

.001), 5% and 63% ($p < .001$), 5% and 100% ($p < .001$), 25% and 100% ($p < .001$), and 63% and 100% ($p = .020$). There was also a difference between 25% and 63% that did not reach significance ($p = .072$). This indicates that population excitatory activity is quite sensitive to the differences between the contrasts whether or not there is locomotion, compared to local activity (Figure 5.4 (4, A)). There is also a significant main effect of locomotion ($F(2, 625) = 43.193$, $p < .001$), and activity was significantly different between the three locomotion groups, suggesting population excitatory activity differentiates between these different patterns of locomotion, where the local excitatory calcium responses did not (Figure 5.4 (4, A); Figure 5.2 (2, A; 3, A)). Specifically, 'Loco before & during stim' was greater than 'No loco' ($p < .001$); 'Loco during stim' was also greater than 'No loco' ($p < .001$), and was also greater than 'Loco before and during stim' ($p = .006$). Somewhat consistently with the local calcium data, there was also a significant interaction between contrast and locomotion ($F(6, 625) = 2.148$, $p = .046$). This appears to be due to a reduced sensitivity to the differing contrasts within the 'Loco during stim' group specifically (Figure 5.4 (2, A)), while both the 'No loco' and 'Loco before & during stim' retain the response (Figure 5.4 (1, A; 3, A)).

There was also a significant main effect of spatial frequency ($F(1, 625) = 8.985$, $p = .003$) in which 0.04 cycles per degree elicited a greater response than 0.2 cycles per degree, unlike within the local excitatory activity, which showed no significant effect of spatial frequency. There was a significant interaction between contrast and spatial frequency ($F(3, 625) = 3.161$, $p = .024$) as certain contrasts appear to show greater differences in responses elicited by differing spatial frequencies than others; and also a significant interaction between contrast, spatial frequency and locomotion ($F(6, 625) = 2.604$, $p = .017$). This is likely due to the differing contrasts at which there appears to be a difference between the responses: there is a general pattern of responses to 0.04 cycles per degree increasing more than 0.2 cycles per degree as contrast increases; however the contrasts at which this difference between spatial frequencies is greater appears to differ with the level of locomotion (Figure 5.4 (1, A; 2, A; 3, A)).

Within population SST interneuron activity, as with local SST, there was a significant main effect of contrast ($F(3, 635) = 13.087$, $p < .001$). However, unlike the local activity, this increased from 5% to 25% contrast (Figure 5.4 (4, B)), but plateaued as contrast increased from 25%. This is shown by the Bonferroni test, which showed significant differences only between 5% and 25% ($p < .001$), 5% and 63% ($p < .001$), and 5% and 100% ($p < .001$). There was also a significant effect of locomotion ($F(2, 635) = 26.157$, $p < .001$), whereby locomotion increased the SST response to the stimulus, but 'Loco during stim' and 'Loco before & during stim' were not significantly different from one another as shown by a Bonferroni test ($p = .344$). There were however significant differences between 'No loco' and 'Loco during stim' ($p < .001$) and between 'No loco' and 'Loco before & during stim' ($p < .001$). Population SST interneurons here therefore only appear to differentiate between presence and absence of locomotion during stimulus presentation (Figure 5.4 (1, B; 2, B; 3, B)).

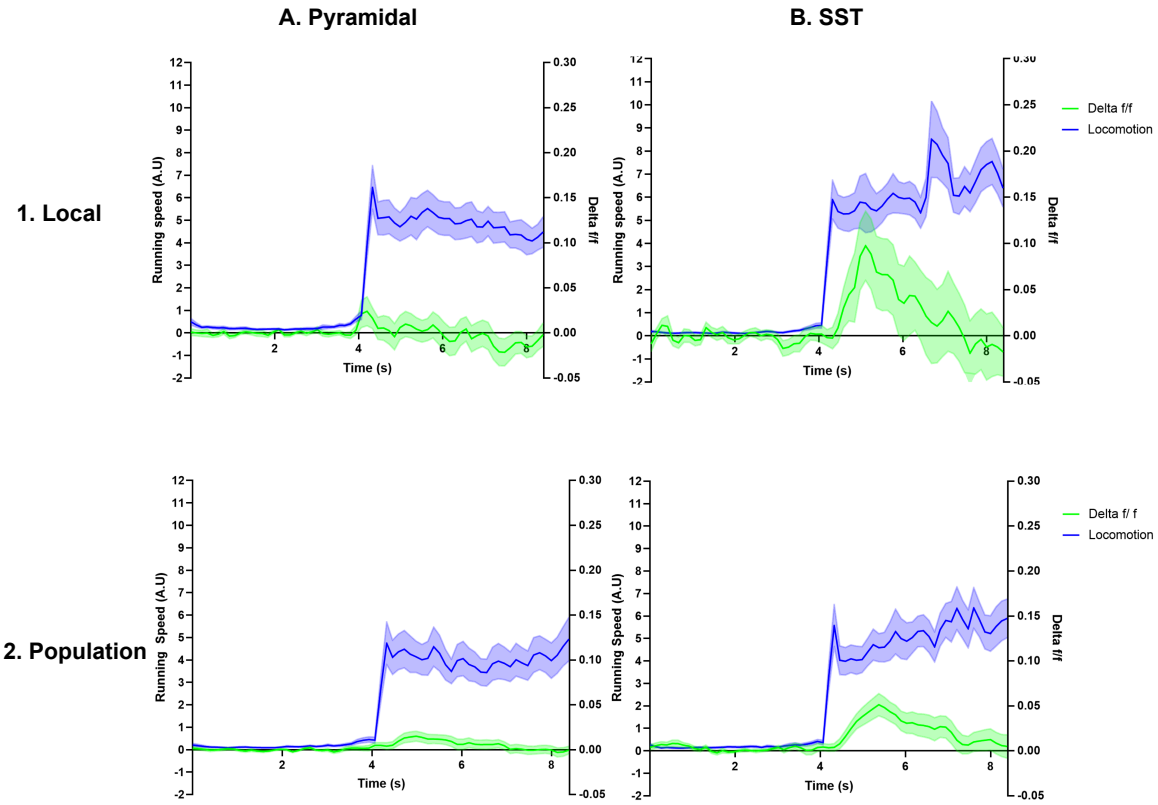

Figure 5.7. Averaged excitatory and SST-expressing interneuron activity (Delta f/f) (green), and spontaneous locomotion traces (arbitrary units) (blue) within local and population neuronal activity (+/- 1SEM).

*Locomotion level is shown in blue, locomotion onset that occurred spontaneously (with no stimulus, but screens switched on) is shown in all conditions above. Excitatory activity (**A**) and SST interneuron activity (**B**) are shown in green, both locally to the vessel (**1**) (Pyramidal N = 31; SST N = 30) and at the population level (**2**) (Pyramidal N = 31; SST N = 32).*

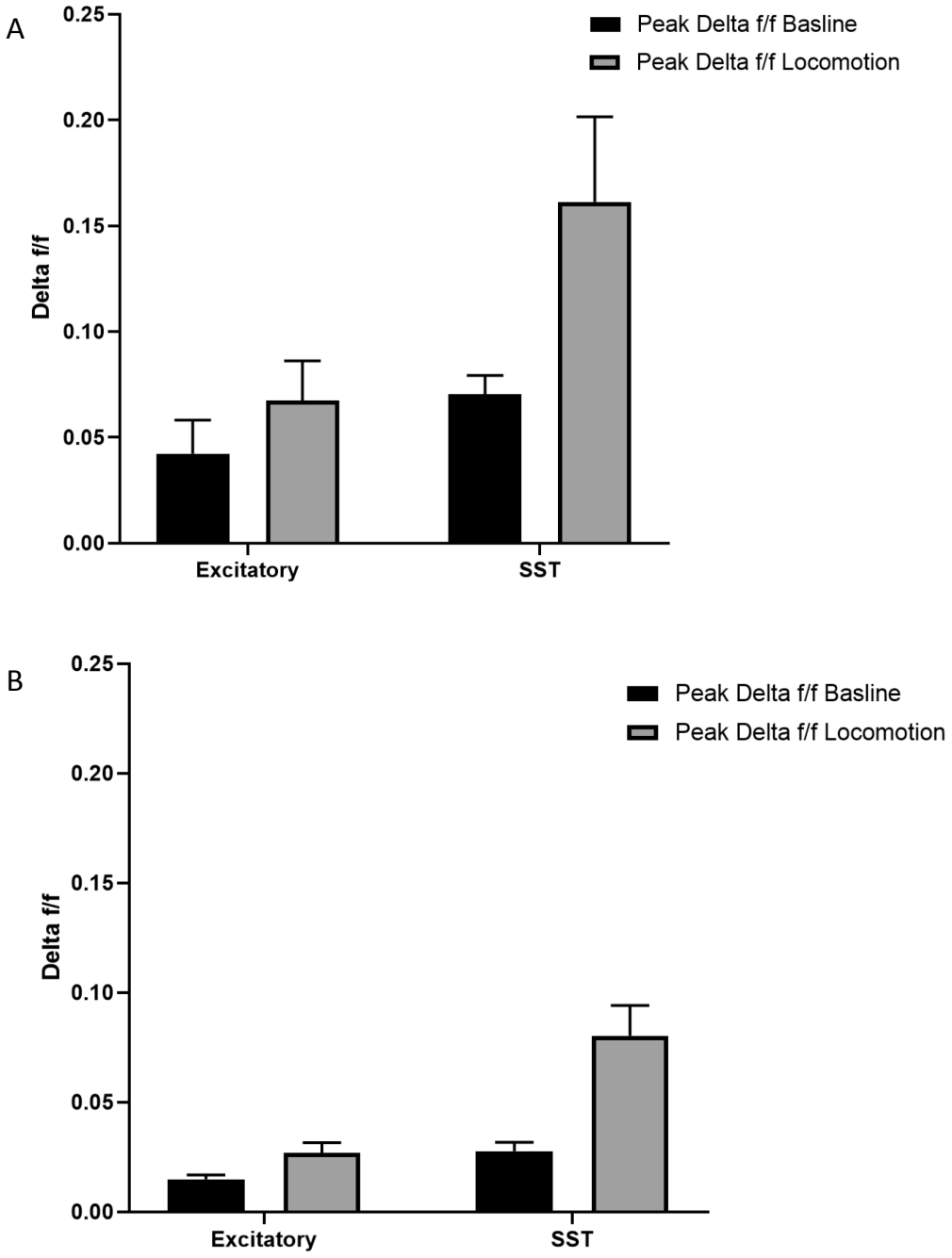

Figure 5.8. Mean peak Δf/f during baseline and spontaneous locomotion onset (+/- 1 SEM).
*Comparison of peak Δf/f during the baseline period, and locomotion onset within excitatory and SST interneuron activity. This is shown for both **A** the neuronal activity local to the vasculature and **B** the neuronal activity as a population.*

5.3.6 Neuronal Response to Spontaneous Locomotion

Locomotion onset traces are shown in figure 5.7 with their corresponding excitatory and SST interneuron neuronal responses. The pattern of locomotion shows a gradual small increase that then sharply increases from the 4-second time-point (Figure 5.7 (1, A; 1, B; 2, A; 2, B)). As a population, both excitatory and SST interneuron activity increases with locomotion, however, locally to a vessel, the excitatory response to locomotion onset is apparent but more variable than as a population. SST interneuron activity showed an increase in activity locally to the vessel. Although it can be seen that locomotion was sustained for a further 4 seconds, during this period, both the excitatory and SST interneuron activity return back to baseline, implying that this there is a response to initial locomotion onset, that is not maintained throughout locomotion.

Within the activity that occurred locally to the vasculature, there was significantly greater SST interneuron than excitatory activity ($F(1, 113) = 6.314$, $p = .013$). There was also significantly greater activity overall during the locomotion onset period than during the baseline period ($F(1, 113) = 5.959$, $p = .016$). There was not a significant interaction between the neuronal subtype and whether the baseline period or locomotion period was measured from within the local activity. Although there does appear to be more of a visible increase in the peak activity of SST interneurons, the variability in the local data renders this non-significant (Figure 5.8 A).

Within population activity, like the local activity, SST interneuron activity was significantly greater than excitatory ($F(1, 122) = 18.315$, $p < .001$), and overall activity during locomotion onset was significantly greater than the baseline period ($F(1, 122) = 17.461$, $p < .001$). Unlike the local activity, there was also a significant interaction between these two variables ($F(1, 122) = 6.871$, $p = .01$), and the pattern shown in figure 5.8 B indicates that the peak activity of SST-interneurons is more increased during locomotion onset from the baseline than is the excitatory activity.

5.4 Discussion

Two-photon imaging was used to investigate the patterns of activity of excitatory pyramidal cells and SST-positive interneurons to variations in a visual stimulus and locomotion.

5.4.1 Results Summary and Interpretation

5.4.1.1 Responses to Contrast Changes

Both pyramidal cell and SST interneuron activity increase significantly with increasing contrast, both locally to vessels and as a population. The vascular findings (chapter 4) also indicated significant increases in maximum diameter change with increasing contrast; based on this data, it therefore appears both of these neuronal subtypes have the potential to be correlated with the vascular response. There was overall greater SST-interneuron than pyramidal cell activation to the stimuli at all contrasts. As responses were normalised to pre-stimulus baseline activity, this is likely to reflect more stimulus-specific activation, as there is overall more pyramidal cell expression in layers I and II/III of the visual cortex (where most of the imaging took place) (Pakan et al., 2016).

This increase that occurred with increasing contrast from both excitatory cells and interneurons is congruent with Adesnik's (2017) findings, however those findings also reported increased excitatory activity at lower contrasts, and increased inhibitory activity at higher contrasts. This was not a prominent pattern in the current data, and in fact in the population data, pyramidal activity appeared to increase more than SST activity with increasing contrast when the mouse was not running (Figure 5.4 (1, A; 1,B)). This is likely due to our focus on SST-expressing interneurons, rather than interneuron activity as a collective. As this subtype of interneuron is thought to be integral in surround suppression in the context of increasing contrast (Johnson et al., 2018), it is unsurprising that its pattern of activity might deviate from that of interneurons of other subtypes that have not been implicated in this function.

For the purposes of this study, our interests do not inherently lie in the ratios of excitatory to inhibitory activity themselves, but in our ability to dissociate SST interneuron and pyramidal cell activity for the purpose of understanding the relationship of each with the vasculature. Within the context of changing contrast, this has been achieved through studying the interaction between contrast and locomotion. While the effect of contrast appears fairly consistent between excitatory cells and SST interneurons in the absence of locomotion, within the pyramidal cells, there appears to be an interaction with locomotion (although this was more prominent in the population than the local data in terms of significance), whereby increases in pyramidal cell activity with increasing contrast were somewhat masked by locomotion. This did not occur within SST interneurons, where there was no interaction between locomotion and the contrasts shown. This indicated that it is possible to use contrast in conjunction with locomotion in order to dissociate the responses of these neuronal subtypes.

It is of note that there were some differences between the local and population neuronal activity. Firstly, population excitatory activity responded significantly to contrast where local activity did not. In the locomotion groups, there is a visible increase with contrast as a population where there is not so clear within local activity. However this does appear less consistent and linear than the population response in the absence of locomotion, supported by a significant interaction between contrast and locomotion within this subset of the data. It is possible that this difference occurred due to lower N within the locomotion groups compared to the ‘No loco’ group, as running behaviour was relatively uncommon, leading to more variability.

The significant response to contrast within population excitatory activity could be due to the greater number of cells sampled from compared to local activity, which may have allowed more consistency within the results to allow effects to reach significance where they might not within the local data. A further difference of note was a significant effect of spatial

frequency within the population data, which was not apparent within the local data. The increased activity that occurred in response to the 0.04 cpd is congruent with previous research, which reported 0.03 cpd (Runyan et al., 2010) and 0.035 (Okun et al., 2015) as optimal spatial frequencies for various neuronal subtypes. It is of interest that this also interacted with contrast, especially within pyramidal cells. The lack of previous research probing spatial frequency specifically and intentionally means that this has, to the author's knowledge, not previously been probed. It appears in the current research that as contrast decreases, selectivity for spatial frequency also decreases, perhaps due to the decreasing visibility of the grating pattern. There is some evidence of increased response to 0.04 cpd within the local activity also, however in this case it was not significant. Again, this could be caused by a reduced number of cells sampled by the nature of imaging locally to the vasculature instead of with a wide field view.

This might also explain the reason why the population activity distinguished between the two locomotion groups ('Loco during stim' and 'Loco before and during stim'), where local activity did not. However, looking at the locomotion traces themselves of 'Loco before and during stim', it is evident that within the local activity, the locomotion appears to be increasing towards the stimulus period. Therefore, although there is locomotion throughout this period, it appears that the running speed is at its highest during the stimulus presentation. This however is less evident when looking at the same locomotion condition within the local activity. This difference is more evident within pyramidal cells, but could in addition to the effect of an increased number of sampled cells; contribute to the effect by increasing the pre-stimulus baseline activity levels.

5.4.1.2 Responses to Stimulus Size Changes

While there was a difference in activation of pyramidal cells and SST interneurons between the different sized stimuli, this did not occur in the expected direction based on the previous literature. It has previously been reported that SST interneuron activity increases, and

excitatory pyramidal cell activity decreases as stimulus size increases (Adesnik et al., 2012). However, in the current research, both of these neuronal subtypes increased with increasing stimulus size. Likewise when the mouse was running, this should have elicited a similar pattern of increased SST but decreased excitatory activity to the large stimulus and the reverse pattern in response to the small stimulus (Dipoppa et al., 2016), whereas the current study showed the expected increased SST activity to the larger stimulus, but no difference in pyramidal cell activity between the stimulus sizes. This lack of congruence with the literature regarding the stimulus size manipulation is likely due to difficulties with placement of the smaller stimulus, which was probably not optimal for the receptive fields of the sampled cells. There was some difficulty within the experimental procedure in finding the optimal position, and it could only be ensured that there was some activity from the cells in response to the small stimulus presentation. There is previous research suggesting that gamma power increases as stimulus size increases, while LFP of cells for which the receptive fields align with the position of the stimulus increase their activity in response to the smaller stimulus (Berens et al., 2010; Gieselmann & Thiele, 2008). It therefore seems likely that activity was measured with the stimulus in a non-optimal position, especially as other factors that affected neuronal response, such as appearance and movement of the stimulus, as well as locomotion very much complicated the determination of optimal positioning.

For the purposes of the current study, it is unimportant that previous findings regarding increased activity elicited by a smaller size stimulus were not replicated. The purpose of the stimulus manipulation was to differentially alter the activity of pyramidal cells and SST interneurons, and this was achieved. This can therefore be investigated in conjunction with changes in local blood vessel diameter in order to determine each neuronal subtype's respective association with vessel dilation.

The results were consistent with the previous results looking at local activity in response to contrast changes. There was also a change to the presence and absence of locomotion,

and within the pyramidal cells, the presence of locomotion appeared to mask any effect of the change of the stimulus, thus differentiating between excitatory and SST interneuron activity. There also wasn't any change in response based on spatial frequency. This is interesting, as the spatial frequency of 0.04 cycles per degree viewed as a small (20 degree), round stimulus wasn't visible as sinusoidal 'stripes', as with all of the other forms of stimulus (see chapter 2), but rather it would appear as half black and half white, entirely black, or entirely white at any given time point. It would therefore be intuitive to expect that this stimulus size might yield a larger difference between the spatial frequencies due to its more dramatic change in appearance. With this in addition to the findings of some differences between the local and population data within contrast changes, it could therefore be interesting to look into to what extent these results are reflected when looked at as a population as well as locally to the vessel; and whether there are similar differences as seen within the altered contrast dataset.

5.4.1.3 Responses to Spontaneous Locomotion

Within the local activity, both neuronal subtypes responded to locomotion onset, and there was overall more SST interneuron activity than pyramidal cell activity. However, when peak activity was compared between the pre-locomotion and locomotion onset period and between neuronal subtypes as an interaction, statistically there was not more of a peak response from SST to locomotion than pyramidal cells, in spite of extremely similar running speeds between neuronal subtypes. This is somewhat surprising considering the visible difference in the data, and considering that within population activity this interaction is significant, this could be due to variability in the data due to a lower N of cells.

It is important to note that mice in the current experiment did not run in complete darkness during spontaneous locomotion, as the screens in front of them were switched on. The responses found here were therefore congruent with those of Pakan (2016), who found that pyramidal cells and SST interneurons only increased activity to locomotion in the presence

of a grey screen and not in absolute darkness. Here, the mice were not in absolute darkness, but nor was the stimulus as obvious as that used in Pakan (2016). This raises interesting questions about the threshold at which a stimulus is considered visible enough in order to elicit a response from locomotion, and how different stimuli might affect the degree to which locomotion elicits responses from these neuronal subtypes. Considering the results yielded here when looking at these neuronal subtype responses to changing contrast as a population, it appears that the pattern of activity does somewhat change, especially within pyramidal cells when locomotion and changes in visual stimulus are studied in interaction. However the current results would suggest that the visual context actually becomes less important and has less of an effect on pyramidal cell activity with locomotion, but the current data also does not take factors such as running speed and arousal level into account, and so the findings would benefit from extension through investigation of these complexities of locomotion.

5.4.2 Limitations of the Current Study

As mentioned previously (chapter 4), here locomotion was studied in terms of whether it was present or not in relation to the stimulus. There is more complexity of locomotion to be explored that could be looked at further in future studies.

The comparison of local and population activity is also somewhat problematic in the context of the current study, due to the inherent increased variability of the local data, which has a reduced number of cells sampled by comparison to the population data. This could lead to apparent differences that are due to a larger N of cells with the wide field view, that increase consistency within the population data and allow differences to reach significance where they do not in the local view. This could lead to apparent differences that might not be valid, and could lead to a potentially false impression that the local activity is not reflected in the cells as a population. It is very difficult to tell where this might be the case, and therefore makes this comparison rather difficult to interpret.

In addition, a subset of SST interneurons have been shown to be co-localised with nNOS, (Perrenoud, Geoffroy, et al., 2012), an enzyme catalysing the production of NO, which dilates blood vessels (Faraci & Brian, 1994). So although previous studies have demonstrated vascular constriction in response to SST activity (Cauli et al., 2004), it is possible that some SST interneurons elicit in vasodilation. Here, we were only able to study SST interneurons in general, some of which might have been dilatory, and some of which may have been constrictive. As there may be SST interneurons with differing functions in relation to the vasculature, it would have been very useful to be able to separate out the respective activity of SST interneurons that were and were not co-localised with nNOS, especially locally to the vasculature, both in order to probe whether there are any differences in responses to the stimuli, and to later correlate the activity of each with vascular constriction and dilation.

5.4.3 Future Directions

Although the current study attempted to image activity of other subtypes of interneuron, including VIP and PV, we were unable to elicit expression from these subtypes. This would therefore be interesting to look at in future research, both in order to get a more well-rounded view of what is occurring within interneuron activity, and to elucidate the potential individual roles of other interneurons in neurovascular coupling. While there are studies suggesting that SST interneurons possess the capacity to dilate vessels (Perrenoud, Geoffroy, et al., 2012), VIP is also known to be a potent vasodilator (Yaksh, Wang, Go, & Harty, 1987), and in brain slices, channelrohdopsin-2 based photostimulation of PV expressing interneurons leads to constriction of penetrating arterioles (Urban et al., 2012). It would therefore be interesting to correlate the activity of both of these alternative interneuron subtypes with vascular dilation in order to better understand their potential roles in NVC.

Possible future work could also work further on understanding behavioural state, beyond merely whether or not there was locomotion, in order to improve our understanding of what is really underpinning the neuronal activity that we see. There is already evidence that there is a difference between the neuronal activity caused by arousal vs. locomotion per se (Vinck et al., 2015), and pupillommetry could be used to try to somewhat disentangle their respective effects here.

5.4.4 Conclusions

We were able to manipulate excitatory and SST interneuron activity through changing contrast and stimulus size, and their respective patterns of activity were differentiated from one another particularly well through the use of locomotion. These data will therefore next be used to correlate with vascular data detailed in chapter 4 (in which degree of dilation to the same stimulus manipulations was measured) in order to explore the relative roles of these neuronal subpopulations in NVC.

Chapter 6

Neurovascular Coupling in V1 of the Visual Cortex

6.1 Introduction

The previous chapters assessed how both vessel diameter and activity of pyramidal cells and SST interneurons change in V1 as a visual stimulus was manipulated. The current chapter will combine the results found in chapters 4 and 5 in order to assess how well pyramidal cell and SST interneuron activity relate to the vessel response. Looking at these data in conjunction will both: 1. Reveal the activity that correlates with blood vessel dilation specifically for SST interneurons and pyramidal cells (thus informing the level of activity from these subtypes that might occur when we see a BOLD response in V1), and 2. Provide some indication of the potential these neuronal subtypes might have to drive the blood vessel dilation response.

6.1.1 Vascular Diameter Change by Excitatory Cells and SST Interneurons

Prior research using ex vivo and in vivo pharmacology and optogentics has shown that activation of N-methyl-D-aspartate (NMDA) receptors in pyramidal cells leads to a COX-2-mediated release of prostaglandin E2 that leads to vasodilation in the rat cortex (Lacroix et al., 2015). Lecrux et al. (2011) characterised pyramidal cells in somatosensory cortex as 'neurogenic hubs' in NVC, in an experiment in which c-Fos was upregulated in pyramidal cells during CBF, and impairment of the cerebral blood flow response occurred through inhibition of COX-2 (expressed on a subset of pyramidal cells but not astrocytes) and through inhibition of astroglial oxidative metabolism; indicating importance of pyramidal cells and astrocytes in driving CBF response. Furthermore blockade of both GABA-A and NMDA receptors drove an additive decrease in CBF, thus indicating a joint action between these neuronal subtypes (Lecrux et al., 2011). It therefore seems that pyramidal cells in collaboration with interneurons and astrocytes, play a key role in driving vasodilation.

The ability of SST-expressing interneurons to dilate blood vessels is somewhat more questionable. Previous work in cortical slices showed that vascular dilation was induced by neurons expressing vasoactive intestinal peptide (VIP) or nitric oxide synthase (NOS),

however interneurons expressing SST elicited constriction from vessels (Cauli et al., 2004). However, this study yielded a low vessel response rate (only one SST neuron out of ten was shown to constrict a vessel), and looking at a single active neuron in relation to changes in vascular tone is unlikely to reflect the complex interactions between neuronal activity and vascular diameter change in vivo. Further in vivo research employing separate optogenetic stimulation of both NOS- and SST-expressing interneurons found that while activating NOS interneurons elicited a positive haemodynamic response, a short 2-second stimulation of SST-interneurons led to increased blood volume, while a longer, 16-second stimulation yielded the negative hemodynamic response; akin to the negative BOLD response (Lee et al., 2019). This raises interesting questions about how naturalistically evoked SST activity might affect CBF; as well as what effect activation of interneurons that might co-express SST and NOS might enact on the vasculature. Research looking into the GABAergic neurons in which neuronal nitric oxide synthase (nNOS) is expressed in the barrel cortex found that both type I and type II nNOS expressing neurons expressed SST (Perrenoud, Geoffroy, et al., 2012). Neuronal nitric oxide synthase is a catalyst of nitric oxide (NO), a potent vasodilator (Huang et al., 1995); and nNOS expressing interneurons can be divided into high and low expression of nNOS as type I and type II. Within the high-expression type I subtype, 91.5% expressed SST, and within the lower expression type II subtype, 18.7% expressed SST. This SST-nNOS colocalisation therefore suggests that it is possible that a subset of SST expressing interneurons dilate vessels.

6.1.2 Different vessel types in NVC

One factor that might affect the degree of NVC that occurs between a vessel and its local neuronal activity is the characteristics of the vessel itself, i.e. whether it might be considered to be an arteriole or a capillary. First order vessels have previously been found to dilate before the penetrating arteriole (Hall et al., 2014), and further work has shown that capillary endothelial cells sense neuronal activity and communicate this through potassium channels to upstream arterioles to signal them to dilate (Longden et al., 2017), which suggests that capillaries might better reflect their local neuronal activity than arterioles.

However, the current work has not found any difference in the time course over which vessels of different branch orders dilate (see chapter 2), which casts some doubt on whether NVC might vary at all over different branch orders. Other studies have indicated the importance of layer as the context for the direction in which propagation occurs. It was found in one study that dilation starts in deeper layers, then propagates upstream to the arteriole in shallower layers, before propagating to the local capillary bed within the shallower layers (Tian et al., 2010). As the majority of the current work was completed in layer 1, with some imaging in layer 2/3 and very little in layer 4; it might be expected that there will be little difference between arterioles and capillaries in the degree of NVC. Thirdly, it could be the case that the larger penetrating arterioles that supply the capillary network might better reflect the general dilation and neuronal activity of the region, and so might not be directly influenced by the local activity, but may still reflect it more closely due to it supplying the capillary bed.

6.1.3 Aims and Justifications for Current Study

The current research aims to use the same dataset used in chapters 4 and 5 in order to correlate the neuronal and vascular responses within pyramidal cells and SST interneurons, in order to gain an improved understanding of the neuronal subpopulations that are active during blood vessel dilations. Means from experimental conditions were compared in order to compare the overall pattern of activity that occurred within pyramidal cells and SST interneurons, and how this compared to the vessel dilations that occurred. Furthermore, binning the data into the mean groups allowed comparison of neuronal activity that occurred both locally to the vessel and as a population in order to assess to what extent local and population neuronal activity reflect blood vessel dilation. Individual vessel dilations were then plotted against their specific concurrent local neuronal activity in order to visualise the relationship between these variables and the degree of variability incurred. Further to this, as there is evidence that the degree of local NVC might vary by vessel type (Longden et al., 2017), correlations were also split up by branch order and resting vessel diameter.

Furthermore, as there is evidence discussed in chapter 5 regarding locomotion-induced pyramidal cell and SST-interneuron activity, which has not before been looked at in conjunction with vascular dilation, the dataset was also divided by the locomotion that occurred during presentation of the stimulus, and NVC during spontaneous locomotion was also looked at separately in order to judge whether NVC might vary with behavioural state.

It was hypothesised that pyramidal cell activity would have a strong correlation with vessel dilation that is consistent across vessel types due to previous research showing pyramidal cell activity elicits dilation across vessel types through both interneurons and astrocytes (Mishra et al., 2016), as well as findings of their direct dilation of the vasculature (Lacroix et al., 2015). It was also hypothesised that SST activity would likely correlate positively with blood vessel dilation due to previous studies indicating that their stimulation leads to increased CBV (Lee et al., 2019), however the relationship between blood vessel dilation and SST is not as well researched, and some research has indicated that this subpopulation constricts blood vessels (Cauli et al., 2004). It might therefore be expected that the relationship between SST activity and vessel dilation is more varied and less consistent than pyramidal cells, and might depend more on factors such as the location of the vessel within the vascular network.

6.2 Methods and Materials

Details of the methods used in this chapter can be found in the main methods section (chapter 2).

6.2.1 Animal Subjects

Adult male and female C57BL mice aged between 3 – 8 months were used in these experiments. Transgenic mice, (Thy1 GCaMP (n = 3) and heterozygous SST cre GCaMP crossed (n = 5)) in which increased intracellular calcium elicited fluorescent signal were used to measure changes in neuronal activity in either excitatory pyramidal cells, or SST interneurons. Animals were housed in a 12-hour reverse light/dark cycle to encourage locomotion during imaging.

6.2.2 Experimental procedure

After recovery, habituation of the mice was carried out detailed in main methods (chapter 2).

Mice were injected with a fluorescent dye (see chapter 2) to visualise the vascular lumen, and the intracellular calcium release was concurrently measured as described in section 5. The region of interest was tested for responsiveness (see section 5 for elaboration), and mice were then presented with a drifting grating that was varied as described in section 5.

6.2.3 Cell Processing

Details of calcium analysis are provided in chapter 2, and a brief overview of the process is provided in the chapter 5 methods.

6.2.4 Vessel Processing

Details of vessel analysis are provided in chapter 2, and a brief overview is provided in the chapter 3 methods.

6.2.5 Data Analysis

Data were then divided into groups based on the variable to be looked at. Where differing stimulus types and locomotion groups were analysed, all vessel types were included from the dataset. Where differing vessel branch orders or diameters were examined, all locomotion groups (except spontaneous) and stimulus types were included in the analysis. All data analysis was performed using MATLAB (MathWorks) and GraphPad Prism 8. Fisher r-to-z transformations were calculated to compare correlations using the website http://vassarstats.net/rdiff.html.

6.3 Results

In chapter 4, the response of vessels to changes in contrast ((5%, 25%, 63%, 100%) and stimulus size (20 degrees, or 220 degrees (full screen)), as well as concurrent and spontaneous (without the stimuli) locomotion were characterised. In chapter 5, the concurrently recorded local neuronal activity of excitatory cells and SST interneurons was characterised in response to the same stimulus manipulations. Additionally, population activity was recorded in order to show whether this reflects the local activity, but this was not carried out concurrently with the vessel due to the wide field view.

Here, these findings are combined in order to look at the relationship between vascular diameter change and activity of neuronal subtypes in order to understand which subtypes are active during CBF change. The data garnered in chapters 4 and 5 are shown here side-by-side in order to better assess any potential relationship between activity of each neuronal subtype and vessel response in figure 6.1 and 6.2. Based on this comparison, SST appears to more closely match the vascular response, as excitatory activity does look like it dissociates from the vessel response under certain circumstances. This is especially evident in figure 6.1 A, in which it appears that excitatory cells fail to maintain response to stimulus during running, while the vessel continues to show this response (as does SST) (see chapters 4 and 5 for statistical analysis). This effect appears more subtle during contrast manipulation, but it was the case that while the vessel was still sensitive to contrast change regardless of whether the mouse was running (figure 6.2); both local (figure 6.2 A) and population (figure 6.2 C) excitatory activity were less sensitive to changing contrast during running. SST (figure 6.2 B, D) however, did not vary in its sensitivity to contrast across locomotion conditions (more akin to the pattern shown by the vessel) (see chapters 4 and 5 for statistical analysis).

In the case of the contrast manipulation, the mean neuronal subtype activation for different experimental groups and the mean corresponding blood vessel response could be directly

correlated (as there were 4 contrast groups to correlate). Figure 6.3 shows the correlations between vessel dilation and both local and population activity within pyramidal cells and SST interneurons. Both local and population excitatory cells and SST interneurons correlated significantly with vessel dilation when the mice weren't running (see figure 6.3 for r and p values), and these correlations were not significantly different from each other, indicating that both could potentially underpin blood vessel dilation. Furthermore for each type of neuron, the correlations were no different whether neurons were sampled locally to the vessel or across the wider population (see figure 6.3 for comparisons between correlations, however the small N of averaged groups lowers the power of this comparative test).

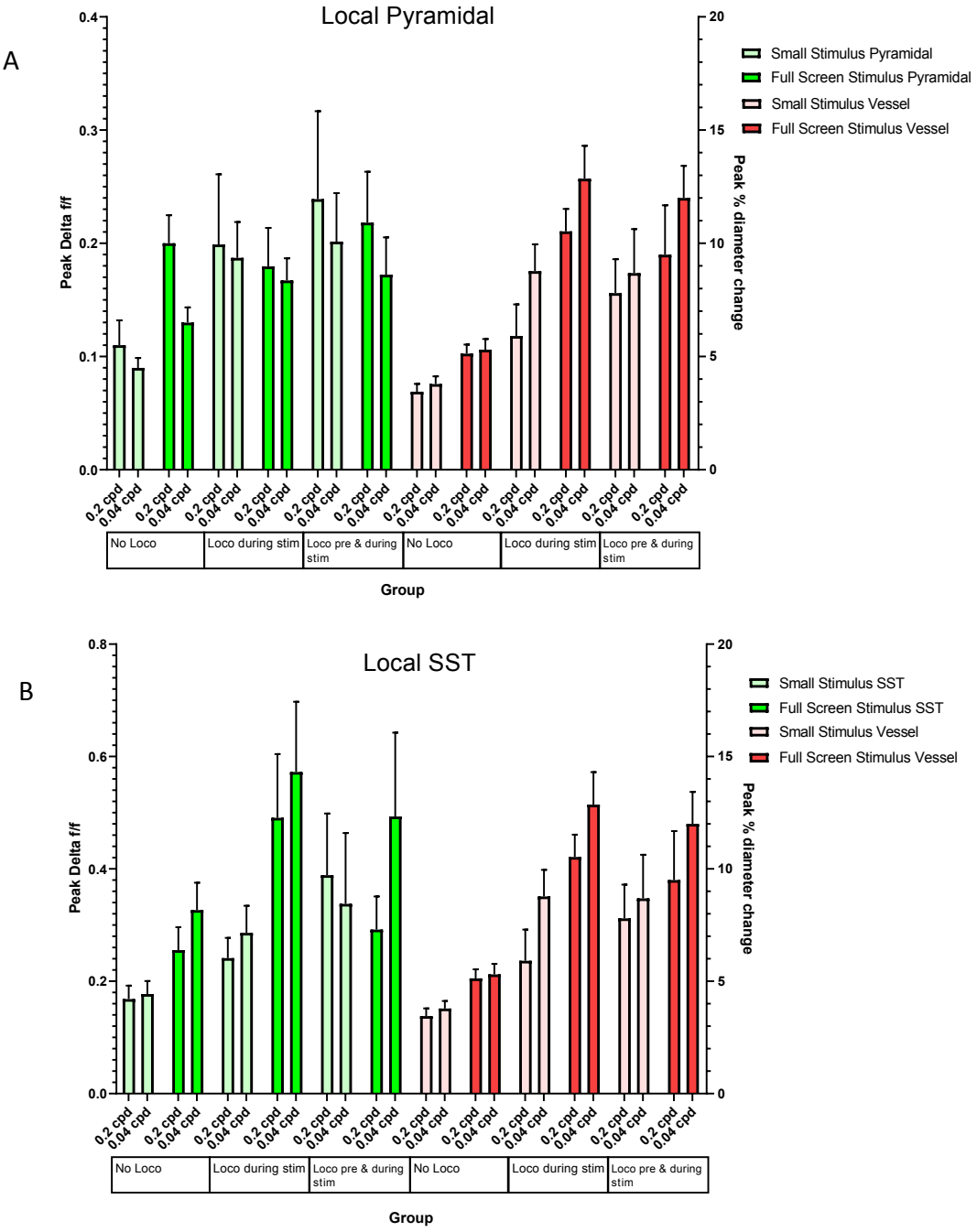

Figure 6.1. Comparison of (A) excitatory and (B) SST activity with degree of blood vessel response when stimulus size was manipulated.
No Loco: N = 109-113; Loco during stim: N = 23-47; Loco before and during stim: N = 19-24.

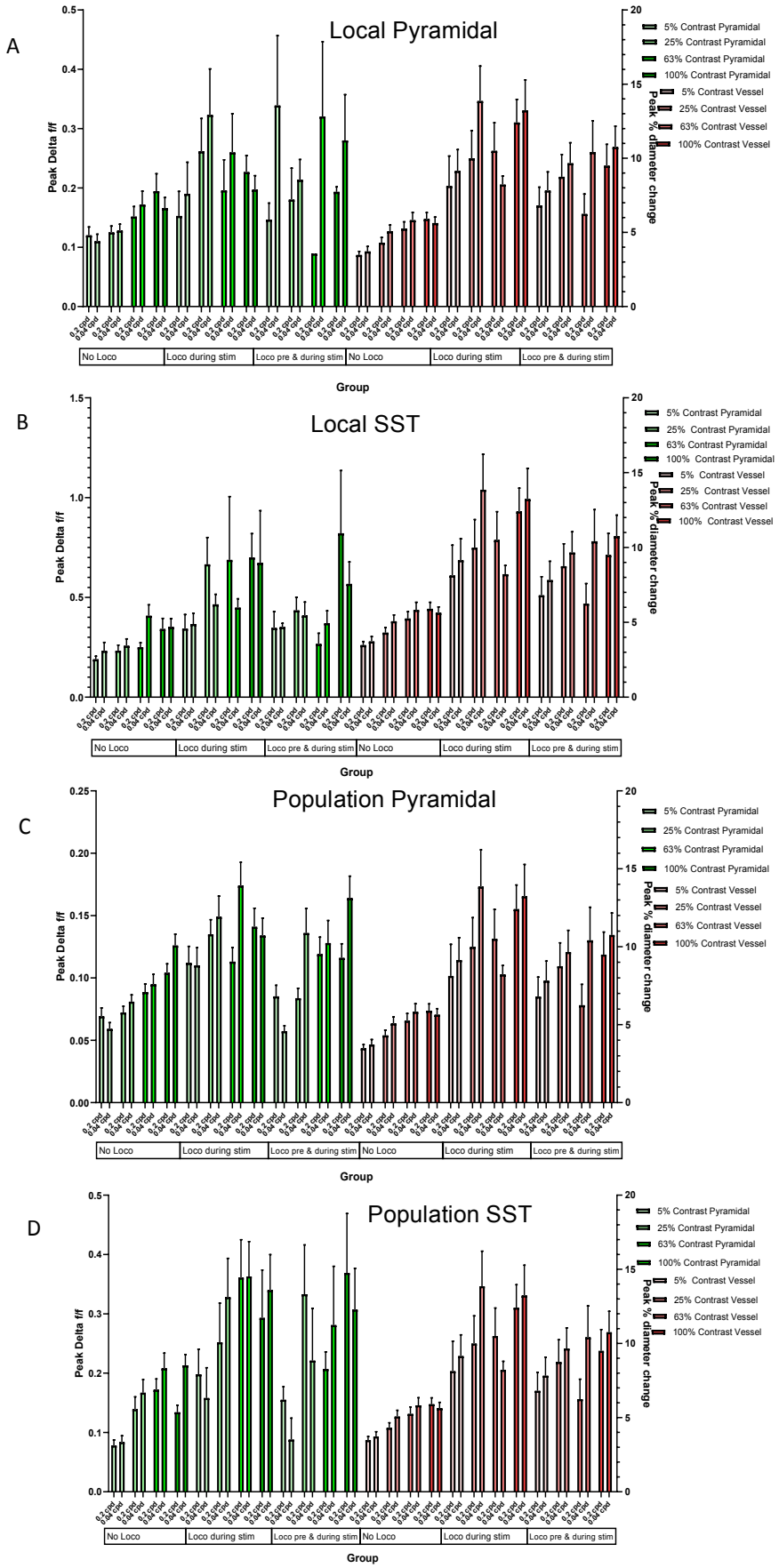

Figure 6.2. Comparison of (A, C) excitatory and (B, D) SST activity with degree of blood vessel response when contrast was manipulated.

*Activity that was local to the vessel is shown in **A** and **B**, population activity (not recorded concurrently with vascular response) is shown in **C** and **D**. No loco: N = 97-112; Loco during stim: N = 14-38; Loco before and during stim: N = 10-25.*

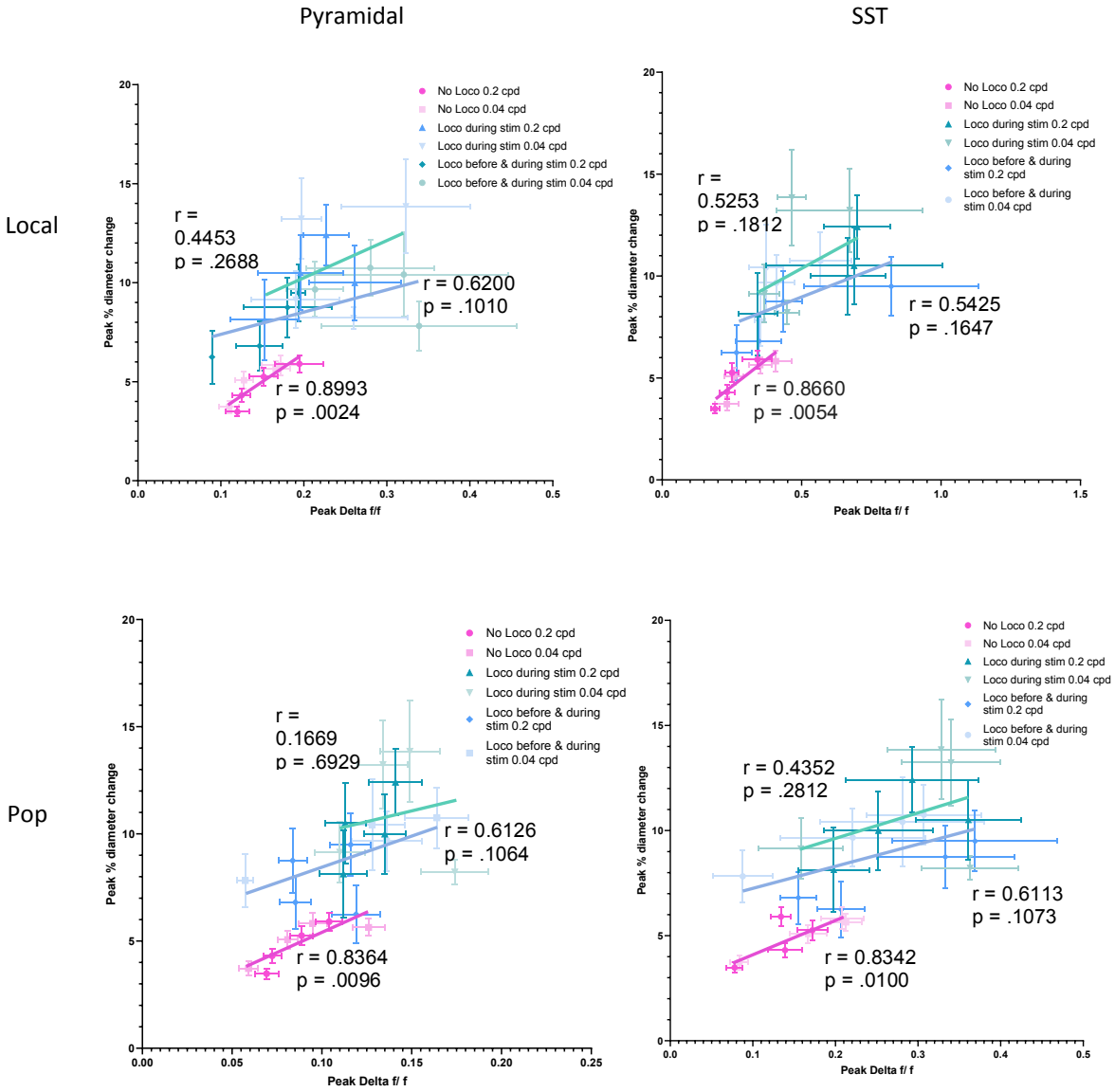

Figure 6.3. Correlation of the means between Pyramidal and SST Neuronal activity and Vessel diameter change with changing contrast and locomotion (+/- 1SEM).
(Top) *Activity local to the vessel, and (**Bottom**) activity as a population (not recorded concurrently with vessel response) from (**left**) excitatory pyramidal cell activity and (**right**) SST interneuron activity. Linear regression lines collapse across spatial frequency groups.*
Comparisons for each neuronal subtype between local and population activity showed no difference: Pyramidal, No Loco: z = .0.41, p = .6818; Pyramidal, Loco during stim: z = 0.49, p = .6241; Pyramidal, Loco before & during stim: z = 0.02, p = .984; SST, No Loco: z = 0.18, p = .8572; SST, Loco during stim: z = 0.19, p = .849; SST, Loco before and during stim: z = 0.16, p = .8729.
Comparisons between neuronal subtypes: Local, no loco: z = 0.24,, p = .8103; Local, loco during stim: z = -0.17, p = .865; Local, loco before & during stim: z = -0.17, p = .865; Pop, no loco: z = 0.01, p = .992; Pop, loco during stim: -0.47, p = .6384, Pop, loco before & during stim: z= < .0001, p = 1.000.

6.3.1 Response to differing stimulus types

If neurons are acting very locally to dilate vessels, the correlations between individual pairs of calcium and vessel responses should be better correlated than the means presented above. Therefore, having established the relationship between the neuronal subtypes and vessel diameter change in terms of the group means, the peak vascular and neuronal response gained for each vessel was extracted in order to correlate this for both excitatory cells and SST interneurons and characterise the relationship further. In order to test this, a linear regression was carried out, which yielded information about the R square value, the F statistic, and p value. The R square value yields a number between 0 and 1 that indicates how good a fit the data are to the linear regression line, and therefore indicates how well the model explains the variability in the data. The F value indicates the degree to which the slope is non-zero. The model we have is compared against a model with no predictors in order to yield an F value and a p value, which tells us whether our model explains the data significantly better than the model with no predictors. A Pearson's r value was also calculated inform the strength of the association. Where appropriate, correlations were also compared using the Fisher r-to-z transformation, yielding a z value and p value.

A linear regression for all data collected across stimulus types and locomotion groups is shown in figure 6.4, and further supports the previous data suggesting that SST activity more closely follows vessel diameter change than does excitatory activity. There was a great deal of variation around linear regression lines, and activity of neither neuronal subtype predicted vascular diameter to the extent that it could be concluded that one is solely responsible. However, SST interneurons predicted vascular diameter changes significantly better than excitatory cells, and a greater degree of vascular dilation could occur in the absence of excitatory activity than SST interneuron activity, indicating that a different neuronal subtype other than pyramidal cells must have been driving that dilation. It is theoretically possible that it could be population excitatory activity driving this, however the fact that SST-interneurons yielded a smaller y-intercept indicates that less vessel

dilation could comparatively occur in the absence of local SST interneuron activity, and it is therefore more integral in potentially dilating the vessel

When the data were split up by locomotion group (i.e. whether mice were running during the stimulus, before and during stimulus, or not at all), SST showed stronger and more consistent correlations with blood vessel diameter change across locomotion groups than did pyramidal cells. The data were then split further into the individual stimulus manipulations in order to understand whether there was consistency between contrast and size manipulations. Generally there was still a trend towards greater correlations between SST interneuron activity and vessel dilation, but this was not consistent, nor significant, although the pattern of vascular dilation occurring in the absence of excitatory vs. SST interneuron activity was fairly consistent with the overall dataset. The significantly weaker correlation between SST activity and vessel dilation during stimulus size manipulation compared to contrast manipulation indicates that this is some degree of genuine decoupling.

SST also trended towards a stronger NVC relationship during spontaneous locomotion, however, this was not significantly greater than excitatory cells, so it appears both cell types might be related to vessel dilation in response to locomotion to some degree (Figure 6.7). However, due to the lower N within spontaneous locomotion data, this trend towards a stronger SST correlation might still indicate a similar relationship between the neuronal subtypes and blood vessel dilation as is seen within the stimulus presentation data, however greater N may be required in order to more confidently establish whether or not the relationship between activity of the neuronal subtypes tested and blood vessel dilation is consistent across behavioural states.

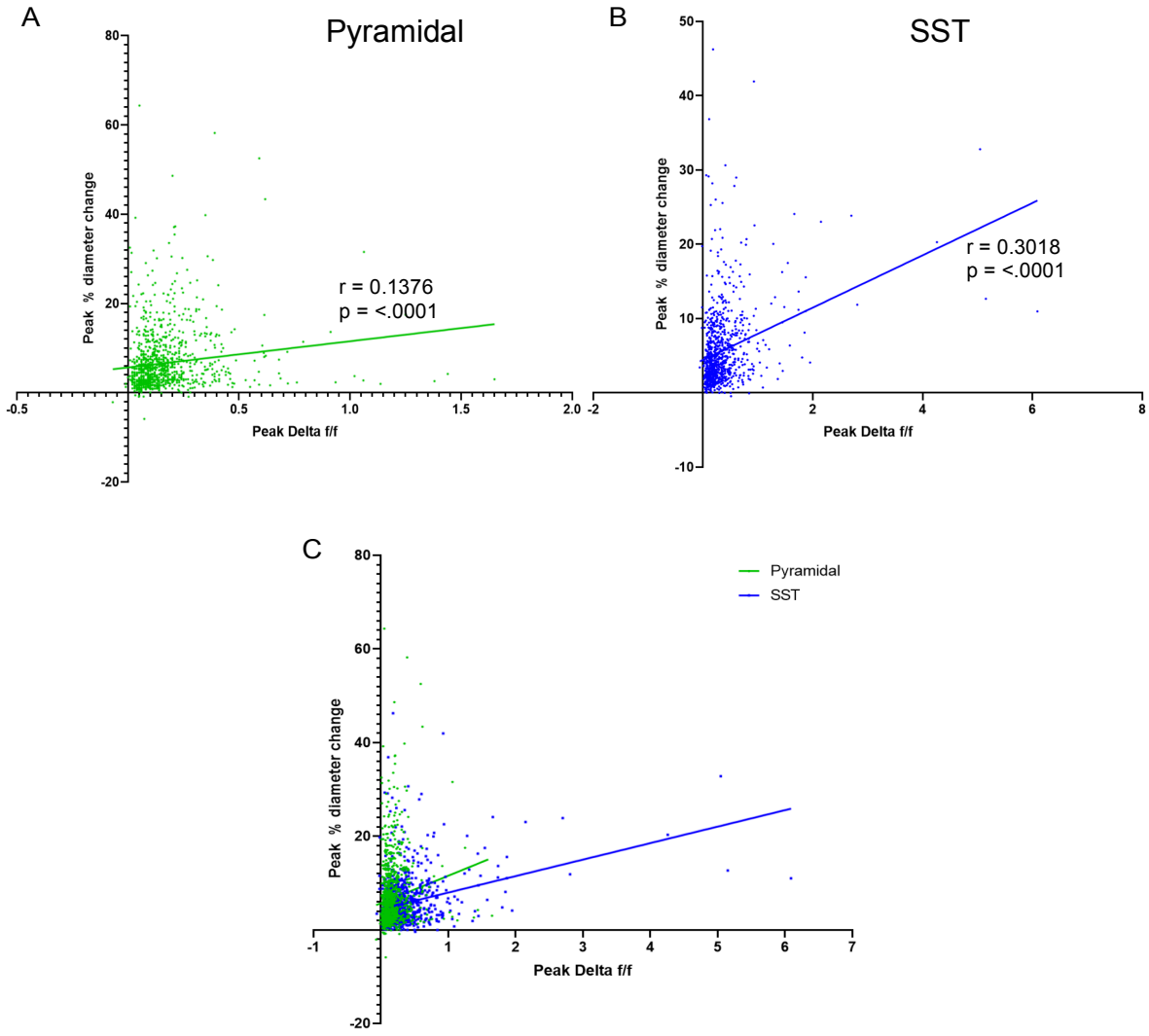

Figure 6.4. Correlations between peak vessel diameter change and peak change in neuronal activity to all stimulus types (including all locomotion groups).
A *pyramidal cell activity (N = 1373),* ***B*** *SST interneuron activity (N = 890),* ***C*** *pyramidal cell and SST interneuron activity together for comparison. Difference between correlations, z = -4.02, p = .0001.*

When taken altogether, looking at all stimulus types (all conditions with contrast and stimulus size; and all locomotion groups); there was a small positive correlation between pyramidal cell activity and corresponding blood vessel response ($F(1, 1371) = 26.46$, $R^2 = 0.019$, $r = 0.1376$, $p < .0001$) (Figure 6.4 A). There was also a stronger positive correlation between SST interneuron activity and blood vessel response ($F(1, 888) = 89.02$, $R^2 = 0.091$, $r = 0.3018$, $p < .0001$) (Figure 6.4 B). The correlations are significantly different from one another ($z = -4.02$, $p = .0001$), indicating tighter coupling between SST interneuron activity and blood vessel response compared to excitatory activity. Furthermore the greater y-intercept of pyramidal cell activity indicates that more dilation occurs in the absence of pyramidal cell activity compared to SST activity, and that this dilation must be driven via an alternative mechanism. Notably, these correlations are both relatively weak in terms of how well the data fits the model, and it is likely that other neuronal subtypes might also explain some of the variation in vessel response.

As pyramidal cells and SST interneurons responded differently to co-occurring locomotion and stimulus manipulation, the overall dataset was then split up into the different locomotion groups. Within pyramidal cells, there was only a significant correlation with vessel response when there was locomotion before and during stim ($F(1, 95) = 7.353$, $R^2 = 0.07184$, $p = .0079$), and there was a significant difference between the No loco and Loco before and during stim correlations ($z = -2.25$, $p = .0244$) (Figure 6.5 A). However, the correlations between SST calcium and vessel responses were significant for all loco groups (No loco ($F(1, 578) = 32.10$, $R^2 = 0.0526$, $p < .0001$); Loco during stim ($F(1, 155) = 11.72$, $R^2 = .0703$, $p = .0008$); and Loco before & during stim ($F(1, 124) = 8.950$, $R^2 = .0673$, $p = .0033$)), with no significant differences between the correlations (see figure for statistical analysis) (Figure 6.5 B). As vascular response is always predicted by SST interneuron activity regardless of the pattern of locomotion occurring, and excitatory activity is not, this strongly indicates that an increase in CBF is a closer report of the SST activity than it is the pyramidal cells activity. Of note here (figure 6.5 A) the correlation between single excitatory activity and blood vessel responses was weak and not significant when the mouse was at

rest, unlike when looking at mean data (figure 6.1 A; figure 6.2 A). This might mean that vessel dilation isn't being driven by such local excitatory cells, but by activity over a wider area; or that although on average, vessel dilation increases and excitatory activity increases, for example, as stimulus contrast increases; it is an alternative neuronal subtype also demonstrating this pattern of activity that is directly dilating vessels rather than pyramidal cells.

The NVC that occurred within specific types of stimulus presentation (contrast and size manipulation) was next established in order to check the consistency of results between stimulus manipulations and also ascertain whether there was any difference in the abilities of changing stimulus contrast and size to reveal any differences in NVC between neuronal subtypes (Figure 6.6). SST calcium correlated with vessel responses better when contrast was being varied, compared to when stimulus size was being varied. Pyramidal cell calcium was consistent in its correlation with blood vessel response across contrast or stimulus size manipulations. Excitatory activity appears to correlate significantly with dilation during stimulus size manipulation when the mouse was running before and during the stimulus, however this did not actually differ significantly from the non-significant SST correlation in the same group. There were groups in which the correlation with vessel dilation was significant for SST but not pyramidal cells, but only when contrast was manipulated (No loco: $p < .0001$; Loco during stim: $p = .0030$; and Loco before & during stim: $p = .0117$). However there were still only significant differences between pyramidal cell and SST activity correlations in the No loco condition (see figure 6.6 for analysis), and there were no significant correlations between SST activity and vessel dilation when stimulus size was manipulated. Moreover, the difference between the correlations between SST activity and vessel dilation were significant between stimulus manipulation types when the mouse was not running ($z = 2.6$, $p = .0093$). The general lack of significant differences between neuronal subtypes could be due to the reduced N that is yielded by dividing the overall dataset into these locomotion and stimulus groups. This could also easily bias the dataset through variation in factors such as vessel resting diameters, which are shown later

to affect degree of NVC (see figure 6.10). However the average diameter across contrast and stimulus size manipulations was approximately the same (5.6 μm and 5.9 μm for contrast and stimulus size respectively). The comparative lack of blood vessel response to SST activation when stimulus size was manipulated compared to when contrast was manipulated might therefore be a genuine example of dissociation between SST activity and vessel dilation and suggests that while SST still appears to be a better predictor of the vessel dilation than excitatory activity does, it is still far from a perfect predictor, and may dissociate from vascular response during stimulus size manipulation.

Within the stimulus size dataset, neither neuronal subtype correlated significantly with the degree of vascular dilation for the most part; and there were no significant differences between the neuronal subtype correlations. Within the loco before & during stim group, there was a significant correlation within the pyramidal cells with vascular diameter change, however the difference between the SST and pyramidal cell correlations was not significant, (see figure 6.6 for analysis).

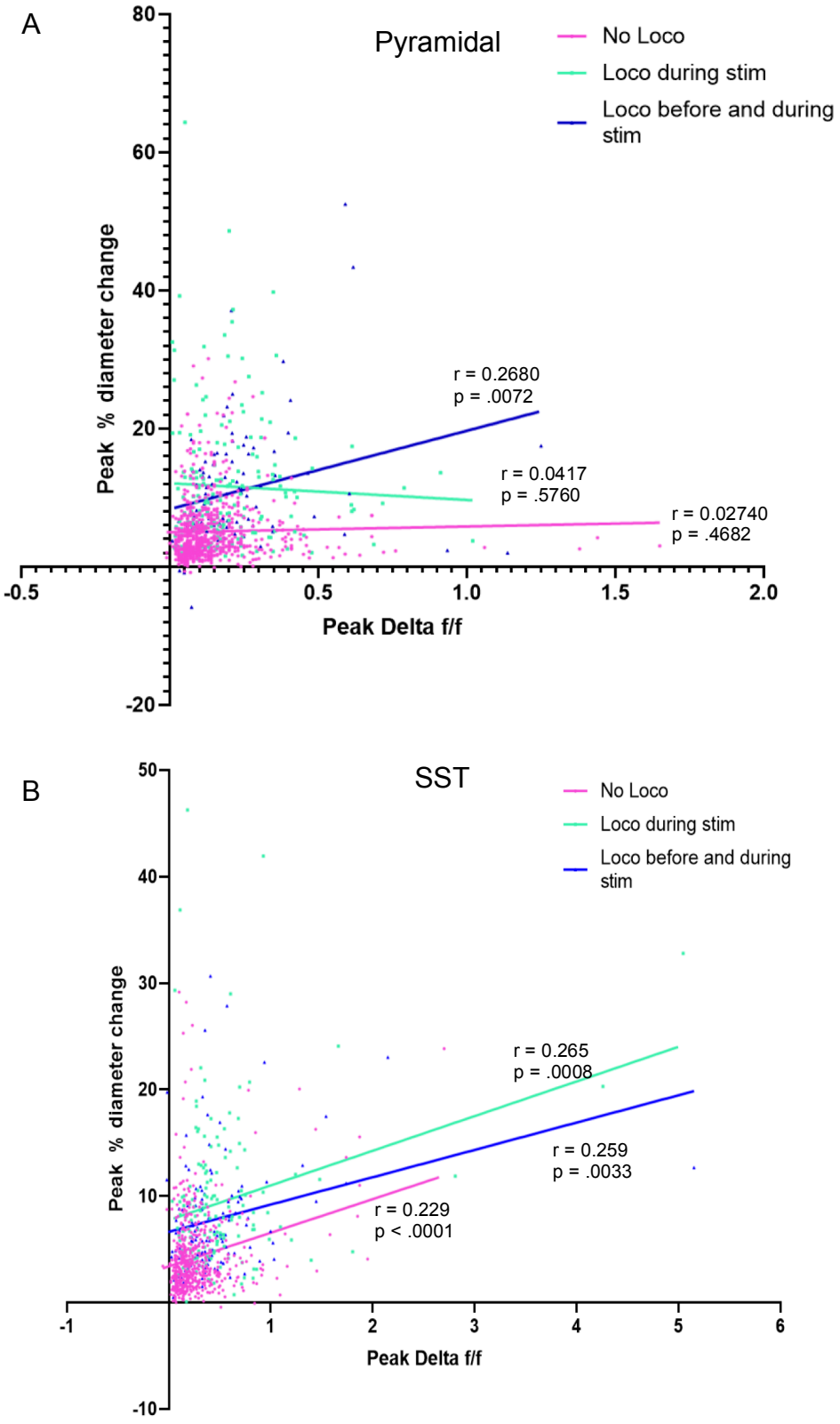

Figure 6.5. Correlations between peak vessel diameter change and peak change in neuronal activity to all stimulus types split up by locomotion group.
A *Correlations within pyramidal cells; No Loco: N = 703; Loco during stim: N = 182; Loco before and during stim: N = 97;* ***B*** *Correlations within SST interneurons; No Loco: N = 580; Loco during stim: N = 157; Loco before and during stim: N = 126.*
Differences between correlations: ***A*** *No Loco and loco during stim: z = -.17, p = .865; No Loco and Loco before and during stim: z = -2.25, p = .0244; Loco during stim and loco before and during stim: z = -1.83, p = .0673.*
B *No Loco and loco during stim: z = -.42, p = .6745; No Loco and Loco before and during stim: z = -0.32, p = .3745; Loco during stim and loco before and during stim: z = 0.05, p = .9601.*

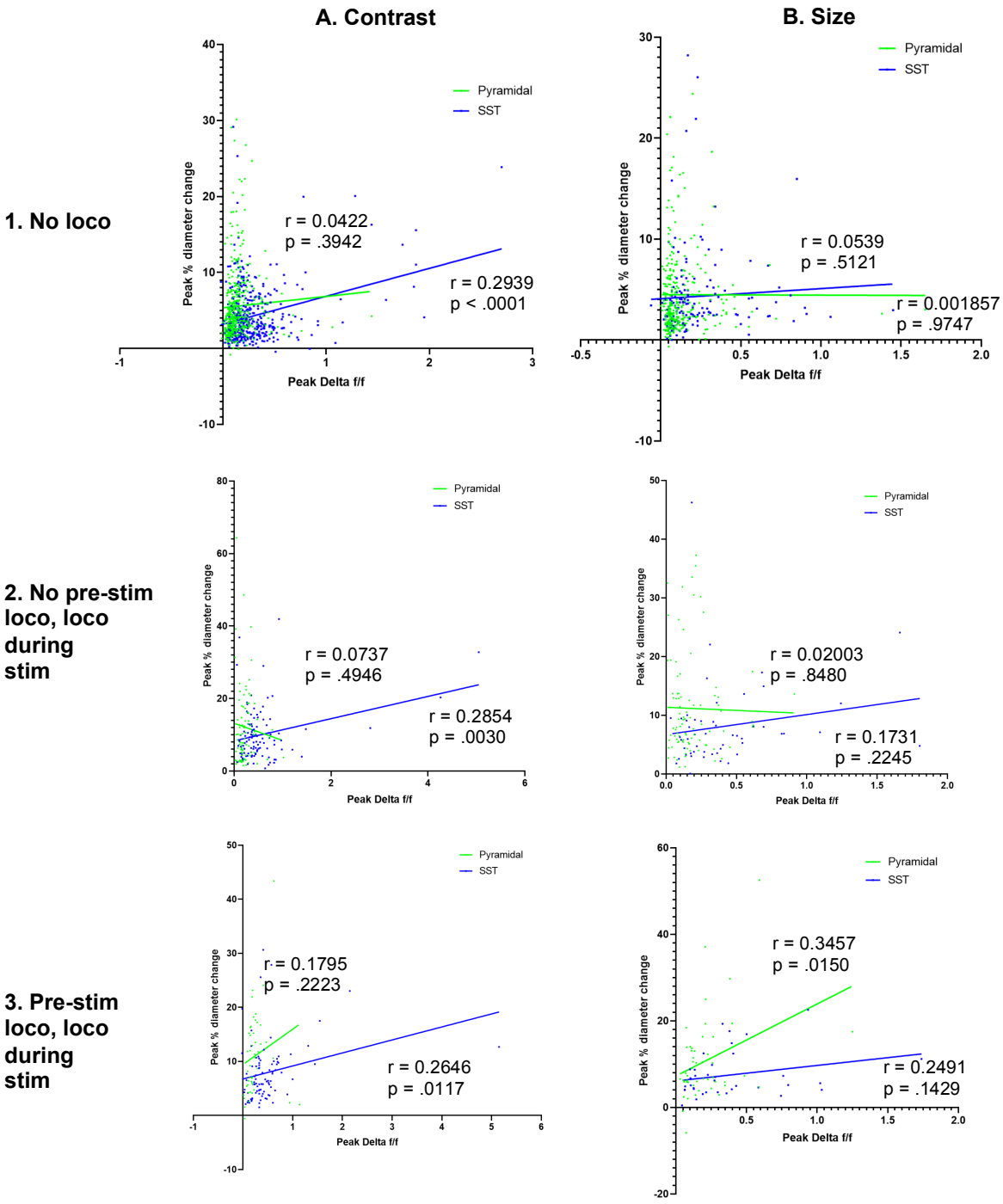

Figure 6.6. Correlations between peak vessel diameter change and peak change in neuronal activity to all stimulus types, split up by locomotion group and stimulus manipulation type.
*Diameter vs calcium changes for **A** contrast manipulation, **B** stimulus size manipulation for the three locomotion (**1-3**). Difference between correlations: **1**. Contrast: N = 409-430, z = -3.76, p = .0002; Stim size: N = 150-294, z =-.0.52, p = .6031; **2** Contrast: N = 88-106, z = -1.5, p = .1336; Stim size: N = 51-94, z = -0.87, p = .3843; **3** Contrast: N = 48-90, z = -0.49, p = .6241; Stim size: N = 36-49, z = 0.47, p = .6384.*

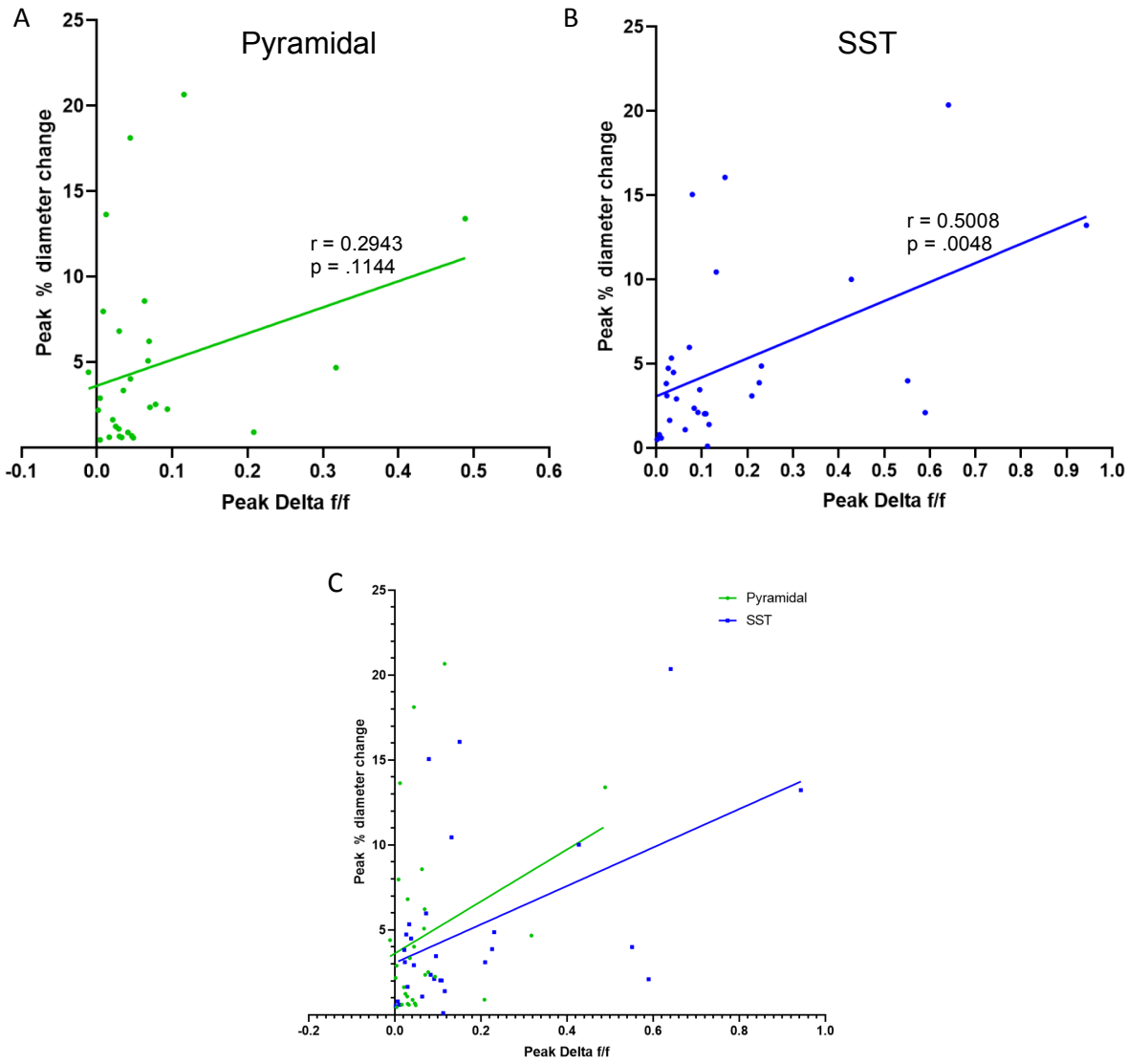

Figure 6.7. Correlations between peak vessel diameter change and peak change in neuronal activity to spontaneous locomotion.
A *shows pyramidal cell activity,* ***B*** *shows SST interneuron activity,* ***C*** *shows pyramidal cell and SST interneuron activity together for comparison.*
N = 30 and 30, difference between correlations: z = -0.91, p = .3628.

When mice spontaneously ran (in low ambient light without periodic visual stimulus) there was a significant, medium correlation between SST interneuron activity and vascular diameter change ($F(1, 28) = 9.375$, $R^2 = 0.2508$, $p = .0048$), while the correlation between excitatory activity and vascular diameter change was smaller and not significant. However, the difference between the correlations was non-significant, and the Y-intercepts were also not significantly different from one another. Therefore based on these data alone (with a relatively small sample size of 30 responses for each neuron type), we can't conclude that SST interneurons more strongly drive vascular responses to running than do pyramidal cells (Figure 6.7).

6.3.2 Differences between vessel types

Vessels were then split up by their branch order (using the alternative method of determining branch order; chapter 3) and resting diameters in order to assess whether activity of certain types of vessels was more strongly coupled to activity from either neuronal subtype. This was carried out due to previous findings of different NVC mechanisms to capillaries and arterioles (Mishra et al., 2016).

Both branch order and resting diameter were shown to affect the degree of NVC. Branch order only affected the relationship between SST neurons and the vasculature, not that between excitatory cells and the vasculature. Baseline diameter modulated NVC for both types of neurons Overall, the general pattern was that higher branch order; higher diameter vessels demonstrated a stronger NVC relationship, as assessed by the strength of the correlations, with both neuronal subtypes. A slight divergence from this rule was seen within the penetrating arteriole, where responses in the vessel section after the first branch showed a higher correlation with local SST activity than with either more superficial or deep sections. No differences were found between dilation of different sections of the penetrating arteriole and pyramidal cell activity.

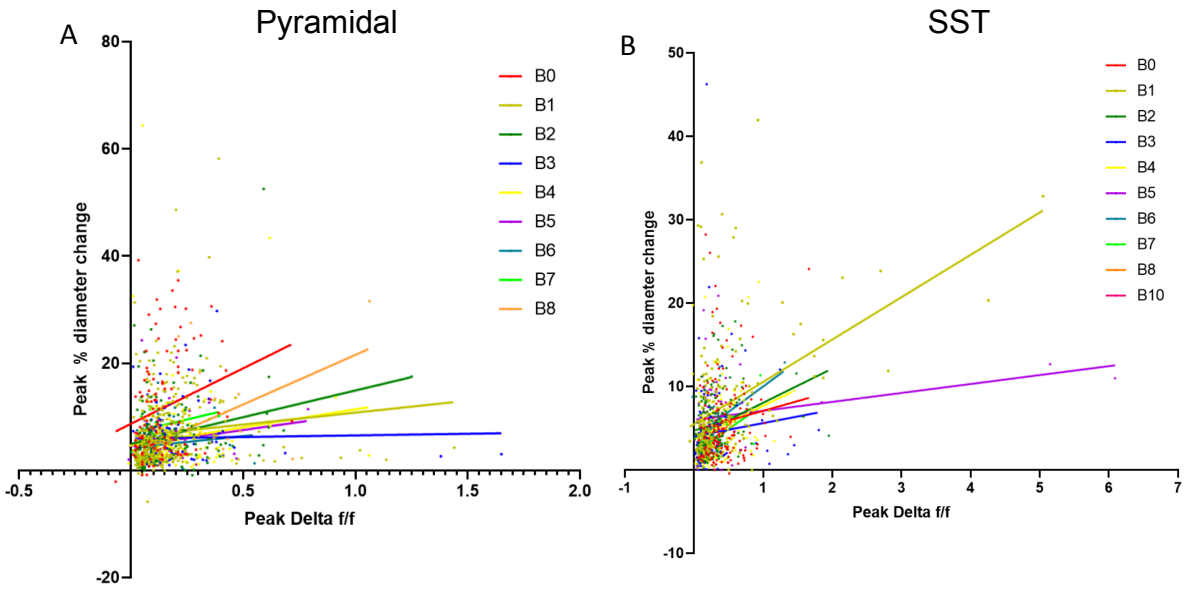

Figure 6.8. Correlations between peak vessel diameter change and peak change in neuronal activity to all stimulus types and locomotion levels divided by branch order using the alternative method
A *shows correlations within pyramidal cells, N = 14-332;* ***B*** *shows responses from SST interneurons, N = 9-194.*

Branch Order	0	1	2	3	4	5	6	7	8
F	7.13	3.38	11.8	0.0804	2.64	1.73	0.746	1.24	11.3
R^2	0.0614	0.0101	0.0674	0.000658	0.0177	0.0295	0.0183	0.0937	0.281
r	0.2477	0.1005	0.2596	0.02565	0.1330	0.1718	0.1353	0.3061	0.5301
P value	.0088	.0671	.0008	.7774	.1063	.1933	.3928	.2867	.0022
N	111	332	165	124	149	59	42	14	31

Table 6.1. Statistics corresponding to Figure 6.8 A, showing pyramidal cell correlations. *Degrees of freedom (left to right): 1, 109; 1, 330; 1, 163; 1, 122; 1, 147; 1, 57; 1, 40; 1, 12; 1, 29*

Branch Order	0	1	2	3	4	5	6	7	8	9	10
F	1.87	43.2	17.0	1.09	6.46	3.25	9.13	14.3	4.77		1.39
R^2	0.0127	0.192	0.0814	0.00909	0.0524	0.0598	0.246	0.405	0.462		0.148
r	0.1127	0.4382	0.2853	0.09534	0.2289	0.2445	0.4960	0.6364	0.6797		0.3847
P value	.1735	<.0001	<.0001	.2981	.0123	.0775	.0053	.0011	.0667		.2716
N	147	184	194	121	119	53	30	23	9		10

Table 6.2. Statistics corresponding to Figure 6.8 B, showing SST correlations. *Degrees of freedom (left to right): 1, 145; 1, 182; 1, 192; 1, 119; 1, 117; 1, 51; 1, 28; 1, 21; 1, 8.*

Looking across all branches on and beyond the penetrating arteriole, the branch with the strongest correlation within each subtype was selected and compared against the other branches. There were no significant differences between correlations with excitatory cells. For SST cells, the strongest correlation occurred for branch 1 vessels (Figure 6.8, B), and was significantly difference from other branch orders including 0 ($z = 3.19$, $p = .0014$); 3 ($z = 3.16$, $p = .0016$); and 4 ($z = 1.99$, $p = .0233$), indicating that SST activity was more closely matched with blood vessel dilation on branch order 1. To compare between neuronal subtypes, the branches that correlated most strongly in their dilation with the activity of pyramidal cells and SST interneurons respectively are compared. Branch order 1 (the branch on which coupling between vessel dilation and SST activity was strongest) had a significantly stronger relationship between its dilation and SST neuronal activity than pyramidal cell activity ($z = 3.99$, $p = .0001$). Branch order 2 (the branch on which coupling between vessel dilation and pyramidal cell activity was strongest) did not show a difference between its coupling to pyramidal cell or SST activity ($z = -0.12$, $p = .7949$). This might further indicate that branch order is more useful in determining the relationship between neuronal activity and vessel dilation across the vasculature specifically when looking at SST NVC rather than pyramidal cell NVC.

This suggests that the degree of NVC that occurs between a vessel and its local SST activity varies across branch orders. However within both neuronal subtypes, the pattern of significance was somewhat erratic, (see Tables 6.1 and 6.2). Within pyramidal cells, the correlation within branch order 0 and branch order 2 were significant, while within branch order 1 it was not (although it was close to significance) (Table 6.1). Within SST interneurons, branch order 3 is non-significant despite the immediate lower and higher branch orders being significant (Table 6.2). There is no reason to expect the significance to change between branch orders in this manner, and this might indicate inconsistency in using branch order as a method of characterising the relationship between these particular neuronal subtypes with the vasculature. Furthermore, branch orders farther from the penetrating arteriole than branch order 2 did not correlate significantly with pyramidal cell

activity; except the farthest branch order (branch order 8) (Table 6.1). Again it might be expected that high branch order capillaries would correspond similarly to one another in terms of their dilation and how this relates to the neuronal activity around them, and so these differences between capillary correlations at different branch orders is not expected. Taken together, this suggests that branch order might not be a very consistent method to use in order to characterise the relationship between neuronal activity and vessel dilation across the vascular tree, however the smaller sample size of certain branches might be affecting this.

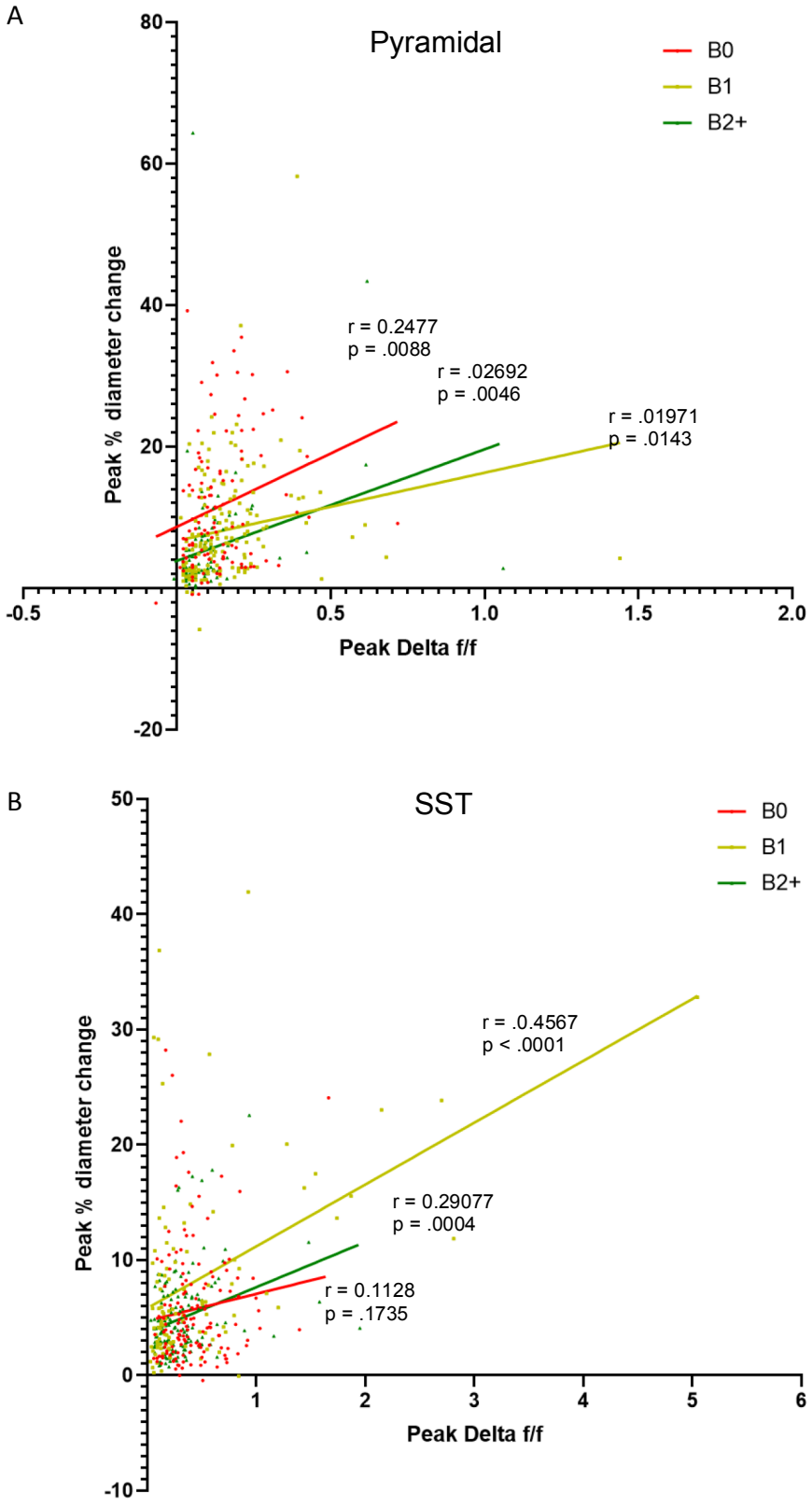

Figure 6.9. Correlations between peak vessel diameter change and peak change in neuronal activity to all stimulus types and locomotion levels divided by branch order on the penetrating arteriole itself.
A *Correlations within pyramidal cells, N = 109-154.* ***B*** *correlations within SST interneurons, N = 101-147.*
A *Difference between correlations B0 and B1: z = 0.42, p = .6745; B0 and B2+: z = -0.17, p = .865; B1 and B2+: z = -0.6, p = 0.5485*
B *Difference between correlations B0 and B1: z = -2.9, p = .0037; B0 and B2+: z = -1.58, p = .1141; B1 and B2+: z = 1.48, p = 0.1389*

Branch orders within the penetrating arteriole were then compared to determine how NVC varied across the length of the penetrating arteriole, particularly as chapter 3 showed heterogeneity in the contractile ability along the length of this vessel, so we might expect parallel variations in correlations between local calcium and vessel responses.

Vessel responses and pyramidal cell activity were significantly correlated to the same degree across all sections of the penetrating arteriole. However correlations between dilations and SST calcium were not significant for the first section of the vessel (branch 0), though later sections (branch order 1 and above) were significantly correlated and the correlations between branch orders 0 and 1 were significantly different (see figure 6.9 for analysis). This is interesting, as branch orders 0 and 1 dilated to the same extent though their coupling to local SST activity is different. The proximity of these branches to one another might mean that a high degree of neuronally-driven dilation of branch order 1 is reflected in branch order 0 as well. As this branch should be high in elastin (see chapter 3), it makes sense that this might allow a large degree of mechanical diameter change in response to diameter changes that might be driven nearby it (Wagenseil & Mecham, 2012). This indicates that there are changes in the coupling of SST interneuron activity and dilation along the length of the penetrating arteriole, but that this does not correspond with dilatory capacity.

We then investigated whether the resting vessel diameter affected the relationship between local neuronal activity and vessel dilations, as baseline diameter is an alternative way to branching order to identify different functional zones within the vascular tree. For both neuronal subtypes, dilation was significantly correlated with neuronal activity across all resting vascular diameters. However, the correlations of different sized vessels were significantly different from one another, being stronger for vessels with a larger resting diameter. Therefore the relationship between local neuronal activity and vessel dilation is more consistent for larger vessels, and also demonstrates a greater change in blood vessel dilation for a given change in calcium (Figure 6.10, see tables 6.3 and 6.4 for statistics).

This did not appear to vary between pyramidal cell and SST activity: comparisons between the diameter ranges at which the strongest correlations occurred between vessel dilation and neuronal activity for each neuronal subtype did not differ significantly between pyramidal cells and SST interneurons, thus indicating that one neuronal subtype does not show greater coupling to certain diameter vessels over another.

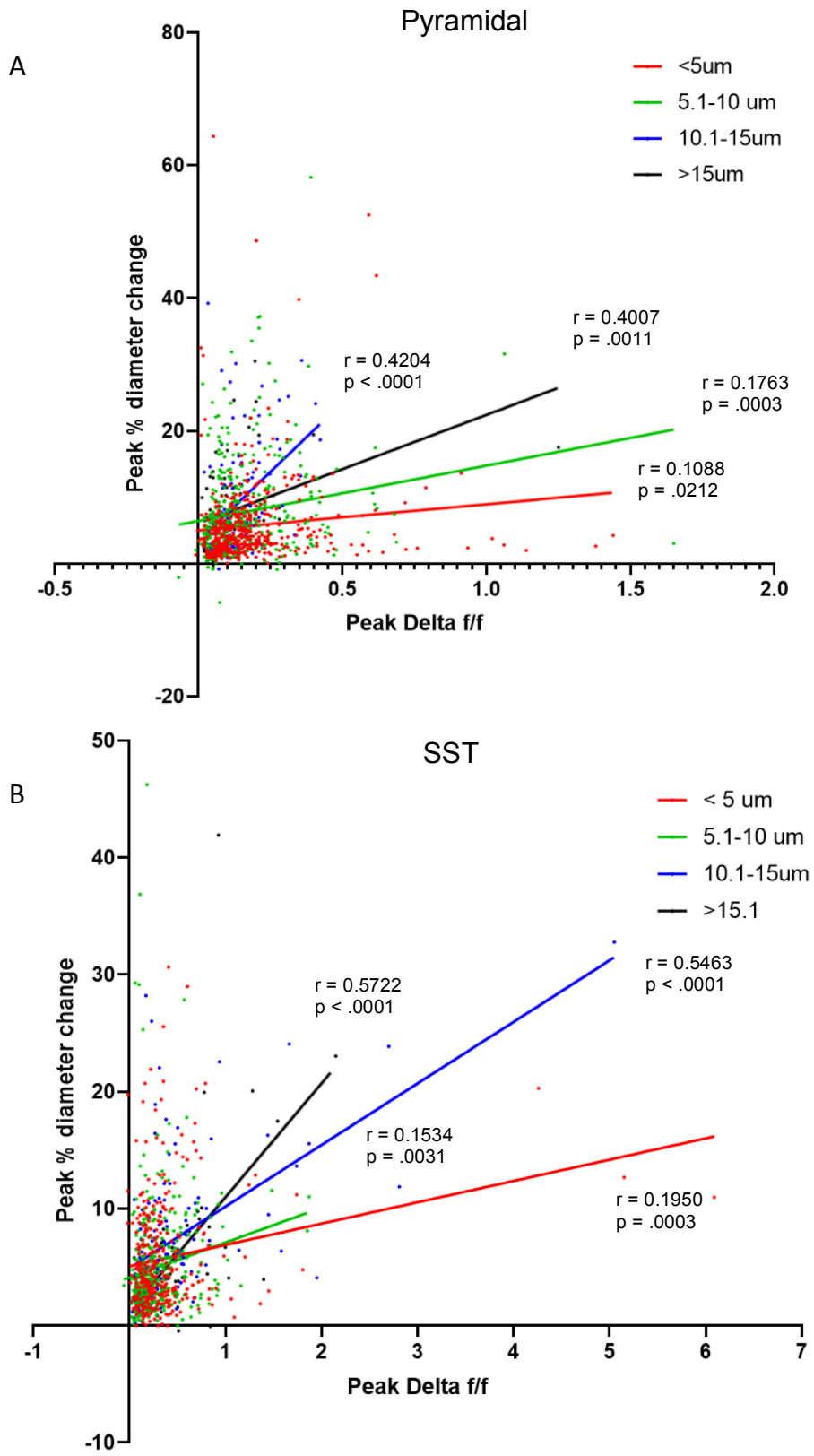

Figure 6.10. Correlations between peak vessel diameter change and peak change in neuronal activity to all stimulus types and locomotion levels divided by binned vascular lumen diameter.
*Correlations within **A** pyramidal cells N = 63-449; **B** SST interneurons N =54-370.*
***A** Correlation between <5 and 5.1-10: z = -1.01, p = .3125; <5 and 10.1-15: z = -3.06, p = .0022; <5 and >15.1: z = -2.29, p = .022; 5.1-10 and 10.1-15: z = -2.42, p = .0155; 5.1-10 and >15.1: z = -1.78, p = .0751; 10.1-15 and > 15.1: z = 0.14, p = .8887.*
***B** Correlation between <5 and 5.1-10: z = 0.57, p = .5687; <5 and 10.1-15: z = -3.95, p = .0001; <5 and >15.1: z = -3.02, p = .0025; 5.1-10 and 10.1-15: z = -4.4, p < .0001; 5.1-10 and >15.1: z = -3.32, p = .0009; 10.1-15 and > 15.1: z = -0.23, p = .8181.*

Diameter (uM)	< 5	5.1-10	10.1-15	>15
F	5.35	13.3	21.67	11.7
R^2	0.0118	0.0311	0.177	0.161
r	0.1088	0.1763	0.4204	0.4007
P value	.0212	.0003	< .0001	.0011

Table 6.3. Statistics corresponding to Figure 6.10 A, showing pyramidal cell correlations. *Degrees of freedom (left to right): 1, 447; 1, 413; 1, 101; 1, 61.*

Diameter (uM)	< 5	5.1-10	10.1-15	>15
F	13.4	8.87	52.8	25.3
R^2	0.0380	0.0245	0.299	0.327
r	0.1950	0.1534	0.5463	0.5722
P value	.0003	.0031	< .0001	< .0001

Table 6.4. Statistics corresponding to Figure 6.10 B, showing SST interneuron correlations. *Degrees of freedom (left to right): 1, 338; 1, 368; 1, 124; 1, 52.*

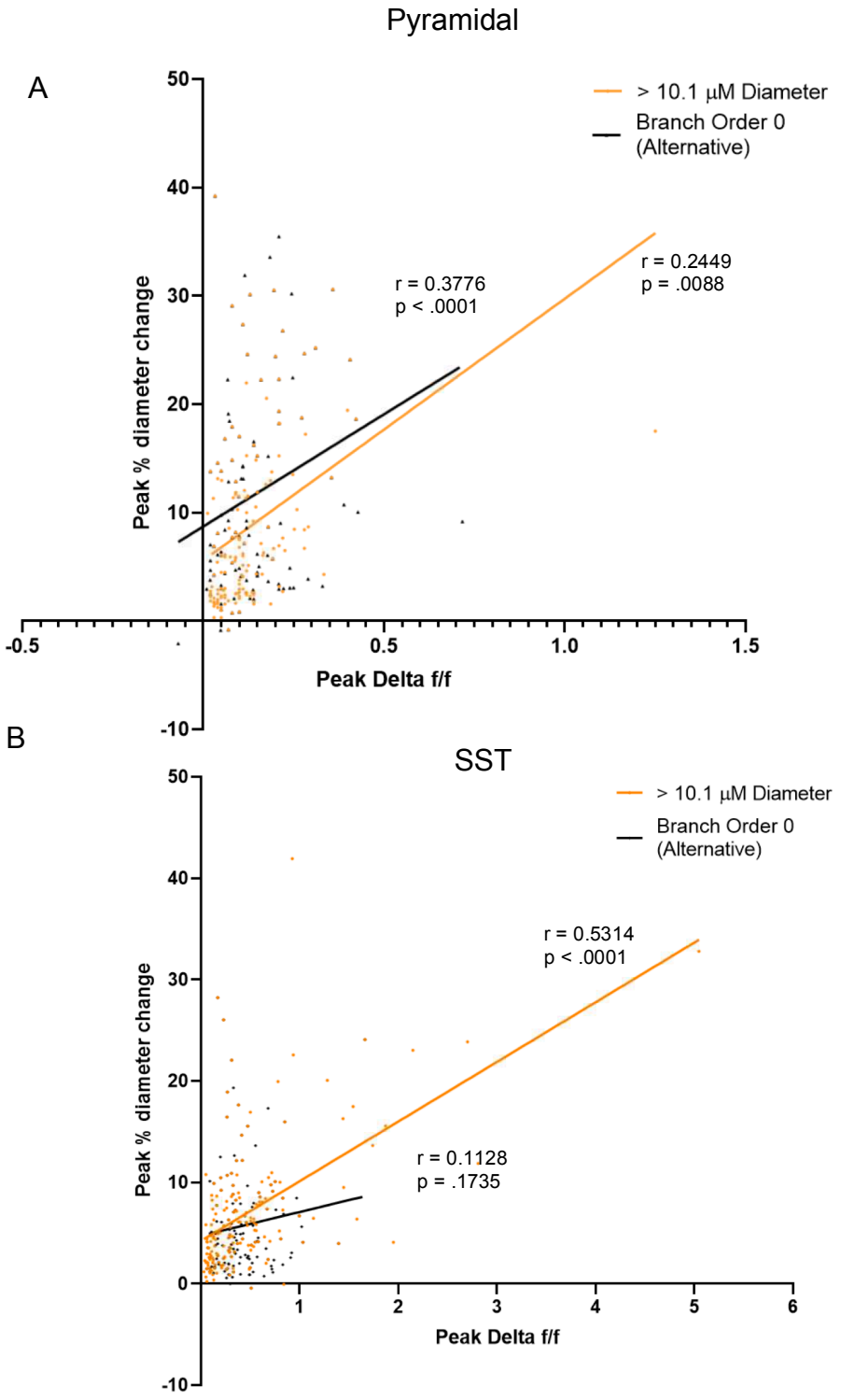

Figure 6.11. Correlations between peak vessel diameter change and peak change in neuronal activity to all stimulus types and locomotion levels divided by different methods of defining an arteriole.
A *Correlations within pyramidal cells, N = 111-166, difference between correlations: z = 1.16, p = .246;* ***B*** *correlations within SST interneurons, N = 147-180, difference between correlations: z = 4.27, p < .0001.*

Differing methods of defining the arteriole were then directly compared, using either branch order or diameter. While within pyramidal cells there was no effect of how an arteriole was defined on the relationship between neuronal activity and vessel dilation; within SST interneurons, the resting diameter was a more reliable and stronger predictor of the NVC between neuronal activity and vessel dilation than was branching order, due to the significant different between correlations (Figure 6.11).

6.4 Discussion

Two-photon imaging was used to concurrently measure changes in pyramidal cell or SST interneuron activity with local blood vessel diameter change while a visual stimulus was manipulated, and changes in locomotion occurred spontaneously.

6.4.1 Results Summary and Interpretation

Overall, both neuronal subtypes showed some degree of correlation with blood vessel response, although this was stronger within SST interneurons. There was a lot of variability in this relationship, and so correlations were relatively weak, and both neuronal subtypes had y-intercepts above zero, meaning that dilation could occur in the complete absence of their local activity. Activity of neither SST nor pyramidal cells was perfect in predicting the degree of dilation from vessel, though SST activity correlated more strongly and consistently (e.g. regardless of whether the mouse was running) than did pyramidal cell activity.

There are several reasons why only relatively weak correlations were observed between the activity of the neuronal subtypes and vessel dilation. The first being that there is an alternative neuronal subtype that is somewhat correlated with the current neuronal subtypes tested, that is driving all of the vascular responses (consistently regardless of vessel point, layer etc.). There are other interneuron subpopulations that have been shown to dilate vessels, for example VIP-expressing interneurons (Cauli et al., 2004), 5-HT expressing interneurons (Perrenoud, Rossier, et al., 2012), and NOS-expressing interneurons (Echagarruga, Gheres, & Drew, 2019; Lee et al., 2019) which could be driving the vascular responses we see. Based on work by Dipoppa et al. (2016); we know that during locomotion VIP activity should be less activated by pyramidal cells and more inhibited by SST interneurons as stimulus size increases. Although the current work found that dilation increases to a larger stimulus compared to a smaller stimulus, we also found changes in neuronal activity that were not congruent with the previous literature (increased pyramidal cell activity to a larger stimulus). It is therefore likely that issues with placing the

stimulus may have prevented the surround suppression response from occurring. If this experiment were repeated and surround suppression could be replicated, it might therefore help elucidate the role of VIP: if dilation decreases to a larger stimulus, then that would suggest a potential role for VIP in mediating this as its activity is also weaker under these conditions. Furthermore, it could be that only a subset of SST interneurons are driving neuronal activity, as there are variations in the literature as to whether SST activity possessed the capacity to dilate (Cauli et al., 2004; Perrenoud, Geoffroy, et al., 2012). In recent research it appears that NOS positive neurons are key in evoking dilation (Echagarruga et al., 2019; Lee et al., 2019), and as this is expressed in multiple interneuron subtypes, including SST (Perrenoud, Geoffroy, et al., 2012); it might be the case that these specific NOS-positive interneurons are driving the dilations.

Alternatively, it might be that another cell type is responsible for driving dilation just under certain conditions, and is therefore driving some of the vascular responses we observed. For example, coupling between SST activity and blood vessel dilation is markedly weaker at lower diameter vessels. It is possible that some of these smaller vessels might just be passively dilating, as it has been argued that capillaries lack the αSMA to dilate and constrict (Hill et al., 2015) and therefore might not be coupled to their local activity. This is still a controversial area, and it might also be the case that these smaller diameter vessels with dilations that correlate poorly with SST interneurons might specifically be being driven by another subtype.

Lastly it's possible that vascular responses reflect summed activity over a wider area than was imaged when measuring locally to the vessel. It's possible that the few cells that were captured locally to the vessel didn't always reflect the general neuronal activity of the area and that it is necessary to compare vessel dilation and wide field neuronal activity concurrently in order to assess the NVC that occurs and assess if the relationships differ at all. This doesn't appear likely based on the very similar correlations with vessel dilation yielded between local and population activity when this data was binned into experimental

groups in figure 6.3, however it might be the case that averaging across the local activity might actually be an approximation of population activity. Furthermore, research that has been carried out since this project was started has indicated that population activity doesn't control haemodynamic signals, and instead implicated a small group of nNOS-positive neurons, whose activity does not always correlate well with the activity of the neuronal population (Echagarruga et al., 2019); it therefore seems unlikely that population activity is driving vascular response.

SST correlations with vessel dilation were more consistent across locomotion groups than were pyramidal cell correlations, suggesting that the blood vessel response across locomotion states might better reflect SST. Based on the means for each condition (i.e. changing stimulus size or contrast, see Figures 6.1 and 6.2), when there was no locomotion, pyramidal cell activity and vessel dilation both changed similarly as the contrast or size of the stimulus was manipulated. Conversely when the mouse ran, pyramidal cell activity increased with locomotion, but no longer reflected the change in vessel dilation that still occurred in response to stimulus change. Furthermore, when neuronal activity and vessel diameter change were directly compared for individual vessels, there was no correlation between pyramidal cell activity and dilations when the mouse wasn't running and pyramidal cells are only well-matched to vessel dilation when the mouse was running before and during stimulus presentation. This appears to be just because more of the signal (both neuronal and vascular) when the mouse runs throughout the trial is driven by locomotion rather than visual input. In short, individual vessel dilations only reflect local pyramidal cell activity insofar as they are both activated by running, while SST interneurons and vessels are matched in activity during both visual stimulus presentation and locomotion. Some very recent research has revealed that modulating pyramidal cell activity has very little effect on arterial dilation (Echagarruga et al., 2019), further supporting the that pyramidal cell activity is less important in eliciting vessel dilation than might intuitively be believed.

This means that vessel responses are more informative about SST interneuron activity than excitatory principal neuron activity. On average, as SST and pyramidal cells' activity are usually correlated, vascular responses are usually informative about both cell types' activity. However, during locomotion vessel responses really only reflect SST activity. This impacts on what information is carried in the BOLD signal. Though humans are not locomoting while in the fMRI scanner, they may experience a change in arousal. Because locomotion and arousal are well-correlated (Vinck et al., 2015) and we cannot distinguish between the two in our current experiment, we do not know whether locomotion per se or associated arousal is driving the uncoupling of vascular responses from excitatory activity. If arousal is the key mediator of this change, changing arousal states within the scanner may produce a disconnect between the excitatory activity and BOLD response.

An interesting result acquired was that SST activity correlated with vessel dilation to a greater degree when the contrast was manipulated, than when stimulus size was manipulated. The fact that regardless of whether or not the mouse was running, SST activity never correlated significantly with blood vessel response when stimulus size was manipulated, and that the difference in the correlations between SST activity and vessel dilation that were yielded between the stimulus manipulation types was significant, indicates that during stimulus size manipulation there is a real reduction in the closeness of the relationship between SST activity and vessel dilation. This indicates further that there is likely an alterative neuronal subtype that correlates more closely with the vessel response across different conditions.

The current study found that branch order had a bearing on the relationship between SST interneuron activity and the degree of dilation from the vessel. The general pattern of this was for lower branch orders to show greater NVC than higher branch orders. Pyramidal cells however did not demonstrate significantly closer NVC depending on the branch order tested, even though differences in correlations between pyramidal cell activity and vessel dilation were found between different resting diameter vessels. Interestingly, branch order

of the penetrating arteriole specifically showed different degrees of SST NVC at different branch orders (specifically, the sections before and after the first branch, which were shown in chapter 3 to dilate similarly). This is likely due to elastin expression and smooth muscle cells allowing changes in diameter as dilation is propagated upstream towards arterioles; the lack of intracranial pressure so close to the surface of the brain that might otherwise mechanically reduce any dilation (Gao, Greene, & Drew, 2015); along with potential changes in local morphology (such as the Virchow-Robin space (Iadecola, 2017)) that might indicate a change in functionality along this vessel, such that it is more akin to a pial vessel at branch order 0, than to an arteriole that is coupled to its local SST activity. It is very interesting that branch order appears to be a reliable marker for this apparent change in functionality along the penetrating arteriole, specifically in relation to SST interneurons, as there was no significant change in the degree of excitatory cell coupling to the degree of dilation across different branch orders. This suggests that branch order is a useful method to use to probe NVC with SST across the vascular tree, where it appears not to be so for excitatory cells.

Both neuronal subtypes demonstrated a stronger relationship with vessel dilation within vessels with a higher resting diameter than vessels with a lower resting diameter. The closer coupling between SST activity and vessel dilation within larger vessels seems to support that SST interneurons might dilate arterioles specifically via NO, as dilation of arterioles has previously been shown to be mediated by interneurons (Mishra et al., 2016). However, pyramidal cells also demonstrated a resting diameter-mediated variability in NVC. It might be expected that SST and pyramidal cell activity are related due to the necessity of glutamate acting on the AMPAR of vasodilatory interneurons in order to generate adequate synaptic activity to release ATP, that acts on P2X1 receptors on astrocytes to mediate capillary dilation (Mishra et al., 2016). However, the fact that both neuronal subtypes demonstrate decreased coupling with smaller diameter vessel response suggests that the most likely explanation of the current findings is that generally, arterioles might better reflect the summed change in blood flow to a region as they supply the

capillary bed, and therefore are most likely to also reflect the change in neuronal activity that occurs in that region.

6.4.2 Limitations of the Current Study

There is evidence of a capacity to constrict vessels by SST interneurons (Cauli et al., 2004), and the current research implicates this neuronal subtype in underlying dilation. This indicates further subtypes within the SST interneuron, which were not possible to discriminate between in the current study. Although there is utility in understanding the general pattern of SST activity, it would be hugely informative to understand the activity of SST interneurons that do and do not express nNOS. The function of SST in relation to the vasculature appears to be diverse, and more work is needed to understand this.

It would have been interesting to look at layer due to factors such as the density of pyramidal cells in layer 5 (Pakan et al., 2016), and preferential expression of nNOS expressing interneurons in layers 2/3 and 4 (Perrenoud, Geoffroy, et al., 2012); however the current study also had too small N to separate out by both layer and vessel type (whether it was more akin to an arteriole or capillary, depending on diameter and/or branch order), and as the average diameter of a vessel changes as it progresses from an arteriole capillary (Attwell et al., 2015), and in the cortex the arteriole dives down into the tissue, this has the potential to interfere with any effect of layer. It would be of benefit to elucidate the relative contributions of vessel type and layer, as they are likely to overlap and potentially bias the results when attempting to look at each variable in isolation.

6.4.3 Future Directions

The current study implicated both neuronal subtypes in underpinning vascular response to locomotion in the absence of visual stimulus, at least to some degree. However, the current study measured response to spontaneous locomotion with the screens left switched on, providing some source of light (i.e. mice did not run in total darkness); and it has previously

been indicated that neither SST interneurons nor excitatory cells demonstrate increased activity to locomotion in absolute darkness (Pakan et al., 2016). It would therefore be interesting to look at the response from the vasculature under these circumstances in order to investigate whether the potentially reduced neuronal activity is reflected by the vessel response or if they dissociate, which would more strongly suggest that an alternative neuronal subtype that is still increased (such as VIP and PV interneurons (Pakan et al., 2016)) is responsible for mediating dilations.

With the mice used in the current study, analysis of vessel characteristics in relation to NVC was limited to branch order and diameter, which were indicated in section 3 to not be the most consistent characteristics to use in terms of functional markers. It would have been useful to be able to visualise vascular mural cells, and therefore future research might cross NG2 DsRed mice (that allow visualisation of vascular mural cells) with the GCaMP mice in order to make it possible to image intracellular calcium as well as the smooth muscle cells and pericytes on the vessels.

Future research could also optogenetically prevent activation of certain neuronal subtypes in order to not just understand which neuronal subtypes correlate with vessel dilation (therefore informing the activity that might co-occur with the BOLD response); but to also establish causality in the NVC process, and gain further understanding of which neuronal subtypes are directly implicated in dilating specific vessel types, thus helping inform answers to further questions. For example, whether the arteriole dilation is propagated from the capillary bed via the endothelium, and therefore the stronger NVC correlation within this vessel type is due to this vessel generally representing blood flow change in the region; or whether nitric oxide is dilating the arteriole, and this stronger correlation is due to the local SST interneuron activity causing a release of this nitric oxide, which would also explain the stronger NVC relationship within this vessel type.

6.4.4 Conclusions

SST interneuron activity is better correlated with vessel dilation than is excitatory activity, however correlations are fairly weak and both appear to dissociate under certain conditions. The characteristics of the vessel also appear to have some bearing on the degree of NVC within both neuronal subtypes, but the precise mechanisms of this require further investigation. It appears likely that an alternative neuronal subtype that is correlated with the neuronal subtypes tested here might be more integral in driving dilations.

Chapter 7

Discussion

7.1 Summary of the Research Findings

7.1.1 Aim 1: To gain clarification of how vessel function changes throughout the vascular tree

We aimed to understand how vascular function evolves throughout the vascular network, and to be able to use functional properties of the vessel and its position within the network to estimate its likely function. To achieve that, key aims devised were to: 1. Determine how different vascular functions change through the vascular network, and 2. Assess the usefulness of different potential descriptors of vessels within this network to discriminate between vessels with different functional properties.

One point of contention within this was whether the entirety of the penetrating arteriole should be considered as one functionally homogenous unit, or whether functionality transitions as the penetrating arteriole branches, as we assume it does throughout the rest of the vascular tree. It was found that in terms of dilatory capacity, the section of the penetrating arteriole closest to the pia (including sections before and after the first branch) is functionally homogenous. After the second branch off the main penetrating arteriole, the penetrating arteriole dilates to a similar degree to all of the other branches. All branches off the penetrating arteriole dilated to the same degree. This suggests that branch order is capable of discriminating different sections of varying contractile ability, and that this is likely a useful method for the purpose of predicting the degree of dilation, but that classifying the penetrating arteriole homogenously as branch order 0 does not capture this. Conversely, it was not possible to predict the degree of dilation based on vessel diameter or IS distance. There was a great deal of variability in the correlations between these vessel descriptors and dilation, which is speculated to be due to the great deal of homogeneity of dilation that was found throughout most of the branches,

We then studied how these results corresponded with functional markers. It was found that the marker for contractile ability (αSMA) did not align with branch order in any intuitive way

(i.e. its termination didn't correspond with branches at which capacity to dilate decreased). It is more ambiguous as to whether αSMA expression corresponded with the degree of dilation that was elicited at different IS distances and vessel diameters, but there is no clear decrease in dilation at the expected αSMA termination points using either diameter or IS distance, and as these characteristics of the vessel predict dilation relatively poorly, they are unlikely to be of great utility for the purpose of charactering contractile function across the vascular network.

Through use of a wider variety of functional markers, each associated with more arteriole- or capillary-like functionality, the change in function across the vascular network was then characterised. Using branch order, IS distance, and diameter allowed these methods of identifying the vasculature to be assessed in terms of how consistently they could label the start and termination points of the various functional markers. Classically considered capillary-associated markers GLUT-1 and PDGFRβ were expressed throughout the vasculature; and the start point of capillary-associated marker nestin expression overlapped with the arteriole-associated marker αSMA to various degrees using all three methods of identifying points of the vasculature. This suggests a lack of discrete function between arterioles and capillaries, and suggests that function transitions in a more gradual manner. The most consistent method of identifying marker start and termination points was IS distance, but understanding the nature of the relationship between IS distance and diameter (which showed a medium correlation) can facilitate the use of diameter instead where it is not possible to visualise vascular mural cells.

7.1.2 Aim 2: To improve understanding of the relationship between activation of specific subpopulations of neurons and blood vessel dilation

Previous research has manipulated a drifting grating by size and contrast and shown dissociation between excitatory and inhibitory activity, as well as a specific role for SST interneurons in suppression of excitatory and inhibitory activity (Adesnik, 2017).

Additionally, the activation of SST interneurons and other interneuron subtypes with pyramidal cells has been characterised with locomotion in differing visual contexts (Dipoppa et al., 2016; Pakan et al., 2016). The current research aimed to utilise these methods of manipulating activation of different neuronal subpopulations in order to test the relationship between activation of specific neuronal subtypes and local blood vessel diameter change. This activation was also tested with a wide field view in order to test whether activity of neurons locally to blood vessels is reflected in the population activity.

The general findings regarding neuronal activity were that both neuronal subtypes increased their activity with increasing contrast, consistent with work by Adesnik (2017); but with increased stimulus size, activity of both neuronal subtypes also increased, which is incongruent with what might be expected from the literature (that excitatory activity would decrease due to increasing SST activity with increasing stimulus size (Adesnik, 2017)). Locomotion also increased activity of both subtypes as might be expected based on the increased activity to stimulus in response to locomotion found previously (Niell & Stryker, 2010). However, while SST still responded to the stimulus shown regardless of locomotion, excitatory cells showed an increased response to locomotion but were then less sensitive to the stimulus shown. While based on the aforementioned studies, increased excitatory activity to locomotion in the presence of some form of stimulus is to be expected (Dipoppa et al., 2016; Niell & Stryker, 2010; Pakan et al., 2016); there is nothing to indicate based on these findings that this increase in activity to locomotion would lead to loss of discrimination between stimuli shown. It was also shown that spontaneous locomotion elicited increases in both neuronal subtypes, but similarly to stimulus presentation, locomotion-induced activity increases were larger in SST than pyramidal neurons. Lastly, population activity that was sampled reflected that of the local activity, but did appear to be more sensitive to differences, likely due to the larger number of cells sampled using a wide field view.

Looking at vessel response, this was more closely matched to SST, as the vasculature maintained an ability to discriminate between stimuli during locomotion, as did SST, where

pyramidal cells activity did not. When the individual concurrent responses in neurons and vessels were compared directly, both neuronal subtypes showed significant positive correlations with vascular response, but SST demonstrated a stronger relationship with the vessel diameter change. Any correlation between excitatory activity and vessel dilation appears to actually be driven by locomotion, as it was found that individual concurrent responses between pyramidal cell activity and vessel dilation only correlated when the mouse was running throughout the trial (i.e. when both excitatory activity and the vessel response were less sensitive to changes in the stimulus due to the locomotion signal during the baseline and stimulus periods). All of this suggests that because pyramidal cell activity dissociates from vessel response, that this is a poor candidate to be consistently driving dilations. SST activity was much more consistent in its correlation with vessel response, however, it did correlate less strongly with dilation during the stimulus size manipulation, suggesting there are also conditions under which this neuronal subtype is more weakly coupled to vessel dilation. During the stimulus size manipulation, the weaker correlation was characterised by a lack of vessel dilation where SST activity increased, suggesting an alternative mechanism is driving the response under these conditions. The relationship between the activity of neuronal subtypes and vessel dilation was also affected by the branch order and diameter of the vessel tested. Lower branch order vessel dilation showed a stronger correlation with SST interneuron activity than did higher branch order vessel dilation, but this was not the case with excitatory activity. However, larger diameter vessel dilation correlated more strongly with both SST and pyramidal cell activity than smaller diameter vessel dilation.

7.2 Wider Context

If the literature is generally in agreement that vascular mural cells are contractile up to branch order 4 (see chapter 1 for review), then it is interesting that vessels dilate to the same extent throughout the vascular tree (bar the initial section of the penetrating arteriole close to the pia). We can conclude from this that capillary dilation outside of αSMA expression is just as extensive as within the zones with αSMA expression. This might mean

that there are alternative contractile pathways, and/or that we are seeing passive dilations, but that these passive dilations could potentially be hugely important. Prior research has revealed that thin-strand pericytes closer to the mid-capillary exhibit decreases in calcium, which are driven by local synaptic activation. The authors speculate that this might act to relax the capillary wall and facilitate a passive dilation (Rungta et al., 2018). Furthermore capillaries underlie most of the vascular bed resistance (Blinder et al., 2013), and accounting for passive dilation from the capillary bed is required to accurately model resting blood flow and functional hyperaemia (Rungta et al., 2018). This adds further credence to the notion that these mid-capillary dilations, while perhaps passive, are greatly important in the hyperaemic response.

Furthermore, the current work found consistent termination of αSMA expression at vessels of a diameter of 6 – 7 μm. This didn't show any particular predictive ability regarding the degree of dilation that occurred within vessels that are greater or smaller than that, nor did the predicted presence or absence of αSMA appear to impact the strength of the correlation between activation of either neuronal subtype and dilation when comparing between < 5 um diameter vessels and 5.1-10 μm diameter vessels. And so this doesn't indicate any difference in the NVC mechanism before vs. after αSMA termination, which might in part be due to ability of even mid-capillary pericytes to sense synaptic activity through decreased calcium (Rungta et al., 2018). However, it is also likely that a different neuronal subtype that was not tested here is driving NVC, which might vary in the strength of its correlation with dilation depending on αSMA presence. Indeed, previous work has implemented a threshold of 10 μm to distinguish between capillaries and arterioles, which found astrocytes to mediate NVC in < 10 μm diameter capillaries, and NO release from interneurons to mediate dilation of vessels larger than this (Mishra et al., 2016); thus demonstrating differing NVC mechanisms between arterioles and capillaries. Although the expression profiles of functional markers that might correspond with this are not known, based on the vessel diameter that corresponded with αSMA termination in the current

work, it seems like there should have been variable expression of αSMA in pericytes that were dilated via astrocytes.

SST activity demonstrated a stronger correlation with vessel dilation than did pyramidal cells in the current study, but the extent to which pyramidal cell activity did not reflect the vessel response when studied at the level of individual vessels and their corresponding activity was surprising. Glutamate release from excitatory cells should regulate vessel dilation through interneurons or astrocytes (Mishra et al., 2016). Blockade of NMDA receptors has been shown to reduce CBF response (Lecrux et al., 2011); and optogentic stimulation of excitatory cells leads to blood vessel dilation (Uhlirova et al., 2016). However, correlationally, the relationship between pyramidal cell activity and vessel dilation was very inconsistent here. This lack of consistent relationship between pyramidal cell activity and vessel response has however recently been supported. Echagarruga et al. (2019) found that pyramidal neurons drove large changes in population neuronal activity, but without changing arterial diameter in awake mice. This work found instead that a small group of nNOS positive neurons played a large role in controlling vessel diameter, and that these neurons are usually correlated with pyramidal neurons (but can become decoupled). This pattern makes sense in the current study, as the overall pyramidal cell activity was usually similar to that of the vessel when average responses were compared (i.e. overall it correlated with whatever subtype is driving dilations), but on the level of individual vessels and their local neuronal activity, the relationship was very weak. If changes in vessel dilation here were NO-driven, this might reflect a general positive correlation between nNOS-positive neuronal activity and pyramidal cell activity, but the same lack of individual pyramidal cell driven dilations. Furthermore as NO is released during exercise (Cristina, Lacerda, Marubayashi, Balthazar, & Coimbra, 2006), this might support NO-driven dilations when the mouse was running (Cristina et al., 2006).

Both excitatory cell and SST interneuron activity were more closely correlated with dilation of larger diameter vessels than smaller diameter vessels, and SST activity specifically

correlated more strongly with dilation from higher order branches than lower order branches. This is despite general homogeneity of degree of vessel dilation across the majority of the branches (shown in chapter 3). Furthermore, the gradual nature in which correlations between neuronal activity and dilation weakened as diameter decreased between the binned groups (figure 6.10) indicates that this is not mediated by the difference in dilatory capacity between the top section of the arteriole and the rest of the vasculature. In addition to this, within the top section of the arteriole (which dilates homogenously, and to a greater degree than the rest of the branches), there is a stark difference between coupling to local SST activity, perhaps as vessel function changes from arteriole to pial vessel. Taken together, all of this suggests that the degree of dilation that a given point in the vasculature is capable of doesn't reliably predict the strength of its relationship with neuronal activity. This might explain the relatively weak, variable correlations between peak dilations of individual vessels and activity of SST interneurons and pyramidal cells over the entire dataset (figure 6.4): perhaps at lower diameter, higher branch order vessels, there is a similar degree of dilation to the majority of the rest of the vascular network, but less corresponding local neuronal activity. This possibility is supported by our current data, as in the correlations between responses of each vessel and local SST and excitatory activity; the y-intercepts indicate that within both neuronal subtypes, there is dilation present in the absence of neuronal activity. Peak dilation might correlate more strongly to cell activity that directly drives dilation, or it might be the case that these dilations are passive and being driven by neuronal activity elsewhere.

7.3 Limitations

One limitation of the current study was aside from the categorical manner of locomotion detection and potential entanglement of locomotion and arousal (discussion in section 4); that different degrees of NVC can occur depending on body movement, which would not be captured by a rotary encoder (Winder, Echagarruga, Zhang, & Drew, 2017). NVC is weak during 'true' rest (i.e. in the absence of any body movement), and so it would be more informative to record the physical state of the animal. However the study that yielded these

findings was conducted in the absence of overt stimulation, and was also conducted in the somatosensory cortex; and so it is difficult to be sure of the applicability to visual cortex research, especially in the context of visual stimulation.

A further limitation that might have affected the current study is the swelling of the vessel that can occur in response to the laser, which was observed on some occasions, and could affect the dilations that might be observable from the vessel. This was avoided by attempting to use a suitable laser power for the depth at which the tissue was imaged; by avoiding imaging the vascular tree in a systematic order (i.e. avoiding imaging from top to bottom or visa versa in order that one section of the vessel might not be disproportionately affected by this potential phenomenon); and by randomising the order in which the stimuli were shown in order that this wouldn't disproportionally affect one type of stimulus (e.g. high contrast) over another. It is therefore possible that this affected the dilation of some of the vessels, but through randomisation implemented in the experimental procedure and avoiding using too high of a laser power, should be minimised and should not have a disproportionate effect on one type of vessel or stimulus over another.

Furthermore, it is not possible to be sure of the recovery of the V1 region post-surgery. Immunohistochemistry was conducted at the end of experimentation, which ascertained that by this point (usually approximately 3-6 months post-surgery), astrocyte and microglia expression appeared normal at a distance of 100 μm or more from the window (where most imaging took place). Previous research has indicated that microglial inflammation returns to normal after 7-10 days, and astrocyte inflammation after a month (Holtmaat et al., 2009). The time frame in which imaging took place should therefore mean the recovery of the region was completed or close to completion for the first imaging sessions, however it is not possible to be sure, or indeed to know how window placement in general may have affected CBF (e.g. through capillary stalling, which has been observed in cranial window fitted mice (Cruz Hernández et al., 2019), but for which it is unknown to what extent window

placement itself might affect this phenomenon through factors such as dura removal, pressure change or vascular damage that might occur).

Another factor to be considered is the depth at which it was possible to image. The current study was limited to mostly layers 1 and 2/3, and it was rarely possible to achieve adequate signal to noise in deeper layers. However, Tian et al. (2010) indicated that the fastest response occurs in the deeper layers, while a more delayed response occurs in layer 1. This might indicate that the closest NVC in terms of direct effects on the blood vessel by local neuronal activity occurs in these deeper layers, and that the relationship between neuronal subpopulation activity and vessel diameter change should also be probed in deeper layers with a greater N than was possible in the current study, including layers 5 and 6 which were unexplored.

It has been found that mice are able to fall asleep during imaging while head fixed (Yüzgeç, Prsa, Zimmermann, & Huber, 2018). It is possible that this could have occurred in the current study, as pupilommetry was not used in order to measure pupil diameters and ascertain whether this was occurring. Blood flow rate can change with changing sleep state (Braun et al., 1997), as does the metabolic rate of the brain (Buchsbaum et al., 1989). This could have affected the results yielded here, however, only for data in which no locomotion was observed. Future research might use pupilommetry in order to detect any bouts of sleep during imaging.

7.4 Future Directions

Future research might attempt to also look at VIP and PV interneurons as previously discussed in chapter 5. However it has previously been indicated, at least during locomotion, that PV interneuron activity is tightly related to pyramidal cell activity, and so it might be expected that this will reflect the pyramidal cell activity found here. Additionally, prior research has indicated an important role for PV in mediating response to contrast and

size of a grating stimulus in tandem (Nienborg et al., 2013), and so this could be of use in determining the role of PV interneurons specifically.

Factors such as 5-HT receptor expression have also been shown to be particularly important in NVC (Perrenoud, Rossier, et al., 2012), and Neuropeptide Y has been found to correlate with CBF (Kocharyan et al., 2008); and so it appears that there is great complexity in trying to unpick the specific subtypes of interneuron that might be involved in NVC, all of which could be tested in conjunction with other potentially overlapping subtypes. It might be of interest to look at this in a more holistic manner and get a general picture of the pattern of neuronal activity that is occurring through studying the overall balance between excitatory and inhibitory activity, which would yield results regarding the general ratio that underlies the BOLD signal, and how the shifting of both general levels of excitatory and inhibitory activity, as well as the change in ratio observed by Adesnik (2017) might relate to changing blood vessel dilation. This should be relatively achievable in future research through a panneuronal viral injection in a tdTomato mouse in which interneurons fluoresce.

It might also be interesting to probe whether the degree of NVC between specific neuronal subpopulations and the vasculature remains stable or varies between regions. This can easily be probed among cortical regions, for example the whisker barrel cortex through whisker stimulation; or perhaps more interestingly, subcortical regions. Subcortical regions have been shown to demonstrate different NVC from the cortex in terms of linearity (Devonshire et al., 2012), and could also be studied through aspiration of the cortex. This might serve to aid our understanding of what pattern of neuronal activity underlies the different BOLD response observed subcortically, and whether there is commonality in the mechanism of NVC, but a different pattern of neuronal activity driving it; or if the importance of for example SST is actually different in these regions when compared to alternative subpopulations and pathways.

Furthermore, comparing regions in the context of understanding the vascular tree and how its functionality transitions would also be of great utility. Intracranial pressure has been demonstrated to play a role in the degree of dilation elicited from a vessel (Gao et al., 2015), which is greater deeper into the tissue; and there is also a different vascular structure in regions such as the hippocampus compared to the visual cortex (Kira Shaw, personal communication). It might therefore be interesting to study in subcortical regions whether there is consistency in how factors such as diameter and inter soma distance relate to vascular response, as well as their relationship with the functional markers explored in the current work within the cortex.

7.5 Final Conclusions

Manipulation of a drifting grating by contrast and size, as well as with different patterns of locomotion was successfully used to alter the degree of vascular and neuronal response; and using a full screen high contrast stimulus, it was possible to yield differences in how different points of the vasculature responded to the stimulus. Spontaneous locomotion also appears to elicit neuronal and vascular response. Importantly, it appears that SST-interneuron response is more strongly associated with vascular dilation than is excitatory activity, despite previous findings indicating that it constricts vessels (Cauli et al., 2004), although it does not correlate perfectly with vessel dilations. Branch order is useful in predicting the degree of dilation, and was used to identify two homogenous zones with similar dilatory capacity, although this does not match up with the expected corresponding functional marker expression.

It seems that the function of the vasculature changes in a continuous manner, and that categorisations of vessel types (arteriole or capillary) or their vascular mural cells (smooth muscle cell or pericyte) are of little utility in terms of understanding what is being expressed at different points along the vascular tree. For this, it might therefore be of greater use to

characterise the vasculature in a more continuous manner, using a measure such as inter soma distance between vascular mural cells.

It is hoped that further research will extend the current findings to elucidate the patterns of activity of other neuronal subpopulations during blood vessel dilations, and to reveal the specific pathways that underpin vessel response across the whole vascular network.

References

Adesnik, H. (2017). Synaptic Mechanisms of Feature Coding in the Visual Cortex of Awake Mice. *Neuron*, *95*(5), 1147-1159.e4. https://doi.org/10.1016/j.neuron.2017.08.014

Adesnik, H., Bruns, W., Taniguchi, H., Huang, Z. J., & Scanziani, M. (2012). A neural circuit for spatial summation in visual cortex. *Nature*, *490*(7419), 226–231. https://doi.org/10.1038/nature11526

Alarcon-Martinez, L., Yilmaz-Ozcan, S., Yemisci, M., Schallek, J., Kılıç, K., Can, A., … Dalkara, T. (2018). Capillary pericytes express α-smooth muscle actin, which requires prevention of filamentous-actin depolymerization for detection. *ELife*, *7*. https://doi.org/10.7554/eLife.34861

Armulik, A., Genové, G., Mäe, M., Nisancioglu, M. H., Wallgard, E., Niaudet, C., … Betsholtz, C. (2010). Pericytes regulate the blood–brain barrier. *Nature*, *468*(7323), 557–561. https://doi.org/10.1038/nature09522

Astrup, J., Heuser, D., Lassen, N. A., Nilsson, B., Norberg, K., & Siesjd, B. K. (2008). Evidence Against H^+ and K^+ as main Factors for the Control of Cerebral Blood Flow: A Microelectrode Study. In *Ciba Foundation symposium* (pp. 313–337). https://doi.org/10.1002/9780470720370.ch16

Attwell, D, Buchan, A. M., Charpak, S., Lauritzen, M., MacVicar, B. A., & Newman, E. A. (2010). Glial and neuronal control of brain blood flow. *Nature*, *468*(7321), 232–243. https://doi.org/10.1038/nature09613

Attwell, D, & Laughlin, S. B. (2001). An energy budget for signaling in the grey matter of the brain. *Journal of Cerebral Blood Flow and Metabolism*, *21*(10), 1133–1145. https://doi.org/10.1097/00004647-200110000-00001

Attwell, David, Buchan, A. M., Charpak, S., Lauritzen, M., Macvicar, B. A., & Newman, E. A. (2010). Glial and neuronal control of brain blood flow. *Nature*, *468*(7321), 232–243. https://doi.org/10.1038/nature09613

Attwell, David, Mishra, A., Hall, C. N., Farrell, F. M. O., & Dalkara, T. (2015). What is a pericyte? *Journal of Cerebral Blood Flow and Metabolism*, 6–10. https://doi.org/10.1177/0271678X15610340

Attwell, David, Mishra, A., Hall, C. N., O'Farrell, F. M., & Dalkara, T. (2016). What is a pericyte? *Journal of Cerebral Blood Flow and Metabolism : Official Journal of the International Society of Cerebral Blood Flow and Metabolism*, *36*(2), 451–455. https://doi.org/10.1177/0271678X15610340

Bandopadhyay, R., Orte, C., Lawrenson, J. G., Reid, A. R., De Silva, S., & Allt, G. (2001). Contractile proteins in pericytes at the blood-brain and blood-retinal barriers. *Journal of Neurocytology*, *30*(1), 35–44. https://doi.org/10.1023/A:1011965307612

Berens, P., Logothetis, N., & Tolias, A. (2010). Local field potentials, BOLD and spiking activity – relationships and physiological mechanisms. *Nature Precedings*, *5*, 1–1. https://doi.org/10.1038/npre.2010.5216.1

Bernier, L.-P., Hefendehl, J. K., Lewis, C.-A., Rossie, F. M., Underhill, M. T., & A, M. B. (2018). Brain pericytes are mesenchymal progenitors that support cerebrovascular regeneration after stroke. *Poster Session Presented at the Society for Neuroscience Annual Meeting*.

Bicher, H. I., Reneau, D. D., Bruley, D. F., & Knisely, M. H. (1973). Brain oxygen supply and neuronal activity under normal and hypoglycemic conditions. *The American Journal of Physiology*, *224*(2), 275–282. Retrieved from http://ajplegacy.physiology.org/content/224/2/275.abstract

Birbrair, A., Zhang, T., Wang, Z.-M., Messi, M. L., Mintz, A., & Delbono, O. (2015). Pericytes at the intersection between tissue regeneration and pathology. *Clinical Science (London, England : 1979)*, *128*(2), 81–93. https://doi.org/10.1042/CS20140278

Blinder, P., Tsai, P. S., Kaufhold, J. P., Knutsen, P. M., Suhl, H., & Kleinfeld, D. (2013). The cortical angiome: an interconnected vascular network with noncolumnar patterns of blood flow. *Nature Neuroscience*, *16*(7), 889–897. https://doi.org/10.1038/nn.3426

Braun, A. R., Balkin, T. J., Wesensten, N. J., Carson, R. E., Varga, M., Baldwin, P., … Herscovitch, P. (1997). *Regional cerebral blood flow throughout the sleep-wake cycle An H 2 15 O PET study* (Vol. 120). Retrieved from https://watermark.silverchair.com/1201173.pdf?token=AQECAHi208BE49Ooan9kkhW_Ercy7Dm3ZL_9Cf3qfKAc485ysgAAAkowggJGBgkqhkiG9w0BBwagggI3MIICMwIBADCCAiwGCSqGSIb3DQEHATAeBglghkgBZQMEAS4wEQQMgaN4hZv_Mt5p65mcAgEQgIIB_WAJmiuFfUGNLtilAAT0zrvUwqnvEj6bh8_aXcWhUYFBfyirb0PMvkXsb6B842t30vMb3---SUEUk5sGWb83VpXxFzblNtQSRHIpq8WWjF3qf1oNQr12ujoLAzREfRB77iC0hNwrnEf0sa5VzAAB3vzR5t7d_71D7kyAzk_DL5PfN-jaPAE5D5c8dIu-T2oq4SwuppwOdLPCxFYdPELzh9gk_pdprfA5wfijn-5H1ZckAPmib8NZah0fMFFMd7RLb3Qul4ah6va5VY4Z_6XNwE07nmNHKr4qukyjlN-fbc_UX3MljI7pEzcgHG4WQ8Bf10CFNjYIfZ4SiJyfYIXgmsg0VGZtGiwAlQzWjWQUmvXK_Jqnh2ZeuykXFtqgU1cdvhmVqu0-RH8OHLVXET5k_T491Kz7I94lK7Am_s6WfohAfS1cy7PflS6gz13sv1HrmLhrjoeLSBEAMHI2YVzp48jHXc-BsEszFA1wJdDrSVbkla6hoaN56Fpj4jIMILzWbRik8y5osRgT0kVQtkhALoYnXEK8pN5OVGwxbHBO147__nubvKVUYZecKJMEQFqwy7TGNsCMsoUYmYOLS2UAAUQTZzdDhqvhPB6wagvIg7NHmPEo-hc4fJJiwzOeVrBP6Dp4QvJ_T7HOzGCFTypvPqcyL7DbwilTU0wCxRYL

Brozovich, F. V, Nicholson, C. J., Degen, C. V, Gao, Y. Z., Aggarwal, M., & Morgan, K. G. (2016). Mechanisms of Vascular Smooth Muscle Contraction and the Basis for Pharmacologic Treatment of Smooth Muscle Disorders. *Pharmacological Reviews*, *68*(2), 476–532. https://doi.org/10.1124/pr.115.010652

Buchsbaum, M. S., Gillin, J. C., Wu, J., Hazlett, E., Sicotte, N., Dupont, R. M., & Bunney, W. E. (1989). Regional cerebral glucose metabolic rate in human sleep assessed by positron emission tomography. *Life Sciences*, *45*(15), 1349–1356. https://doi.org/10.1016/0024-3205(89)90021-0

Cauli, B., Tong, X.-K., Rancillac, A., Serluca, N., Lambolez, B., Rossier, J., & Hamel, E. (2004).

Cortical GABA interneurons in neurovascular coupling: relays for subcortical vasoactive pathways. *The Journal of Neuroscience : The Official Journal of the Society for Neuroscience*, *24*(41), 8940–8949. https://doi.org/10.1523/JNEUROSCI.3065-04.2004

Cervós-Navarro, J., Kannuki, S., & Nakagawa, Y. (1988). Blood-brain barrier (BBB). Review from morphological aspect. *Histology and Histopathology*, *3*(2), 203–213. Retrieved from http://www.ncbi.nlm.nih.gov/pubmed/2980226

Cipolla, M. J. (2009). Control of cerebral blood flow. In S. Rafael (Ed.), *The Cerebral Circulation*. CA: Morgan & Claypool Life Sciences.

Cossell, L., Iacaruso, M. F., Muir, D. R., Houlton, R., Sader, E. N., Ko, H., … Mrsic-Flogel, T. D. (2015). Functional organization of excitatory synaptic strength in primary visual cortex. *Nature*, *518*(7539), 399–403. https://doi.org/10.1038/nature14182

Cristina, A., Lacerda, R., Marubayashi, U., Balthazar, C. H., & Coimbra, C. C. (2006). Evidence that brain nitric oxide inhibition increases metabolic cost of exercise, reducing running performance in rats. *Neuroscience Letters*, *393*, 260–263. https://doi.org/10.1016/j.neulet.2005.09.076

Cruz Hernández, J. C., Bracko, O., Kersbergen, C. J., Muse, V., Haft-Javaherian, M., Berg, M., … Schaffer, C. B. (2019). Neutrophil adhesion in brain capillaries reduces cortical blood flow and impairs memory function in Alzheimer's disease mouse models. *Nature Neuroscience*, *22*(3), 413–420. https://doi.org/10.1038/s41593-018-0329-4

Dadarlat, M. C., Michael, X., & Stryker, P. (2017). Systems/Circuits Locomotion Enhances Neural Encoding of Visual Stimuli in Mouse V1. https://doi.org/10.1523/JNEUROSCI.2728-16.2017

Dai, J., & Wang, Y. (2012). Representation of Surface Luminance and Contrast in Primary Visual Cortex. *Cerebral Cortex*, *22*(4), 776–787. https://doi.org/10.1093/cercor/bhr133

Damisah, E. C., Hill, R. A., Tong, L., Murray, K. N., & Grutzendler, J. (2017). A fluoro-Nissl dye identifies pericytes as distinct vascular mural cells during in vivo brain imaging. *Nature Neuroscience*. https://doi.org/10.1038/nn.4564

Daneman, R., Zhou, L., Kebede, A. A., & Barres, B. A. (2010). Pericytes are required for blood–brain barrier integrity during embryogenesis. *Nature*, *468*(7323), 562–566. https://doi.org/10.1038/nature09513

Devonshire, I. M., Papadakis, N. G., Port, M., Berwick, J., Kennerley, A. J., Mayhew, J. E. W., & Overton, P. G. (2012). Neurovascular coupling is brain region-dependent. *NeuroImage*, *59*(3), 1997–2006. https://doi.org/10.1016/j.neuroimage.2011.09.050

Devor, A., Sakadzic, S., Saisan, P. A., Yaseen, M. A., Roussakis, E., Srinivasan, V. J., … Boas, D. A. (2011). "Overshoot" of O_2 is required to maintain baseline tissue oxygenation at locations distal to blood vessels. *The Journal of Neuroscience : The Official Journal of the Society for Neuroscience*, *31*(38), 13676–13681.

https://doi.org/10.1523/JNEUROSCI.1968-11.2011

Dipoppa, M., Ranson, A., Krumin, M., Pachitariu, M., Carandini, M., & Harris, K. D. (2016). Vision and locomotion shape the interactions between neuron types in mouse visual cortex. *BioRxiv*, 058396. https://doi.org/10.1101/058396

Echagarruga, C., Gheres, K., & Drew, P. J. (2019). An oligarchy of NO-producing interneurons controls basal and evoked blood flow in the cortex. *BioRxiv*, 555151. https://doi.org/10.1101/555151

Faraci, F. M., & Brian, J. E. (1994). Nitric oxide and the cerebral circulation. *Stroke*, *25*(3), 692–703. https://doi.org/10.1161/01.str.25.3.692

Friedland, R. P., & Iadecola, C. (1991). Roy and Sherrington (1890): a centennial reexamination of "On the regulation of the blood-supply of the brain". *Neurology*, *41*(1), 10–14. https://doi.org/10.1212/wnl.41.1.10

Gao, Y.-R., Greene, S. E., & Drew, P. J. (2015). Mechanical restriction of intracortical vessel dilation by brain tissue sculpts the hemodynamic response. *NeuroImage*, *115*, 162–176. https://doi.org/10.1016/j.neuroimage.2015.04.054

Gieselmann, M. A., & Thiele, A. (2008). Comparison of spatial integration and surround suppression characteristics in spiking activity and the local field potential in macaque V1. *European Journal of Neuroscience*, *28*(3), 447–459. https://doi.org/10.1111/j.1460-9568.2008.06358.x

Girouard, H., Bonev, A. D., Hannah, R. M., Meredith, A., Aldrich, R. W., & Nelson, M. T. (2010). Astrocytic endfoot Ca2+ and BK channels determine both arteriolar dilation and constriction. *Proceedings of the National Academy of Sciences of the United States of America*, *107*(8), 3811–3816. https://doi.org/10.1073/pnas.0914722107

Goense, J. B. M., & Logothetis, N. K. (2008). Neurophysiology of the BOLD fMRI Signal in Awake Monkeys. *Current Biology*, *18*(9), 631–640. https://doi.org/10.1016/J.CUB.2008.03.054

Gold, I. (1999). Does 40-Hz Oscillation Play a Role in Visual Consciousness? *Consciousness and Cognition*, *8*(2), 186–195. https://doi.org/10.1006/CCOG.1999.0399

Goldey, G. J., Roumis, D. K., Glickfeld, L. L., Kerlin, A. M., Reid, R. C., Bonin, V., … Andermann, M. L. (2014). Removable cranial windows for long-term imaging in awake mice. *Nature Protocols*, *9*(11), 2515–2538. https://doi.org/10.1038/nprot.2014.165

Grant, R. I., Hartmann, D. A., Underly, R. G., Berthiaume, A.-A., Bhat, N. R., & Shih, A. Y. (2019). Organizational hierarchy and structural diversity of microvascular pericytes in adult mouse cortex. *Journal of Cerebral Blood Flow and Metabolism : Official Journal of the International Society of Cerebral Blood Flow and Metabolism*, *39*(3), 411–425. https://doi.org/10.1177/0271678X17732229

Hall, C., Howarth, C., Kurth-Nelson, Z., & Mishra, A. (2016). Interpreting BOLD: towards a dialogue between cognitive and cellular neuroscience. In *Philosophical Transactions B: Biological Sciences*.

Hall, C. N., Reynell, C., Gesslein, B., Hamilton, N. B., Mishra, A., Sutherland, B. A., … Attwell, D. (2014). Capillary pericytes regulate cerebral blood flow in health and disease. *Nature*, *508*, 55–60. https://doi.org/10.1038/nature13165

Hamilton, N. B., Attwell, D., & Hall, C. N. (2010). Pericyte-mediated regulation of capillary diameter: A component of neurovascular coupling in health and disease. *Frontiers in Neuroenergetics*, *2*(5). https://doi.org/10.3389/fnene.2010.00005

Harper, S. L., Bohlen, H. G., & Rubin, M. J. (1984). Arterial and microvascular contributions to cerebral cortical autoregulation in rats. *American Journal of Physiology-Heart and Circulatory Physiology*, *246*(1), H17–H24. https://doi.org/10.1152/ajpheart.1984.246.1.H17

Hartmann, D. A., Underly, R. G., Grant, R. I., Watson, A. N., Lindner, V., & Shih, A. Y. (2015). Pericyte structure and distribution in the cerebral cortex revealed by high-resolution imaging of transgenic mice. *Neurophotonics*, *2*(4), 041402. https://doi.org/10.1117/1.NPh.2.4.041402

Hawkins, B. T., & Davis, T. P. (2005). The Blood-Brain Barrier/Neurovascular Unit in Health and Disease. *Pharmacological Reviews*, *57*(2). Retrieved from http://pharmrev.aspetjournals.org/content/57/2/173.short

Hill, R. A., Tong, L., Yuan, P., Murikinati, S., Gupta, S., & Grutzendler, J. (2015). Regional Blood Flow in the Normal and Ischemic Brain Is Controlled by Arteriolar Smooth Muscle Cell Contractility and Not by Capillary Pericytes. *Neuron*, *87*(1), 95–110. https://doi.org/10.1016/j.neuron.2015.06.001

Holtmaat, A., Bonhoeffer, T., Chow, D. K., Chuckowree, J., De Paola, V., Hofer, S. B., … Wilbrecht, L. (2009). Long-term, high-resolution imaging in the mouse neocortex through a chronic cranial window. *Nature Protocols*, *4*(8), 1128–1144. https://doi.org/10.1038/nprot.2009.89

Huang, P. L., Huang, Z., Mashimo, H., Bloch, K. D., Moskowitz, M. A., Bevan, J. A., & Fishman, M. C. (1995). Hypertension in mice lacking the gene for endothelial nitric oxide synthase. *Nature*, *377*(6546), 239–242. https://doi.org/10.1038/377239a0

Hughes, J. R. (2008). Gamma, fast, and ultrafast waves of the brain: their relationships with epilepsy and behavior. *Epilepsy & Behavior : E&B*, *13*(1), 25–31. https://doi.org/10.1016/j.yebeh.2008.01.011

Huo, B.-X., Smith, J. B., & Drew, P. J. (2014). Systems/Circuits Neurovascular Coupling and Decoupling in the Cortex during Voluntary Locomotion. https://doi.org/10.1523/JNEUROSCI.1369-14.2014

Hutter-Schmid, B., & Humpel, C. (2016). Platelet-derived Growth Factor Receptor-beta is

Differentially Regulated in Primary Mouse Pericytes and Brain Slices. *Current Neurovascular Research*, *13*(2), 127–134. Retrieved from http://www.ncbi.nlm.nih.gov/pubmed/26891660

Iadecola, C. (2017). The Neurovascular Unit Coming of Age: A Journey through Neurovascular Coupling in Health and Disease. *Neuron*, *96*, 17–42. https://doi.org/10.1016/j.neuron.2017.07.030

Ince, C., Coremans, J. M. C. C., & Bruining, H. A. (1992). In Vivo NADH Fluorescence (pp. 277–296). Springer, Boston, MA. https://doi.org/10.1007/978-1-4615-3428-0_30

Jennings, M., & Berdoy, M. (2010). Guiding Principles for Preparing for and Undertaking Aseptic Surgery. In *A report by the LASA Education, Training and Ethics section*.

Johnson, J. K., Geng, S., Hoffman, M. W., Adesnik, H., & Wessel, R. (2018). Stimulus information is isolated from single whole-cell recordings in the visual cortex of awake mice by exploiting high-dimensional representations of dynamics. *Society for Neuroscience Annual Meeting*.

Jong, G. I., Vos, R. A. I., Steur, E. N. H. J., & Luiten, P. G. M. (1997). Cerebrovascular Hypoperfusion: A Risk Factor for Alzheimer's Disease?. *Annals of the New York Academy of Sciences*, *826*(1 Cerebrovascul), 56–74. https://doi.org/10.1111/j.1749-6632.1997.tb48461.x

Kety, S. S. (1950). Circulation and metabolism of the human brain in health and disease. *The American Journal of Medicine*, *8*(2), 205–217. https://doi.org/10.1016/0002-9343(50)90363-9

Kim, D.-S., Ronen, I., Olman, C., Kim, S.-G., Ugurbil, K., & Toth, L. J. (2004). Spatial relationship between neuronal activity and BOLD functional MRI. *NeuroImage*, *21*, 876–885. https://doi.org/10.1016/j.neuroimage.2003.10.018

Kocharyan, A., Fernandes, P., Tong, X.-K., Vaucher, E., & Hamel, E. (2008). Specific Subtypes of Cortical GABA Interneurons Contribute to the Neurovascular Coupling Response to Basal Forebrain Stimulation. *Journal of Cerebral Blood Flow & Metabolism*, *28*(2), 221–231. https://doi.org/10.1038/sj.jcbfm.9600558

Krueger, M., & Bechmann, I. (2010). CNS pericytes: Concepts, misconceptions, and a way out. *Glia*, *58*(1), 1–10. https://doi.org/10.1002/glia.20898

Kwong, K. K., Belliveau, J. W., Chesler, D. A., Goldberg, I. E., Weisskoff, R. M., Poncelet, B. P., … al., et. (1992). Dynamic magnetic resonance imaging of human brain activity during primary sensory stimulation. *Proceedings of the National Academy of Sciences of the United States of America*, *89*(12), 5675–5679. https://doi.org/10.1073/pnas.89.12.5675

Lacroix, A., Toussay, X., Anenberg, E., Lecrux, C., Ferreirós, N., Karagiannis, A., … Cauli, B. (2015). COX-2-Derived Prostaglandin E2 Produced by Pyramidal Neurons Contributes to Neurovascular Coupling in the Rodent Cerebral Cortex. *The Journal of Neuroscience : The*

Official Journal of the Society for Neuroscience, *35*(34), 11791–11810. https://doi.org/10.1523/JNEUROSCI.0651-15.2015

Lassen, N. A., Ingvar, D. H., & Skinhøj, E. (1978). Brain Function and Blood Flow. *Scientific American*. Scientific American, a division of Nature America, Inc. https://doi.org/10.2307/24955823

Le Bihan, D. (1996). Functional MRI of the brain principles, applications and limitations. *Journal of Neuroradiology. Journal de Neuroradiologie*, *23*(1), 1–5. Retrieved from http://www.ncbi.nlm.nih.gov/pubmed/8767912

Lecrux, C., Toussay, X., Kocharyan, A., Fernandes, P., Neupane, S., Lévesque, M., … Hamel, E. (2011). Pyramidal neurons are “neurogenic hubs” in the neurovascular coupling response to whisker stimulation. *Journal of Neuroscience*, *31*(27), 9836–9847. https://doi.org/10.1523/JNEUROSCI.4943-10.2011

Lee, L. M., Boorman, L., Glendenning, E., Christmas, C., Sharp, P., Redgrave, P., … Howarth, C. (2019). Key aspects of neurovascular control mediated by specific populations of inhibitory cortical interneurons. *BioRxiv*, 550269. https://doi.org/10.1101/550269

Lindauer, U., Leithner, C., Kaasch, H., Rohrer, B., Foddis, M., Fü Chtemeier, M., … Dirnagl, U. (2010). Neurovascular coupling in rat brain operates independent of hemoglobin deoxygenation. *Journal of Cerebral Blood Flow & Metabolism*, *30*, 757–768. https://doi.org/10.1038/jcbfm.2009.259

Logothetis, N. K., Pauls, J., Augath, M., Trinath, T., & Oeltermann, A. (2001). Neurophysiological investigation of the basis of the fMRI signal. *Nature*, *412*(6843), 150–157. https://doi.org/10.1038/35084005

Longden, T. A., Dabertrand, F., Koide, M., Gonzales, A. L., Tykocki, N. R., Brayden, J. E., … Nelson, M. T. (2017). Capillary K+-sensing initiates retrograde hyperpolarization to increase local cerebral blood flow. *Nature Neuroscience*, *20*(5), 717–726. https://doi.org/10.1038/nn.4533

Longden, T. A., Hill-Eubanks, D. C., & Nelson, M. T. (2015). Ion channel networks in the control of cerebral blood flow. *Journal of Cerebral Blood Flow & Metabolism*, *36*(3), 0271678X15616138. https://doi.org/10.1177/0271678X15616138

Maffei, L., & Fiorentini, A. (1973). The visual cortex as a spatial frequency analyser. *Vision Research*, *13*, 1255–1267. Retrieved from https://pdf.sciencedirectassets.com/271122/1-s2.0-S0042698900X04555/1-s2.0-0042698973902010/main.pdf?x-amz-security-token=AgoJb3JpZ2luX2VjEPj%2F%2F%2F%2F%2F%2F%2F%2F%2F%2FwEaCXVzLWVhc3QtMSJHMEUCIQD8CBF60YU8WkMDHDLSNQKVf9%2BDlCQuETPDc4RG%2BX08BwIgKbp0%2FzO

Mergenthaler, P., Lindauer, U., Dienel, G. A., & Meisel, A. (2013). Sugar for the brain: the role of glucose in physiological and pathological brain function. *Trends in Neurosciences*, *36*(10), 587–597. https://doi.org/10.1016/j.tins.2013.07.001

Miners, J. S., Schulz, I., & Love, S. (2017). Differing associations between AB accumulation, hypo perfusion, blood-brain barrier dysfunction and loss of PDGFRB pericyte marker in the precuneus and parietal white matter in Alzheimer's disease. *Journal of Cerebral Blood Flow*, *38*(1), 103–115. https://doi.org/10.1177/0271678X17690761

Mintun, M. A., Lundstrom, B. N., Snyder, A. Z., Vlassenko, A. G., Shulman, G. L., & Raichle, M. E. (2001). *Blood flow and oxygen delivery to human brain during functional activity: Theoretical modeling and experimental data* (Vol. 98). Retrieved from www.pnas.orgcgidoi10.1073pnas.111164398

Mishra, A., Reynolds, J. P., Chen, Y., Gourine, A. V, Rusakov, D. A., & Attwell, D. (2016). Astrocytes mediate neurovascular signaling to capillary pericytes but not to arterioles. *Nature Neuroscience*, *19*(12), 1619–1627. https://doi.org/10.1038/nn.4428

Mosso, A. (1880). Sulla circolazione del cervello dell'uomo. *Atti Della R/ Accademia Dei Lincei*, *5*, 237–358.

Muthukumaraswamy, S. D., & Singh, K. D. (2008). Spatiotemporal frequency tuning of BOLD and gamma band MEG responses compared in primary visual cortex. https://doi.org/10.1016/j.neuroimage.2008.01.052

Nakagawa, S., Deli, M. A., Kawaguchi, H., Shimizudani, T., Shimono, T., Kittel, Á., … Niwa, M. (2009). A new blood–brain barrier model using primary rat brain endothelial cells, pericytes and astrocytes. *Neurochemistry International*, *54*(3), 253–263. https://doi.org/10.1016/j.neuint.2008.12.002

Nehls, V., & Drenckhahn, D. (1991). Heterogeneity of microvascular pericytes for smooth muscle type alpha-actin. *Journal of Cell Biology*, *113*(1), 147–154. https://doi.org/10.1083/jcb.113.1.147

Niell, C. M., & Stryker, M. P. (2010). Modulation of Visual Responses by Behavioral State in Mouse Visual Cortex. *Neuron*, *65*(4), 472–479. https://doi.org/10.1016/J.NEURON.2010.01.033

Nienborg, H., Hasenstaub, A., Nauhaus, I., Taniguchi, H., Huang, Z. J., & Callaway, E. M. (2013). Systems/Circuits Contrast Dependence and Differential Contributions from Somatostatin-and Parvalbumin-Expressing Neurons to Spatial Integration in Mouse V1. https://doi.org/10.1523/JNEUROSCI.5320-12.2013

Nizar, K., Uhlirova, H., Tian, P., Saisan, P. A., Cheng, Q., Reznichenko, L., … Devor, A. (2013). In vivo stimulus-induced vasodilation occurs without IP3 receptor activation and may precede astrocytic calcium increase. *The Journal of Neuroscience*, *33*(19), 8411–8422. https://doi.org/10.1523/JNEUROSCI.3285-12.2013

Okun, M., Steinmetz, N., Cossell, L., Iacaruso, M. F., Ko, H., Barthó, P., … Harris, K. D. (2015). Diverse coupling of neurons to populations in sensory cortex. *Nature*, *521*(7553), 511–515. https://doi.org/10.1038/nature14273

Ozerdem, U., & Stallcup, W. B. (2003). Early Contribution of Pericytes to Angiogenic Sprouting and Tube Formation. *Angiogenesis*, *6*(3), 241–249. https://doi.org/10.1023/B:AGEN.0000021401.58039.a9

Pakan, J. M., Lowe, S. C., Dylda, E., Keemink, S. W., Currie, S. P., Coutts, C. A., & Rochefort, N. L. (2016). Behavioral-state modulation of inhibition is context-dependent and cell type specific in mouse visual cortex. *ELife*, *5*(AUGUST). https://doi.org/10.7554/eLife.14985

Peng, X., & Van Essen, D. C. (2005). Areas V1 and V2 Peaked Encoding of Relative Luminance in Macaque Downloaded from. *Journal of Neurophysiology on March*, *1*, 1620–1632. https://doi.org/10.1152/jn.00793.2004

Peppiatt, C. M., Howarth, C., Mobbs, P., & Attwell, D. (2006). Bidirectional control of CNS capillary diameter by pericytes. *Nature*, *443*(7112), 700–704. https://doi.org/10.1038/nature05193

Perrenoud, Q., Geoffroy, H., Gauthier, B., Rancillac, A., Alfonsi, F., Kessaris, N., … Gallopin, T. (2012). Characterization of Type I and Type II nNOS-Expressing Interneurons in the Barrel Cortex of Mouse. *Frontiers in Neural Circuits*, *6*, 36. https://doi.org/10.3389/fncir.2012.00036

Perrenoud, Q., Rossier, J., Férézou, I., Geoffroy, H., Gallopin, T., Vitalis, T., & Rancillac, A. (2012). Activation of cortical 5-HT(3) receptor-expressing interneurons induces NO mediated vasodilatations and NPY mediated vasoconstrictions. *Frontiers in Neural Circuits*, *6*, 50. https://doi.org/10.3389/fncir.2012.00050

Picot, A., Dominguez, S., Liu, C., Tessier, G., Forget, C., Correspondence, V. E., … Emiliani, V. (2018). Temperature Rise under Two-Photon Optogenetic Brain Stimulation Article Temperature Rise under Two-Photon Optogenetic Brain Stimulation. *CellReports*, *24*, 1243-1253.e5. https://doi.org/10.1016/j.celrep.2018.06.119

Pisauro, M. A., Dhruv, N. T., Carandini, M., & Benucci, A. (2013). Systems/Circuits Fast Hemodynamic Responses in the Visual Cortex of the Awake Mouse. https://doi.org/10.1523/JNEUROSCI.2130-13.2013

Powers, W. J., Hirsch, I. B., & Cryer, P. E. (1996). Effect of stepped hypoglycemia on regional cerebral blood flow response to physiological brain activation. *The American Journal of Physiology*, *270*(2 Pt 2), H554-9. https://doi.org/10.1152/ajpheart.1996.270.2.H554

Ricard, C., Coles, J. A., Serduc, R., van der Sanden, B., Verant, P., & Vial, J.-C. (2009). Two-Photon Imaging. *Encyclopedia of Neuroscience*, 1221–1229. https://doi.org/10.1016/B978-008045046-9.00863-9

Riedemann, T., Straub, T., & Sutor, B. (2018). Two types of somatostatin-expressing GABAergic interneurons in the superficial layers of the mouse cingulate cortex. *PLOS ONE*, *13*(7), e0200567. https://doi.org/10.1371/journal.pone.0200567

Roy, C. S., & Sherrington, C. S. (1890). On the Regulation of the Blood-supply of the Brain. *The*

Journal of Physiology, *11*(1–2), 85–158. https://doi.org/10.1113/jphysiol.1890.sp000321

Rungta, R. L., Chaigneau, E., Osmanski, B.-F., & Charpak, S. (2018). Vascular Compartmentalization of Functional Hyperemia from the Synapse to the Pia. *Neuron*, *99*(2), 362-375.e4. https://doi.org/10.1016/J.NEURON.2018.06.012

Runyan, C. A., Schummers, J., Van Wart, A., Kuhlman, S. J., Wilson, N. R., Huang, Z. J., & Sur, M. (2010). Response Features of Parvalbumin-Expressing Interneurons Suggest Precise Roles for Subtypes of Inhibition in Visual Cortex. *Neuron*, *67*(5), 847–857. https://doi.org/10.1016/J.NEURON.2010.08.006

Schmidt, C. F., & Hendrix, J. P. (1938). The action of chemical substances on cerebral blood vessels. *Research Publications - Association for Research in Nervous and Mental Disease*, *18*, 229–276.

Sokoloff, L. (1960). The metabolism of the central nervous system in vivo. In *Handbook of physiology, section I, Neurophysiology 3* (pp. 1843–1864).

Sun, W., McConnell, E., Pare, J.-F., Xu, Q., Chen, M., Peng, W., … Nedergaard, M. (2013). Glutamate-dependent neuroglial calcium signaling differs between young and adult brain. *Science (New York, N.Y.)*, *339*(6116), 197–200. https://doi.org/10.1126/science.1226740

Suzuki, S., Namiki, J., Shibata, S., Mastuzaki, Y., & Okano, H. (2010). The Neural Stem/Progenitor Cell Marker Nestin Is Expressed in Proliferative Endothelial Cells, but Not in Mature Vasculature. *Journal of Histochemistry and Cytochemistry*, *58*(8), 721–730. https://doi.org/10.1369/jhc.2010.955609

Teichert, M., Lehmann, K., & Bolz, J. (2018). Visual performance in mice: physiology meets behaviour. *Journal of Behavioral Neuroscience*, *1*(1). Retrieved from https://www.pulsus.com/scholarly-articles/visual-performance-in-mice-physiology-meets-behaviour-4460.html

Tian, P., Teng, I. C., May, L. D., Kurz, R., Lu, K., Scadeng, M., … Devor, A. (2010). Cortical depth-specific microvascular dilation underlies laminar differences in blood oxygenation level-dependent functional MRI signal. *Proceedings of the National Academy of Sciences of the United States of America*, *107*(34), 15246–15251. https://doi.org/10.1073/pnas.1006735107

Tian, R., Vogel, P., Lassen, N. A., Mulvany, M. J., Andreasen, F., & Aalkjaer, C. (1995). Role of extracellular and intracellular acidosis for hypercapnia-induced inhibition of tension of isolated rat cerebral arteries. *Circulation Research*, *76*(2), 269–275. https://doi.org/10.1161/01.res.76.2.269

Tiret, P., Chaigneau, E., Lecoq, J., & Charpak, S. (2009). Two-Photon Imaging of Capillary Blood Flow in Olfactory Bulb Glomeruli (pp. 81–91). Humana Press. https://doi.org/10.1007/978-1-59745-543-5_4

Tootell, R. B. H., Hadjikhani, N. K., Vanduffel, W., Liu, A. K., Mendola, J. D., Sereno, M. I., &

Dale, A. M. (1998). *Neuroimaging of Human Brain Function* (Vol. 95). Retrieved from www.pnas.org.

Tricoire, L., & Vitalis, T. (2012). Neuronal nitric oxide synthase expressing neurons: a journey from birth to neuronal circuits. *Frontiers in Neural Circuits*, *6*, 82. https://doi.org/10.3389/fncir.2012.00082

Tseng, Q., Wang, I., Duchemin-Pelletier, E., Azioune, A., Carpi, N., Gao, J., … Balland, M. (2011). A new micropatterning method of soft substrates reveals that different tumorigenic signals can promote or reduce cell contraction levels. *Lab on a Chip*, *11*(13), 2231. https://doi.org/10.1039/c0lc00641f

Uhlirova, H., Kılıç, K., Tian, P., Thunemann, M., Desjardins, M., Saisan, P. A., … Devor, A. (2016). Cell type specificity of neurovascular coupling in cerebral cortex. *ELife*, *5*(MAY2016). https://doi.org/10.7554/eLife.14315

Urban, A., Rancillac, A., Martinez, L., & Rossier, J. (2012). Deciphering the Neuronal Circuitry Controlling Local Blood Flow in the Cerebral Cortex with Optogenetics in PV::Cre Transgenic Mice. *Frontiers in Pharmacology*, *3*, 105. https://doi.org/10.3389/fphar.2012.00105

Vinck, M., Batista-Brito, R., Knoblich, U., & Cardin, J. A. (2015). Arousal and Locomotion Make Distinct Contributions to Cortical Activity Patterns and Visual Encoding. *Neuron*, *86*(3), 740–754. https://doi.org/10.1016/J.NEURON.2015.03.028

Vrselja, Z., Brkic, H., Mrdenovic, S., Radic, R., & Curic, G. (2014). Function of circle of Willis. *Journal of Cerebral Blood Flow & Metabolism*, *34*(10), 578–584. https://doi.org/10.1038/jcbfm.2014.7

Wagenseil, J. E., & Mecham, R. P. (2012). Elastin in large artery stiffness and hypertension. *Journal of Cardiovascular Translational Research*, *5*(3), 264–273. https://doi.org/10.1007/s12265-012-9349-8

Webb, R. C. (2003). Smooth muscle contraction and relaxation. *Advances in Physiology Education*, *27*(1–4), 201–206. Retrieved from http://www.ncbi.nlm.nih.gov/pubmed/14627618

Winder, A. T., Echagarruga, C., Zhang, Q., & Drew, P. J. (2017). Weak correlations between hemodynamic signals and ongoing neural activity during the resting state. *Nature Neuroscience*, *20*(12), 1761–1769. https://doi.org/10.1038/s41593-017-0007-y

Xu, X., Roby, K. D., & Callaway, E. M. (2010). Immunochemical characterization of inhibitory mouse cortical neurons: Three chemically distinct classes of inhibitory cells. *The Journal of Comparative Neurology*, *518*(3), 389–404. https://doi.org/10.1002/cne.22229

Yaksh, T. L., Wang, J.-Y., Go, V. L. W., & Harty, G. J. (1987). Cortical Vasodilatation Produced by Vasoactive Intestinal Polypeptide (VIP) and by Physiological Stimuli in the Cat. *Journal of Cerebral Blood Flow & Metabolism*, *7*(3), 315–326.

https://doi.org/10.1038/jcbfm.1987.69

Yüzgeç, Ö., Prsa, M., Zimmermann, R., & Huber, D. (2018). Pupil Size Coupling to Cortical States Protects the Stability of Deep Sleep via Parasympathetic Modulation. *Current Biology*, *28*(3), 392-400.e3. https://doi.org/10.1016/J.CUB.2017.12.049

Zimmermann, K. W. (1923). Der feinere Bau der Blutcapillaren. *Zeitschrift Für Anatomie Und Entwicklungsgeschichte*, *68*(1), 29–109. https://doi.org/10.1007/BF02593544